UNIVERSITY OF SOUTHAMPTON

Faculty of Natural and Environmental Sciences

School of Chemistry

Understanding Cyclobutenone Rearrangements: A Study Under Flow

by

Mubina Mohamed

A Thesis Submitted for the Degree of Doctor of Philosophy

September 2013

UNIVERSITY OF SOUTHAMPTON

ABSTRACT

FACULTY OF NATURAL AND ENVIRONMENTAL SCIENCES
SCHOOL OF CHEMISTRY

Doctor of Philosophy

UNDERSTANDING CYCLOBUTENONE REARRANGEMENTS: A STUDY UNDER FLOW

By Mubina Mohamed

This thesis describes the work undertaken to get a better understanding of cyclobutenone rearrangements. Thermal rearrangements of aryl- and heteroarylcyclobutenones have become established as useful methods for the synthesis of many polyaromatic and heteroaromatic ring systems, which include natural products with interesting biological activity. Though widely used, little is known about the factors that influence the course of these reactions, or the optimal conditions for effecting them. Herein, the utility of flow chemistry will be presented as a valuable tool that has markedly improved the efficiency of the reactions due to the tight control of reaction conditions. The results obtained were correlated to *in silico* calculations to develop a better understanding of the rearrangement.

The photochemical rearrangement of 4-hydroxycyclobutenones were also investigated under a continuous flow-photo set-up using a simple, low-cost device with an interchangeable low-energy light source. The results obtained challenge the long-established view that the electrocyclic ring opening of cyclobutenones is a torquo-selective process, with the thermochemical and photochemical rearrangements displaying complimentary torquoselectivity.

Contents

Declaration of Authorship

I, Mubina Mohamed declare that the thesis entitled "Understanding Cyclobutenone Rearrangements: A Study Under Flow" and the work presented in the thesis are both my own, and have been generated by me as the result of my own original research. I confirm that:

- this work was done wholly or mainly while in candidature for a research degree at this University;
- where any part of this thesis has previously been submitted for a degree or any other qualification at this University or any other institution, this has been clearly stated;
- where I have consulted the published work of others, this is always clearly attributed;
- where I have quoted from the work of others, the source is always given. With the exception of such quotations, this thesis is entirely my own work;
- I have acknowledged all main sources of help;
- where the thesis is based on work done by myself jointly with others, I have made clear exactly what was done by others and what I have contributed myself;
- parts of this work have been published as:

  Harrowven, D. C.; Mohamed, M.; Gonçalves, T. P.; Whitby, R. J.; Sneddon, H. F., *Chem. Eur. J.*, **2011**, *17*, 13698–13705.

  Harrowven, D. C.; Mohamed, M.; Gonçalves, T. P.; Whitby, R. J.; Bolien, D.; Sneddon, H. F., *Angew. Chem. Int. Ed.*, **2012**, *51*, 4405–4408.

Signed: ……..

Date: ……..

Acknowledgements

I would first like to thank Prof. David Harrowven for giving me the opportunity to work on one of the most treasured subjects within the group. Your full commitment, guidance, enthusiasm, and encouragement on a daily basis has been incredible and much appreciated. A simple thank you cannot express how grateful I am to the vast amounts of proof reading you have carried out for me, but nonetheless, thank you.

A special thanks has to go to Dr. Helen Sneddon for adopting me during my lengthy placements at GSK. The transition from Southampton to GSK could not have been smoother, and that was solely down to you. Your advice and support on all matters were greatly appreciated. Thanks also to Dr. Andy Craven for watching over me from a far, invitations to Friday morning breakfast and brightening my day with your wonderful banter. I am highly indebted to Rob Wheeler for all the invaluable advice and support regarding all things flow; I'd still be clueless as to what 'air' meant if it wasn't for you. Thanks to everyone at GSK that has put up with me during my many placements especially members of lab 2S110 and the NMR analysis team. A special thanks to Dr. Sébastien Campos and Afjal Miah in lab 2S113 for making me feel very welcome, adopting me as an honorary member of their 'PROTAC' team and enlightening me with their weird and wonderful chemistry.

The revolving door of Harrowven group members is many, and I must thank them all for making my time within the group memorable. In particular, I would like to thank Zeshan, Majdouline, Paul, Rob 'Gangster' and Cyril Plouchart for making the past year very enjoyable. The cupcakes, 'hit' biscuits, tea breaks and Friday dinners have been traditions that made late nights in the lab and working at the weekend bearable!! A special thanks to my flow team, Cyril Henry and David Bolien – my PhD wouldn't have been half as fun if you guys weren't beside me and your help every step of the way has been outstanding. Thanks also to all the wonderful chemists of Bldg 30, Floor 3 – everyone in the Linclau, Brown and Whitby labs, the chemistry and non-chemistry banter has been a delight to come back to after every placement.

Thanks must be given to all the support staff with the School of Chemistry. In particular, Dr. Neil Wells for the meticulous running of the NMR rooms. To Dr. John Langley, Ms. Julie Herniman, and Sarah Clark in mass spectroscopy for running a well oiled department and Mark Light and Majduoline Roudias for all the X-ray analysis. Thanks also to the gents in stores; Karl, Keith, and Mark – it's never a dull visit when I'm down in stores, the banter is much appreciated and it always put a smile on my face!

A very special thanks to my family for their support and putting up with my absence. And last but not least, to my partner-in-writing, I cannot thank you enough for your support, encouragement, enthusiasm, and staying up late with me while I work. Your positivity has been infectious and I believe I've done better with you by my side.

MM 2013

Abbreviations

Ac	acetyl	mmol	millimole(s)
app.	apparent	mol	mole(s)
Ar	aryl	MOM	methoxymethyl ether
aq	aqueous	MP	melting point
B3LYP	Becke, 3-parameter, Lee-Yang-Parr	Ms	mesyl
Bn	benzyl	MS	molecular sieves
br.	broad	m/z	mass / charge ratio
Bu	butyl	NBS	*N*-bromosuccinimide
cal	calories	NIS	*N*-iodosuccinimide
CAN	ceric ammonium nitrate	nM	nanomolar
°C	degrees centigrade	NMO	*N*-methylmorpholine-*N*-oxide
cm^{-1}	wavenumber	NMP	N-methylpyrrolidone
d	doublet / deuterated	NMR	nuclear magnetic resonance
d.r.	diastereomeric ratio	*o*	*ortho*
DCM	dichloromethane	*p*	*para*
DMAP	4-*N*, *N*-dimethylaminopyridine	PG	protecting group
DMF	*N*-*N*-dimethylformamide	Ph	phenyl
DMSO	dimethylsulfoxide	ppm	parts per million
EDC	1-ethyl-3-(3-dimethylaminopropyl)carbodiimide	q	quartet
El	electron ionisation	*R*	resonance
ES+	electrospray ionisation (positive mode)	*rac*	racemic
ES-	electrospray ionisation (negative mode)	RT	room temperature
ESl	electrospray ionisation	s	singlet / strong
Et	ethyl	sat.	saturated
g	gram(s)	sxt	sextet
h	hour(s)	t	triplet
HPLC	high performance liquid chromatography	*t*	tertiary
HRMS	high resolution mass spectrometry	*tert*	tertiary
Hz	hertz	TBAF	tetra-^{n}butylammonium fluoride
i	iso	TEA	triethylamine
I	inductive	TES	triethylsilyl
J	coupling constant	Tf	triflate
k	kilo	TFA	trifluoroacetic acid
L	litre(s)	TFAA	trifluoroacetic anhydride
LCMS	liquid chromatography-mass spectrometry	THF	tetrahydrofuran
LDA	lithium diisopropylamide	THP	tetrahydropyran
LHMDS	lithium hexamethyldisilazide	TLC	thin layer chromatography
LRMS	low resolution mass spectrometry	TMS	trimethylsilyl
μwave	microwave	Trisyl	triisopropylbenzenesulfonyl
M	molar	Ts	tosyl
m	medium / multiplet / milli	UV	ultraviolet
m	meta	υ_{max}	absorption maxima
Me	methyl	*viz.*	*videlicet*
*m*CPBA	*m*-chloroperoxybenzoic acid	w	weak
min	minute(s)	W	watt
mL	millilitre(s)		
mM	millimolar		

Chapter 1. Introduction

Substituted cyclobutenones such as **3–6** are readily prepared from squaric acid diesters **2**, and have proven to be useful precursors to an array of highly substituted quinones and condensed quinones (e.g. **7–10**) *via* thermal rearrangement (Scheme 1).[1] Much of the pioneering work in this area was carried out by the Moore[2,3] and Liebeskind[4,5] groups.

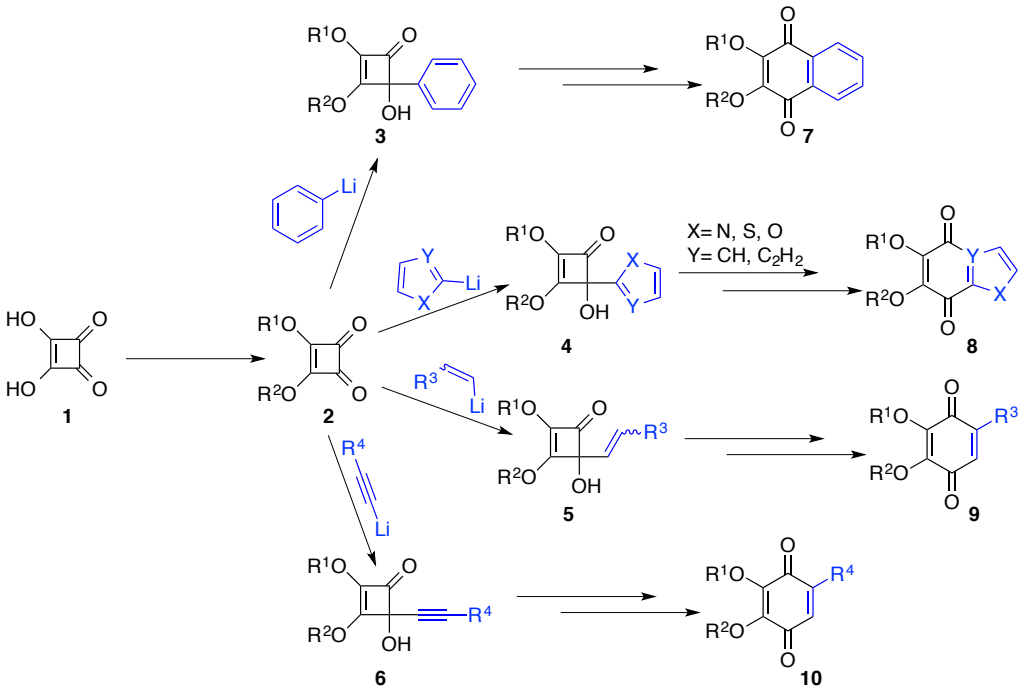

Scheme 1: Scope for the rearrangement of substituted cyclobutenones.

1.1 Rearrangement of 4-Aryl and 4-Vinyl Cyclobutenones

The rearrangement of 4-vinyl-4-hydroxycyclobutenones **11** have been shown to give access to highly substituted hydroquinones, which undergo facile oxidation to quinones. The mechanistic course of the rearrangement was first described by Moore *et al.*[6] who suggested that heating arylcyclobutenone **11** would trigger an electrocyclic ring opening to ketene **14**. In turn, the vinyl ketene undergoes a 6π electrocyclic ring closure to **15** and tautomerisation to hydroquinone **12.** Oxidative workup using air,[7] DMP,[8] CAN,[9] and other oxidants then gives the corresponding quinone **13** (Scheme 2).

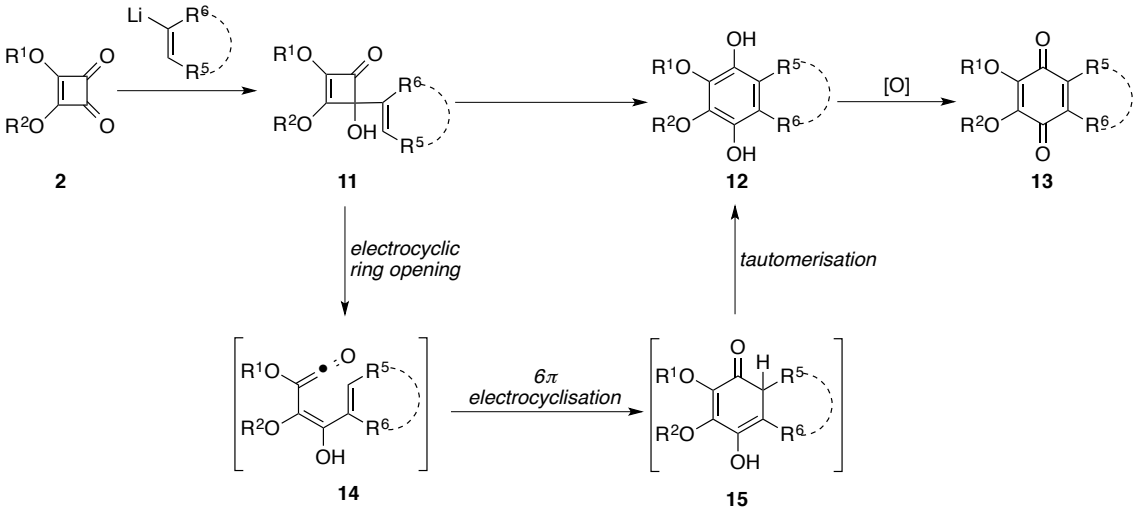

Scheme 2. Thermally induced vinyl-, aryl- and heteroaryl-cyclobutenone rearrangements.

The same course is followed by arylcyclobutenones, as illustrated by the examples shown in Scheme 3. The reaction often displays exquisite regioselectivity, is generally performed at reflux in *p*-xylene (138 °C) and usually proceeds in good to excellent yield. Notably, when 2-substituted arenes are employed, cyclisation occurs towards the unsubstituted C-6 carbon centre (*e.g.* **17c, d → 18c, d**).[6]

Moore suggested that the transformation observed was largely dictated by the nature of the cyclobutenone ring opening. In general, this is governed by the substituents on the saturated carbon where electron-donating substituents such as a hydroxyl group rotate away from the ketene (outwards), while the vinyl or aryl group rotates towards it (inwards). Consequently, the ketene is placed in close proximity to the vinyl or aryl group and is able to participate in a 6π electrocylisation.[1] This rational was supported by the outcome of such thermal rearrangements, which selectively give hydroquinones and benzohydroquinones in good to excellent yield.[9-11]

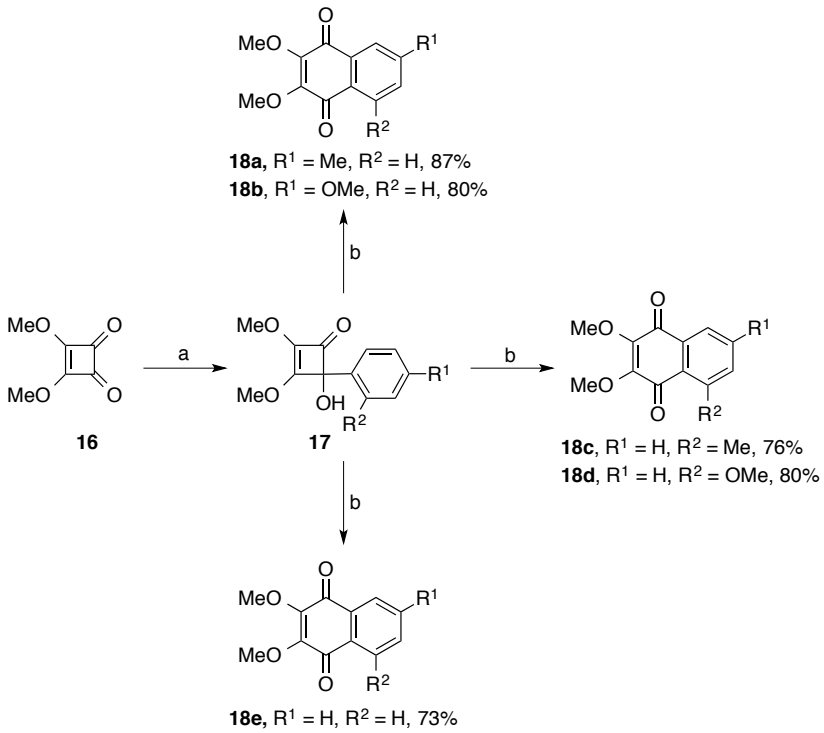

Scheme 3: Rearrangement of 4-arylcyclobutenones **17** to quinones **18.**

Further insight into the mechanism came with the rearrangement of the 2-naphthyl derivative **17f** (Scheme 4). Thermolysis of **17f** could conceivably give polyaromatic quinones **18f** and **19** *via* ring closure at the C-1 or C-3-centres of the naphthalene group. Interestingly, only the unsymmetrical phenanthraquinone **18f** was isolated, suggesting to Moore that the transition state for the rearrangement of **17f** to **18f** requires some electrophilic character, which is provided by the electrophilicity of the C-1-centre.[6]

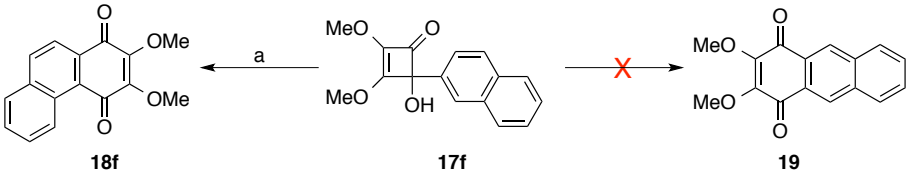

Scheme 4: Rearrangement of 2-naphthyl derivative **17f**.

This hypothesis was supported by the rearrangement of **17g**, where ring closure gave a mixture of cyclohexenedione **21** and 1,4-phenanthrenedione **22**. These products arise from the selective ring closure of the conjugated ketene to the proximal carbon bearing

the methoxy group. Tautomerisation then gives cyclohexenedione **21** while loss of methanol from **21** gives 1,4-phenanthrenedione **22** (Scheme 5).

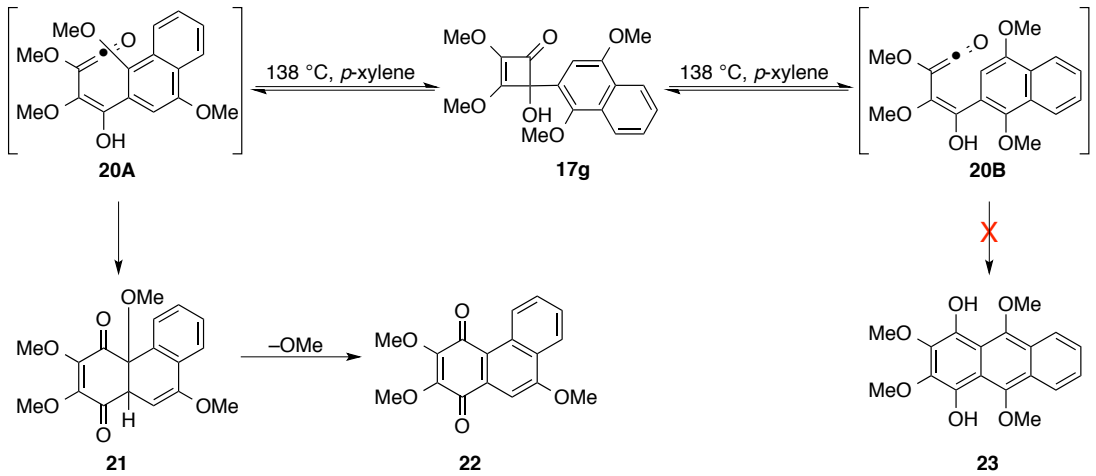

Scheme 5: Thermal rearrangement of **17g**.

4-Chlorocyclobutenones bearing 4-aryl, 4-alkenyl and 4-alkynyl substituents have also been shown to be valuable precursors to highly substituted chlorophenols.[12,13] Their preparation begins from dimethyl squarate **16**, which is readily converted into the regioisomeric cyclobutenones **24** and **25** *via* well-documented methods.[14,15] These regioisomers each gave the same 4-chloro derivative **26** upon treatment with thionyl chloride and pyridine in DCM due to formation of a common cationic intermediate (Scheme 6). Thermolysis of **26** in refluxing *p*-xylene led to chlorophenol **28**.

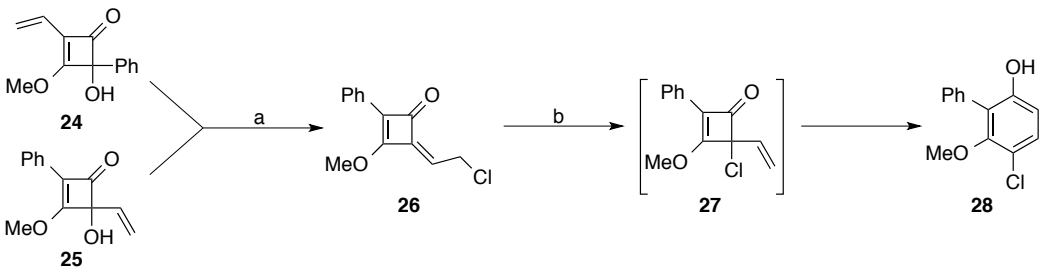

a) $SOCl_2$, pyridine, DCM, 82% (from **24**) and 42% (from **25**); b) *p*-xylene, 138 °C, 3 h, 62%.

Scheme 6: Formation of chloride **26** and its thermolysis.

Reductive dehydroxylation of 4-hydroxycyclobutenones provides a convenient route to highly substituted naphthols. Precursors such as **32** are readily formed from hydroxycyclobutenones (*e.g.* **30**) by treatment with BF_3•OEt_2 and triethylsilane and these

readily expand to the corresponding naphthols on thermolysis (Scheme 7). The regioselectivity of the ionic hydrogenation, and subsequently the substitution pattern of the phenol is dictated by the nature of the substituents on 4-hydroxycyclobutenone **30**, as well as electronic and steric effects and the size of the silane reagents.[16]

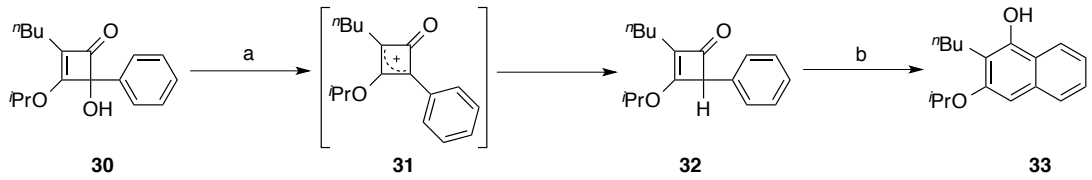

30 **31** **32** **33**

a) Et_3SiH, $BF_3{\bullet}OEt_2$, DCM, RT, 5 h, 75%; b) PhMe, 110 °C, 1 h, 96%.

Scheme 7: Synthesis and rearrangement of protiocyclobutenones to naphthols.

Harrowven *et al.* have extended the scope of vinylcyclobutenones rearrangement[8] with the discovery that thermolysis of vinylcyclobutenone **34** did not follow the classic course depicted in Scheme 2, but instead proceeds *via* a carbonyl-ene reaction (Scheme 8). Thus when a THF solution of **34** was subjected to microwave irradiation at 120 °C, it yielded spirocycle **36**, after oxidation of the crude product mixture with the Dess-Martin periodinane reagent.[17]

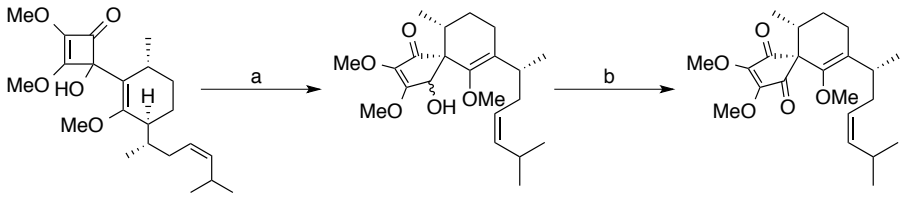

34 (d.r. ~ 3:2) **35** **36**

a) THF, 120 °C, μwave, 30 min; b) Dess-Martin periodinane, DCM, 0 °C, 30 min, 73% over 2 steps.

Scheme 8: Formation of spirocycles from thermolysis of vinylcyclobutenones.

To gain a better understanding of the rearrangement and the factors that influence this pathway, vinylcyclobutenone **37** was thermolysed in the aforementioned reaction conditions and gave a single diastereoisomer of spirocycle **41** in 72% yield. This suggested that the rearrangement proceeds *via* electrocyclic ring opening to ketene **38**, which induces a carbonyl-ene reaction to spirocycle **39**, and tautomerisation to **40**. Oxidation of the crude product mixture then gives cyclopentendione **41** (Scheme 9).

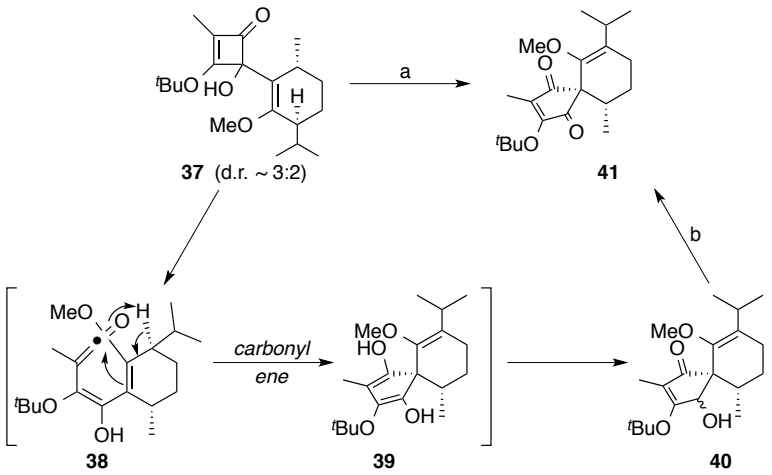

a) THF, 120 °C, μwave, 30 min; b) Dess-Martin periodinane, DCM, 0 °C, 30 min, 72% over 2 steps.

Scheme 9: Thermal rearrangement of cyclobutenone **37** to spirocycle **41**.

Though the rearrangement of vinylcyclobutenones generally give access to hydroquinones, Harrowven *et al.* have shown that the incorporation of a leaving group on the vinyl appendage can induce a domino reaction giving direct access to quinones thereby circumventing the need for an oxidation step.[8] Thermolysis of phenyl vinyl ether **42a** and vinyl sulfide **42b** by microwave irradiation at 120 °C in THF induced electrocyclic ring opening to **43**, which was followed by electrocyclisation to **44** and elimination of PhXH to give quinones **45a** and **45b** (Scheme 10). The successful progress of the transformation **42→45** shows that the course of reactions involving enol ethers is dictated by electronic factors rather than steric effects.

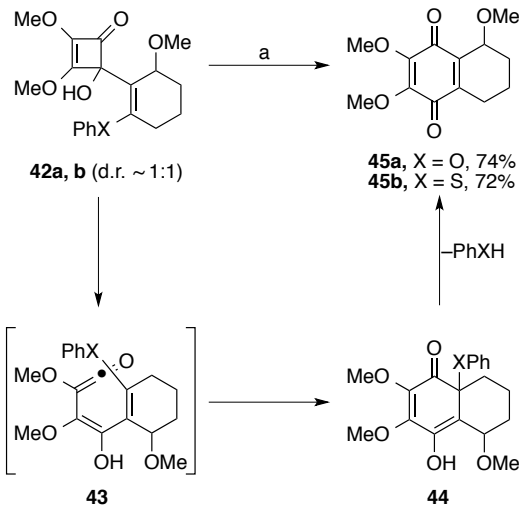

Scheme 10: Direct synthesis of quinones by thermolysis of vinylcyclobutenone **42**.

1.2 Rearrangement of Heteroaromatic Cyclobutenones

The rearrangement has been extended to heteroarylcyclobutenone derivatives, largely through the efforts of the Moore[6] and Liebeskind[9] groups. Thiophenes (**46**→**47**), furans (**48**→**49**), and pyrroles (**50**→**51**) all give the reaction (Scheme 11) in high yields.

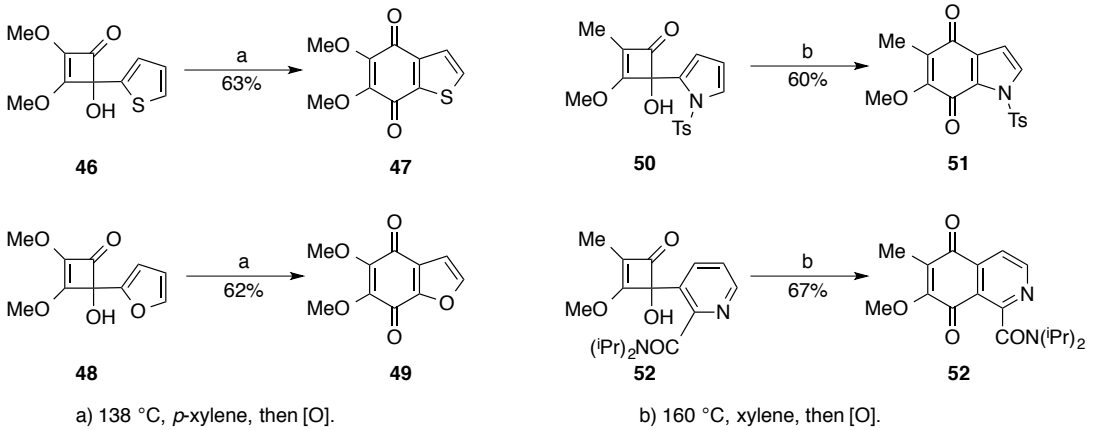

Scheme 11: Synthesis of heteroaromatic quinones.

The methodology was further expanded by Liebeskind and co-workers to include pyridines (**52**→**53**) and related azaheteroaromatic ring systems. Thermolysis of 4-(2-pyridyl)cyclobutenones **55** provided quinolizin-4-one **57** in 86%.[4] Notably, in this case the ketene intermediate **56A** underwent cyclisation to the electron-rich nitrogen atom rather than the C-3 carbon of the heterocycle (Scheme 12).

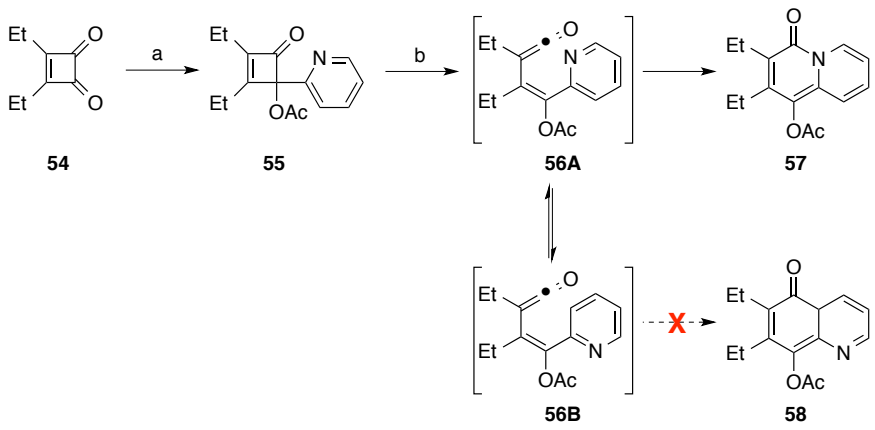

a) 2-bromopyridine, ^{n}BuLi, –78 °C, THF, 25 min, then Ac_2O, –78 °C, 1.5 h, 40%; b) PhMe, 100 °C, 4 h, 86%.

Scheme 12: Synthesis of quinolizinone **57**.

The method proved general enough to be applied to other azaheterocycles.[4] In each case cyclisation occurred towards the proximal nitrogen atom with imidazoles (*e.g.* **59→60**), thiazoles (*e.g.* **61→62**), and benzothiazoles (*e.g.* **63→64**). Notably, cyclisation could be achieved at lower temperatures than was needed for the corresponding arylcyclobutenones (Scheme 13).

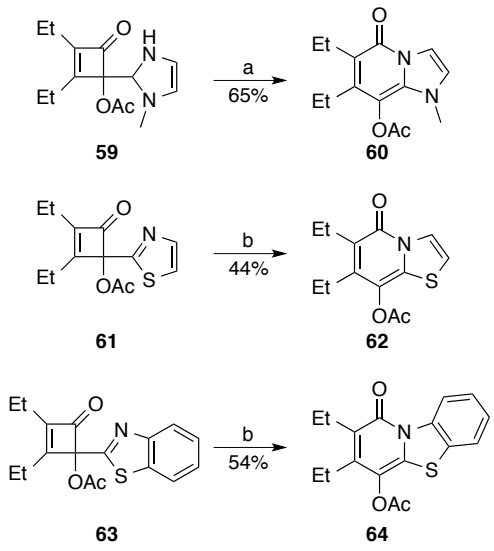

a) DCE, 85 °C, 4 h; b) 1,4-dioxane, 90 °C, 4 h.

Scheme 13: Access into heterocyclic ring-fused pyridones.

Liebeskind *et al.* also developed a complementary strategy to achieve cyclisation to the adjacent carbon atom.[5] To that end, they employed *N*-BOC protection and the corresponding dihydroheterocycles. Notably, *N*-BOC-protected 1,4-dihydropyridine **65** is

readily lithiated at C-2 with ^{s}BuLi in THF at –42 °C. Addition of the resulting organolithium to 3,4-diisopropoxy-3-cyclobutene-1,2-dione **66** then gave 1,2-adduct **67**. To achieve rearrangement to **69**, the crude adduct had to be heated between 160–165 °C for 45 min in an oxygen-free atmosphere. During thermolysis, displacement of the *tert*-butoxy residue from the BOC group occurred leading to the formation of an oxazolone ring **68**. Oxidative aromatisation of **69** was successfully achieved using two equivalents of *o*-chloranil in acetic acid[18] to provide the substituted quinolone quinones in good overall yield (Scheme 14).

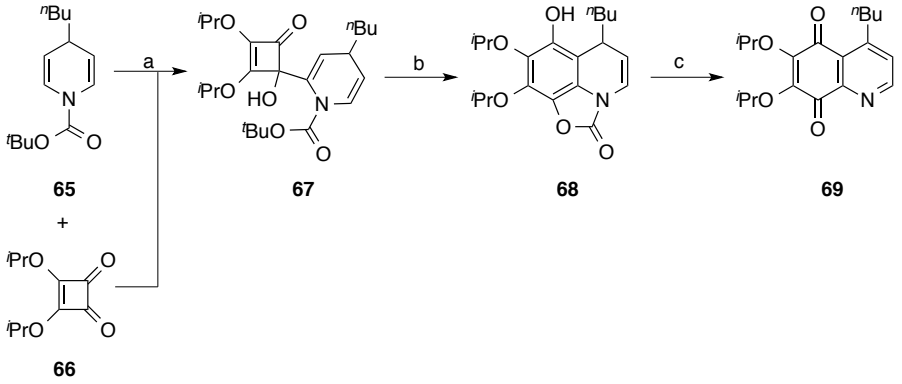

a) **65**, ^{s}BuLi, –78 °C→–42 °C, THF, 3 h, then, **66**, –78 °C, THF, 2 h; b) 160–165 °C, neat, 45 min, 65% over two steps; c) AcOH, *o*-chloranil, RT, 5 h, 93%.

Scheme 14: Synthesis of quinoline quinones using dihydroquinolines.

Thermal expansion of 4-alkyl-4-hydroxycyclobutenones bearing a heteroatom in the alkyl chain can also result in capture of the ketene by the heteroatom.[19] For example, thermolysis of the 1,3-dithianyl adduct **70** in refluxing *p*-xylene gave spirobutenolide **76** in excellent yield. The mechanism postulated for the transformation involves nucleophilic capture of the ketene **71** leading to the zwitterion **72**. It collapses to thiolactone **73** and induces a transannular ring closure to zwitterion **74**. Heterolytic cleavage to ketene **75** is followed by cyclisation to the observed product **76** (Scheme 15).

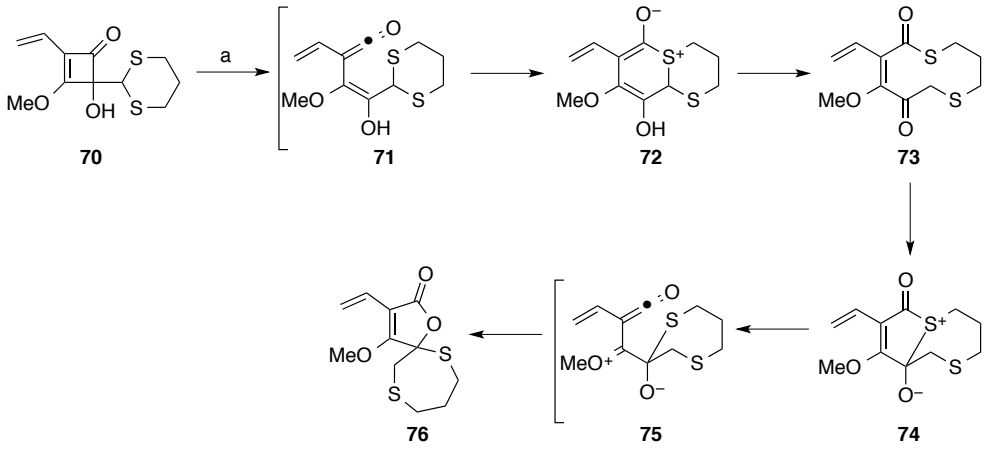

a) *p*-xylene, 138 °C, 3 h, 90%.

Scheme 15: Synthesis of spirobutenolides **76** from dithiacycloalkyl-cyclobutenones **70**.

The scope of the above study was expanded to include 4-oxiranylcyclobutenones such as **78**.[19] Cyclobutenone **78** was readily prepared by the addition of 1-lithio-2-phenyloxirane[20] **77** to dimethyl squarate **16** in THF at –78 °C in the presence of TMEDA and with a subsequent quench with TMSCl. In analogy to the mechanism discussed above the first formed ε-lactone **79** rearranges to the observed 5*H*-furanone product **82** in 90% yield *via* zwitterionic intermediate **81** (Scheme 16).

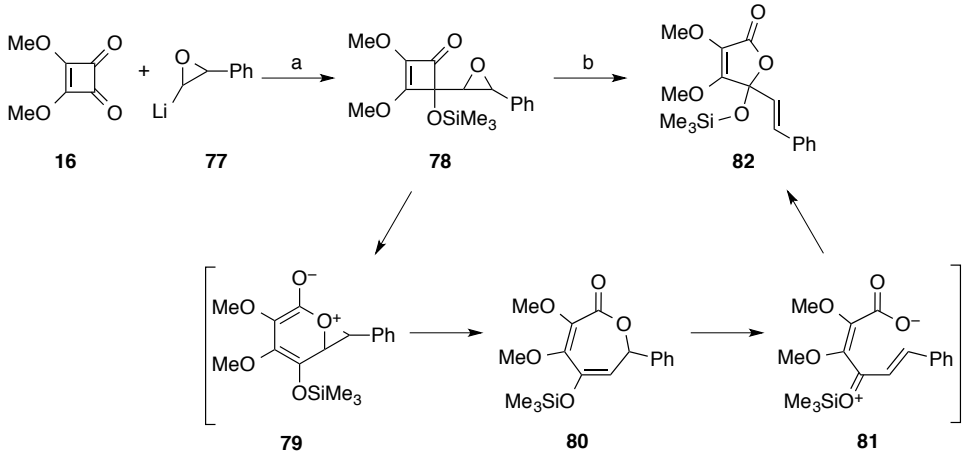

a) –100 °C, 30 min, TMSCl, –100 °C→RT, 32%; b) *p*-xylene, 138 °C, 5 h, 90%.

Scheme 16: Rearrangement of 4-oxiranylcyclobutenones **78**.

1.3 Rearrangements of 4-Alkynylcyclobutenones

Thermal rearrangements of 4-alkynyl-4-hydrocyclobutenones **83** were first reported by Moore *et al.* in 1985, who found that they readily transformed into quinones **87** or

cyclopentenediones **88** on themolysis.[1,21-25] Their initial postulate that the reaction proceeded *via* zwitterionic intermediates **85B** and **86B** was soon revised when computational studies and trapping experiments provided strong evidence to support the involvement of diradical intermediates **85A** and **86A**. Notably, reactions led to *O*- to *C*-migration of the group (E) attached to the C-4 oxygen when it was a proton, silyl[23] or allyl[1,26] group. Moreover, the course of the rearrangement appeared to be governed by the alkynyl substituent R^3.[23] When this was capable of stabilising an α-anion or radical intermediate, cyclopentendione formation predominated. By contrast when the R^3-substituent was an alkyl residue, quinone formation was observed (Scheme 17).

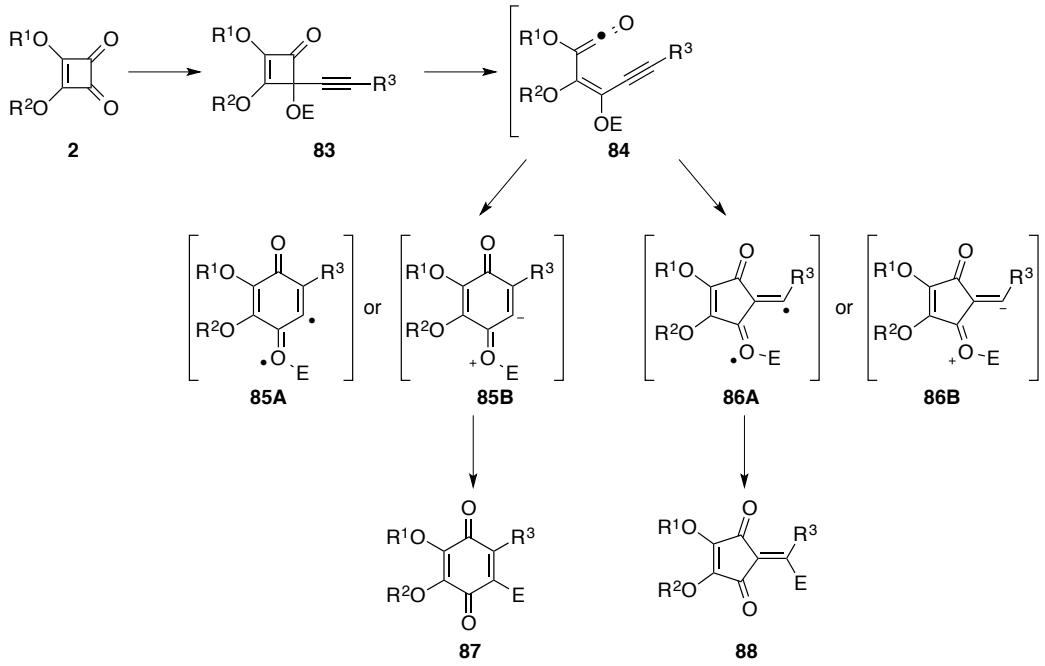

Scheme 17: Rearrangement of 4-alkynyl-4-hydrocyclobutenones **83**.

The scope of the reaction was demonstrated by the ease with which an array of 4-alkynyl-2,3-dimethoxy-4-(trimethylsiloxy or hydroxy)cyclobutenones **89a-h** were transformed into quinones. The precursors were readily synthesised from dimethyl squarate **16** by treatment with the corresponding lithium acetylide and quenching with trimethylsilyl chloride or ammonium chloride respectively. Thermolysis in *p*-xylene at 138 °C gave the 1,4-quinones **90a-h** in moderate to good yields (Scheme 18).[23]

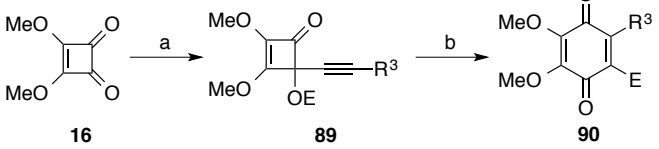

a) i) $R^3C{\equiv}CLi$, THF, –78 °C, then $ClSi(CH_3)_3$ or NH_4Cl, –78 °C→RT, 50–90%; b) *p*-xylene, 138 °C, 55–80%.

89	R^3 =	E =	Yield 90 (%)
a	H	H	48
b	H	$Si(CH_3)_3$	75
c	$^nC_4H_9$	H	78
d	$^nC_4H_9$	$Si(CH_3)_3$	75
e	CH_2OTHP	H	47
f	CH_2OTHP	$Si(CH_3)_3$	41
g	$CH_2C_6H_5$	H	71
h	$CH_2C_6H_5$	$Si(CH_3)_3$	74

Scheme 18: Synthesis of benzoquinones **90** from 4-alkynylcyclobutenones **89**.

In the above examples, the alkyne moiety bore an alkyl, proton, or benzyl residue. However, when the R^3-substituent was an alkoxy, phenyl or trimethylsilyl group **89i-m**, mixtures of quinones **90** and cyclopentenediones **91** are formed (Scheme 19).

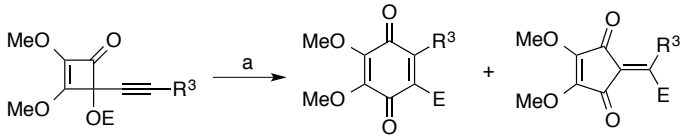

a) *p*-xylenes, 138 °C.

89	R^3 =	E =		Yield 90 (%)	Yield 91 (%)
i	C_6H_5	H		21	46
j	C_6H_5	$Si(CH_3)_3$		52	13
k	OC_2H_5	H		25	50
l	OC_2H_5	$Si(CH_3)_3$		23	55
m	$Si(CH_3)_3$	H		41	5

Scheme 19: Rearrangement of 4-alkynylcyclobutenones **89**.

Moore observed the exclusive formation of cyclopenetenediones when the alkynyl substituent – R^3 was an ester **89n,o** and alkene group **89p** (Scheme 20). They presumed that this led to stabilisation of the adjacent vinyl radical intermediate and favoured diradical intermediate **86A** over **85A** (Scheme 17).[23]

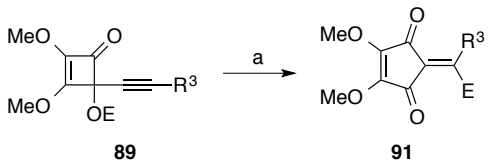

89	R^3 =	E =	Yield 91 (%)
n	$CO_2C_2H_5$	H	66
o	$CO_2C_2H_5$	$Si(CH_3)_3$	33
p	$CH{=}CHOCH_3$	H	49

a) *p*-xylenes, 138 °C.

Scheme 20: Synthesis of cyclopenetenediones **91** from 4-alkynylcyclobutenones **89**.

To establish whether *O*- to *C*-migration of the substituent E was an intramolecular process,[23] Moore *et al.* took equimolar amounts of silyl ether **89h** and its deuterated

analogue d-**89h** and subjected them to thermolysis at 138 °C in refluxing *p*-xylene. No crossover products were observed in the resulting product mixture, with the rate of formation of **90h** and d-**90h** being nearly equivalent by ^{1}H NMR analysis. Moore thus concluded that the diradical **85A** or zwitterionic intermediate **85B** (Scheme 17) induces intramolecular migration of the trimethylsilyl group to give the corresponding quinones **90h** and d-**90h** (Scheme 21).

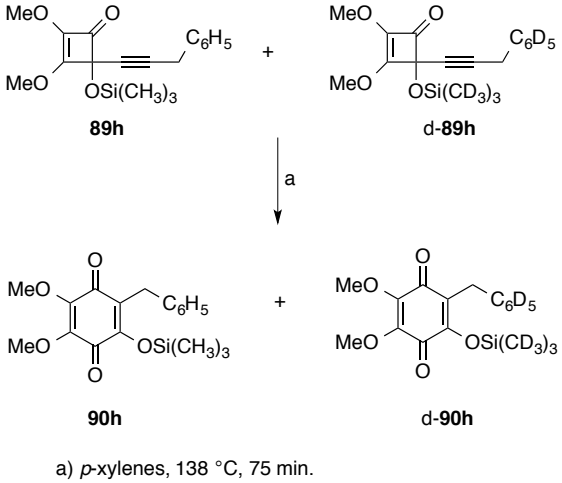

Scheme 21: Thermolysis of **89h** and its deuterated analogue d-**89h**.

Moore and co-workers had earlier shown that allyl group migration from *O*- to *C*- is a facile process. They suggested that this occurred *via* a zwitterionic intermediate **94**. The starting material **92** was prepared from dimethyl squarate **16** by sequential alkynyllithium addition followed by allylation of the resulting alcohol to yield **92**. Thermolysis for 1 h in *p*-xylene gave quinone **95** in 76% yield. (Scheme 22).[1]

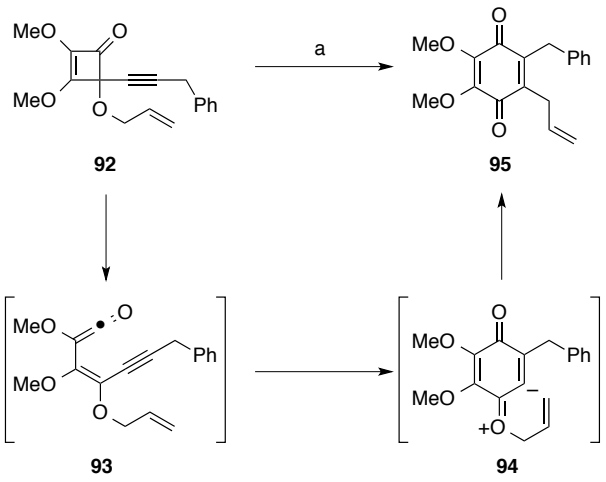

a) *p*-xylenes, 138 °C, 1 h, 76%.

Scheme 22: Allyl group migration *via* zwitterionic intermediate **94**.

Subsequently, Moore *et al.* reported further examples of the rearrangement. Thermolyses of **96a-c** each gave the corresponding quinones **98a-c** in good yields. On this occasion it was suggested that allyl group migration occurred *via* the diradical intermediate **97** leading to allyl-substituted quinones **98a-c** (Scheme 23).[23]

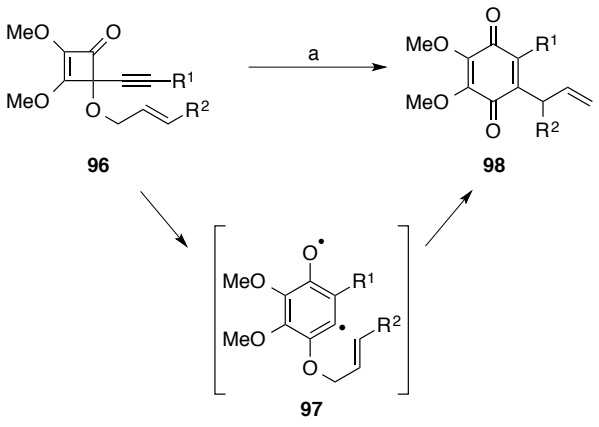

96	R^1 =	R^2 =	Yield 98 (%)
a	$CO_2C_2H_5$	H	66
b	$CO_2C_2H_5$	$Si(CH_3)_3$	33
c	$CH{=}CHOCH_3$	H	49

a) *p*-xylenes, 138 °C.

Scheme 23: Allyl group migration to give **98a-c**.

In a related study, thermolyses of cyclobutenones **99** were found to be concentration dependent.[27] Rearrangement of **99a** in refluxing toluene at high dilution (3.86 x 10^{-3} M) gave the annulated quinone **104a** as the major product along with quinone **102a** in a 23:1 ratio (deduced by ^{1}H NMR) and an overall yield of 84%. In contrast, thermolysis at higher concentration (1.2 M) gave quinone **102a** as the major product in a 7:1 ratio with **104a** (deduced by ^{1}H NMR) and an overall yield of 70% (Scheme 24). A similar observation was

made with diyne **99b**, which gave only **104b** at low concentrations and a 1:1 mixture of **104b** and **102b** at high concentration (1.0 M). Moore reasoned that the formation of **104** arose from 5-*exo*-dig cyclisation of the aryl radical intermediate **101** to the proximal alkyne moiety giving **103**. H-atom abstraction from the proximal hydroxy group then gives quinone **104**. The rearrangement of **99** to **102** follows the same course except that the diradical intermediate **101** favours H-atom abstraction from the proximal phenol over cyclisation (Scheme 24).

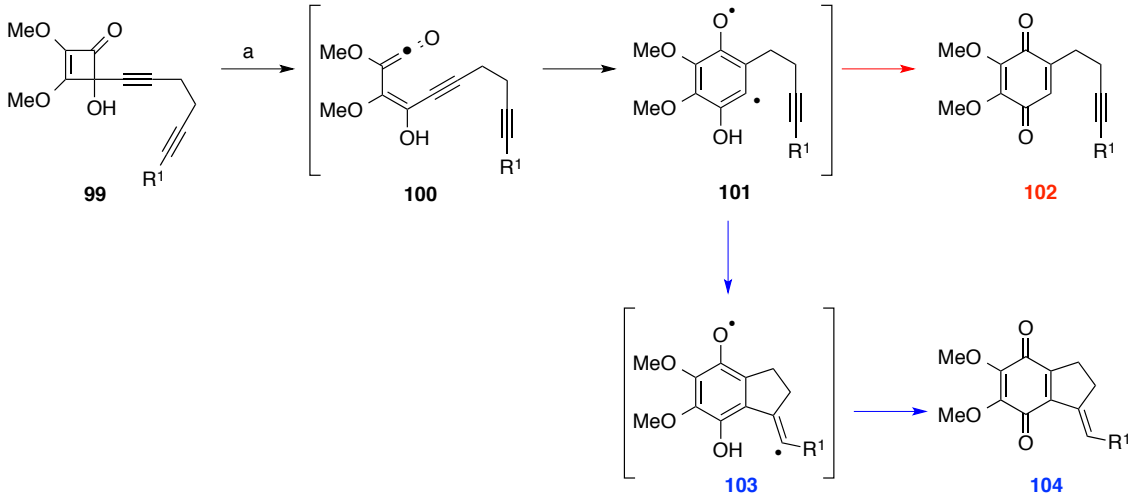

a) PhMe, 110 °C, 2 h.

99	R¹ =	Conc^{n} (M)	Ratio 102:104	Overall Yield (%)
a	*n*-C_4H_9	3.86 x 10^{-3}	1:23	84
	n-C_4H_9	1.2	7:1	70
b	$(CH_2)_3CH{=}CH_2$	2.43 x 10^{-3}	0:1	57
	$(CH_2)_3CH{=}CH_2$	1.0	1:1	77

Scheme 24: Concentration dependent rearrangement of **99**.

Moore reasoned that the concentration dependence was due to the instability of the diradical intermediate **101**. When generated at a high concentration, he argued that the relatively stable ketenes might stack leading to high local concentrations of the reactive diradical intermediate **101**. This would promote intermolecular H-atom abstraction from the hydroxyl group of one partner by the aryl radical centre of another, leading directly to two molecules of the corresponding non-annulated quinone **102**. Under dilute condition, stacking of the ketene intermediate would be reduced so intramolecular reactions of the diradical intermediate would predominate, *i.e.* [**101**]→[**103**]→**104**.[2,27]

In a related study, thermolysis of the methyl protected analogues **105** in refluxing toluene led to the annulated spiroepoxycyclohexadienones **109** in excellent yield.[27] The rearrangement was explained by involving diradical intermediate **106** and previously

seen 5-*exo*-dig radical cyclisation to vinyl radical intermediate **107**. H-atom abstraction from the proximal methyl ether then gives **108**, a precursor to the spiroepoxides **109** (Scheme 25).

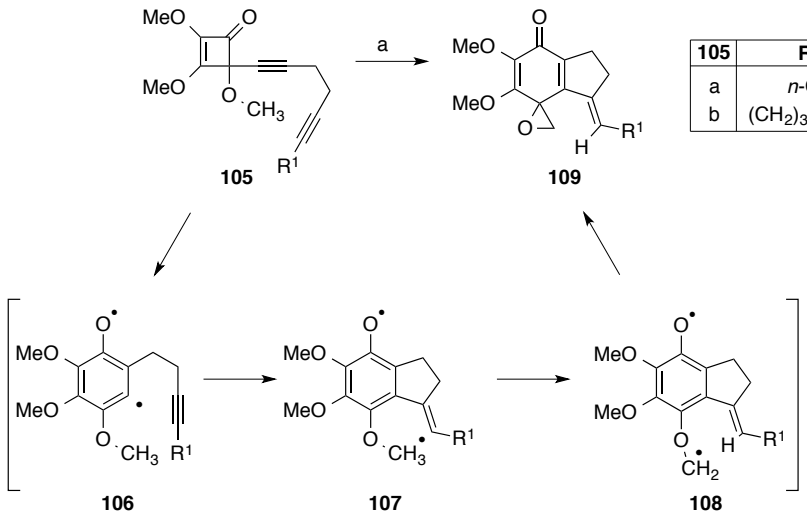

105	R^1 =	Yield 109 (%)
a	n-C_4H_9	87
b	$(CH_2)_3CH{=}CH_2$	70

a) PhMe, 110 °C, 2 h.

Scheme 25: Rearrangement of the methyl-protected diyne **105**.

Moore and co-worker were confident in their analysis due to previous work with the deuterated analogue d-**110**. In this case thermolysis gave spiroepoxide d-**113** in 37% yield. Here the aryl radical in **111** has the option of H-atom abstraction from the methyl group or D-atom abstraction from the methylene group of the ethoxy substituent leading to a stabilised radical centre **112**. The latter proved more facile (Scheme 26).

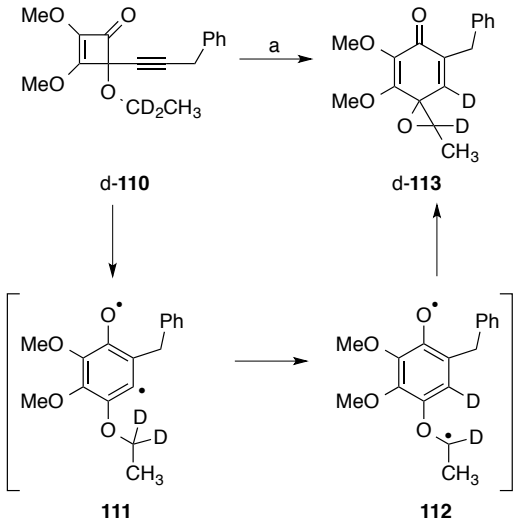

Scheme 26: Rearrangement of deuterated analogue **110** to give spiroepoxide d-**113**.

The efficiency of such annulation reactions depends on the length of the carbon chain separating the two alkyne groups in the starting 4-dialkynylcyclobutenones. If an additional methylene group is added, the reaction followed the same course as before when the hydroxyl group is unprotected, *e.g.* **114a** (Scheme 27), with the diradical intermediate **115a**, undergoing a 6-*exo*-dig cyclisation, followed by termination *via* 1,5-H transfer from the adjacent hydroxyl group to give the annulated quinone **119** in 63% yield. However, in this case hydroxyl group protection, as with analogue **114b** switches the course of the reaction (Scheme 27). H-atom abstraction from the propargylic carbon is now favoured over addition to the alkyne group leading to **116**. The newly formed diradical intermediate then undergoes radical-radical combination to give chromanol **117** in 76% yield. Moore suggested that the protecting group may hinder cyclisation on steric grounds or render the cyclisation **115b→118b** reversible by removing the facile H-atom abstraction pathway (**118→119**).[27]

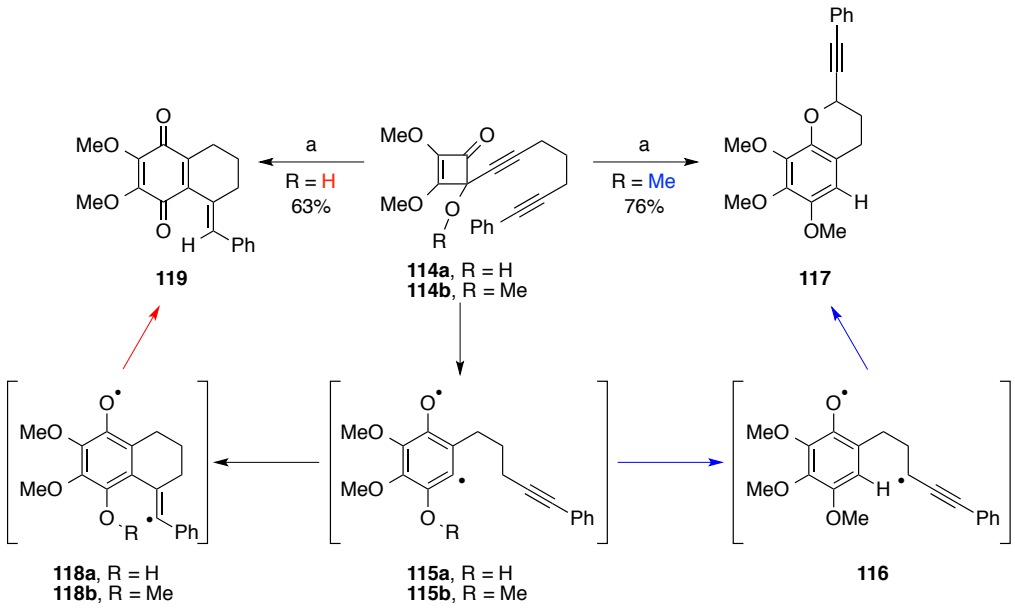

a) PhMe, 110 °C.

Scheme 27: Switch in the mechanism when hydroxyl group is protected.

Thermolysis of 4-chlorocyclobutenone **120** gives a similar result to that seen for the protected 4-hydroxylcyclobutenone **114b**. In this case, the aryl radical in **121** abstracts a hydrogen atom from the terminal methyl group to generate **122**. Ring closure then gives a 2:1 mixture of benzopyran **123** and spirocycle **124** (Scheme 28).

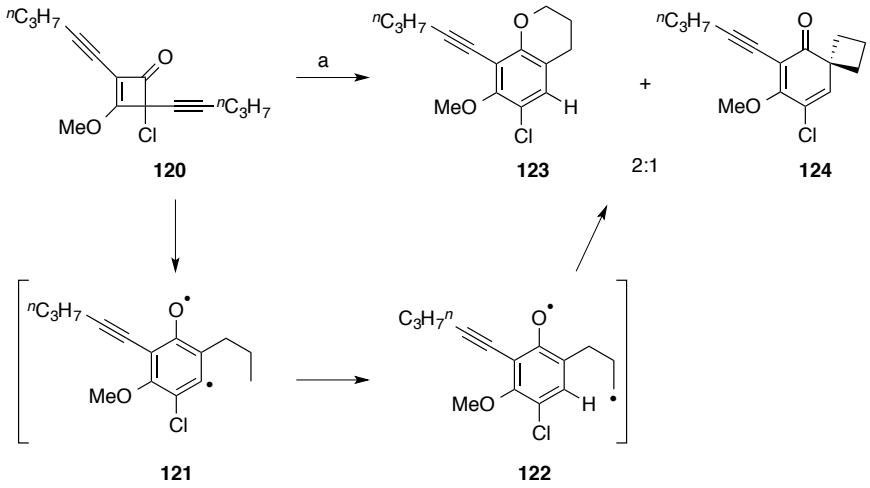

a) *p*-xylene, 138 °C, 52%.

Scheme 28: Thermolysis of 4-chlorocyclobutenone **120**.

When a hydroxyl group is functionalised as a propargyl ether, the system gives access to methylenebenzofurans[26] *via* addition of the aryl radical intermediate to the proximal

alkyne group (*viz* **126→127**). Thus, thermolysis of **125** in refluxing *p*-xylene leads to the diradical intermediate **126**. This undergoes a 5-*exo*-dig cyclisation to the vinyl radical intermediate **127**. Intramolecular H-atom abstraction then gives **128**, which collapses to alkene **129** following a second H-atom abstraction (Scheme 29).

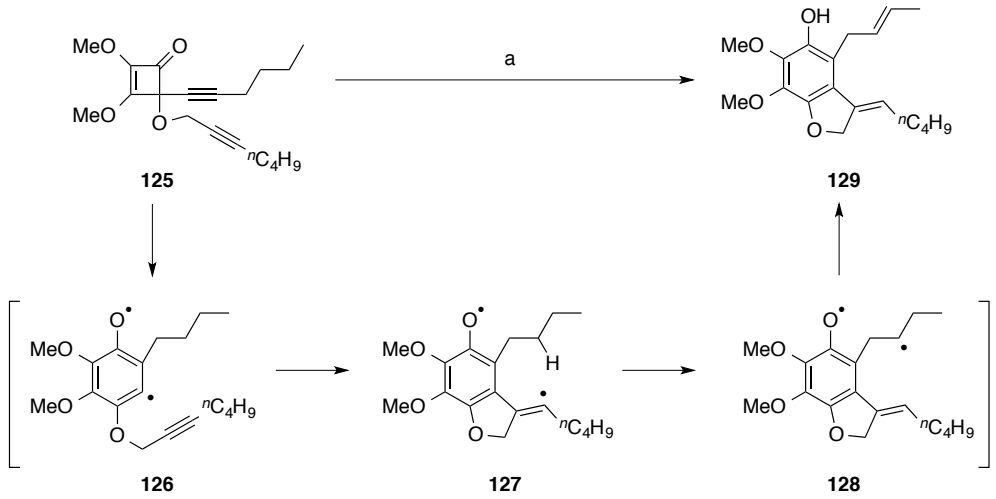

a) *p*-xylene, 138 °C, 30 min, 73%.

Scheme 29: Synthesis of methylbenzofuran **129** from thermolysis of **125**.

It should be noted that both of the proposed H-atom abstraction steps proceed *via* seven-membered transition states. This was confirmed by deuterium labelling studies[3] with the deuterated derivative of d-**125** giving the analogous product d-**129** where deuterium is incorporated on both alkenyl groups (Scheme 30).

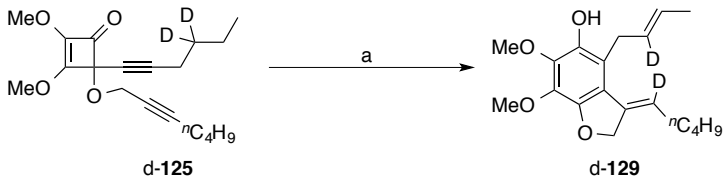

a) *p*-xylene, 138 °C, 30 min, 73%.

Scheme 30: Thermolysis of deuterium labelled **125** showing deuterium transfer**.**

The 4-alkynylcyclobutenone ring expansion methodology has also proved to be an attractive strategy for the construction of *N*-heterocyclic ring systems such as piperidinoquinones[24] and benzophenanthridines.[25,28] The piperidinoquinone skeleton is prevalent as a subunit in many naturally occurring *N*-heterocyclic quinones such as the cyanocycline and saframycin families.[29-34] Following the addition of the lithium salt of the diyne **130** to dimethyl squarate **16** in THF at –78 °C, the resulting 4-alkynyl-4-

hydroxycyclobutenones **131** was thermolysed directly in refluxing toluene to give piperidinoquinone **134** in 55% overall yield. In analogy to the discussion presented above, the transformation was envisaged to occur *via* the diradical intermediates **132** and **133**. The exocyclic double bond was assigned with (*E*)-stereochemistry due to the configuration of the diradical intermediate **133**. Though this is likely to be in configurational equilibrium, intramolecular H-atom abstraction from the proximal hydroxyl group can only provide a pathway to the (*E*)-isomer of **134** (Scheme 31).[24]

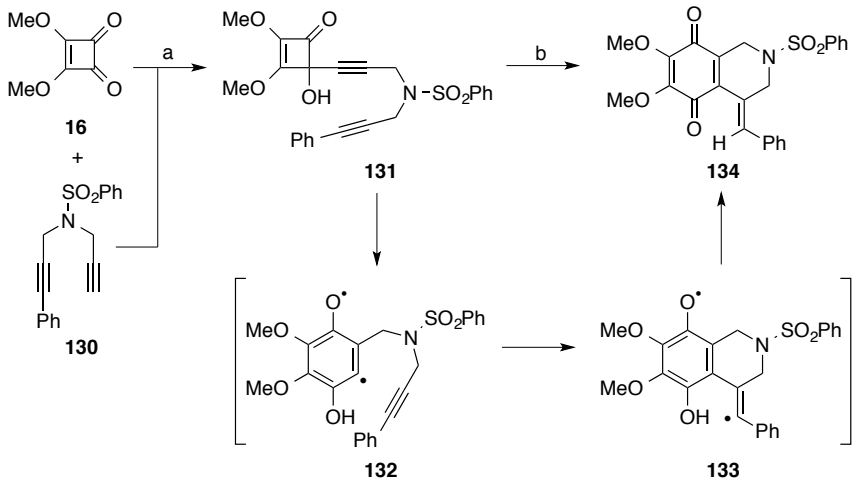

a)**130**, ^{n}BuLi, –78 °C, THF; b) PhMe, 110 °C, 1 h, 55% over 2 steps.

Scheme 31: Synthesis of piperidinoquinones **134**.

The above methodology was further extended by Wipf and Hopkins[28] to prepare the isoquinoline-3,5,8-trione ring system **139** (Scheme 32), which is found as a central core in several natural products. They were able to show sterically hindered amides such as **136** are able to participate in ring annulation if the conformation of the amide side chain is favourably disposed to interception by the diradical intermediate **137**. They suggest that the *s-cis* arrangement of the propargyl and alkene residue of the amide is necessary for isoquinoline formation. Otherwise the substrates led to decomposition as seen during the thermolysis of **140** (Scheme 33).

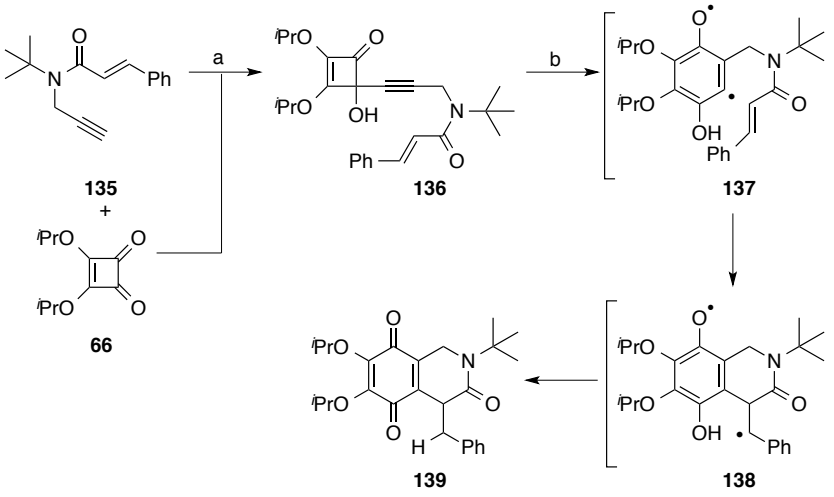

a) LHMDS, **66** , –78 °C, 2 h, THF, 69%; b) xylenes, 138 °C, 20 min, 62%.

Scheme 32: Synthesis of isoquinoline-3,5,8-trione ring system **139** by Wipf and Hopkins.

Cyclobutenone **140** does not undergo ring expansion to the isoquinoline trione skeleton (Scheme 33) because the most favoured amide rotamer in **140** has a *s-trans* arrangement for the *N*-propargyl and styryl substituent. This conformation keeps the aryl radical and styryl groups separated in **141** and hence prevent annulation to **139** (Scheme 32).

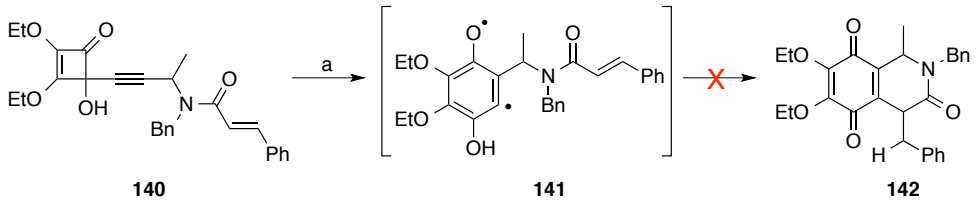

a) xylenes, 138 °C, 20 min, *decomposition.*

Scheme 33: Unfavoured conformation of **140** due to *s-trans* arrangement**.**

The rearrangement also provides a route to the benzophenanthridine ring systems found in many alkaloids.[35-37] Access is achieved *via* addition of the lithium salt of *N*-methyl-*N*-propargyl-1-naphthyl-amine[38] **143** to dimethyl squarate **16** in THF at –78 °C. Thermolysis of the resulting cyclobutenone **144** in refluxing chlorobenzene gave benzophenanthridine **145** in 68% yield (Scheme 34).

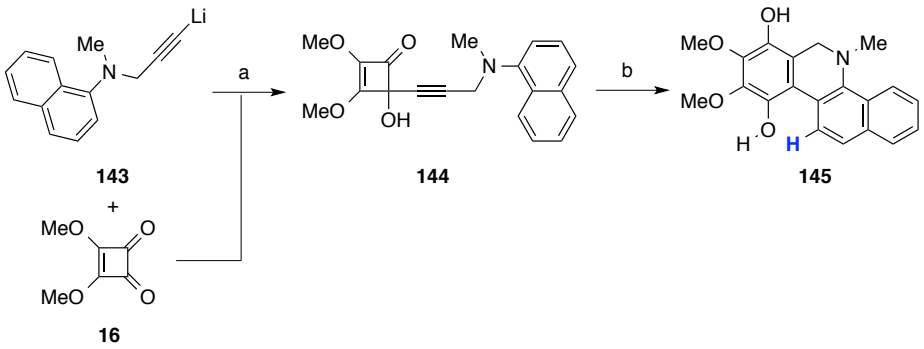

a) **16**, –78 °C, 55 min, THF, 87%; b) PhCl, 131 °C, 1.5 h, 68%.

Scheme 34: Synthesis of benzophenanthridines **145**.

To gain further insight on the course of the reaction, and to rule out products with similar spectral characteristics, the deuterated analogue[25] of **144** was prepared (d-**144**) and subjected to the thermal rearrangement in refluxing chlorobenzene for 1.5 h. Following an aqueous workup the product given was identified as **145** and showed no incorporation of deuterium. The result ruled out the formation of **148** by D-atom abstraction by the aryl radical in **147** and the formation of d-**150** due to its cyclisation to the proximal aromatic ring. Instead, the result provided evidence for the identity of the isolated product, where loss of a H-atom from intermediate **149** leads to the product **145** (Scheme 35).

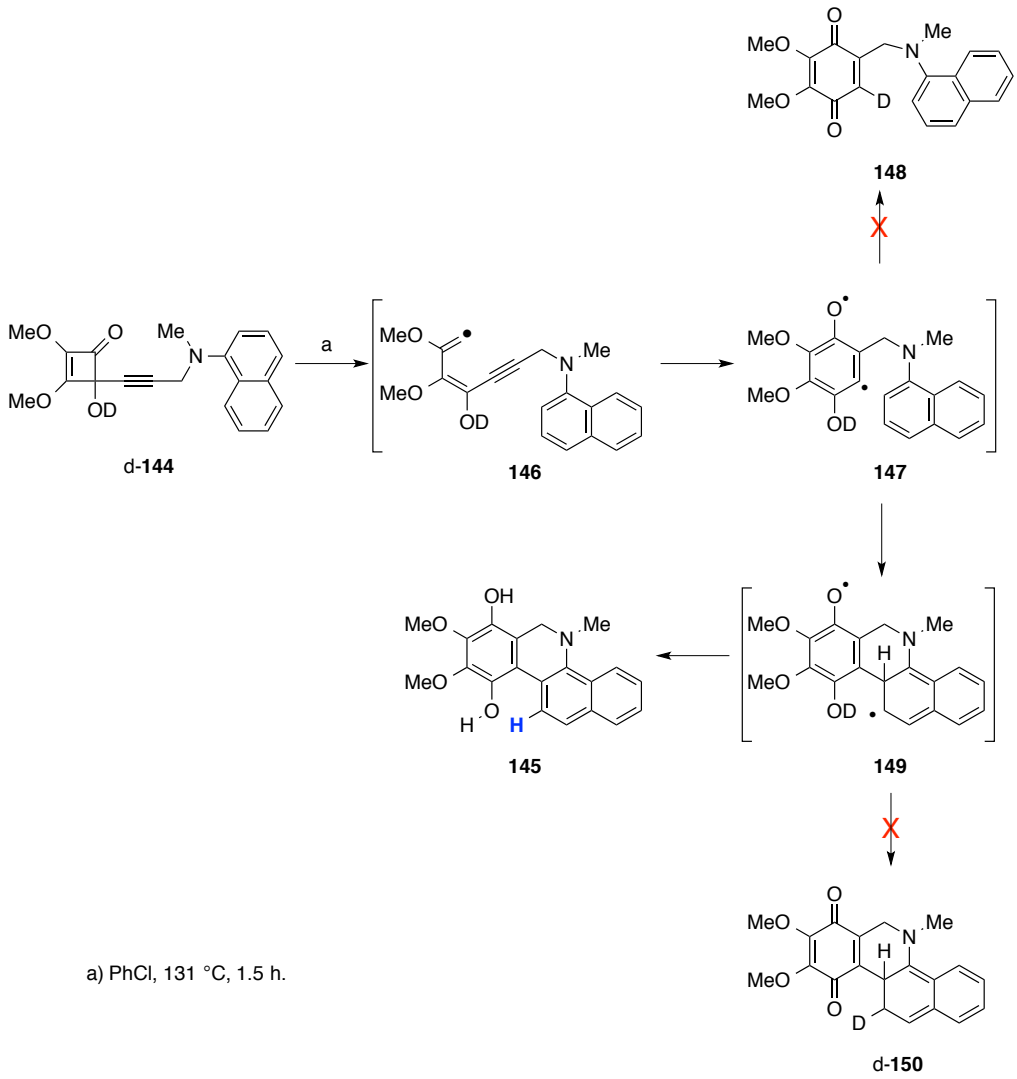

Scheme 35: Thermolysis of deuterated analogue **144** to confirm product formed.

An example involving radical cyclisation to a proximal ring system followed by H- or D-atom abstraction[39] by the newly formed radical centre was developed by Moore and co-workers during studies directed towards the synthesis of pyranoquinones **154** (Scheme 36). Specifically, thermolysis of the deuteroxy analogue **151** (85% enriched in deuterium) led to diradical intermediate **152**, promoting addition of the aryl radical centre to the proximal alkene. D-atom abstraction by the resulting alkyl radical **153** then gave pyranoquinone **154**. Notably, the latter proceeded in a stereospecific manner leading to *cis*-addition overall.

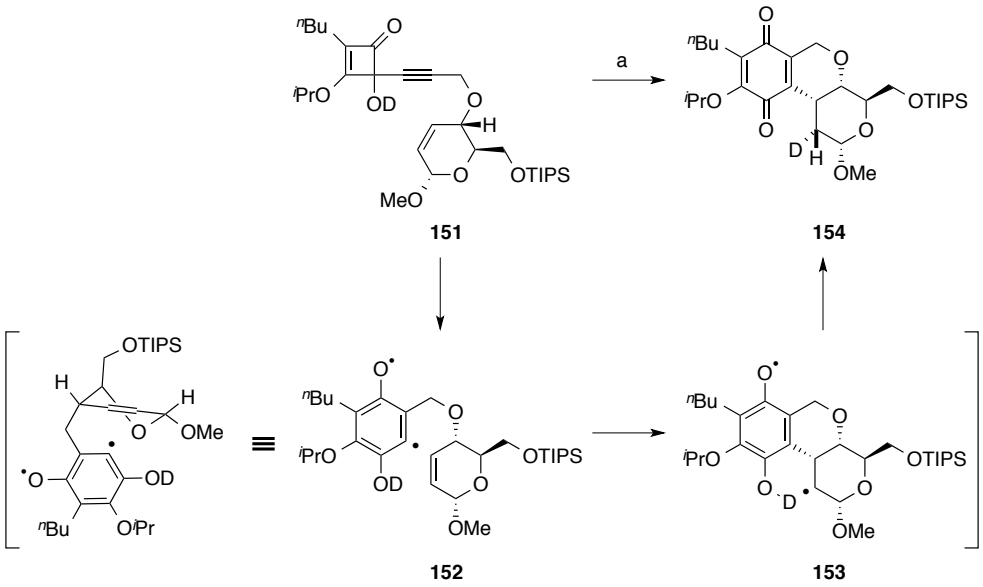

Scheme 36: Moore's synthesis of pyranoquinones **154**.

The examples presented above provide strong evidence for the involvement of a diradical intermediate **85A** in the rearrangement of 4-alkynyl-4-hydroxycyclobutenones **83** to quinones **87** (Scheme 17).[23] The structure of that diradical intermediate **85A** has been the subject of much speculation as it could also be viewed as the strained cyclic allene **85C**. Though cyclic allenes in rings sizes of less than nine members cannot attain their preferred linear geometry, the highly strained 1,2-cyclohexadiene **85C** is conceivable. Indeed, Moore *et al.* have suggested that it may be in equilibrium with the zwitterionic form **85B**. To date, experimental evidence for the existence of these species is lacking. Moreover, the diradical intermediate **85A** would be expected to be favoured over the allene form **85C** due to the lower strain energy and the gain in aromatic stabilisation (Scheme 37).

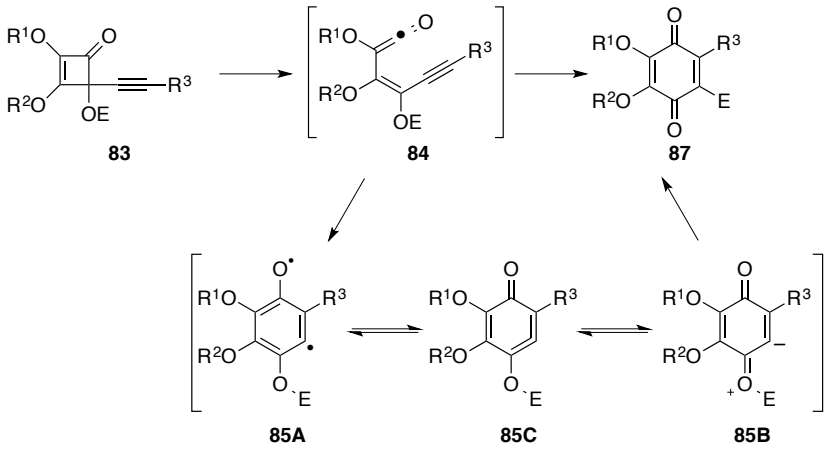

Scheme 37: Different possible forms for the diradical intermediate **85A**.

1.4 Synthesis of Natural Products and Related Compounds from Cyclobutenones

Many of the cyclobutenone rearrangements highlighted above have been used as key steps in the total synthesis of natural products. The first example reported was by Moore and co-workers[40] in the total synthesis of lonapalene **158**, a selective 5-lipoxygenase inhibitor for the treatment of psoriasis.[41] Their target **158** was efficiently synthesised in four steps from dimethyl squarate **16** and 4-bromochlorobenzene **155** (Scheme 38). Thus, following the addition of 1-chloro-4-lithiobenzene to dimethyl squarate **16** the resulting cyclobutenone **156** was subjected to thermolysis to furnish hydroquinone **157**. Acetylation of **157** with acetic anhydride then provided lonapalene **158** in 52% overall yield. Notably, the synthesis could be accomplished in "one pot" with no isolation of the intermediates.

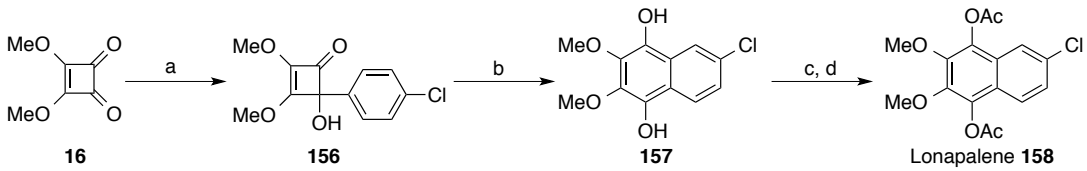

a) 4-bromochlorobenzene **155**, ^{n}BuLi, THF, –78 °C, 15 min; b) *p*-xylene, 138 °C, 3 h; c) H_2, Pd/C, *p*-xylene, RT, 3.5 h; d) Ac_2O, pyridine, DMAP, 10 h, 52% over 4 steps.

Scheme 38: Moore's total synthesis of lonapalene **158**.

A similar strategy was used in a synthesis of the furochromonone natural product khellinone **166**.[42,43] Khellinone was isolated from the fruits and seeds of *Amni visnaga L.*

Interest in such furochromone analogues results from their lipid-altering abilities, which may make them useful as anti-atherosclerotic agents.[44] The synthesis was completed in seven steps from diethyl squarate **159** and began with addition of lithiated trimethylsilyl acetylene. Hydrolysis of the adduct **160** with TFAA next provided cyclobutenone **161** in 97% yield. Addition of 2-lithiofuran to **161** then provided cyclobutenone **162**, which was thermolysed in refluxing toluene for 1 h to give hydroquionone **163**. To prevent aerial oxidation, this was not isolated. Rather, it was treated directly with methyl iodide, potassium carbonate and 18-crown-6 to give the protected hydroquinone **164** in 90% yield. Mercury(II) catalysed hydrolysis of the alkyne in **164** next installed the acetyl side chain (**165**), enabling the selective deprotection of the 6-ethoxy group with BF_3•Et_2O to khellinone **166** (Scheme 39).

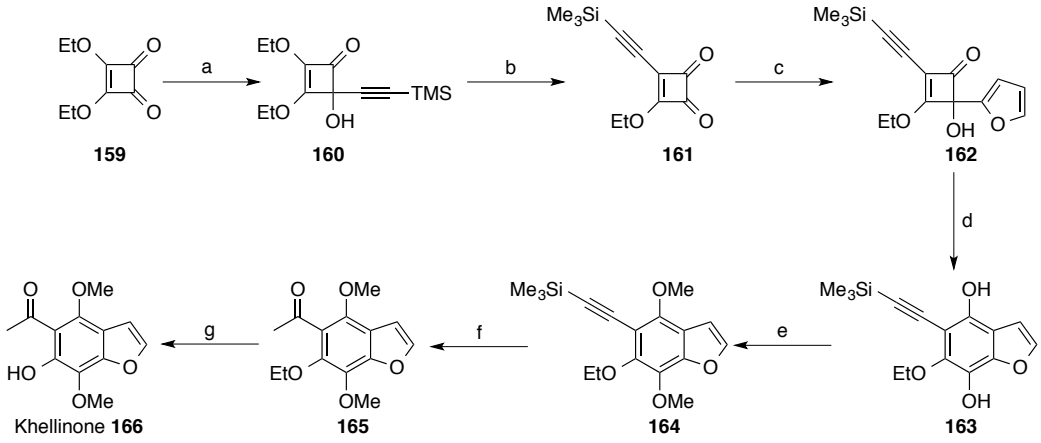

a) $Me_3SiC{\equiv}CLi$, THF, 78 °C, 88%; b) TFAA, pyridine, Et_2O, 0 °C, 91%; c) 2-lithiofuran, THF/Et_2O (1:1), –100 °C, 75%;
d) PhMe, 110 °C, 1 h; e) MeI, K_2CO_3, 18-crown-6, RT, 90% over 2 step; f) $HgSO_4$, H_2SO_4, THF, 99%; g) BF_3•Et_2O, DCM, RT, 97%.

Scheme 39: Route towards the total synthesis of khellinone **166**.

Intermediate **164** proved to be a valuable precursor as it also allowed syntheses of pimpinellin **167**, isophellopterin **168** and isopsoralenquinone **169** to be realised (Scheme 40).[42]

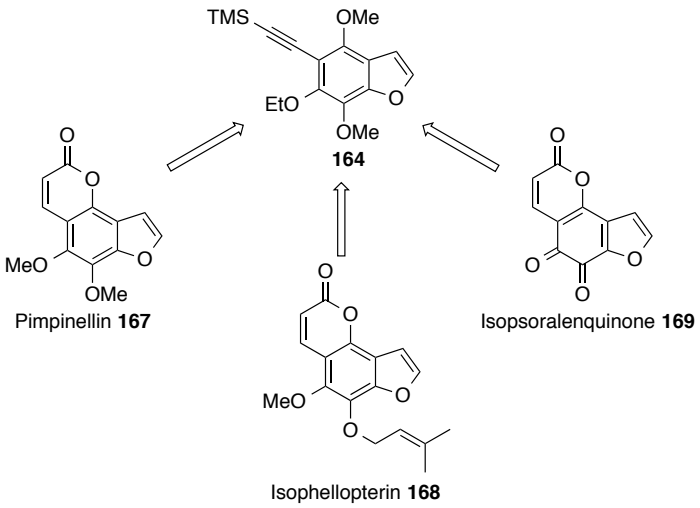

Scheme 40: Synthesis of other furocoumarins from intermediate **164**.

More recently, Trost and co-workers have used the arylcyclobutenone rearrangement to prepare natural products with a naphthoquinone core such as furaquinocin E **177**.[45] To achieve the correct regioselectivity they employed a protecting group strategy to reverse the natural chemoselectivity of organolithium additions to cyclobutenediones.[46] Thus, the more reactive C-2 carbonyl group in **172** was protected as the imine **173** in good yield. To this was added the organolithium derived from bromide **171**. Hydrolysis of the resulting imine **174** under mild acidic conditions then gave 4-arylcyclobutenone **175** in 50% yield. Thermal rearrangement of **175** followed by oxidation in air led to the desired naphthoquinone **176**. Deprotection of the silyl ethers with TBAF in THF provided furaquinocin E **177** (Scheme 41). This strategy allowed access to various analogues of furaquinocin E and syntheses of furaquinocin A and B.[45]

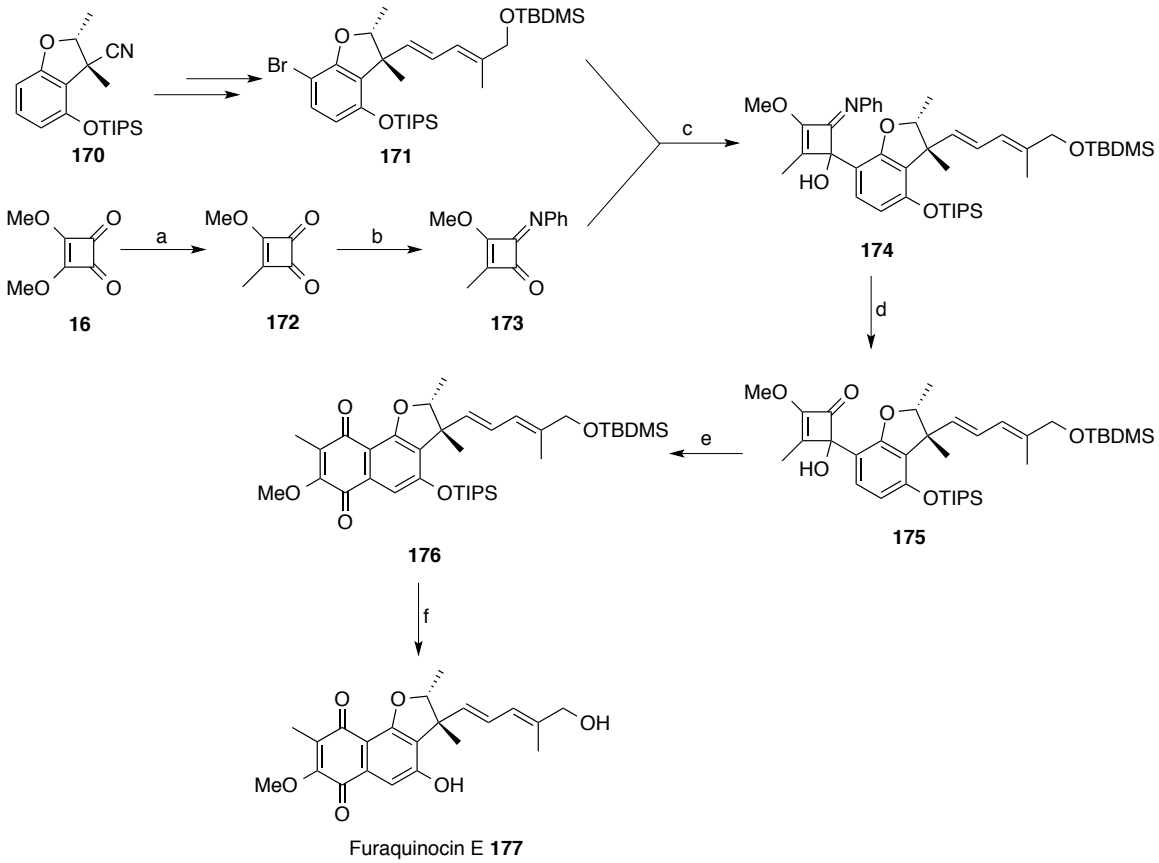

Furaquinocin E **177**

a) MeLi, THF, –100 °C, then TFAA, –78 °C; b) aniline, –78 °C→–15 °C, 53% over 2 steps; c) **171**, ^{n}BuLi, THF, –78 °C, then **173**, THF, –78 °C; d) oxalic acid, THF/H_2O, 50% over 2 steps; e) PhMe, 110 °C, then air, RT, 64%; f) TBAF, THF, 0 °C, 65%.

Scheme 41: Trost's regioselective synthesis of furaquinocin E **177**.

A growing number of naturally occurring naphthoquinones have hydroxyl or alkoxy groups in the 2,5-orientation. As seen from the synthesis above, access to the correct 4-arylcyclobutenone regioisomer can prove difficult. Moore and Lee provided an alternative means to address that problem during a synthesis of lomandrone **184** and aristolindiquinone. The idea was to combine the ring expansion methodology with a Hooker oxidation of the resulting hydroxynaphthoquinones, as the latter induces an oxidative rearrangement resulting in a regiochemical switch.[47] Their synthesis of lomandrone **184** began (Scheme 42) with 2-*tert*-butoxy-3-propylcyclobutenedione **178**, which was converted to cyclobutenone **180** by the addition of 1-lithio-2,3,4-trimethoxybenzene **179**. Addition occurred to the most reactive ketonic carbonyl rather then the vinylogous ester. Ordinarily these modes of addition would be unsuitable for the final product as it gives the wrong regioisomer. Indeed, thermolysis of **180** in refluxing toluene gave hydroxynaphthoquinone **182** in near quantitative yield after deprotection of the *tert*-butyl ether with TFA with the alkyl and hydroxy substituents reversed compared

to the target. However, application of the Hooker oxidation[48-53] ($KMnO_4/OH^-$) induced a regioisomeric switch to the homolog **183** in 81% yield. The total synthesis was completed by removing one methyl ether and installing another.

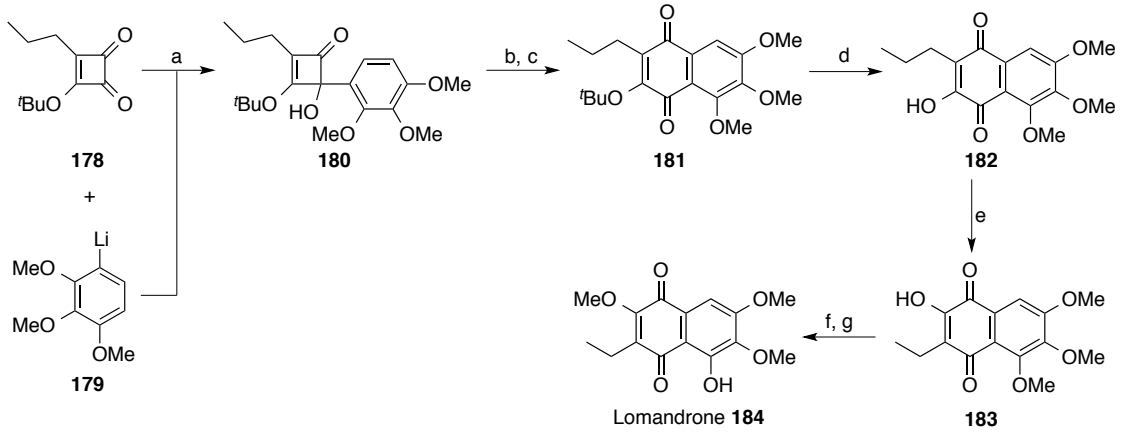

Scheme 42: Synthesis of lomandrone **184** using the Hooker oxidation.

More recently, Harrowven and co-workers have simplified access into the less reactive carbonyl of cyclobutenediones such as **185** by transmetalation of the organolithium salt with $Yb(OTf)_3$.[54] They were able to show that organoytterbium reagents add to the vinylogous ester (C-2 carbonyl) of **185** in stark contrast to the usual mode of addition displayed by organolithium and Grignard reagents. The change in selectivity was attributed to adverse steric interactions between the ytterbium ligands and the *tert*-butyl protecting group as depicted in **187A**, as well as the stronger interaction of the ytterbium-ate complex with the vinylogous ester carbonyl in its pre-reaction complex (**186**) with cyclobutenediones **185** (Scheme 43).

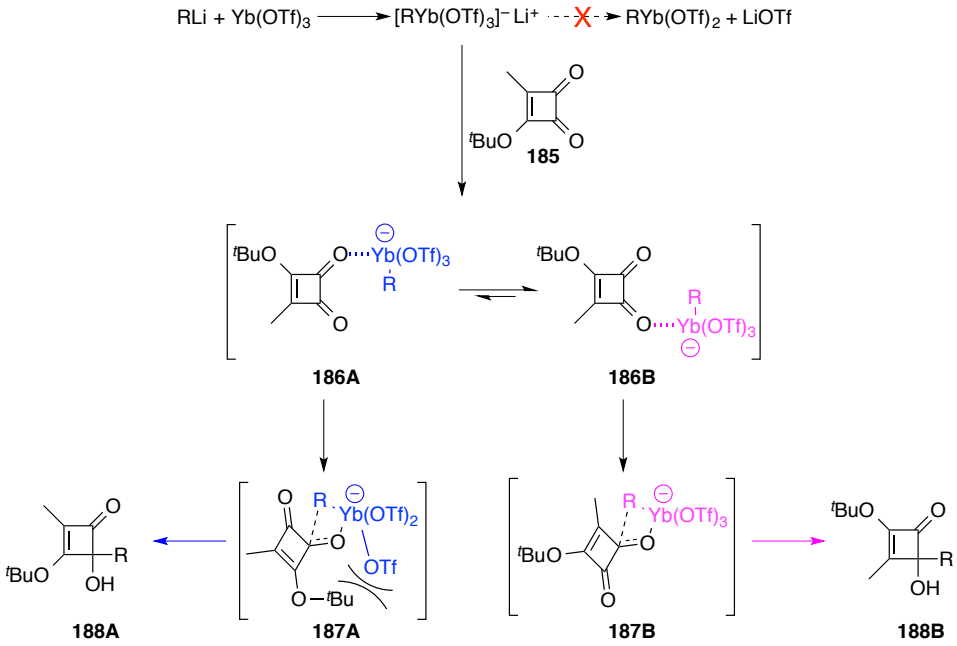

Scheme 43: Regiochemical course of organoyterrbium addition to cyclobutendione **185**.

The value of the method was demonstrated with the first total synthesis of (–)-mansonone B.[55,56] The synthesis began with commercially available (–)-menthone **189**, which was transformed into the corresponding vinyllithium using a Shapiro reaction.[57] Transmetallation with ytterbium triflate, followed by addition of the resulting vinylytterbium ate complex to cyclobutenedione **185** gave the corresponding C-2 adduct **192** in 94% yield with a *d.r.* ~ 7:3. Thermolysis of the mixture under continuous flow at 110 °C followed by aerial oxidation gave the quinone precursor **193** in 84% yield. Deprotection of the *tert*-butyl ether with BF_3•Et_2O gave the target, (–)-mansonone B **194** in excellent yield (Scheme 44).

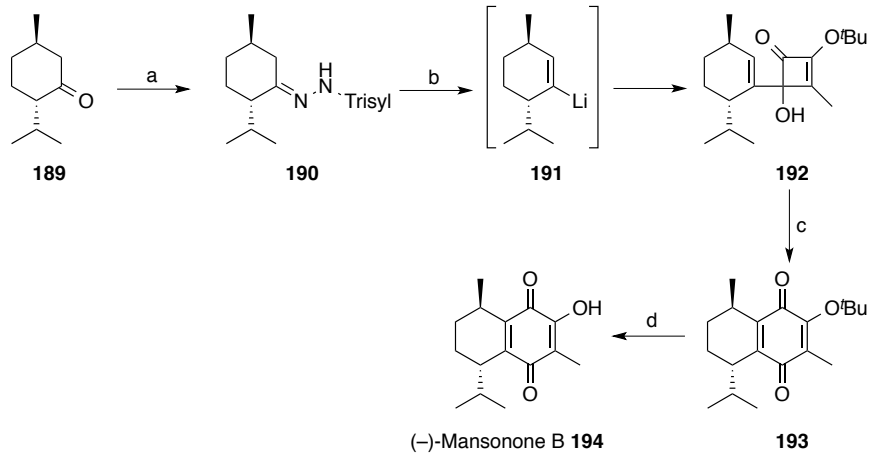

a) TrisylNHNH$_2$, DCM, 0 °C, 2 h, 76%; b) ^{n}BuLi, TMEDA/pentane, –78 °C→RT, 2 h, then Yb(OTF)$_3$, THF, –78 °C, **185**, 94% (*d.r.* ~ 7:3); c) 1,4-dioxane, 110 °C, 1 h, 84%; d) BF_3•Et_2O, DCM, 0 °C, 5 min, 82%.

Scheme 44: First total synthesis of (–)-mansonone B **194** by Harrowven *et al.*

Earlier, the rearrangement of vinylcyclobutenones was used by Harrowven *et al.* to complete the divergent synthesis of (–)-colombiasin A **201** and (–)-elisapterosin B **199** (Scheme 45). They envisaged access to both natural products from a common intermediate – vinylcyclobutene **197**, which was synthesised from (–)-dihydrocarvone **195** in eight steps. The union of (*E*)-dienone **196** and squarate **185** *via* a Shapiro reaction gave the desired vinylcyclobutene **197**. Thermolysis of **197** in THF at 110 °C under microwave irradiation, followed by aerial oxidation gave quinone **198** in 80% yield. Subsequently heating a toluene solution of **198** in the dark at 150 °C induced an intramolecular Diels–Alder cycloaddition to (–)-colombiasin A *tert*-butyl ether **200**. Deprotection with BF_3•OEt_2 gave (–)-colombiasin A **201** in good yield. Importantly, exposing quinone **198** to BF_3•OEt_2 induced both deprotection of the *tert*-butyl ether and an intramolecular [5+2] cycloaddition to give (–)-elisapterosin B **199** in 73% yield.

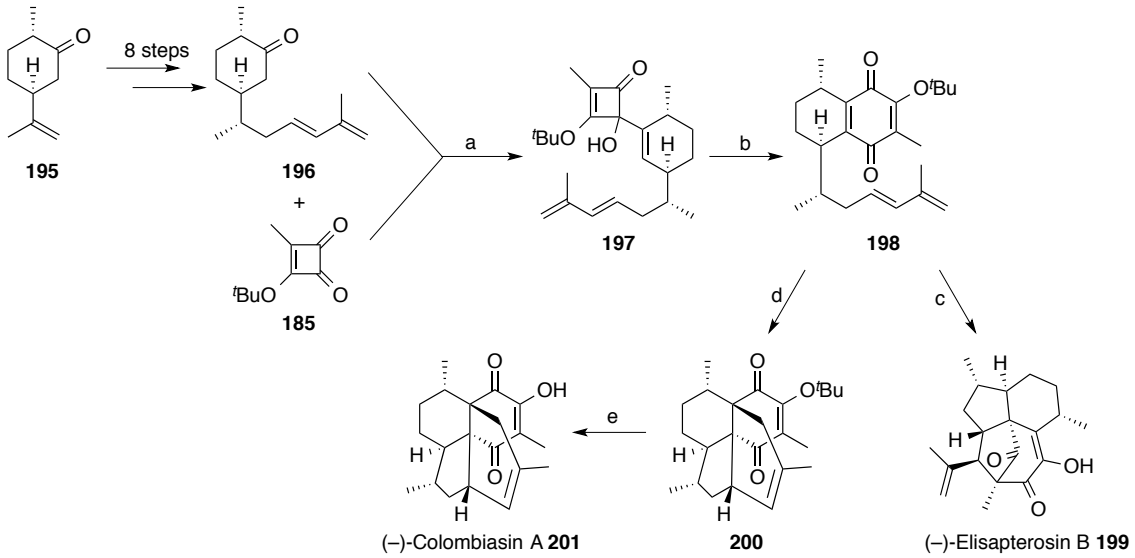

a) **196**, TrisylNHNH$_2$, THF, RT, 2 h, then –78 °C, ^{t}BuLi, 2 h, –78 °C→–20 °C, 20 min, then –78 °C, **185**, 36%; b) PhMe, 110 °C, 30 min, μwave, then air, RT, 80%; c) BF_3•Et_2O, DCM, –78 °C, 1 h, 71%; d) PhMe, 150 °C, 15 h, μwave, 61%; e) BF_3•Et_2O, DCM, 0 °C, 5 min, 78%.

Scheme 45: Divergent total synthesis of (–)-colombiasin A **201** and (–)-elisapterosin B **199**.

The rearrangement of 4-alkynylcyclobutenones to 1,4-benzoquinones has been widely utilised in total synthesis. Natural products prepared using this methodology include arnebifuranone **202**,[23] deoxyfrenolicin **203**,[23] (±)-terreic acid **204**,[58] (±)-perezone **205**[58] and (±)-isoperezone **206**[58] (Scheme 46).

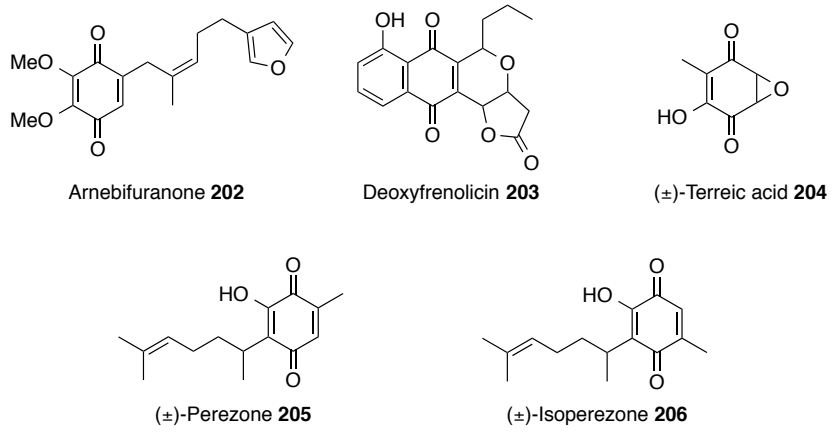

Scheme 46: Natural products that have been synthesised using 4-alkynylcyclobutenone methodology.

The synthesis of (±)-nanaomycin D **213**, a member of the naturally occurring isochroman-1,4-naphthoquinones, provides a good illustration of the methods value, as the target has antimycotics and antineoplastic activity. Following treatment of dione **207** with the

lithium salt of 3-(tetrahydropyranyloxy)propyne, the resulting alcohol **208** was alkylated with allyl iodide and Ag_2CO_3 to give **209** in quantitative yield. Its thermolysis next induced ring expansion to the diradical intermediate **210** and *O*- to *C*-allyl migration to benzoquinone **211** in 71% yield (Scheme 47). A short sequence of steps then gave access to (±)-nanaomycin D **213**.[59,60]

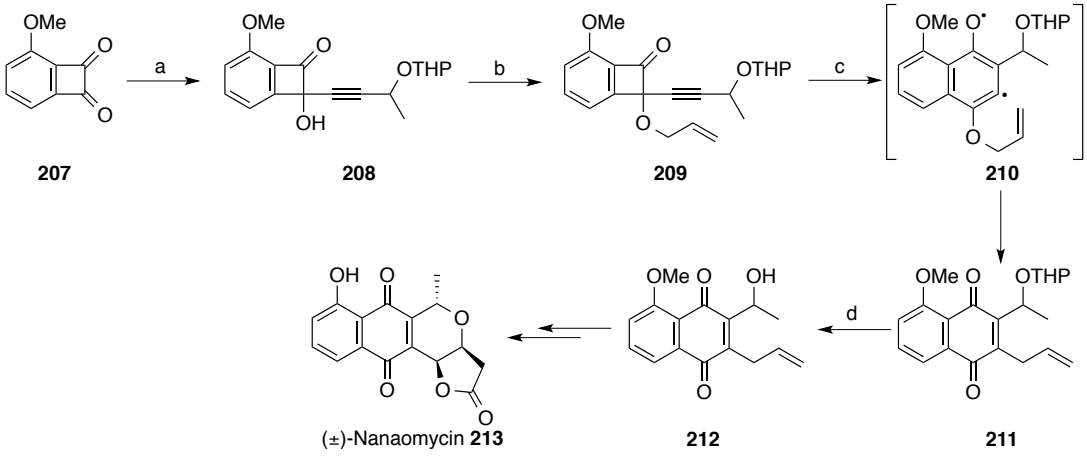

a) (Tetrahydropyranyloxy)propyne, ^{n}BuLi, THF, –78 °C, 58% (2:1); b) allyl iodide, Ag_2CO_3, 99%; c) *p*-xylene, 138 °C, 71%; d) AcOH:THF: H_2O (4:2:1), 72%.

Scheme 47: Synthesis of (±)-nanaomycin D **213**.

A further illustration of the methods power is provided by the efficient syntheses of the natural sesquiterpene quinones (±)-*O*-methylperezone **218** and (±)-*O*-methylisoperezone **219**. The synthesis of these natural products was achieved from a common intermediate **215** that was readily accessible from dimethyl squarate **16**. Adding 2-lithiopropene or 1-lithiopropyne to **215** gave access to cyclobutenones **216** (72% yield) and **217** (81% yield) respectively. Thermolysis of each gave the targets **218** and **219** in high yields. It is worth noting that the use of 4-alkenyl-4-hydroxycyclobutenones such as **216** requires subsequent oxidation to access quinones, while 4-alkynyl-4-hydroxycyclobutenones such as **217** give these directly (Scheme 48).

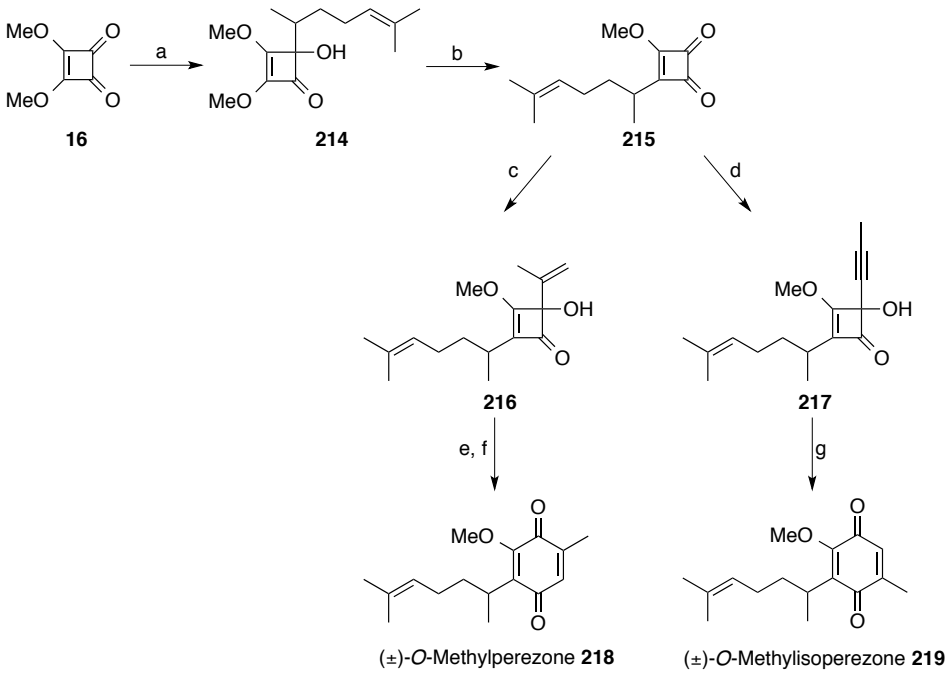

a) $CH_3CHLi(CH_2)_2CH{=}C(CH_3)_2$, hexanes, –78 °C, 20 min, 68%; b) TFAA, pyridine, Et_2O, 0 °C, 25 min, 73%; c) 2-bromopropene, ^{t}BuLi, Et_2O/THF, –78 °C, 20 min 72%; d) propyne, ^{n}BuLi, THF, –78 °C, 40 min, 81%; e) benzene, 80 °C, 2 h; f) 20% Ce^{IV}/SiO_2, DCM, 74%; g) MeCN, 82 °C, 2 h, 76%.

Scheme 48: Synthesis of (±)-*O*-methylperezone **218** and (±)-*O*-methylisoperezone **219**.

Finally, the 4-alkynyl-4-hydroxycyclobutenone ring expansion reaction has been applied in the total synthesis of assoanine **226**, one of a series of biologically active pyrrolophenanthridine alkaloids isolated from various *Crinum* species.[61-64] The short synthesis began with the alkylation of indoline with propargyl bromide, which provided *N*-propargyl indoline **220** in 93% yield.[65] The lithium salt of **220** was generated by treatment with ^{n}BuLi at –78 °C and added to dimethyl squarate **16** in THF to give cyclobutenone **221** in 87% yield. This adduct was thermolysed in refluxing *p*-xylene for 2 h and gave pyrrolophenanthridine **223** in 40% yield along with the undesired nonannulated hydroquinone **224** in 50% yield. The desired product arises from the cyclisation of the diradical intermediate **222** to the proximal aromatic ring, whereas the indole **224** arises from intramolecular H-atom abstraction from C-2 of the indoline moiety. Removal of the phenolic hydroxyl group was achieved by the reductive cleavage of the bis-diethyl phosphate ester **225** using sodium in liquid ammonia, which gave assoanine **226** in 25% yield (Scheme 49).[24]

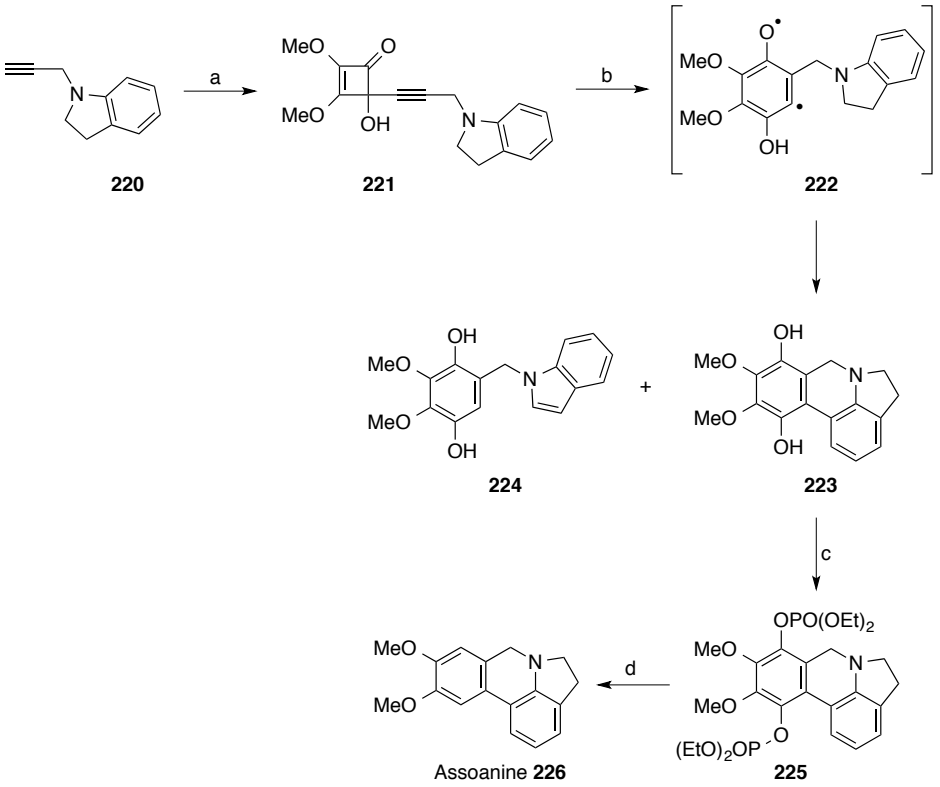

220 **221** **222** **224** **223** **225**

a) ^{n}BuLi, **16**, –78 °C, THF, 55 min, 87%; b) *p*-xylene, 138 °C, 2 h, 90% (1:1.25); c) NaH, $ClPO(EtO)_2$, 0 °C→RT, THF, 16 h, 72%; d) Na/NH_3, –78 °C, Et_2O, 1 h, then RT for 16 h, 25%.

Scheme 49: Synthesis of pyrrolphenanthridine **226**.

Other natural product total synthesis completed using cyclobutenone methodology include, (–)-thespesone[66] **230** (Scheme 50), echinochrome A[67] **233** (Scheme 51) and various xanthones[68] **239** (Scheme 52).

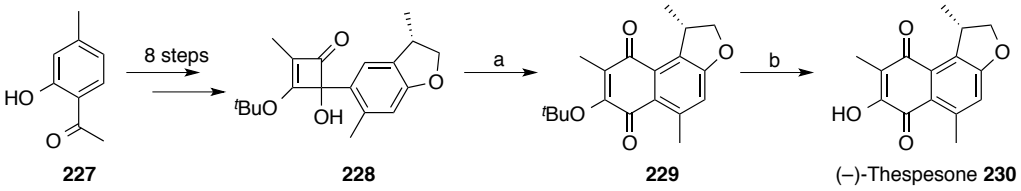

227 **228** **229**

a) PhMe, 110 °C, 2 h, 57% over 3 steps; b) TFA, DCM, 0 °C, 1 h, 77%.

Scheme 50: Schobert's synthesis of (–)-thespesone **230**.

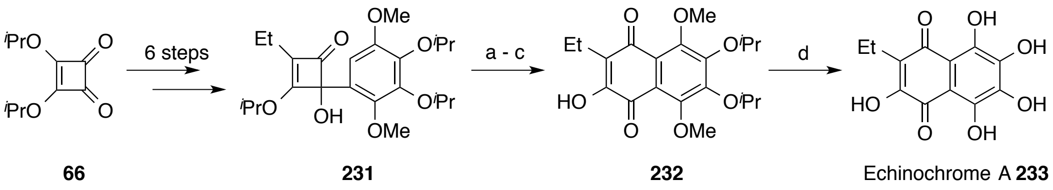

a) neat, 160 °C, 15 min; b) CAN, 25 °C, Et_2O/H_2O; c) air, 7 h, 95 % over 3 steps;
d) BBr_3, DCM, –78 °C → 0 °C, 41%.

Scheme 51: Total synthesis of echinochrome A **233**.

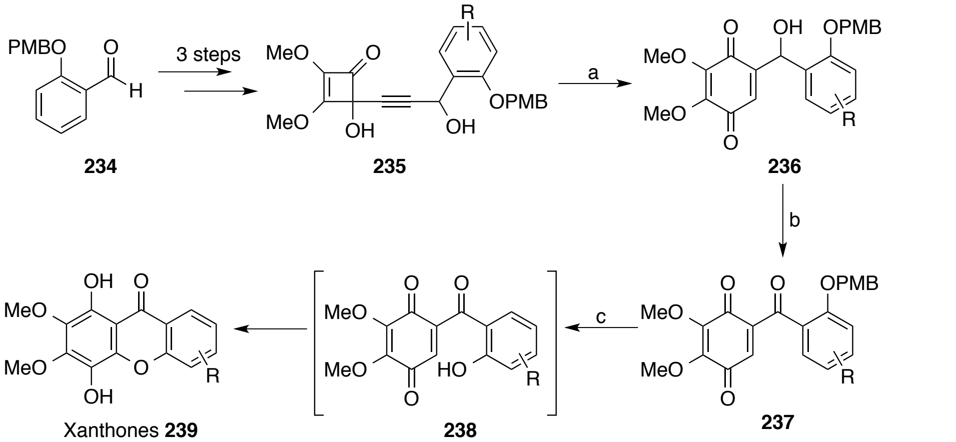

a) PhMe, 110 °C, 4 h, 60–83%; b) CrO_3, H_2SO_4 (aq), acetone, 0 °C, 1 h, 89–99%; c) TFA, DCM, RT, 1 h, 60–81%.

Scheme 52: Synthesis of xanthones **239** from alkynylcyclobutenones **235**.

1.5 Photochemically Induced Cyclobutenone Rearrangements

The photochemical rearrangement of 4-hydroxycyclobutenones **240** was first investigated by Moore *et al.* in 1988.[69] Photolysis of substituted cyclobutenones **240** were carried out in THF at 0 °C using a Quartz immersion well and a 400 W medium-pressure Hanovia lamp. Reaction times varied from 1.5 h to 5.5 h depending on the substituents and were established by monitoring progression by TLC (Scheme 53). The low yields attained (27–60%) were attributed to the decomposition of the 5*H*-furanone products **241** under the reaction conditions. Control experiments showed them to be photochemically unstable.

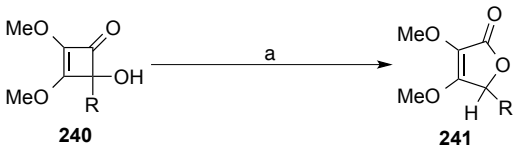

240	R	Time (h)	Yield 241 (%)
a		4 h	27
b		4 h	28
c		5.5 h	39
d		2.5 h	51
e		4 h	60

a) hν, THF, 0 °C.

Scheme 53: Photochemical rearrangement to 5*H*-furanones **241**.

Photochemical rearrangements of cyclobutenones **240** have received less attention but are nonetheless interesting as they follow a different course to the related thermal rearrangement. Moore proposed that thermolysis of 4-hydroxycyclobutenones **240** leads to hydroquinone **12** formation *via* electrocyclic ring opening to (*Z*)-**14** while photolysis leads to 5*H*-furanone **241** *via* electrocyclic ring opening to (*E*)-**14** (Scheme 54).

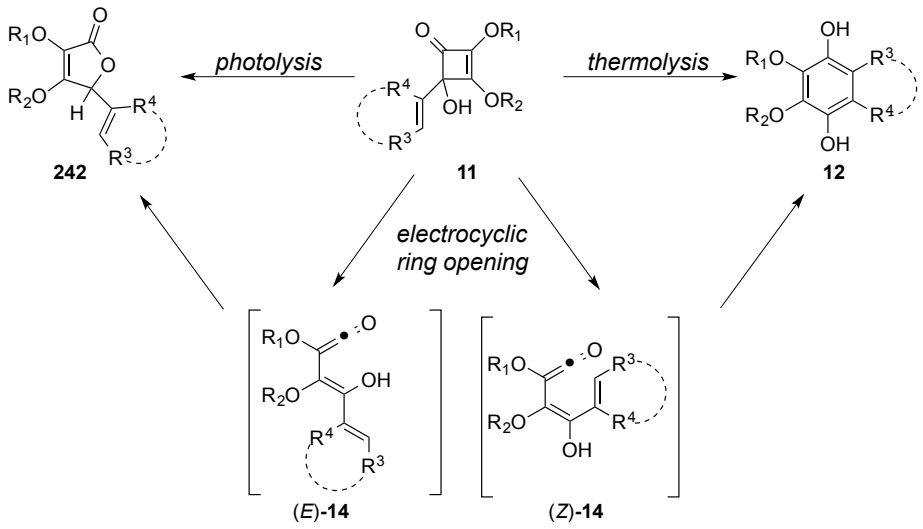

Scheme 54: Thermal or photochemical induced rearrangements of vinyl-, aryl- and heteroaryl-cyclobutenone.

Since the emergence of the above publication by Moore *et al.*,[69] the synthesis of 5*H*-furanones using the above route has seen little use due to the low yields attainted. This was further demonstrated by Yamamoto *et al.* in the construction of chlorinated tetronate derivatives[70] such as **245**. Following the conditions reported by Moore,[69] the photochemical rearrangement of cyclobutenone **243** was carried out in THF at RT using a Quartz immersion well and a 400 W medium-pressure Hanovia lamp to give α-chlorotetronate **245** in 48% yield (Scheme 55).

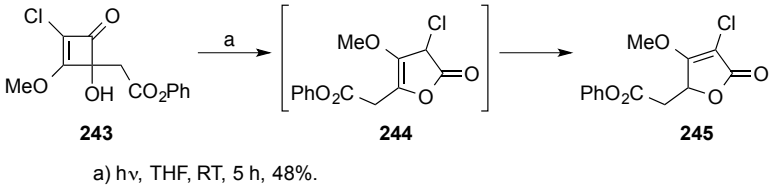

Scheme 55: Photochemical rearragnement to form α-chlorotetronate **243** by Yamamoto *et al.*

Although, the direct formation of a butenolide as a product from the thermolysis of 4-hydroxycyclobutenone **240** is unusual, it has been observed in a few cases. Thermolysis of **240f** at 138 °C (*p*-xylene), for example,[6] gave a mixture of butenolides **247** and **241f** in a 2:1 ratio (89% yield). Treatment of the initially formed crude mixture with silica gel gave exclusively isomer **241f**. The switch in mechanism to give the butenolide in place of the quinone following the thermolysis of **240f** was due to ring closure of the kinetic isomeric ethenyl ketene (*E*)-**246** not competing with that of (*Z*)-**246**, therefore resulting in the butenolide **241f** as the product (Scheme 56).

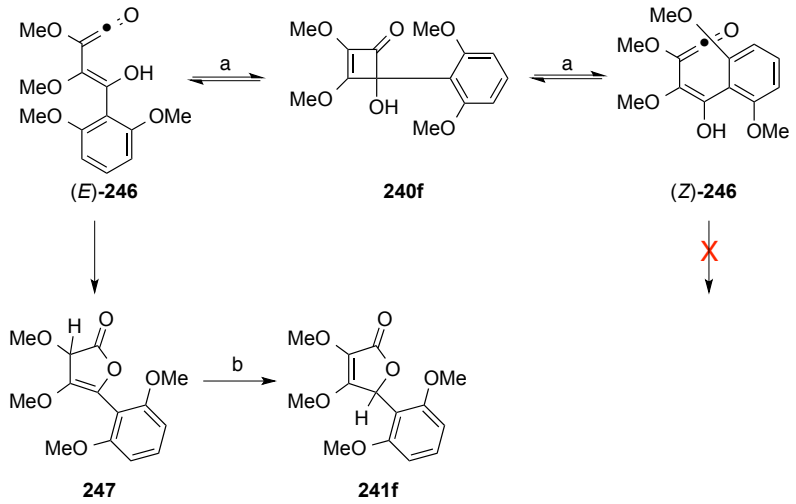

a) *p*-xylene, 138 °C, 16 h; b) SiO_2, DCM, 70% over 2 steps.

Scheme 56: Formation of butenolide **241f** from thermolysis of **240f**.

In an example published by Liebeskind and co-workers, thermolysis of 4-hydroxy-4-(1-methylimidazole-2-yl)-2-cyclobutenone **248** yielded **251** as the sole product.[4] They postulated that the 1,2-adduct **248** exists in a stable hydrogen-bonded conformation that internally protects the imidazole imine nitrogen and thus disfavours intramolecular cyclisation onto the ketene. Instead equilibration of the unfavoured vinylketene **249** into **250** allows closure to the butenolide **251**. As previously shown (Scheme 12), protection of the hydroxyl group as the acetate analogue circumvents the formation of the butenolide to give the expected acetoxypyridinone product (Scheme 57).

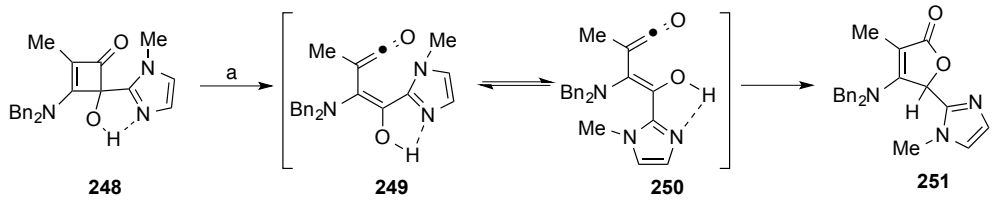

a) 1,4-dioxane, 90 °C, 4 h, quantitative.

Scheme 57: Thermolysis of **248** to give butenolide **251**.

Houk *et al.* addressed the issue of inward *vs.* outward rotation of the hydroxycyclobuteneones and discovered that outward rotation was favoured by groups with π-donor ability. Thus, selectivity in the thermal rearrangement places groups with non-bonding electron pairs outward due to i) a repulsive interaction between the donor non-bonding electrons on the substituent with the C_3-C_4 σ-orbital (inward rotation) and

ii) a stabilising two-electron interaction between the same donor electrons and the empty C_3-C_4 σ*-orbital. In the case of an electron-donating alkoxy substituent (OR), the preference for outward rotation over inward rotation has been reported to be between 14–16 kcalmol^{-1}. Steric effects were reported to be of secondary importance in controlling the direction of the rotation.[10,71] *Ab initio* calculations performed by Houk and co-workers[72] on the ring opening of 3-*tert*-butyl-3-hydroxycyclobutenone **252** was particularly illustrative. The calculations indicated that the *tert*-butyl group prefers to rotate inwards **253** in spite of the large steric effect and the activation energy calculated was 4 kcalmol^{-1} lower than that of the hydroxyl group inwards **254**.

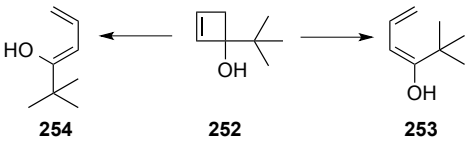

Scheme 58: Rotation of the hydroxyl group inwards (**254**) *vs* outwards (**253**).

Chapter 2.Our Strategies

Though widely used since its introduction by Moore and Liebeskind, little is known about the factors that influence the course of cyclobutenone reactions, or the optimal conditions for effecting the transformations. A typical technique used to investigate the factors that influence the course of a reaction is by establishing a Hammett relationship for the reaction. Structural features such as different substituent groups that enhance electron density on an aromatic ring can be used as an indicator of the degree to which the reaction responds to electronic perturbation. This can be achieved by varying the substituent groups as they can be introduced near the reaction centre but do not take part directly in the reaction. Our strategy is to vary substituents on a 4–arylcyclobutenone at the *para* position of the aromatic ring and rearrange them *via* thermolysis and observe any effects the substitution has on the overall reaction.

Any data obtained from the reactions will be used to establish a Hammett relationship and will be compared and used in conjunction with *in silico* studies to provide new insights into the mechanistic course of the Moore rearrangement.[73,74] In particular we would like to investigate the following:

- Which of the two steps, i.e. the ring opening or the ring closing is the rate determining step.
- What factors influence the course of the reaction.
- What factors influence the selectivity in products formed when the reaction is performed under thermal conditions (formation of quinones) compared with photochemical conditions (formation of 5*H*-furanones).

The study will be performed using flow chemistry due to the many advantages that have been reported in the literature.[75-77] While thermal flow chemistry is widely available, flow-photo chemistry has recently gain momentum.[78-82] Our aim is to develop equipment and a method for doing photochemical reactions under flow to make setting up photochemical reactions simple and more accessible to chemists. Using this new set-up we expect to investigate the photochemical aspect of the Moore rearrangement and determine the cause for the selectivity in conjunction with *in silico* methods.

Chapter 3.Results and Discussion: Thermal Rearrangements of Arylcyclobutenones

3.1 Synthesis and Rearrangement of 4-Arylcyclobutenones

The correlation established between the structure of a compound and its chemical reactivity can be a great indicator of the mechanism of the reaction. Consequently, the effect of substituents (X) on the reactivity of a side chain functional group (Y) in compound series (G) have received considerable attention (Figure 1).[83] [84]

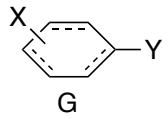

255

Figure 1

Substituent groups (X) can induce electronic perturbation near the reaction centre without taking part in the reaction directly. Common substituents include –OH, –Me, –Cl, –F, $–NO_2$, –CN, amongst other. The changes these induce in reaction affinity are of interest, and their impact must be assessed relative to a standard substituent that is considered to be neutral electronically. Hydrogen is normally adopted as the 'zero' substituent, and therefore the other groups are categorised as electron–donating or electron–withdrawing relative to it.[85]

Keeping in mind the above, our investigation into the mechanism of the Moore rearrangement started with the synthesis of various arylcyclobutenones containing a variety of *p*-substituents (X) on the aromatic ring. Our synthesis began with dimethyl squarate **16**, which was synthesised using a literature procedure involving the heating of squaric acid in methanol containing trimethyl orthoformate. An aryllithium, formed by lithium-halogen exchange, was added at –78 °C to form the required 4-aryl-4-hydroxy cyclobutenone adducts **258a–i** (Scheme 59) with variable success.

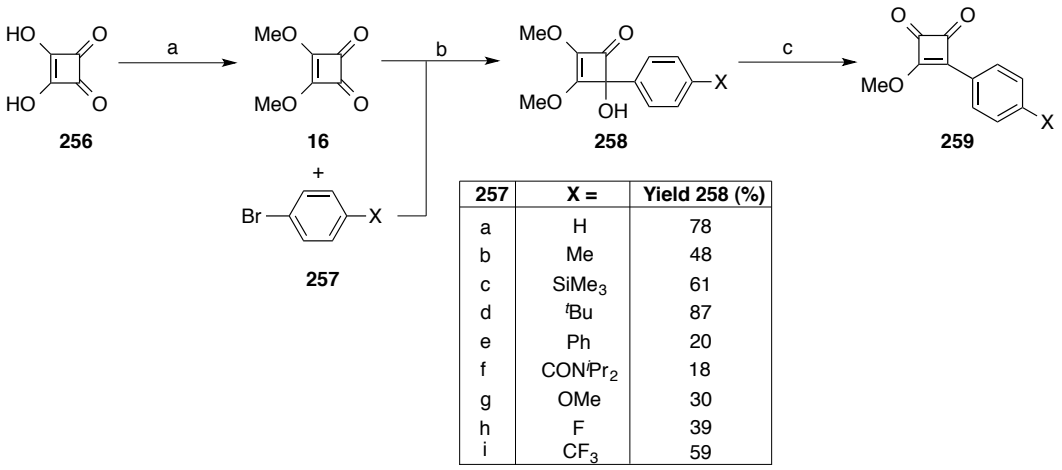

257	X =	Yield 258 (%)
a	H	78
b	Me	48
c	$SiMe_3$	61
d	^{t}Bu	87
e	Ph	20
f	CON^iPr_2	18
g	OMe	30
h	F	39
i	CF_3	59

a) $HC(OCH_3)_3$, MeOH, 65 °C, 16 h, 88%; b) **257**, ^{n}BuLi, –78 °C, THF, then NH_4Cl; c) H^+.

Scheme 59. Synthesis of 4-substituted-4-hydroxy cyclobutenone **258a–i**.

The low yields attained for some of the targets could be attributed to their sensitivity. Decomposition to dione **259** (Scheme 59) was evident if samples were kept at RT for prolonged periods or exposed to trace acid making purification by column chromatography using silica gel difficult in some cases. The addition of trace amounts of TEA to the eluent aided purification in some instances.

With these arylcyclobutenones **258a-i** to hand, our attention turned to the thermal rearrangement, **258→260** + **261** (Scheme 60). In batch, reactions of this type are usually conducted in *p*–xylene at reflux (~135 °C) and typically give yields of 70–85% after 2–3 h.[1,6] Our plan was to see if conversions could be improved by the application of flow technology.

Flow chemistry is a useful alternative to traditional batch methods. It has the capacity for automation, and potential for performing sequential reactions. The reduced costs that arise from continuous processes allow for greater reproducibility.[86] In addition, flow reactors afford significant processing advantages, which include improved thermal management and mixing control, the ability to handle extreme conditions and rapid exotherms and the ability to use dissolved gaseous reagents.[87]

The flow system chosen for our study was the Vapourtec R4/R2+ device (Figure 1).[88] Its set-up is user-friendly and comes with a self-calibrating dual pumping system, injection loops that can be pre-loaded with reagents, and a T-piece that conveniently allows two different flow streams to mix before progressing into the flow heat reactor. The Vapourtec

R4 reactor module is capable of supporting four different temperature zones. Due to the design of the stainless steel tubing in the reactor, each zone can be set at a temperature between ambient and 250 °C (Figure 3). In-line back pressure regulators (BPR) are incorporated into the system to prevent the vapourisation of solvents when heated above their normal boiling points.

Figure 2. Vapourtec R4/R2+ flow device.

Figure 3. High temperature reactor.

Preliminary investigations on the thermal rearrangement of 4-phenylcyclobutenone **258a** were conducted in toluene using the high temperature reactor consisting of a stainless steal tubing of 1 mm diameter. Pleasingly, the reaction proceeded in near quantitative yield on heating at 110 °C for 1 h. However, when seeking to extend the study to cyclobutenone **258b-i**, we found that many of our substrates displayed poor solubility in toluene at ambient temperature. Consequently, the solvent was changed to 1,4-dioxane. The thermolysis of 4-phenylcyclobutenone **258a** was repeated and smoothly rearranged to benzohydroquinone **260a** after 30 min of residence time at 150 °C. The isolated benzohydroquinone **260a** was stirred in air for 2 h to promote the facile aerial oxidation to the corresponding quinone **261a,** which was isolated in 99% yield (Scheme 60). We attributed the marked improvement in efficiency to the tight control of temperature across the narrow tubing. Indeed, when these conditions were applied over the range of arylcyclobutenone substrates **258b–i** (Scheme 60) each gave 'spot to spot' reactions. Unexpectedly, each case reaction took longer to proceed to completion than the parent compound **258a** with electron–withdrawing substituents (such as F, CF_3, amide) and some electron donors (such as OMe, ^{t}Bu) slowing the reaction significantly.

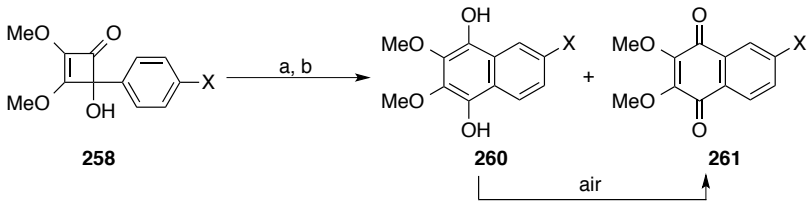

258	X =	Time	Yield 261 (%)
a	H	30 min	99
b	Me	2 h	94
c	$SiMe_3$	2 h	94
d	^{t}Bu	2 h	94
e	Ph	3 h	95
f	CON^iPr_2	1.5 h	84
g	OMe	4 h	94
h	F	4 h	93
i	CF_3	4 h	93

a) i) 1,4-dioxane,150 °C, flow; b) aerial oxidation.

Scheme 60. Rearrangements of aryl-cyclobutenone **258** under flow.

To understand the nature of these substituent effects, we decided to establish a Hammett relationship. In order to establish a Hammett relationship for the rearrangement, substituents must be located at either the *meta* or *para* positions on the benzene ring since *ortho* substituents introduce a steric component. The substituents chosen for our study were –H, –Me, –$SiMe_3$, –^{t}Bu, Ph, an amide (–CON^iPr_2), –OMe, –F and –CF_3 in order to cover the spectrum of electronic contribution for both mesomeric and inductive effects. The near quantitative yields attained under flow made this possible as it allowed the progress of each reaction to be determined from an assessment of the substrate to product ratio at various residence times. For our purposes this was achieved by ^{1}H NMR analysis. The extent of conversion was determined by comparison of the integrals of key signals in the starting material and product samples taken after various residence times (Figure 4).[89] Though complicated by incomplete aerial oxidation of the product hydroquinones **260** to their respective benzoquinones **261**, the method proved reliable and allowed us to establish a rate constant (*k*) for each reaction by applying the values to the first order rate equation (Figure 4).

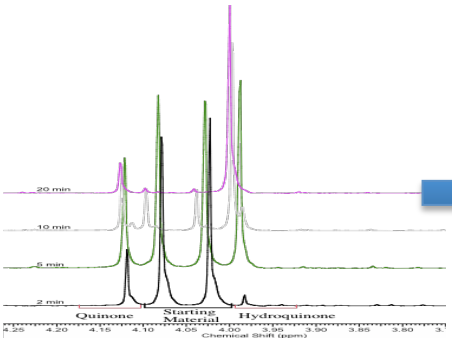

1st Order Rate Equation ⇒ Rate = $k[SM]_t$

$\ln [SM]_t = -kt + \ln [SM]_0$

∴ A plot of $\ln [SM]_t$ vs t gives a gradient = $-k$

Figure 4: Obtaining kinetic data from ^{1}H NMR and determining the rate constant from 1st order rate equation.

Notably, each plot showed the reaction obeyed first order kinetics to give a straight line with a R^2 values being greater than 0.96 (Graph 1).

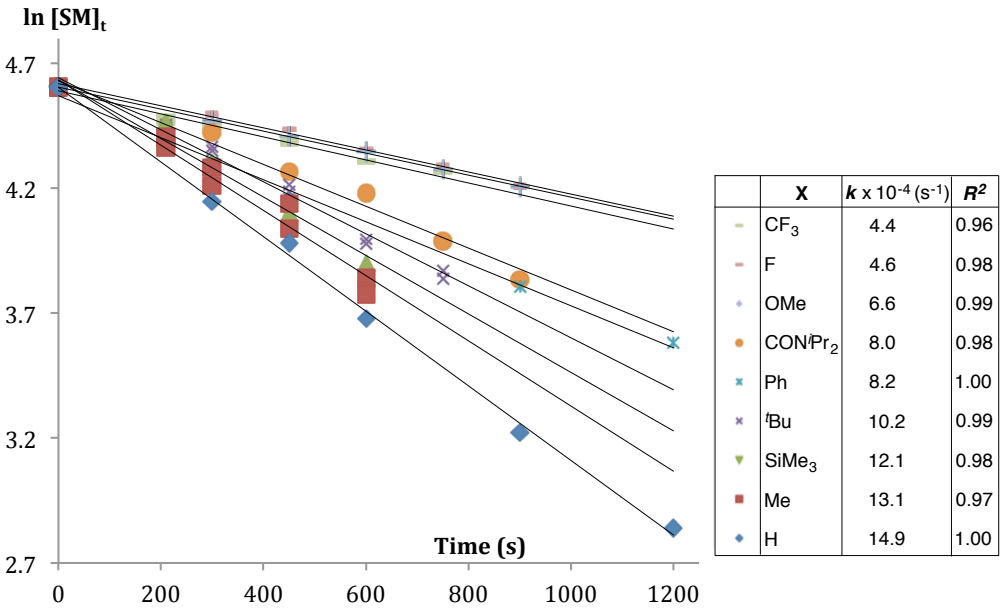

	X	k x 10^{-4} (s^{-1})	R^2
	CF_3	4.4	0.96
	F	4.6	0.98
	OMe	6.6	0.99
	$CONiPr_2$	8.0	0.98
	Ph	8.2	1.00
	tBu	10.2	0.99
	$SiMe_3$	12.1	0.98
	Me	13.1	0.97
	H	14.9	1.00

Graph 1: Determination of rate constants for **258→260 + 261**.

3.2 Hammett Relationship

Using the rate data obtained (Graph 1), we now sought to determine a Hammett relationship for the reaction. L. P. Hammett introduced the equation:[90]

$$\log \frac{k_X}{k_0} = \rho \sigma$$

The parameter k_0 is the rate given when the substituent is –H, while k_X is the rate constant observed for a given substituent group – X to study the influence of a *meta* and *para* substituent on the rate of a reaction that is compared relative to the rate constant of the parent compound (X = H). ρ was defined as the *reaction constant*,[91] and provides a measure of the electronic demands of the reaction in question by indicating susceptibility to electronic effects. σ is the *substituent constant*. It is a characteristic of the substituent group –X. In general, electron-withdrawing substituents have a positive σ value, while electron-donating ones have negative values.[92-94] σ values were determined experimentally and come in many guises. For example, σ_I related to the inductive character of a substituent, so the effect is far greater at the *meta* position than at the *para*. σ_R assesses the resonance effect (mesomeric effect). Here the effect is greater when the substituents are located *para* rather than *meta*. Effects on the reaction for the *meta* and *para* substituents relate to the combined influence of inductive and mesomeric effects.

The kinetic data obtained from our flow rearrangement were first correlated to σ_p values (Graph 2). This seemed a logical choice, as the substituents (X) were all *para* relative to the side chain. No correlation was seen with this parameter set.

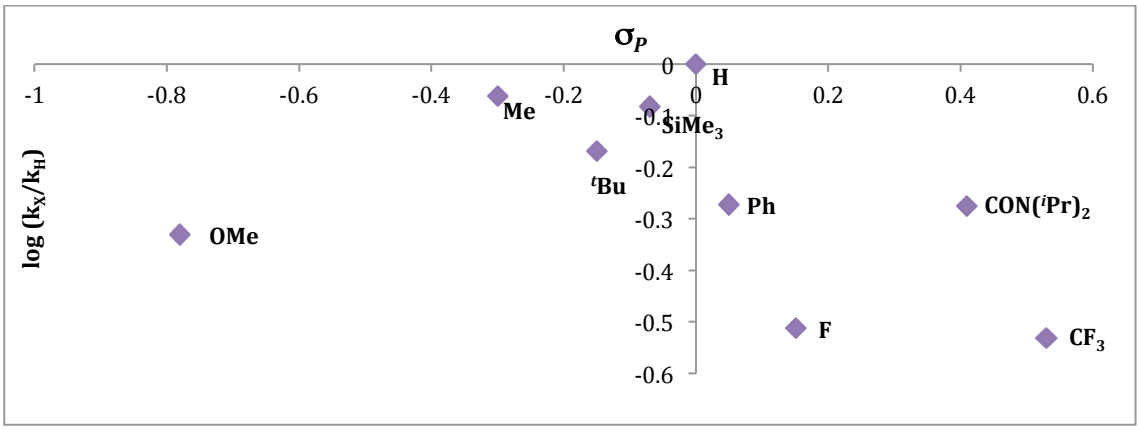

Graph 2: Hammett plot showing no correlation to σ_p.

A plot of the rate constant with σ_m values (Graph 3) was then examined as the substituent was *meta* to the centre of reactivity. The correlation observed was poor with a R^2 value of 0.692 for the line of best fit.

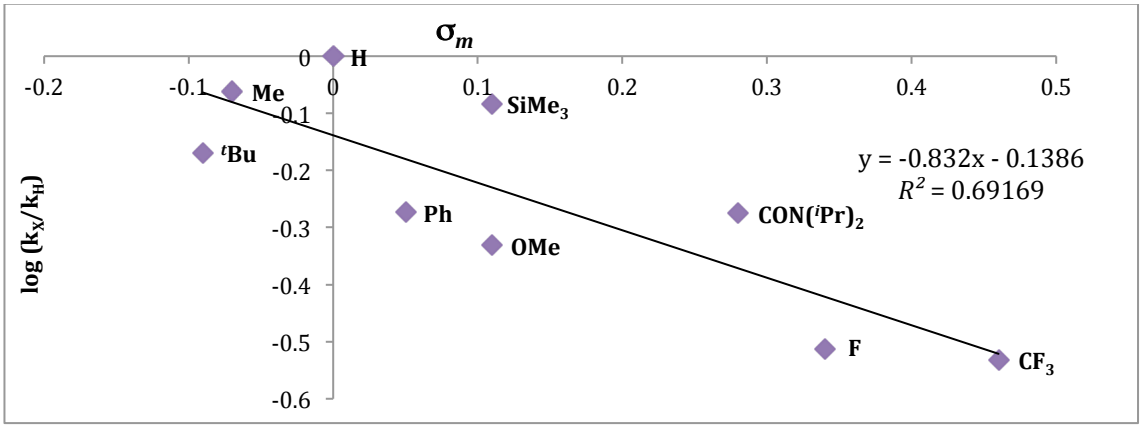

Graph 3: Hammett plot showing a poor correlation to σ_m.

As it seemed likely that the rate determining step involved electrocyclic ring closure, we next examined the resonance effect (σ_R). To our surprise, this led to points scattered around the graph (Graph 4) suggesting minimal influence on the course of the reaction.

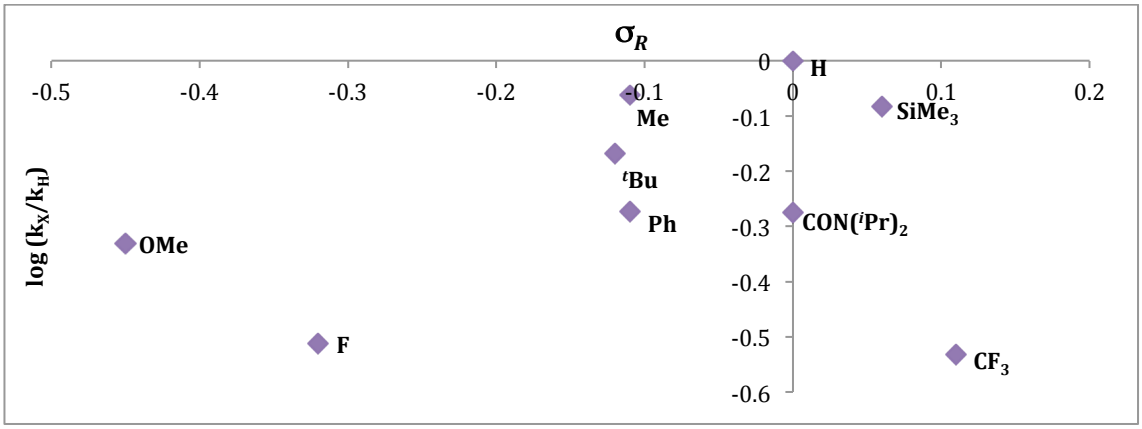

Graph 4: Hammett plot showing no correlation to σ_R.

Indeed, the only reasonable correlation given was with the σ_I parameter set[95] (Graph 5) which gave a straight line fit with R^2 = 0.858. Closer inspection of these data revealed that the substrates showing greatest deviation in the Hammett plot were the parent compound **258a** (X = H) and those bearing large substituents (^{t}Bu, Me_3Si, CF_3). This suggested that the reaction had a steric component.[73,84,96,97]

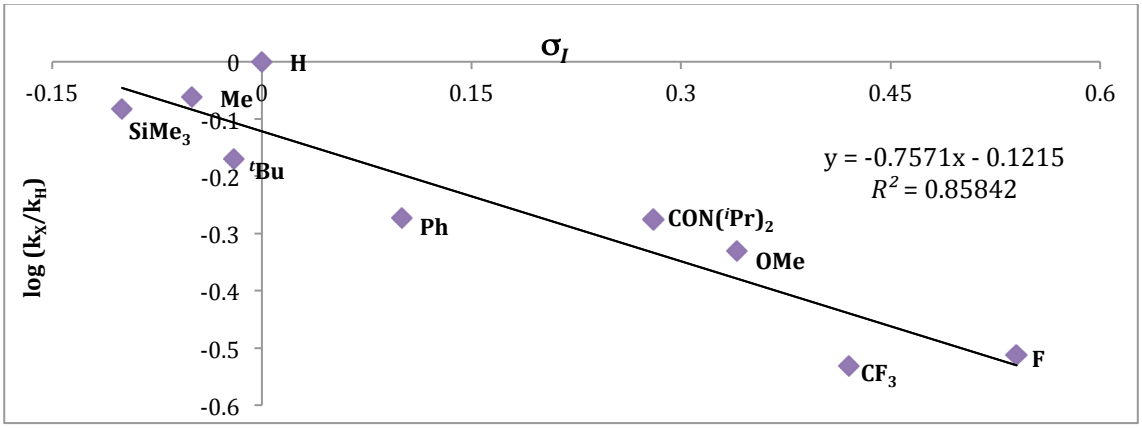

Graph 5: Hammett plot showing a reasonable correlation to σ_I.

To examine the influence of sterics, we next looked at the Taft equation.[98-100] Developed by Robert Taft, this equation allows for inductive, resonance and the steric effects of a substituent to be taken into account. Indeed, by introducing a small steric correction factor the correlation improved significantly (Graph 6 and Graph 7). The best correlation was observed with (σ_I–6% E_s), which gave a R^2 value of 0.989.

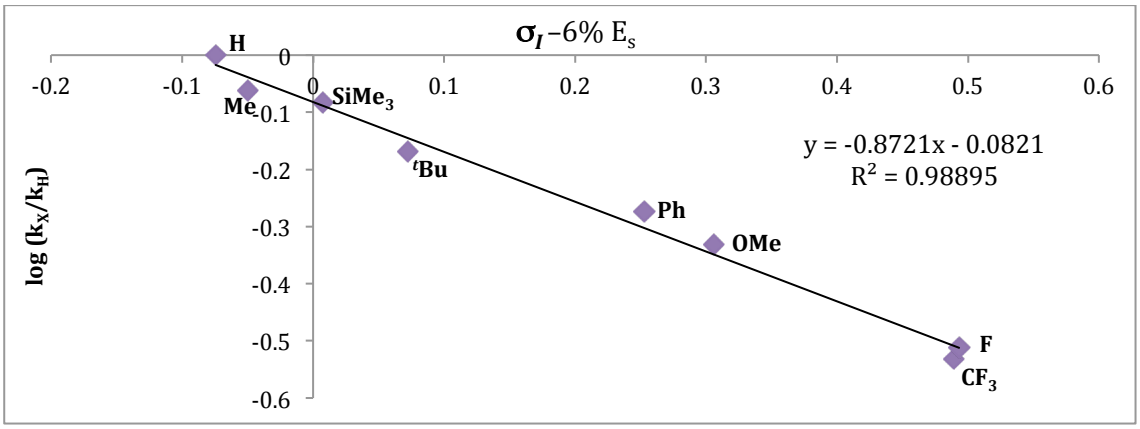

Graph 6: Hammett plot for the arylcyclobutenone rearrangement **258→260 + 261** with the σ_I parameter corrected for the steric factor (6% E_s).

The correlation observed with the σ_I parameter set is instructive in suggesting that the substituents have an influence on the ease of forming the new σ-bond between the arene and the carbonyl (*i.e.* late transition state) **263→265** rather than the initial interaction of the reacting carbons in the π-system (early transition state). Therefore, this indicates that the formation of the new σ-bond is the rate-determining step.

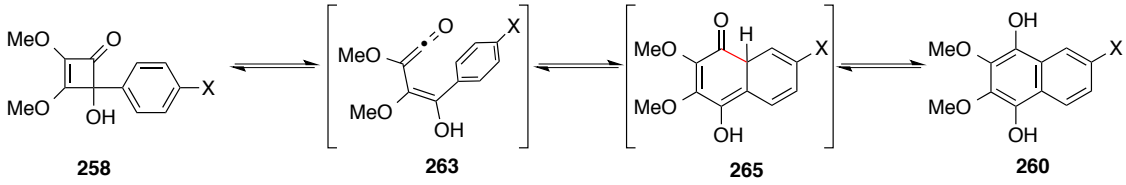

Scheme 61: Reaction mechanism for the rearrangement of 4-arylcyclobutenone **258**.

3.3 Computational Studies

All calculations were performed by Theo P. Gonçlaves at the B3LYP/6-311(d,p) level using Gaussian 09.[101]

To confirm the findings obtained from the Hammett correlation, the course of the reaction was modelled for the rearrangement of **258a→260a** at the B3LYP/6-311G(d,p) level using the Gaussian 09 program.[102,103] The results obtained (Figure 5) showed that the electrocyclisation of ketene **263** to bicyclic ketone **265** was the rate-determining step, and that this intermediate has a late transition state. Thus, **264** is more akin to intermediate **265** than its precursor ketene **263**, with the rate of reaction determined by the ease with which the σ-bond developing between the arene and the carbonyl is established. Pleasingly, the calculations summarised in Figure 5 support our experimental findings.

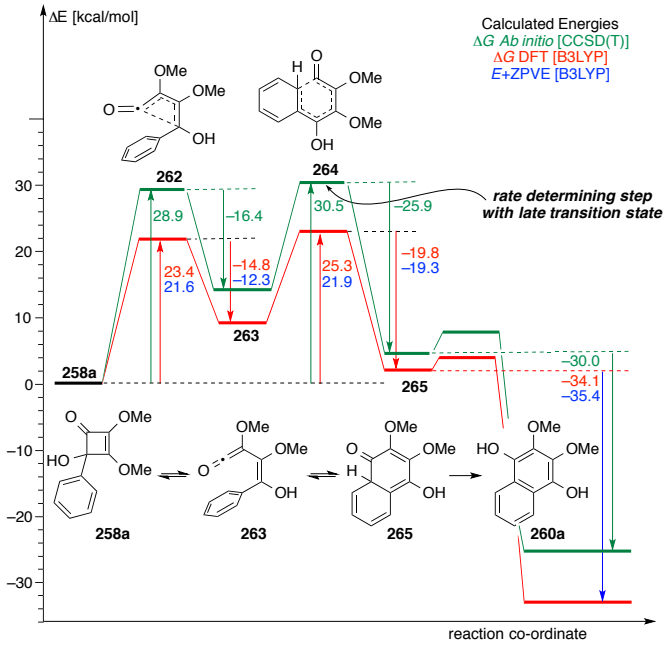

Figure 5. Summary of the energies calculated for the rearrangement of **258→260** in the gas phase at 150 °C using different computational methods.

Importantly, the calculated geometry for transition state **264** indicated that the angle of incidence between the developing σ-bond and the plane of the arene is 41.5°, and reduces to 21.6° as the reaction progresses to intermediate **265** (Figure 6). Thus, interaction between this nascent σ-bond and the residual π-system is limited as it develops to become part of the σ-framework. This is consistent with a late transition state under the influence of inductive rather than resonance effects.

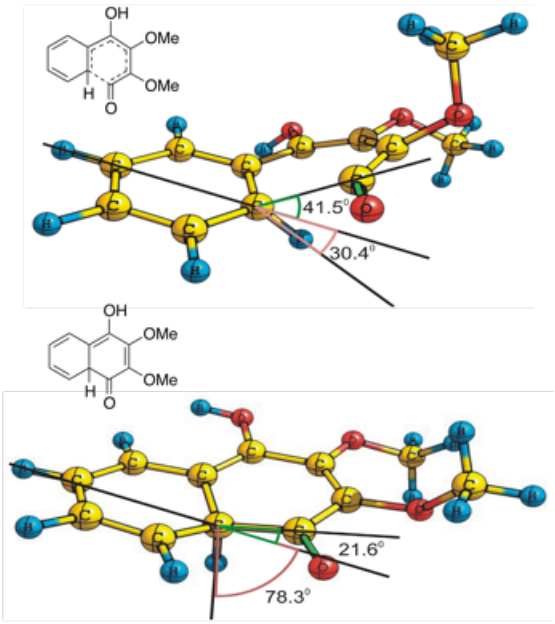

Figure 6. Calculated structures for the transition state **264** and intermediate **265**.[1]

3.4 Synthesis of Heteroarylcyclobutenone

Our attention turned next to the rearrangement of heteroarylcyclobutenones. We limited our study to representative electron-rich (thiophene) and electron-poor (pyridine) systems. The thermolysis of (2-pyridyl)-cyclobutenone **267** provides access to quinolizidone **268**.[104] For the rearrangement of **267**, the standard temperature of 150 °C proved to be too high since after a residence time of only 2 minutes, analysis of the reaction showed it had gone to completion. Therefore the reaction temperature was reduced to 100 °C and after a residence time of just 10 min we observed complete rearrangement of the starting material to quinolizidone **268**, which was isolated in quantitative yield.

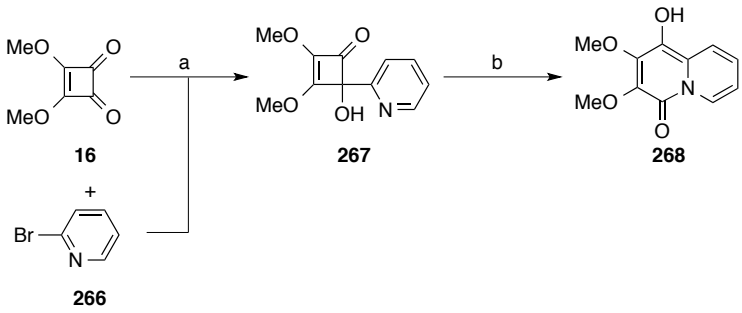

a) **266**, ^{n}BuLi, –78 °C, THF, then NH_4Cl, 62%; b) 1,4-dioxane, 100 °C, 10 min, flow, quantitative.

Scheme 62. Rearrangement of (2-pyridyl)-cyclobutenones **268**.

The solubility of **268** in $CDCl_3$ was poor, so it proved necessary to acquire NMR data in d6-DMSO. A crystal structure provides a possible explanation for this. It revealed that in the solid state the product exists in two slightly different forms, which overlay in an asymmetric unit (Figure 7 and Figure 8).

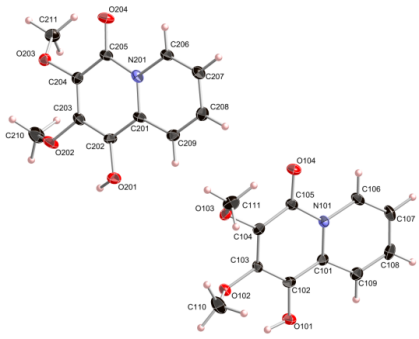

Figure 7. Two different forms of **268**.

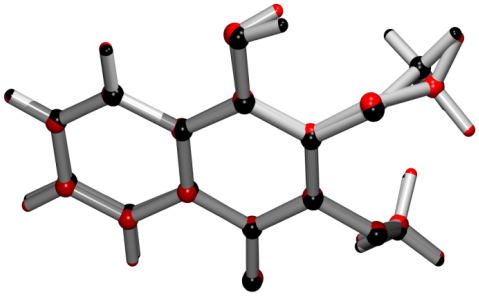

Figure 8. Overlay of the two forms to show an asymmetric unit.

It also showed how these conformers form different and entirely independent hydrogen bond chains along the *c*-axis (Figure 9). This may explain the poor solubility in $CDCl_3$ compared with DMSO.

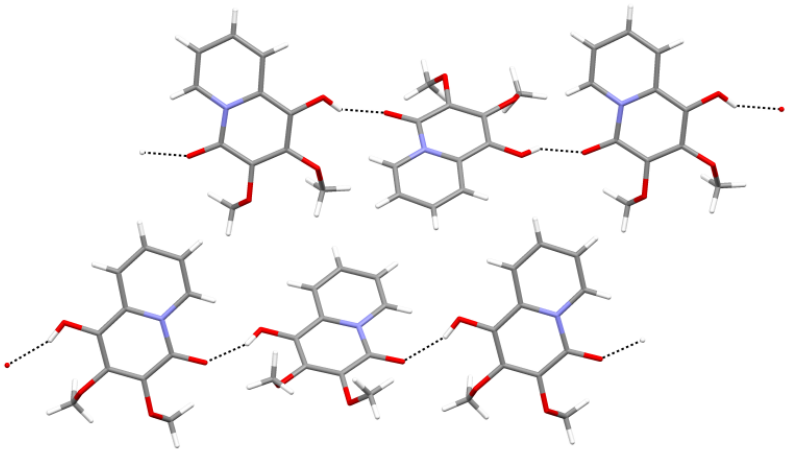

Figure 9: Hydrogen bonding patterns of **268**.

As previously seen, an analogue of **268** had been synthesised using the Moore rearrangement **57** (Scheme 12).[104] However, product isolation required protection of the alcohol moiety formed on addition of 2-lithiopyridine to cyclobutendione **54**. Subsequently, the thermal rearrangement of the pyridyl-cyclobutenone **55** led to quinolizidone **57**.

The related synthesis of quino[*b*]thiophene **272** from thiophene **270** progressed[1,6] as expected in 1,4-dioxane at 150 °C. After an aerial oxidation, the product was given in 99% yield (Scheme 63).

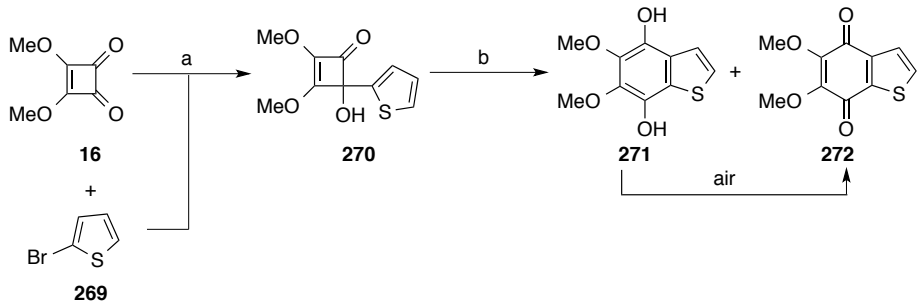

a) **269**, ^{n}BuLi, –78 °C, THF, then NH_4Cl, 32%; b) 1,4-dioxane, 150 °C, 30 min, flow, 99%.

Scheme 63. Rearrangement of thiophene **270**.

3.5 Conclusions

Our investigation of the thermal rearrangement of 4-arylcyclobutenones had led to an enhancement in yields to near quantitative. We have also established a Hammett relationship for the reaction and revealed the influence of the inductive effect (σ_I) on the reaction (Graph 7).

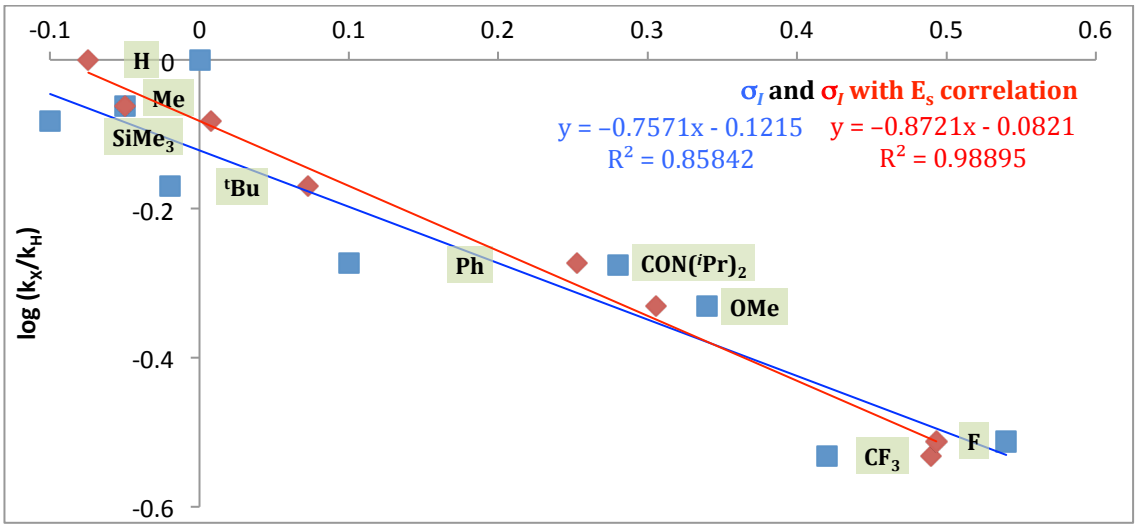

Graph 7: Hammett plot for the arylcyclobutenone rearrangement (*viz* **258→260+261**) using the σ_I parameter set (blue squares) and with a steric correction (σ_I–6% E_s, red diamonds).[105]

Using the above information, in conjunction with *in silico* studies, we were able to show that the electrocyclic ring closure of the ketene **263** to the bicyclic ketone **265** was the rate determining step. The ease of formation of the new σ–bond, is strongly influenced by the inductive effect of the proximal substituents.

3.6 Exemplification of the Method

3.6.1 Cribrostatin 6

To demonstrate the advantages offered by our flow thermochemical methodology, we chose to effect a short and efficient total synthesis of the marine natural product cribrostatin 6 **273**. Over the past few years, a series of biologically active 5,8-isoquinolinedione alkaloids have been isolated from marine sources.[106] Some examples of natural products containing this structural core are shown in Figure 10. They include mimosamycin **274**, which was isolated from the culture filtrate of *Streptomyces lavendulae* and showed antimicrobial activity, particularly against mycobacteria; renierone **278** and

N-formyl-1,2-dihydroreierone **276**, which were the major metabolites isolated from *Reniera* sp.; and mimocin **277** a metabolite from *Streptomyces lavendulae*.

In 2003, Pettit *et al.* reported the isolation and structural determination of cribrostatin 6 **273** (Figure 10) from the blue vase sponge *Cribrochalina* sp. found in coastal waters off the Republic of Maldives. It has been shown to inhibit the growth of cancer cells, and displays antimicrobial activity against antibiotic-resistant Gram-positive bacteria and pathogenic fungi. Further to its important biological activity, Pettit *et al*. noted that cribrostatin 6 was unique in having a tricyclic imidazo[5,1-*a*]isoquinolinedione ring system at its core, making it an ideal target for total synthesis.

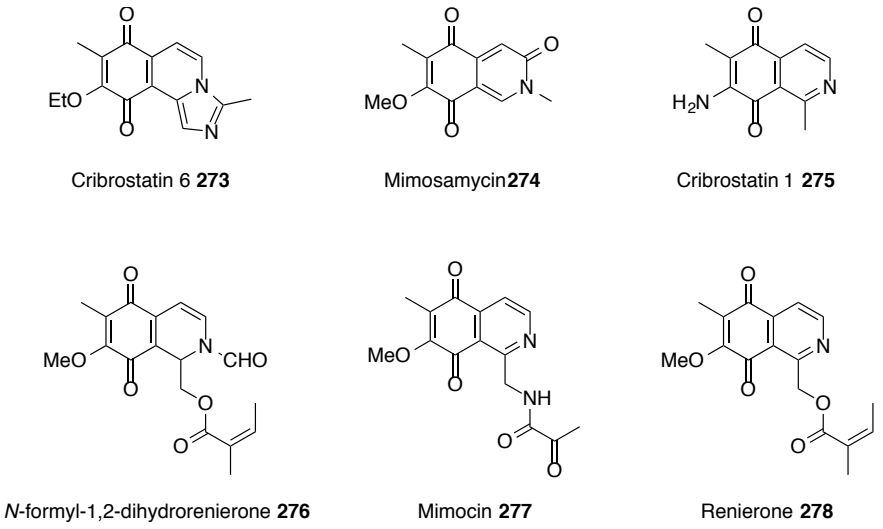

Figure 10: Example of 5,8-isoquinolinedione alkaloids natural products**.**

The first total synthesis of cribrostatin 6 **273** was achieved by Nakahara *et al*. in 2004,[106,107] who used it to showcase a catalytic hydrogenation induced intramolecular *O*- to *N*- acyl group transfer reaction. Thus, phenol **279** was converted into isoquinoline **284** in six steps. Treatment of **284** with *m*-CPBA, followed by TMSCN in NMP next gave the cyanoisoquinoline **285** in 68% yield. Oxidation of **285** with CAN in aqueous acetonitrile for 30 min furnished the desired *p*-quinone **286** in 38% yield together with the corresponding *o*-quinone in 35% yield. Treatment of the *p*-quinone with zinc powder in acetic anhydride provided diacetate intermediate **287** in 33% yield, which on catalytic hydrogenation over 10% Pd-C in MeOH containing HCl induced intramolecular *O*- to *N*-acyl transfer to amide **288** in 82% yield. Sequential treatment of **288** with $POCl_3$, HCl in methanol and air afforded cribrostatin 6 **273** in 61% yield (Scheme 64).

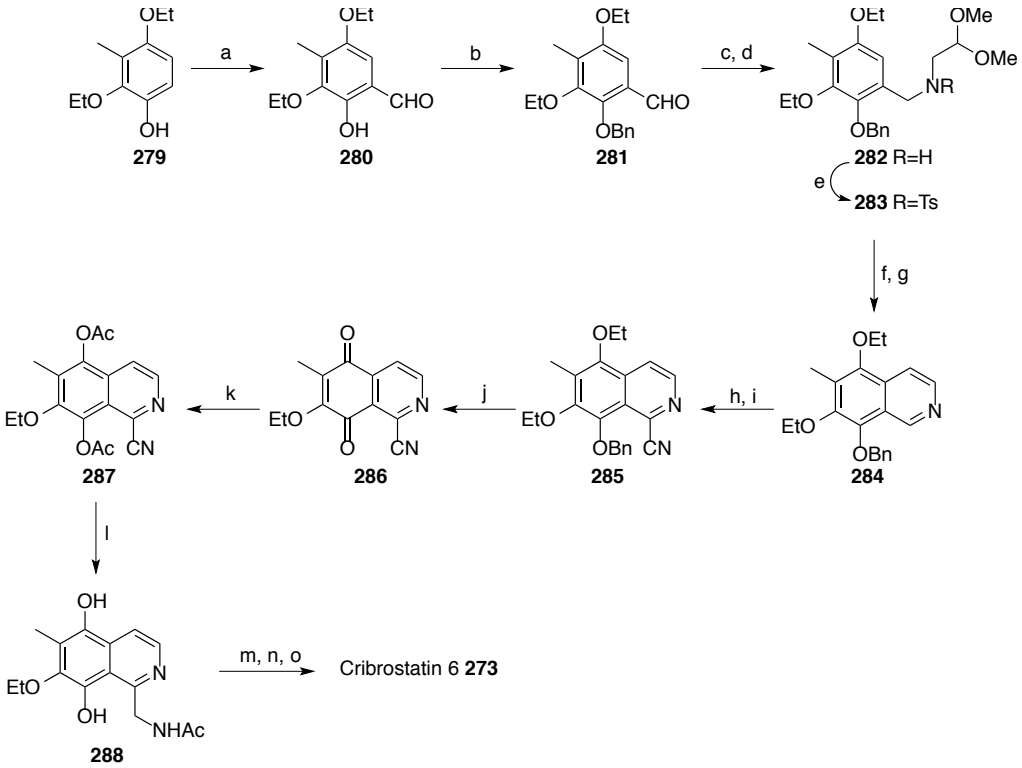

a) Hexamine, AcOH, 135–140 °C, 2 h, 43%; b) BnBr, K_2CO_3, DMF, RT, 48 h, 98%; c) $(MeO)_2CHCH_2NH_2$, benzene, reflux, 3 h; d) $NaBH_4$, MeOH, RT, 1 h, 96% over 2 steps; e) TsCl, pyridine, RT, 20 h, 88%; f) HCl, 1,4-dioxane, reflux. 3.5 h; g) ^{t}BuOK, ^{t}BuOH, 80 °C, 1 h, 80% over 2 steps; h) *m*-CPBA, DCM, RT, 16 h; i) $(Me)_3SiCN$, NMP, 55–65 °C, 50 h, 68% over 2 steps; j) CAN, MeCN, H_2O, 0–5 °C, 0.5 h, 38%; k) Zn, Ac_2O, RT, 1 h, 33%; l) 10% Pd-C, HCl, MeOH, H_2, RT, 3 h, 82%; m) $POCl_3$, PhMe, 110 °C, 15 min; n) HCl, MeOH, RT, 20 h; o) O_2, 61% over 3 steps.

Scheme 64: First total synthesis of cribrostatin 6 **273** by Nakahara *et al*.

Martin *et al.* have achieved the shortest synthesis to date, comprising of five steps from commercially available starting materials. The synthesis began with the activation of alcohol **289** as its tosylate **290** using a known literature procedure. Attempts to generate alkyne **291** from 2-methylimidazole and tosylate **290** failed to give the desired product in significant amounts when bases such as ^{t}BuOK, Cs_2CO_3 and NaH were used. However, by adding excess imidazole to tosylate **290** in acetonitrile at 70 °C afforded the desired alkyne **291** in 92% yield. Deprotonation of **291** with ^{n}BuLi and addition to 3-ethoxy-4-methylcyclobut-3-ene-1,2-dione **292**, (synthesised using literature procedures by Moore *et al.*[14]) gave the key intermediate **293** in 62% yield (Scheme 65).

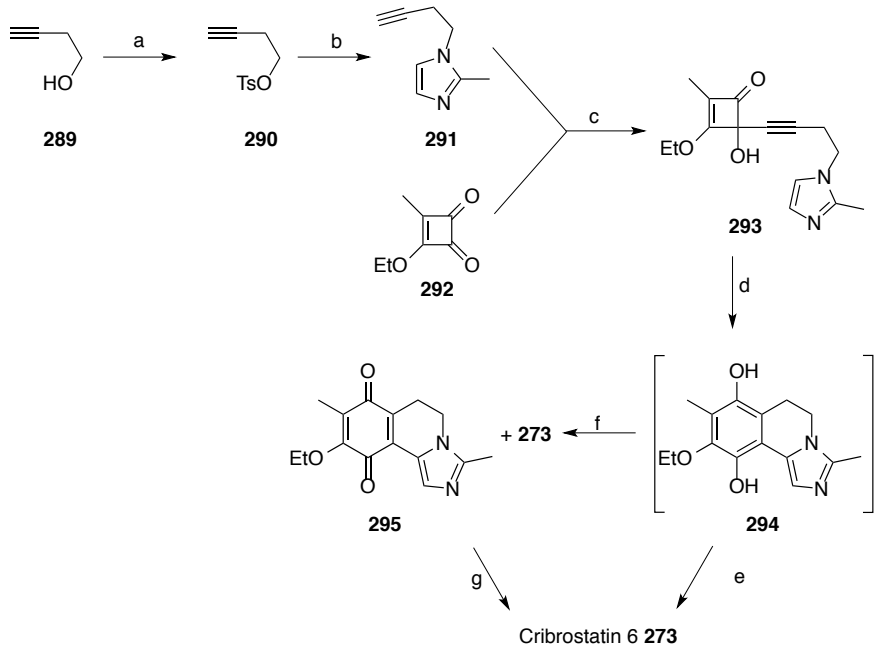

a) ^{n}BuLi, THF, –78 °C→0 °C, then TsCl, 0 °C→RT, 95%; b) 2-methyl-1*H*-imidazole (excess), MeCN, 70 °C, 92%; c) ^{n}BuLi, **291**, THF, –78 °C, then **292**, –78 °C→0 °C, 62%; d) MeCN (0.001 M), 82 °C, 35 min, e) Pd/C MeOH, 80 °C, 4 h, 26%; f) air, RT, 18 h, 24%; g) Pd/C, PhOMe, 90 °C, 4 h, 69%.

Scheme 65: Synthetic route adopted by Martin *et al*.

Their key step envisioned an alkynylcyclobutenone rearrangement[108] with capture of the aryl radical intermediate **297**. Thermochemical opening of alkynylcyclobutenone **293** to ketene **296** would lead to diradical intermediate **297** on ring closure. Diradical intermediate **297** could be captured by imidazole to give **298** *en route* to the desired intermediate **294** (Scheme 66).

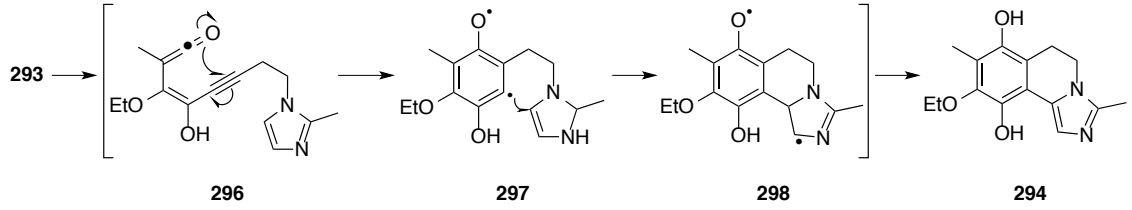

Scheme 66: Key cyclisation reaction to the synthesis of cribrostatin 6 **273** by Martin *et al*.

In practise the key step proved low yielding. The best outcome was seen when a dilute solution of **293** was heated in acetonitrile (0.001 M) for 35 min, which led to a mixture of **295** and **273** in 24% yield (2:1) after stirring the product mixture in air for 18 h. Subjecting the 2:1 mixture to dehydrogenation using Pd/C gave cribrostatin 6 273 in 69% yield (Scheme 65).

3.6.2 Our Approach

Our approach to cribrostatin 6 also envisaged its total synthesis in five linear steps from commercially available starting materials. It relied on a Moore rearrangement of cyclobutenone **303** to cribrostatin 6 **273**. In turn, the precursor **303** could be prepared through 1,2-addition of imidazo-pyridine **302** and to the known cyclobutenone **292**, which will be synthesised using the literature procedure of Moore.[14] Contemporaneously imidazo-pyridine **302** can be synthesised from acetamide **301**, which in turn can be prepared from either the 3-bromopicolinonitrile **298** or the 3-bromopicolinaldehyde **299** by reduction or a reductive amination respectively.

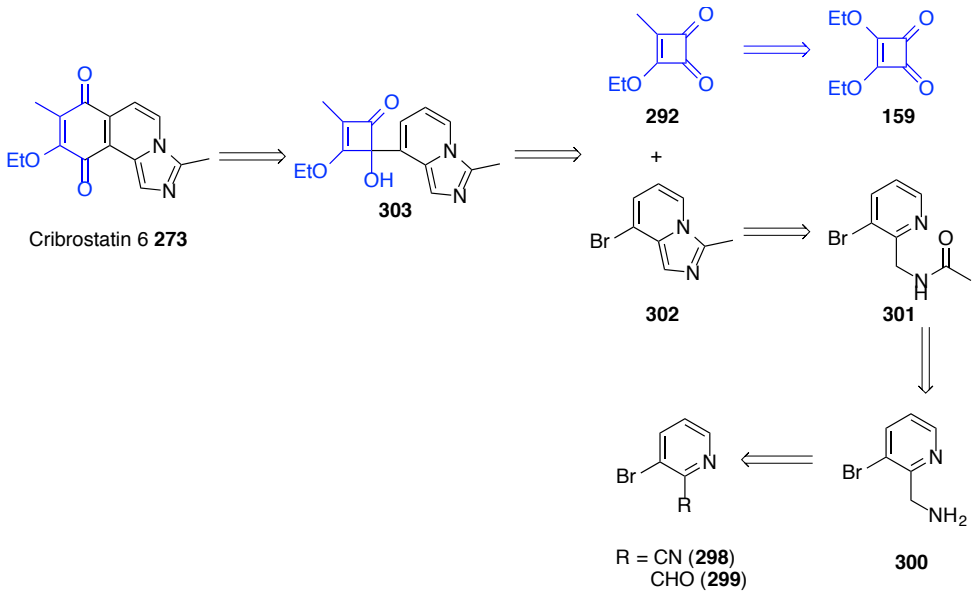

Scheme 67: Retrosynthetic analysis of our approach to cribrostatin 6 **273**.

3.6.3 Synthesis of Cribrostatin 6

Our synthesis of imidazo-pyridine **302** began with the known reduction of nitrile **298** to give the amine **300** using BH_3•THF.[109,110] Analysis of the product mixture by LCMS showed the reaction had gone to completion, however analysis by ^1H NMR led us to conclude that the desired amine **300** was contaminated with various boron residues and complexes (Scheme 68). Repeated attempts to de-complex amine **300** through refluxing the crude reaction mixture in methanol, 2M HCl in methanol, 4M HCl in dioxane, and concentrated HCl were all unsuccessful.

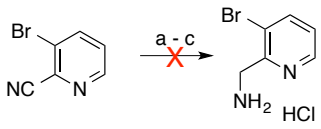

298 **300**

a) BH_3•THF (5 eq), THF, RT, 16 h; b) MeOH; c) 4M HCl in dioxane, reflux, 30 min.

Scheme 68. Reduction of nitrile **298** to amine **300**.

Our attention now turned to alternative ways of synthesising the required amine **300**. Reductive amination of 3-bromopicolinaldehyde **299** was carried out using 7M ammonia in methanol with sodium triacetoxyborohydride as reducing agent.[111] The above conditions failed to furnish the desired product **300** but led instead to the isolation of dimer **304**, suggesting that once formed, the amine product **300** reacts rapidly with the starting aldehyde **299** (Scheme 69).

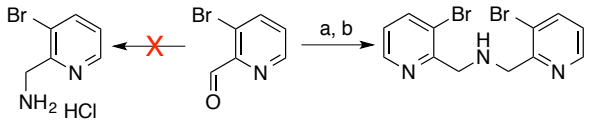

300 **299** **304**

a) 7M NH_3 in MeOH (1.5 eq), $NaBH(OAc)_3$, RT, 15 min; b) 4M HCl in Et_2O, 61%.

Scheme 69: Reductive amination of aldehyde **299**.

Thought then turned to other reducing agents that could be utilised for the selective reduction of **298**. Yoon *et al*.[112] have shown aluminum hydride (alane) is very effective at reducing carboxylic acid and carboxylic ester groups of halogen-containing derivatives without significant dehalogenation. In addition they found alane to be useful in the reduction of nitriles to amines in good yields. This prompted us to use alane for the reduction of nitrile **298** to amine **300**, and to our delight reduction proceeded to completion. Isolation of amine **300** proved difficult due to the high solubility of the free amine **300** in water causing some loss of material on work-up and a moderate yield of 60% (Scheme 70).

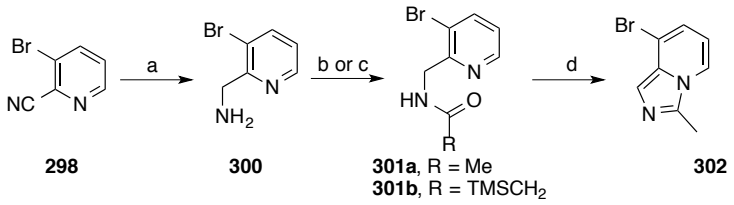

a) Alane•Me_2NEt, PhMe, 0 °C→RT, 16 h, 60%; b) AcOH, EDC, TEA , DCM/DMF, RT, 2 h, 52%; c) EtOC≡$CSiMe_3$, PhMe, 110 °C, 90 min, flow, 89%; d) $POCl_3$, PhMe, reflux, 4 h, 99%.

Scheme 70: Reduction of **298** using alane and synthesis of **300**.

The acylation of **300** using acetic acid and EDC led to the formation of **301** in moderate yield. However, an alternative to acylation with acetic acid was to use (ethoxyethynyl)trimethylsilane that generates trimethylsilane ketene at 110 C to trap the free amine. The procedure was more successful than the predecessor, yielding the acetamide in 89% yield. The cyclisation of **301a** and **301b** with phosphorus oxychloride proceeded smoothly with complete consumption of **301** to form the desired product **302** in quantitative yield (Scheme 70).

The requisite cyclobutendione **292** was prepared by the procedure of Moore *et al.*[14] from diethoxy squarate **159**. The next step was the union of imidazo-pyridine **302** to cyclobutendione **302** *via* 1,2 addition. Treatment of the organolithium adduct of imidazo-pyridine **302** to **292** gave a 3:1 mixture of two regioisomers; the major isomer being the desired product **303** in 56% yield (Scheme 71).

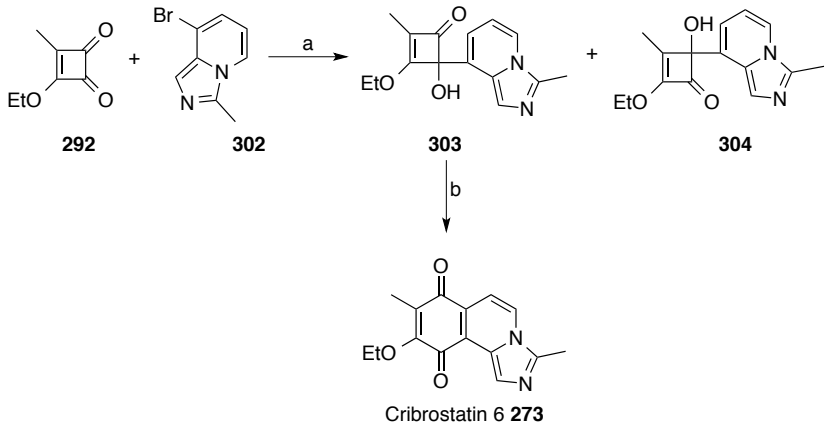

a) **302**, ^{n}BuLi, THF, –78 °C, 30 min, **292**, 30 min, then NH_4Cl (aq), 56% (+ 18% of **304**); b) 1,4-dioxane, 110 °C, 1 h, flow, 90%.

Scheme 71: Union of **292** and **302** to give precursor **303** and rearrangment to **273.**

The final step of the synthesis was carried out under flow, where a solution of **303** in 1,4-

dioxane was injected into the flow apparatus and heated to 130 °C for 20 min. This gave the isolated product **273** in 73% after purification, with the loss of mass balance attributed to some thermal decomposition. Reducing the temperature to 100 ˚C for 1 h did not allow the reaction to go to completion. However, the optimum temperature was established at 110 ˚C for 1 h whereby the reaction gave a yield of 90% (Scheme 71). The synthetic material cribrostatin 6 **273** obtained gave ^{1}H and ^{13}C NMR data consistent with those reported for the natural product.[106,107,113-116]

Chapter 4.Results and Discussion: Photochemical Rearrangement of Hydroxycyclobutenone

4.1 Construction of Flow-Photo Reactor

Following our success in realising the thermal rearrangement of arylcyclobutenones **258** to quinones **261** in near quantitative yields, we wanted to see if we could achieve a similar improvement for the photochemical rearrangement of 4-hydroxycyclobutenones **240** to 5*H*-furanones **241**. Though reported by Moore *et al.* in 1988, it has seldom been used by chemists for synthesis due to the low yields (between 27–51%) reported for the rearrangement.

Our investigation into the photochemical synthesis of 5*H*-furanones **240** began with the construction of a continuous photochemical reactor for use under flow. Traditionally, photochemistry has been performed in solution using immersion well reactors, which typically have the reactor irradiated from within by a high-pressure mercury vapour lamp (Figure 11). The main disadvantage with these systems is their poor applicability for small and large-scale photochemical synthesis. For small scale work, the size and power of the lamps could present practical problems. For large-scale work, the problem is associated with throughput as the majority of the photochemistry occurs within a short radius of the lamp, and therefore the amount of solution that can effectively be irradiated by the lamp is scale dependent.[117]

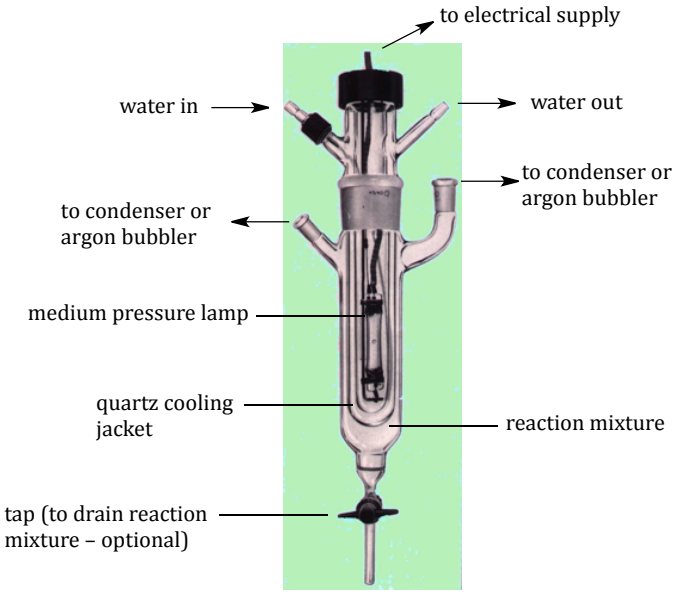

Figure 11: Immersion well photochemical reactor.

Taking inspiration from Booker-Milburn, Berry and co-workers,[117] a photochemical reactor was assembled as shown below. The process started by winding a double layer of perfluoroalkoxy (PFA) tubing (dimensions = 1.6 mm (o.d.) x 1 mm (i.d.)) around a cylindrical Quartz tube (57 mm (d) x 39 cm (l)). In all, 36 m of tubing was used with an internal volume of 28 mL. The coiled Quartz tube was next covered with aluminium foil to promote heat transfer, the recycling of light and to protect the user from stray light. Finally, condenser tubing was wrapped around to facilitate cooling. Importantly, our use of a Quartz tube, open at each end, also facilitated cooling through convection. The set-up used inexpensive 9 W bulbs spanning various wavelengths (supplied by Philips[118]) instead of the more conventional 400–600 W medium-pressure mercury lamps. These were inserted into the cylindrical Quartz tube. Coupling the device to commercial flow chemistry instruments, such as the Vapourtec R4/R2+, allowed for the control of flow rates and residence times (Figure 12).

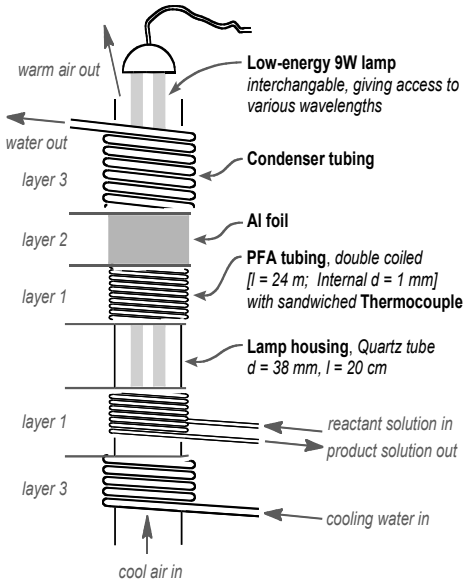

Figure 12: A photochemical reaction set-up under flow.

4.2 Investigations and Insights into the Mechanism

Our investigation into the synthesis of 5*H*-furanones through cyclobutenone rearrangement began with a study of the rearrangement of phenylcyclobutenone **240a** to 5*H*-furanone **241a** as the yield reported in Moore's paper was poor (27%).[69] Our first experiment sought to replicate Moore's conditions under flow, so THF was used as the solvent and a broad spectrum UVB lamp (280–370 nm) was employed. With a residence

time of 30 min this gave the desired product **241a** in 35% yield. Analysis of the crude reaction mixture indicated that the remaining mass balance contained the starting material and some complex by–products that could not be identified (Entry 1, Table 1). The complete consumption of the starting material was achieved by extending the residence time to 100 min and 120 min. These improved the yield of 5*H*-furanones **241a** to 70% and 54% yield respectively but also presented unidentifiable by-products, which compromised recovery of the target product on purification by column chromatography (Entry 2 and 3, Table 1). Increasing the concentration of the reaction from 0.05 M to 0.1 M also proved unfavourable with only 40% conversion to the desired product, the remained being starting material and by-products (Entry 4, Table 1)

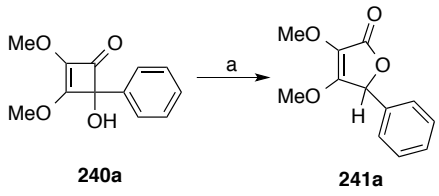

240a **241a**

a) hν, THF, 25 °C.

Entry	*Concentration*	*UV Lamp*	*Time (min)*	*Conversion* Prod:SM:Unknown(s)*
1	0.05M	UVB broad	30	35:55:10
2	0.05 M	UVB broad	100	70:6:24
3	0.05 M	UVB broad	120	54:0:46
4	0.1 M	UVB broad	60	38:37:25
5	0.1 M	UVB narrow	60	46:29:25
* by ^{1}H NMR analysis.				

Table 1: Various conditions used for rearrangement of phenylcyclobutenone **240a→241a.**

An examination of the UV visible spectra of the starting material (Figure 13) and product (Figure 14) indicated that a switch of UV lamp from UVB broad (280–340 nm) to UVB narrow (310–320 nm) might be beneficial. Though the spectra were similar, cyclobutenone **240a** had two absorption bands at 295 and 315 nm, which were not present in the product. By targeting these absorptions, we hoped to reduce side reactions associated with photoexcitation of furanone **241a**. However, only a modest improvement was seen (Entry 4 and 5, Table 1).

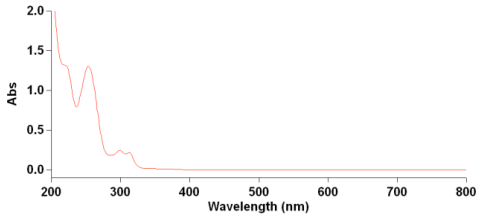

Figure 13: UV visible spectrum for **240a.**

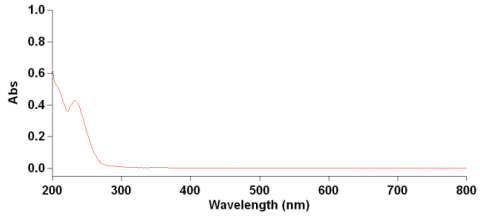

Figure 14: UV visible spectrum for **241a**.

A step change in the performance was realised on changing the solvent from THF to acetonitrile. The rearrangement of **240a→241a** now occurred in near quantitative yield with a residence time of 60 min using the UVB broad lamp (280–370 nm) (Scheme 72).

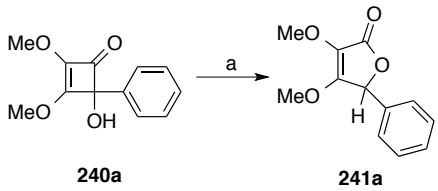

240a **241a**

a) hν, MeCN, 25 °C, 60 min, UVB broad (280-370 nm) 92% (96% conversion).

Scheme 72: Photochemical rearrangement to 5*H*-furanone **240a** using MeCN.

We next decided to examine the effect of wavelength in more detail by inducing the rearrangement of cyclobutenone **240a** with a range of bulbs whilst keeping the concentration and residence time fixed (Table 2). Irradiation using the UVA bulb (360–395 nm), which is outside the absorbance range of the starting material **240a**, showed 8% conversion to the desired product **241a** after 60 min, with the remainder of the mass balance being starting material **240a** (Entry 1, Table 2). In the case of the UVB narrow (310–320 nm) and UVC (254 nm) lamps – which are both within the range of absorbance of **240a** – there was near quantitative consumption of the starting material. However, with the UVC lamp, the crude reaction mixture was less clean, with the appearance of additional signals around the OMe region on the ^{1}H NMR (Figures 15 and 16).

Entry	*Concentration*	*UV bulb*	*Time (min)*	*Conversion* Prod:SM:Unknown*
1	0.05 M	UVA	60	8:92:0
2	0.05 M	UVB narrow	60	97:0:3
3	0.05 M	UVB broad	60	96:4:0
4	0.05 M	UVC	60	N/A
* by ^{1}H NMR analysis.				

Table 2: Effects of different UV bulbs on conversion of **240a→241a**.

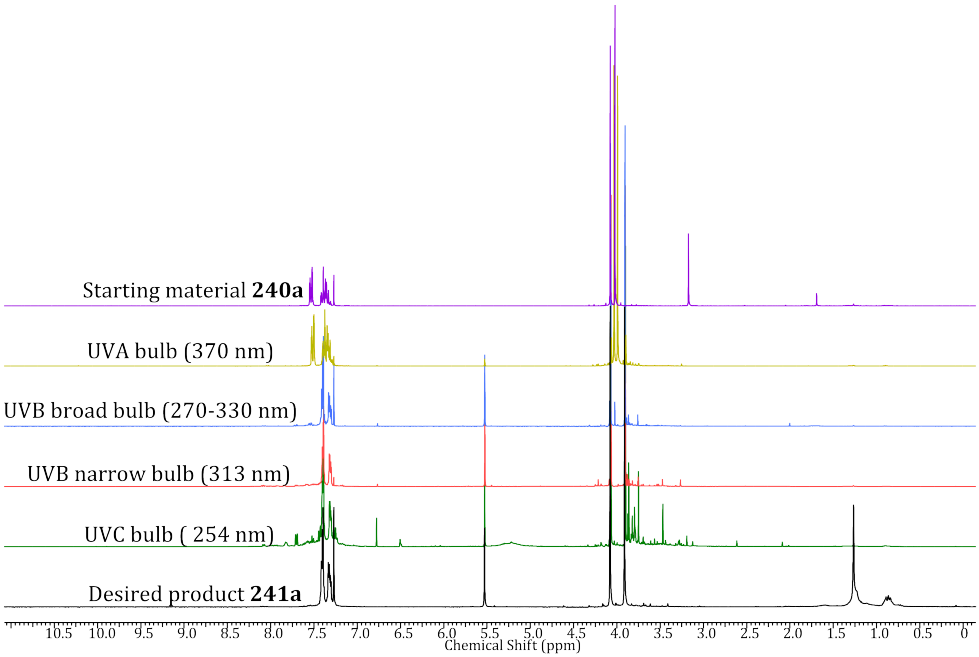

Figure 15: Stacked NMR spectra for 240a→241a using different bulbs.

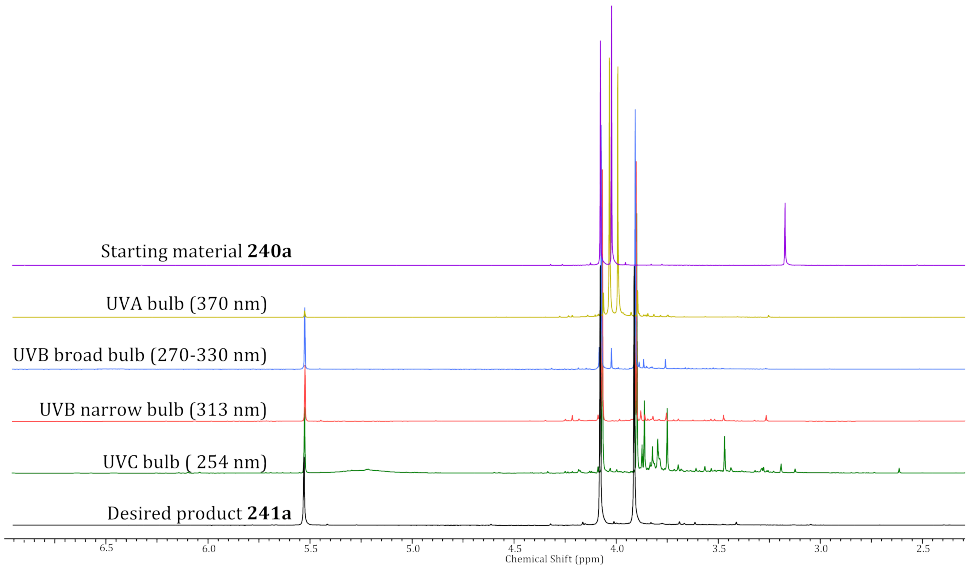

Figure 16: Stacked NMR spectra for **240a→241a** (enlarged OMe region of Figure 5).

Exploring the effect of concentration on the rearrangement showed the reaction to be tolerant of concentrations up to 0.1 M (Entry 1 and 2, Table 3). At higher concentrations there was a drop in efficiency. When the concentration was increased to 0.5 M (Entry 3, Table 3) the conversion to product **241a** decreased to 57% conversion with 39% recovered starting material and some byproduct(s) (*ca.* 4%)(Figure 17).

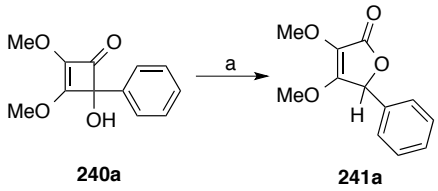

240a **241a**

a) hν, THF, 25 °C.

Entry	*Concentration*	*UV bulb*	*Time (min)*	*Conversion* Prod:SM:Unknown*
1	0.05	UVB broad	60	93:6:0
2	0.1 M	UVB broad	60	95:4:1
3	0.5 M	UVB broad	60	57:39:4
* by ^{1}H NMR analysis.				

Table 3: Effect of concentration on **240a→241a.**

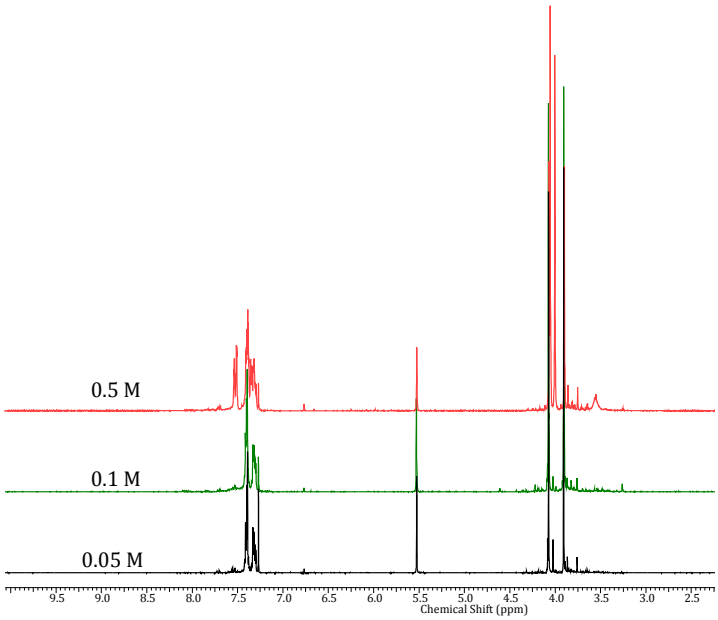

Figure 17: Stacked NMR spectra for **240a→241a** at varying concentrations.

The generality of the above method was explored by first preparing a broad range of 4-hydroxycyclobutanones **240** *via* the addition of alkyl–, aryl– and heteroaryl–lithium reagents to dimethylsquarate **16**. These were then subjected to the optimised reaction conditions for the photochemical rearrangement to give the corresponding 5*H*-furanones **240a-h** in excellent yields (Scheme 73).

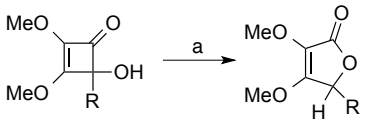

240 **241**

240	R =	Yield 241 (%)
a	Ph	99
b	C≡CPh	95
c	^{t}Bu	97
d	*o*-$MeOC_6H_4$	97
e	^{n}Bu	95
f	*p*-$^{t}BuC_6H_4$	91
g	*p*-$Me_3SiC_6H_4$	92
h	3-pyridyl	94

a) hν, MeCN, 25 °C, 90 min, UVB broad (280–370 nm).

Scheme 73: Summary of the photochemical rearrangement of **240** to **241** under flow.

At this stage, the above results offered credence to the established view that both the thermal and photochemical ring openings of cyclobutenones are tourquoselective processes, with the former giving vinylketene (*Z*)-**14** and the latter its isomer (*E*)-**14** (Scheme 54).

However, when 2-pyridylcyclobutenone **267** was subjected to the aforementioned photochemical conditions, the reaction took longer to run to completion and gave both the expected 5*H*-furanone **241i** and the quinolizinone **268** in roughly equal amounts – the latter being the product attained from the thermal rearrangement of **267**. The remainder of the mass balance was attributed to photochemical decomposition of **268** (Scheme 74).

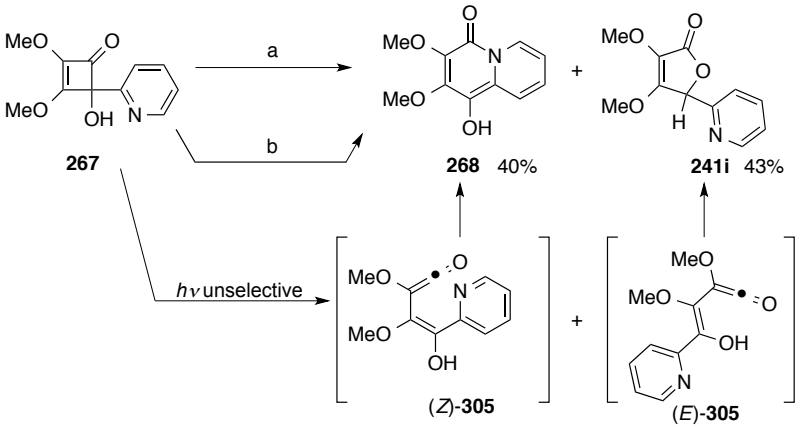

267 **268** 40% **241i** 43%

(*Z*)-**305** (*E*)-**305**

a) hν, MeCN, 25 °C, 150 min, UVB broad (280–370 nm).
b) 1,4-dioxane, 100 °C, flow, 10 min, 99%.

Scheme 74: Photochemical rearrangement of **267**→**268** + **241i**.

This result cast doubt on the view that the photochemical rearrangement of 4-hydroxycyclobutenone **240** proceeds *via* torquoselective ring opening to (*E*)-vinylketene **305** (Scheme 74). Instead, it suggests following photochemical excitation of **240**, the species formed **[240]*** is very high in energy and collapses randomly to give a mixture of (*E*)- and (*Z*)-vinylketenes **306**, with (*E*)-**306** giving cyclisation to furanone **307** *en route* to furanone **241**, while (*Z*)-vinylketene **306** reverts back to the starting cyclobutenone **240** unless it too can be captured by an internal nucleophile, as is the case for 2-pyridylcyclobutenone **267→268** (Scheme 75).

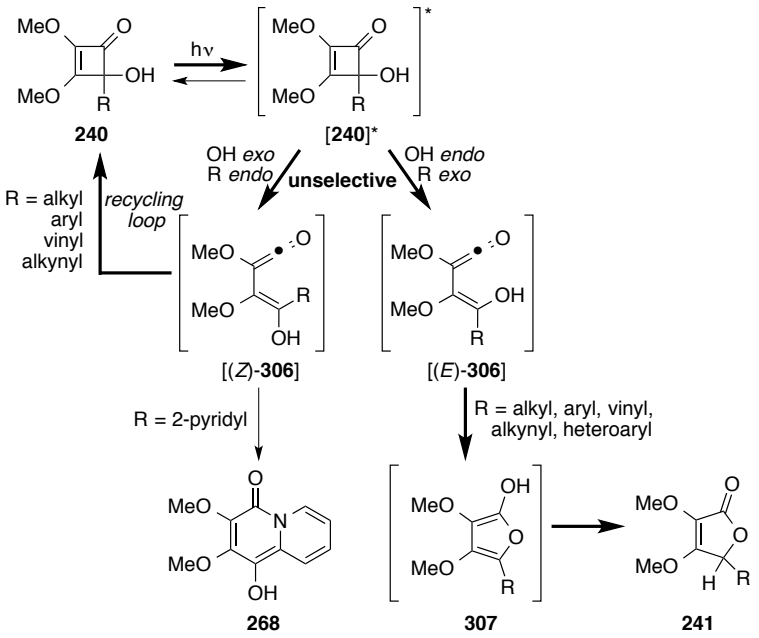

Scheme 75: Revised mechanism for the photochemical rearrangement of 4-hydroxycyclobutenone **240**.

To explore this hypothesis, Theo Gonçalves began a computational investigation of the proposed cyclisation pathways for the intermediate (*E*)- and (*Z*)-vinylketenes **306a** and **305** bearing phenyl and (2-pyridyl) residues respectively. In the case of phenylcyclobutenone **240a**, the calculated barrier for 6π electrocyclic ring closure of vinylketene (*Z*)-**306a** to **308** at 25 °C was 16.7 kcal mol^{-1} and exceeded that for 4π-electrocyclic ring closure back to the starting material **240a** (15.8 kcal mol^{-1}). Pleasingly, this was consistent with our hypothesis for the recycling of intermediate (*Z*)-**306a** (Scheme 76). The situation was reversed for its geometric isomer (*E*)-**306a**, where the calculated barrier for returning back to cyclobutenone **240a** was 20.4 kcal mol^{-1} and exceeded that for cyclisation to furan **307a** (12.4 kcal mol^{-1}). In the thermal

rearrangement of phenylcyclobutenone **240a**, torquoselective ring opening was evident by the higher calculated energy barrier for the formation of (*E*)-vinylketene **306a** (35.0 kcal mol^{-1}) than for (*Z*)-vinylketene **306a** (28.9 kcal mol^{-1}) at 150 °C.

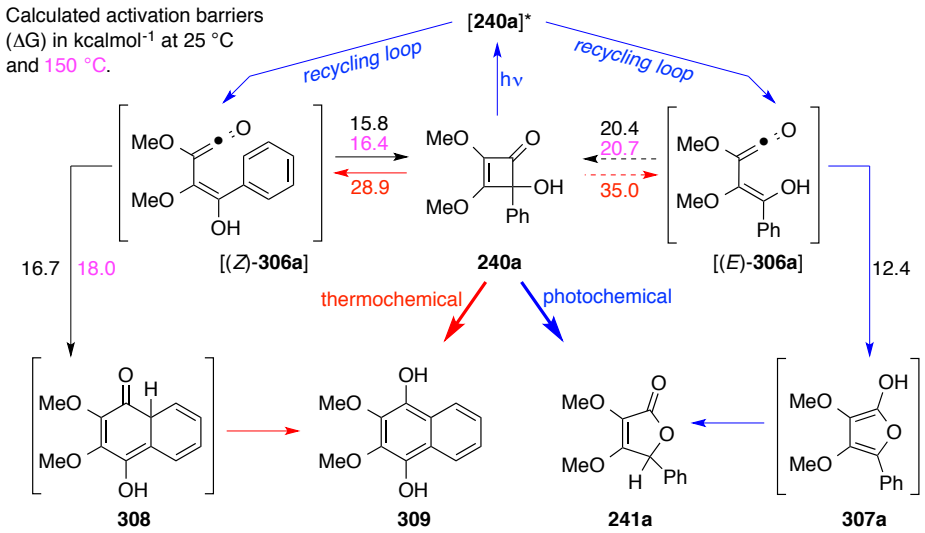

Scheme 76: Calculated energy barriers in rearrangement of **240a.**

In the case of 2-pyridylcyclobutenone **267**, Theo's calculations showed that cyclisation of (*Z*)-vinylketene **305B** to quinolizinone **268** was spontaneous once the appropriate conformer was formed (transformation of (*Z*)-**305A** to (*Z*)-**305B** is lower in energy at 3.5 kcal mol^{-1} than cyclisation of (*Z*)-**305A** to **310**) and therefore diverting it away from the usual recycling loop (Scheme 77). The geometric isomer (*E*)-vinylketene **305** favours cyclisation to furan **307i** (10.9 kcal mol^{-1}) over 4π electrocyclic ring closure back to the starting material **267** (23.2 kcal mol^{-1}) so gives the expected furanone **241i**. Additional calculations showed torquoselectivity in the thermal ring opening of cyclobutenone **267** to (*Z*)-vinylketene **305** and indicated that hydrogen bonding between the pyridine and hydroxyl residue leads to a significant rate enhancement. This was been evident in the thermal rearrangement of 2-pyridylcyclobutenone **267**, which proceeded at a far lower temperature than the related arylcyclobutenones (100 °C for 10 min compared to 150 °C for 1–4 h; Scheme 62).

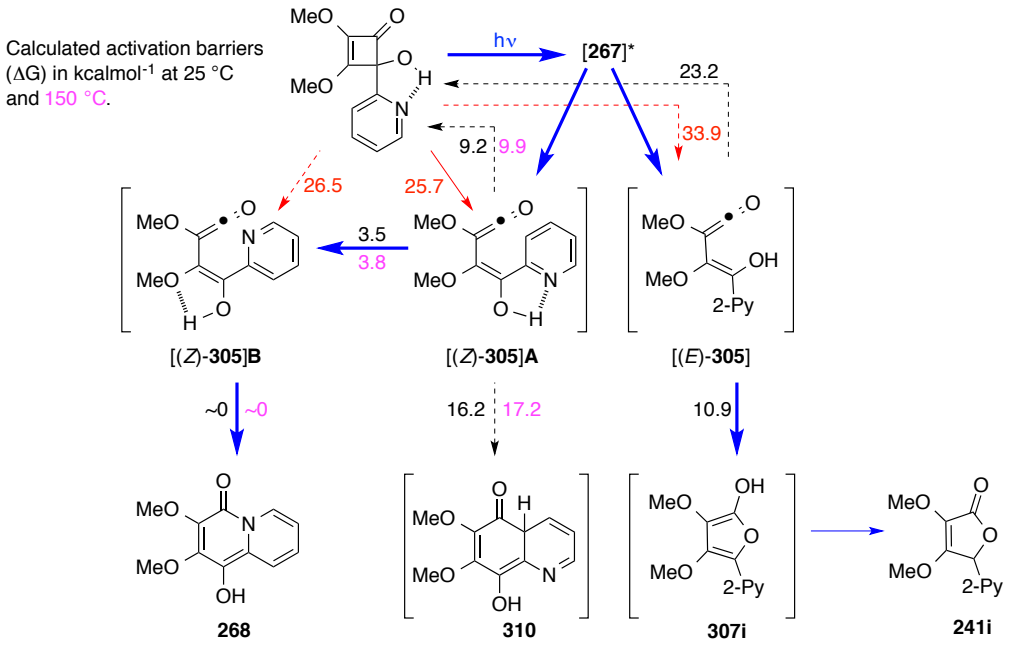

Scheme 77: Calculated activation energies in the photo- and thermochemical rearrangement of **240**.

4.3 Conclusions

Transformations of many 4-hydroxycyclobutenones **240** into 5*H*-furanones **241** have been successfully undertaken in near quantitative yield using an inexpensive flow-photochemical setup. The results attainted allowed an in depth investigation into the mechanistic course of the reaction and cast a doubt on the long-held view that thermal and photochemical rearrangements of cyclobutenones display complementary torquoselectivity in their electrocyclic ring opening to a vinylketene. Rather, results suggest that the photochemical opening of cyclobutenones leads to a mixture of (*E*)- and (*Z*)-vinylketenes **306**. In the case of (*E*)-**306a**, cyclisation to 5*H*-furanone **241a** is facile at ambient temperature and outpaces 4π electrocyclisation back to cyclobutenone **240a**. For (*Z*)-vinylketene **306a**, the opposite is generally true as barriers for their cyclisation are generally higher than the barrier to revert back to starting material. Consequently, it is recycled when no low energy cyclisation path is available to divert it from that course (Scheme 78).

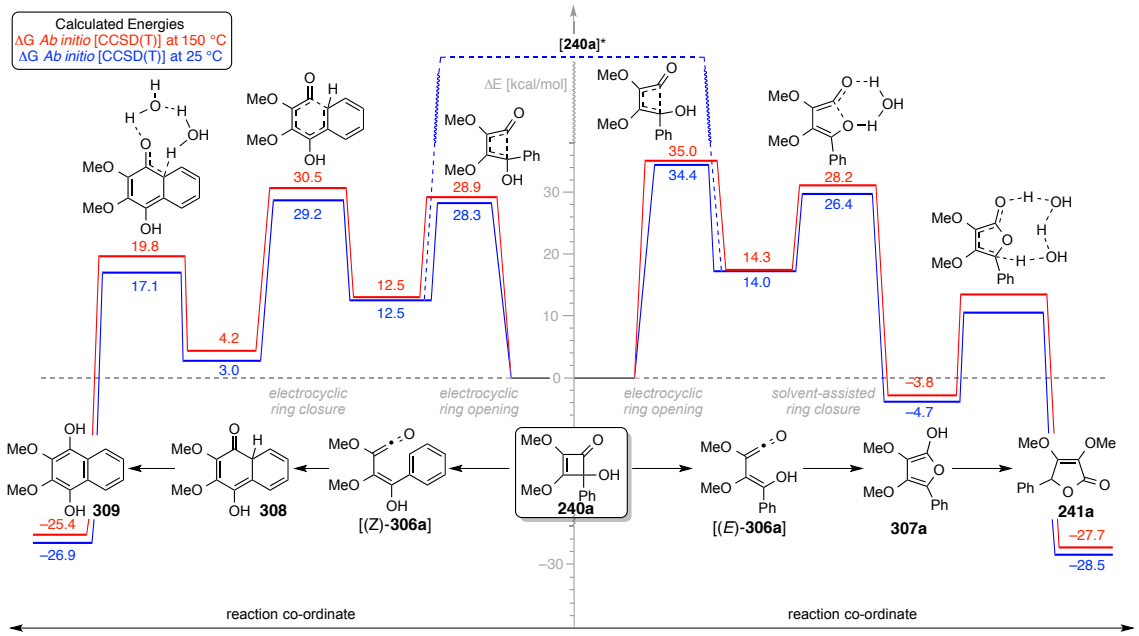

Scheme 78: Summary of data for the rearrangement of **240a** to 5*H*-furanone **241a** and naphthalene **309**.

Chapter 5.Results and Discussion: Rearrangement of Alkynylcyclobutenones

5.1 Strategies and Mechanistic Insights

All calculations were performed by Theo P. Gonçlaves at the B3LYP/6-311(d,p) level using Gaussian 09.

The thermal rearrangement of 4-alkynylcyclobutenones **89** has been the subject of much mechanistic debate since it was first reported by Moore *et al.* in 1985.[21] The formation of quinones **90j** and/or cyclopentendiones **91j**, led to an initial postulate that the reaction proceeded *via* zwitterionic intermediates **312** and **313** (Scheme 79). Although, the mechanism was subsequently revised when computational studies by Hook *et al.* and trapping experiments by Moore and co-workers[23] provided evidence to support the diradical intermediates.

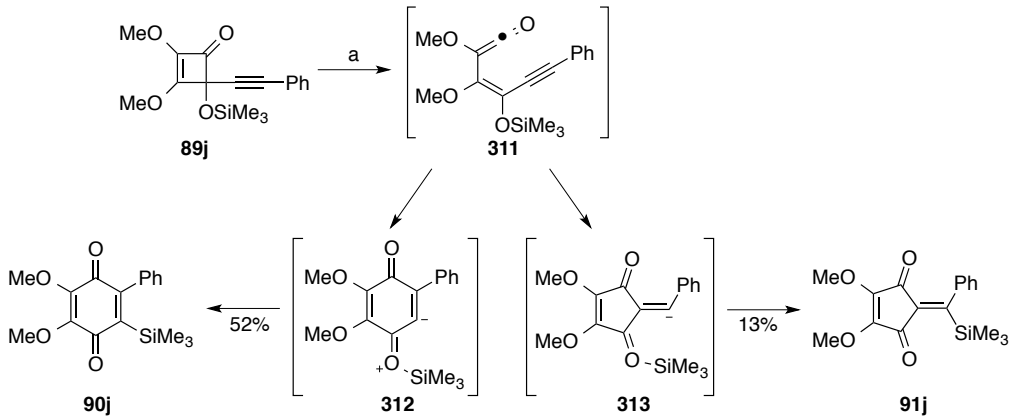

a) *p*-xylene, 135 °C, 2 h.

Scheme 79: Initial postulated mechanism for the thermal rearrangement 4-alkynylcyclobutenones **89** by Moore *et al.*

We first became aware of the importance of the zwitterionic intermediates during studies directed towards the synthesis of isoperezone[22,58] **314** (Scheme 80). Preliminary investigations of the key step on the model system **XX** showed promise. We envisioned that thermolysis of alkynylcyclobutenone **316** would induce ring expansion to diradical intermediate **317**, and hoped that we might use this to induce H-atom abstraction to **318**. Thermolysis at 101 °C in 1,4-dioxane gave the desired product **318** as an inseparable

mixture (1:1 mixture of diastereoisomers) with quinone **320** (1:1 mixture of diastereoisomers) in 60% yield.

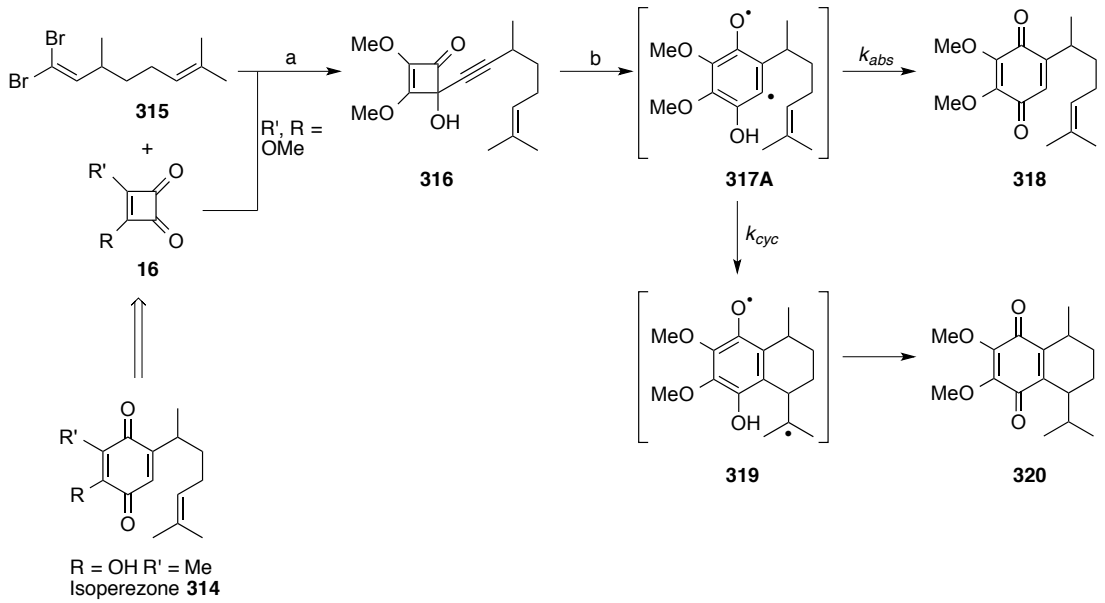

a) **315**, ^{n}BuLi (2 equiv.), –78 °C→RT, 1 h, THF, then **16**, THF –78 °C; b) 1,4-dioxane, 101 °C, 6 h, 63% overall yield containing 24% (**318**) and 36% (**320**).

Scheme 80: Preliminary investigation into the key step for the synthesis of isoperezone **314**.

Consideration of this outcome led us to wonder if we could exploit the deuterium isotope effect to bias the reaction in favour of cyclisation, in order to access an array of related natural products such as (+)-elisabethadione **321**, *O*-methyl-nor-elisabethadione **322** and (–)-mansonone B **194** (Figure 18).

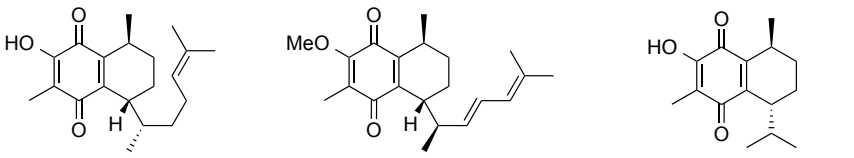

(+)-Elisabethadione **321** *O*-Methyl-Nor-Elisabethadione **322** (–)-Mansonone B **194**

Figure 18: Related natural products to **320**.

We reasoned that deuteration of the phenol in **317A** would slow the rate of H-atom abstraction (k_{abs}) leading to **318**, yet would have little impact on the rate of cyclisation (k_{cyc}) leading to **320**. The experiment was easy to carry out as we simply had to employ D_2O as a co-solvent of the reaction on a simpler substrate **323**. However, the outcome was as remarkable as it was unexpected (Scheme 80). Instead of promoting the radical cyclisation pathway, it shut it down. Indeed, the only product given was the deuterated

quinone d-**325**, which was isolated in 98% yield (Scheme 80). A similar switch in the course of the reaction was observed when the thermolysis was conducted in 1% aqueous 1,4-dioxane, when quinone **325** was given in near quantitative yield.

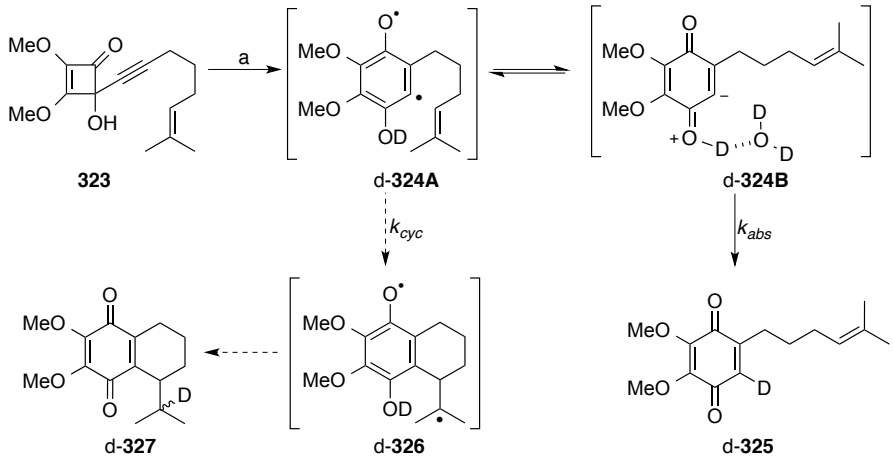

a) 1,4-dioxane (+ 1% D_2O), 150 °C, 30 min, 95%.

Scheme 81: An orbital isomer switch promoted by H_2O and D_2O.

These results made little sense in the context of diradical chemistry, but provided strong evidence for the involvement of the zwitterionic intermediate **324B** (Scheme 80). To test that hypothesis, Theo Gonçalves modelled the course of the reaction using DFT calculations. These showed that in 1,4-dioxane at 150 °C the diradical orbital isomer **324A** was *ca.* 5.2 kcal mol^{-1} lower in energy than its zwitterionic partner **324B**. When water (or D_2O) was included in the calculations the relative stabilities of the diradical and zwitterionic orbital isomers of **324** were reversed, with the latter now favoured by 3.0 kcal mol^{-1}. In this instance, the orbital isomer switch is triggered by the availability of two hydrogen bonds to water (or D_2O), one to the phenol and the other to the carbanion in **324B**. Calculations showed that both the proton transfer **324B**•H_2O→**325**•H_2O and deuterium transfer d-**324B**•D_2O→d-**325**•D_2O steps were spontaneous processes and that, in line with our experimental findings, the barriers presented by the pathways leading to **325** and d-**325** were lower than those for cyclisation of **324A** to **326** or intramolecular H-atom transfer, **324A**→**325**.

Having determined that the C-4 hydroxyl group plays a critical role in promoting the zwitterionic orbital isomer, we next sought to determine how its protection would influence the course of the reaction. To that end, MOM ether **328** was prepared. In line with an earlier observation by Moore (Scheme 27), protection of the alcohol switched the course of the reaction away from **325** in favour of benzopyran **331**, when thermolysis of

328 was conducted at 150 °C in 1,4-dioxane. This is due to the diradical intermediate **329A** favouring H-atom abstraction from the allylic carbon [**329A**]→[**330**] over cyclisation to the alkene [**329A**]→[**332**]. The newly formed diradical intermediate then terminates by radical-radical combination to give **331** in 73% yield.

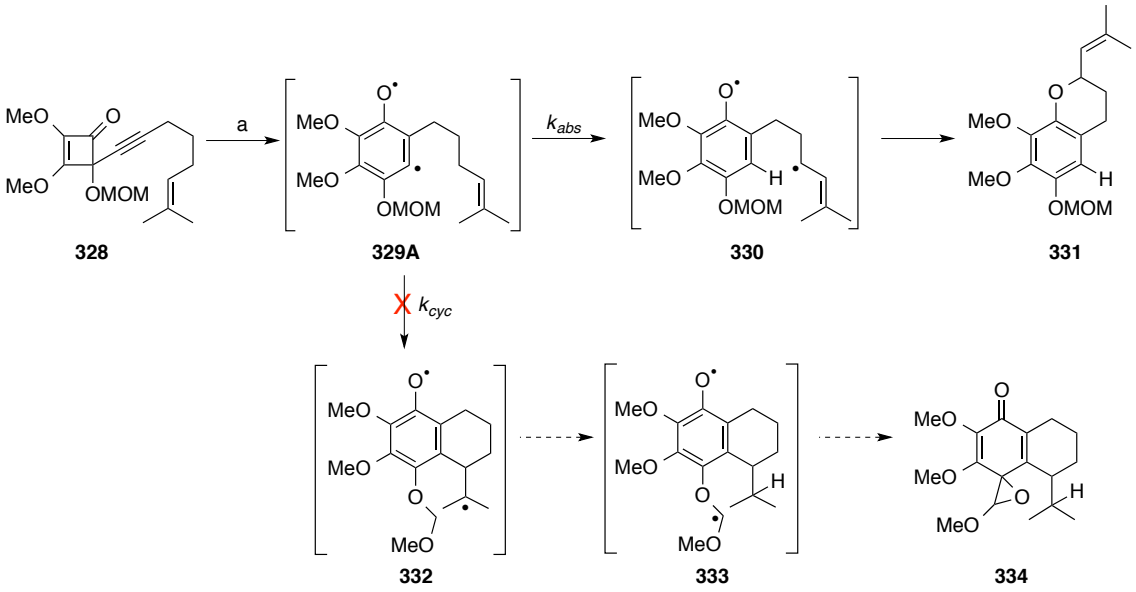

Scheme 82: Influence of the OH protection on the course of the reaction.

Having observed that the thermal rearrangement of alkynylcyclobutenone **323** proceeds *via* the diradical **324A** and zwitterionic oribital isomer **324B**, we began to wonder whether if it could also behave as a cyclohexatrienone. Rearrangements of allyloxyalkynylcyclobutenones, *e.g.* **335→340**, have long been known to proceed with *O*- to *C*-allyl migration. The course of the reaction was rationalised by Moore to proceed *via* a 6-*endo*-trig cyclisation of diradical intermediate **336A** to **339** followed by ring scission to quinone **340**. However, the cyclisation mode this invokes is in stark contrast to the ubiquitous reactivity of *o*-allyloxyaryl radical intermediates, which are commonly used to prepare dihydrobenzofurans *via* 5-*exo*-trig cyclisation, *i.e.* **336A→337** (Scheme 83). To assess whether this proceeds *via* an *ene*-rearrangement, Theo Gonçalves modelled the reaction using DFT calculations and concluded that the reaction proceeded *via* sequential 5-*exo* and 3-*exo* trig cyclisation to **339** and sequential fragmentation to **340** (Scheme 83).

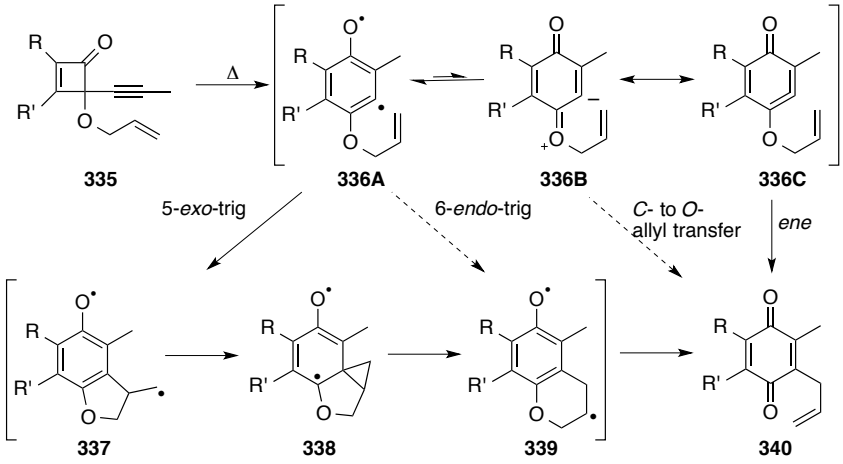

Scheme 83: Rearrangements of allyloxyalkynylcyclobutenones **335**.

Consequently, we needed an alternative approach to trigger the reactivity of the cyclohexatrienone. To that end the C-4 hydroxy group was protected with an acetate group, which was successfully carried out on the unsymmetrical cyclobutendione **185** to give the acetate **341b** in 71% yield. Its thermolysis was then carried out in aqueous 1,4-dioxane at 150 °C and gave a 1:1 mixture of protected hydroquinones **348a** and **348b**. Deprotection of this mixture in 2M aqueous NaOH, gave quinone **349** in 95% yield after aerial oxidation and the structure was confirmed by x-ray cystallogrpahy (Figure 19). The outcome of this reaction provides strong evidence for an intramolecular cyclisation of the acetate group to the proximal cyclohexatrienone **[344C]→[346]** giving intermediate **346**, as its hydrolysis would lead to the primary products **348a** and **348b** (Scheme 84).

In contrast, rearrangement of the unprotected cyclobutenone **341a** in 1,4-dioxane at 150 °C gave a ~1:1 mixture of cyclopentendione **343** and quinone **345**, implicating the diradical intermediates **342A** and **344A** respectively.

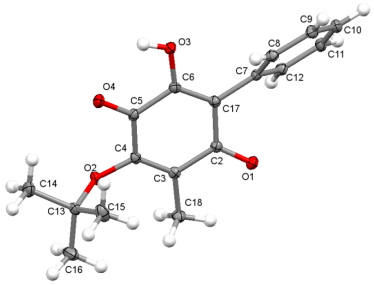

Figure 19: X-ray stricture of **349**.

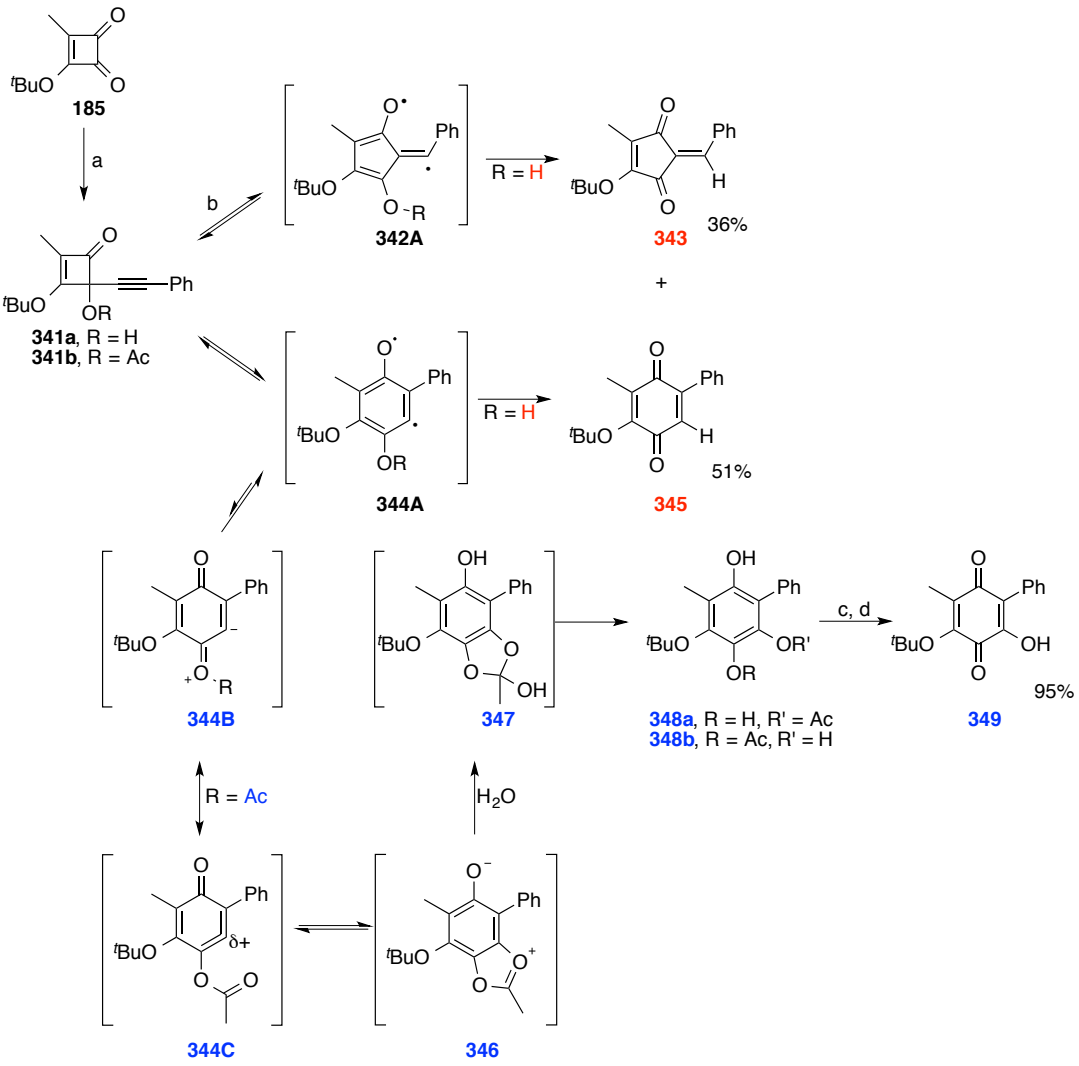

Scheme 84: Rearrangement of cyclobutenone **341**.

5.2 Conclusions

Since the introduction of the thermal rearrangement of 4-alkynylcyclobutenones **83**, the postulated mechanism for the rearrangement to quinones **87** involved diradical intermediate **85A** or zwitterionic intermediate **85B** (Scheme 17). During our studies directed towards the synthesis of isoperezone, we discovered the importance of the diradical intermediate **317A**, which can undergo intramolecular H-atom abstraction to give quinone **318** or radical cyclisation to give **320**. An interesting observation was made with the analogous substrate **323** when the addition of water or D_2O as a co-solvent caused a switch from the diradical intermediate **334A** to its zwitterionic orbital isomer

324B and the shut down of the radical cyclisation pathway. DFT calculations indicated that in 1,4-dioxane at 150 °C the diradical orbital isomer **324A** was *ca.* 5.2 kcal mol^{-1} lower in energy than the zwitterionic isomer **324B**. However, when water (or D_2O) was included in the calculations, the zwitterionic isomer **324B** was more stable than the diradical intermediate **324A** due to hydrogen bonding.

To complete our investigation into the mechanism of alkynylcyclobutenone rearrangements, we wanted to find evidence to implicate cyclohexatrienone **85C**. This was achieved through protection of the hydroxyl group as an acetate **341b**. When subjected to thermolysis, an intramolecular cyclisation of the acetate to the proximal cyclohexatrienone was observed leading to quinone **349** after hydrolysis and oxidation. That outcome, which was predicted by DFT calculations, provides strong evidence for reactivity *via* a cyclohexatrienone.

Chapter 6.Experimental

6.1 General Experimental Techniques

Melting points: Melting points were recorded on a Reichert (Austria) apparatus and are uncorrected.

Infrared Spectra: Infrared spectra were recorded neat as a thin film or a solid compression using the Golden Gate ATR method. Absorption maxima (υ_{max}) are expressed as s, strong; m, medium; w, weak and are quoted in wavenumbers (cm^{-1}).

NMR Spectra: Proton (^{1}H) and carbon (^{13}C) spectra were recorded on a Bruker DPX300 (300/75 MHz), Bruker DPX400 (400/100 MHz) or Bruker DPX600 (600/150 MHz) spectrometer at 298 K. Experiments were carried out in deuterated chloroform ($CDCl_3$) unless otherwise stated, which was supplied by Goss Scientific and stored over dried K_2CO_3 to neutralise trace acidity. Chemical shifts are reported in parts per million (ppm) downfield of tetramethylsilane with residual solvent as the internal standard. Assignments were made on the basis of chemical shifts, coupling constants, DEPT-135, COSY, HMQC and comparison with literature values where available. Resonance are depicted as s (singlet), d (doublet), t (triplet), q (quartet) m (multiplet), dd (double of doublet), dt (doublet of triplets), br. s (broad singlet), br. (broad) and app. (apparent). Coupling constants (*J*) are given in Hz and are rounded to the nearest 0.1 Hz.

Mass spectra: Electrospray mass spectrometry was carried out on a directly injected Waters quadrupole MSD using ES+ or ES– ionisation with MeOH or acetonitrile as solvent. *m/z* values are reported with their respective abundance and the fragment ion. High resolution mass spectra were recorded by Bill Leverns at GlaxoSmithKline or Dr John Langley, Ms. Julie Herniman, or Dr. Jaclyn Johnson at the University of Southampton and are calculated to four decimal places from the molecular formula.

Liquid chromatography-mass spectrometry (LCMS): The analysis was conducted on Waters ZQ machine, using an Acquity UPLC BEH C18 column (50mm x 2.1mm i.d. 1.7µm packing diameter) at 40 ˚C.

The solvents employed for high pH were, A = 10 mM Ammonium Bicarbonate in water adjusted to pH 10 with ammonia solution and B = Acetonitrile, employing a gradient from 0–100% over 2 min.

The solvents employed for low pH were, A = 0.1% v/v solution of Formic Acid in Water and B = 0.1% v/v solution of Formic Acid in Acetonitrile, employing a gradient from 0–100% over 2 min.

Chromatography Technique: Thin layer chromatography was carried out on Merck Silica Gel 60 Å F 254 0.2 mm plates, which were visualised under fluorescence UV (254 nm) followed by staining with aqueous 1% $KMnO_4$, methanolic H_2SO_4, methanolic vanillin and / or iodine. Flash chromatography was carried out under pressure on silica gel with the appropriate solvent system.

Solvents and Reagents: Reagents that were commercially available were purchased and used without further purification unless stated otherwise. All solvents were distilled prior to use. THF, diethyl ether and benzene were all distilled from sodium benzophenone ketyl under argon. Toluene was distilled from sodium under argon. Pyridine, triethylamine and dichloromethane were distilled from calcium hydride under argon. All air sensitive reactions were carried out under argon or nitrogen using flame or oven dried apparatus.

6.2 Experimental Procedures for Chapter 3

3,4-Dimethoxycyclobut-3-ene-1,2-dione; dimethyl squarate (16)

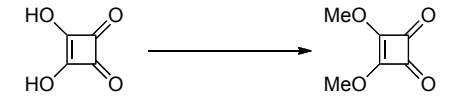

$C_4H_2O_4$
Mol Wt: 114.06

$C_6H_6O_4$
Mol Wt: 142.11

To a suspension of squaric acid (10.0 g, 88 mmol) in MeOH (180 mL) was added trimethyl orthoformate (19.7 mL, 180 mmol). The resulting mixture was refluxed for 24 h then cooled to RT and concentrated *in vacuo* and purified by column chromatography (0%→50% EtOAc:petroleum ether) to afford the title compound as a white solid (11.02 g, 77 mmol, 88%).

Data is consistent with literature.[119]

MP	52–54 °C (EtOAc/petroleum ether).
υ_{max} ($CHCl_3$)	2964 (w), 1811 (m), 1728 (s), 1597 (s), 1480 (s).
δ_H (300 MHz, $CDCl_3$)	4.38 (6 H, s, 2 x OC**H**$_3$).
δ_C (75 MHz, $CDCl_3$)	189.1 (**C** x 2), 184.5 (**C** x 2), 60.9 (**C**H_3 x 2).
LRMS (ES+)	175 ([M+H+MeOH]$^+$, 100%), 197 ([M+Na+MeOH]$^+$, 41%).

4-Hydroxy-2,3-dimethoxy-4-phenylcyclobut-2-enone (258a)

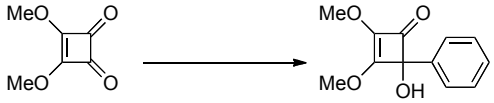

$C_6H_6O_4$
Mol Wt: 142.11

$C_{12}H_{12}O_4$
Mol Wt: 220.22

To a solution of bromobenzene (1.63 mL, 15.5 mmol) in THF (100 mL) at –78 °C was added ^{n}BuLi (2.47 M in hexanes, 6.3 mL, 15.5 mmol) dropwise. After 30 min the resulting solution was added *via* cannula to a solution of dimethyl squarate (2.00 g, 14.1 mmol) in THF (100 mL) at –78 °C, giving a bright yellow solution. After 20 min sat. NH_4Cl (75 mL) was added. The reaction mixture was allowed to warm to RT then extracted with DCM (75 mL x 3). The combined organic layers were washed with brine (50 mL x 2), dried ($MgSO_4$), filtered, concentrated *in vacuo* and purified by flash column chromatography (5%→50% EtOAc:petroleum ether with 2% NEt_3) to afford the title compound as a white solid (2.406 g, 10.93 mmol, 78%).

Data is consistent with literature.[14]

MP	100–102 °C (diethyl ether/petroleum ether).
υ_{max} ($CHCl_3$)	3403 (m), 2986 (w), 2862 (w), 1772 (m), 1624 (s), 1468 (s), 1341 (s), 1049 (m), 984 (w), 836 (s).
δ_H (300 MHz, $CDCl_3$)	7.54 (2 H, dd, *J*=8.8, 1.5 Hz, 2 x Ar**H**)
	7.42–7.34 (3 H, m, 3 x Ar**H**)
	4.08 (3 H, s, OC**H**$_3$)
	4.02 (3 H, s, OC**H**$_3$)
	3.17 (1 H, br. s, O**H**).
δ_C (75 MHz, $CDCl_3$)	183.6 (**C**=O), 165.9 (**C**), 137.1 (**C**), 135.3 (**C**), 128.6 (**C**H x 2), 128.5 (**C**H), 125.8 (**C**H x 2), 87.7 (**C**), 60.2 (O**C**H$_3$), 58.7 (O**C**H$_3$).
LRMS (ES+)	243 ([M+Na]$^+$, 100%), 275 ([M+Na+MeOH]$^+$, 87%).

4-Hydroxy-2,3-dimethoxy-4-(*p*-tolyl)cyclobut-2-enone (258b)

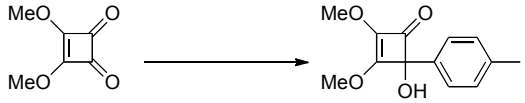

$C_6H_6O_4$
Mol Wt: 142.11

$C_{13}H_{14}O_4$
Mol Wt: 234.25

To a solution of *p*-bromotoluene (1.26 mL, 7.37 mmol) in THF (70 mL) at –78 °C was added ^{n}BuLi (2.47 M in hexanes, 2.99 mL, 7.39 mmol) dropwise. After 30 min the resulting solution was added *via* cannula to a solution of dimethyl squarate (1.00 g, 7.04 mmol) in THF (30 mL) at –78 °C, giving an orange solution. After 1 h sat. NH_4Cl (75 mL) was added. The reaction mixture was allowed to warm to RT and extracted with DCM (50 mL x 3). The combined organic layers were washed with brine (50 mL x 2), dried ($MgSO_4$), filtered, concentrated *in vacuo* and purified by flash column chromatography (5%→40% EtOAc:petroleum ether with 2% NEt_3) to afford the title compound as a white solid (0.746 g, 3.39 mmol, 48%).

Data is consistent with literature.[6]

MP	123–125 °C (diethyl ether/petroleum ether).
υ_{max} ($CHCl_3$)	3387 (m), 2953 (w), 2360 (s), 2343 (s), 1773 (m), 1623 (s), 1467 (m), 1339 (s), 1050 (w), 995 (w), 854 (w).
δ_H (400 MHz, $CDCl_3$)	7.42 (2 H, d, *J*=8.1 Hz, 2 x Ar**H**)
	7.20 (2 H, d, *J*=8.1 Hz, 2 x Ar**H**)
	4.08 (3 H, s, OC**H**$_3$)
	4.02 (3 H, s, OC**H**$_3$)
	2.72 (1 H, s, O**H**)
	2.36 (3 H, s, C**H**$_3$).
δ_C (100 MHz, $CDCl_3$)	184.0 (**C**=O), 166.0 (**C**), 138.3 (**C**), 135.2 (**C**), 134.1 (**C**), 129.3 (**C**H x 2), 125.7 (**C**H x 2), 87.5 (**C**), 60.2 (O**C**H$_3$), 58.7 (O**C**H$_3$), 21.2 (Ar–**C**H$_3$).
LCMS (ES+)	235 ([M+H]$^+$, 70%).

4-Hydroxy-2,3-dimethoxy-4-(4-(trimethylsilyl)phenyl)cyclobut-2-enone (258c)

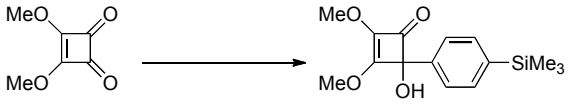

$C_6H_6O_4$
Mol Wt: 142.11

$C_{15}H_{20}O_4Si$
Mol Wt: 292.40

To a stirred solution ^{n}BuLi (2.40 M in hexanes, 3.52 mL, 8.84 mmol) in THF (30 mL) at –78 °C was added 1-bromo-4-(trimethylsilyl)benzene (1.65 mL, 8.44 mmol) dropwise. After 30 min the resulting solution was added *via* cannula to a solution of dimethyl squarate (1.00 g, 7.04 mmol) in THF (30 mL) at –78 °C, giving a red solution. After 20 min sat. NH_4Cl (75 mL) was added. The reaction mixture was allowed to warm to RT then extracted with DCM (50 mL x 3). The combined organic layers were washed with brine (50 mL x 2), dried ($MgSO_4$), filtered, concentrated *in vacuo* and purified by flash column chromatography (0%→40% EtOAc:petroleum ether with 2% NEt_3) to afford the title compound as a white solid (1.26 g, 4.34 mmol, 61%).

MP	150–152 °C (diethyl ether/petroleum ether).
υ_{max} ($CHCl_3$)	2954 (w), 2360 (s), 2341 (s), 1772 (m), 1622 (s), 1467 (s), 1337 (s), 1049 (m), 836 (s).
δ_H (300 MHz, $CDCl_3$)	7.56 (2 H, d, *J*=8.4 Hz, 2 x Ar**H**)
	7.52 (2 H, d, *J*=8.4, Hz 2 x Ar**H**)
	4.10 (3 H, s, OC**H**$_3$)
	4.03 (3 H, s, OC**H**$_3$)
	2.62 (1 H, s, O**H**)
	0.27 (9 H, s, Si(C**H**$_3$)$_3$).
δ_C (75 MHz, $CDCl_3$)	202.0 (**C**=O), 167.0 (**C**), 142.1 (**C**), 138.7 (**C**), 136.5 (**C**), 134.7 (**C**H x 2), 126.2 (**C**H x 2), 88.9 (**C**), 61.5 (O**C**H$_3$), 59.9 (O**C**H$_3$), 0.00 (Si(**C**H$_3$)$_3$).
LRMS (ES+)	356 ([M+MeCN+Na]$^+$, 100%).
HRMS (ES+)	Found 315.1023, $C_{15}H_{20}NaO_4Si$ [M+Na]$^+$ requires 315.1029.

4-(4-(*tert*-Butyl)phenyl)-4-hydroxy-2,3-dimethoxycyclobut-2-enone (258d)

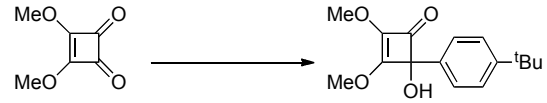

$C_6H_6O_4$
Mol Wt: 142.11

$C_{16}H_{20}O_4$
Mol Wt: 276.33

To a solution of 1-bromo-4-*tert*-butylbenzene (1.5 mL, 8.44 mmol) in THF (30 mL) at –78 °C was added ^{n}BuLi (2.40 M in hexanes, 3.52 mL, 8.44 mmol) over 3 min. After 30 min the resulting solution was added *via* cannula to a solution of dimethyl squarate (1.00 g, 7.04 mmol) in THF (30 mL) at –78 °C, giving an orange solution. After 30 min sat. NH_4Cl (75 mL) was added. The reaction mixture was allowed to warm to RT then extracted with DCM (20 mL x 3). The combined organic layers were washed with brine (20 mL x 2), dried ($MgSO_4$), filtered, concentrated *in vacuo* and purified by flash column chromatography (0%→15% EtOAc:petroleum ether with 2% NEt_3) to afford the title compound as a white solid (1.68 g, 6.10 mmol, 87%).

MP	179–181 °C (diethyl ether/petroleum ether).
υ_{max} ($CHCl_3$)	3385 (m), 2958 (m), 2360 (s), 2341 (s), 1772 (m), 1624 (s), 1467 (s), 1337 (s), 1051 (m), 994 (w), 859 (w).
δ_H (400 MHz, $CDCl_3$)	7.46 (2 H, d, *J*=8.5 Hz, 2 x Ar**H**)
	7.41 (2 H, d, *J*=8.5 Hz, 2 x Ar**H**)
	4.10 (3 H, s, OC**H**$_3$)
	4.02 (3 H, s, OC**H**$_3$)
	2.92 (1 H, s, O**H**)
	1.32 (9 H, s, C(C**H**$_3$)$_3$).
δ_C (100 MHz, $CDCl_3$)	184.5 (**C**=O), 166.4 (**C**), 151.9 (**C**), 135.6 (**C**), 134.5 (**C**), 126.0 (**C**H x 2), 125.9 (**C**H x 2), 87.9 (**C**), 60.7 (O**C**H$_3$), 59.1 (O**C**H$_3$), 35.0 (**C**), 31.7 ((**C**H$_3$)$_3$).
LRMS (ES+)	299 ([M+Na]$^+$, 100%).
HRMS (ES+)	Found 299.1257, $C_{16}H_{20}NaO_4$ [M+Na]$^+$ requires 299.1259.

4-([1,1'-Biphenyl]-4-yl)-4-hydroxy-2,3-dimethoxycyclobut-2-enone (258e)

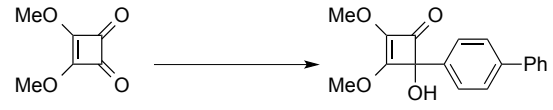

$C_6H_6O_4$
Mol Wt: 142.11

$C_{18}H_{16}O_4$
Mol Wt: 296.32

To a solution of 4-bromobiphenyl (1.00 g, 4.29 mmol) in THF (30 mL) at –78 °C was added ^{n}BuLi (3.15 mL, 1.5 M solution in hexane, 4.72 mmol) dropwise. After 15 min the resulting solution was added *via* cannula to a solution of dimethyl squarate (0.70 g, 4.93 mmol) in THF (30 mL) at –78 °C, giving an orange solution. After 15 min sat. NH_4Cl (75 mL) was added. The reaction mixture was allowed to warm to RT then extracted with DCM (50 mL x 3). The combined organic layers were washed with brine (50 mL x 2), dried ($MgSO_4$), filtered, concentrated *in vacuo* and purified by flash column chromatography (0%→15% EtOAc:petroleum ether with 2% NEt_3) to afford the title compound as a white solid (0.261 g, 0.879 mmol, 20%).

MP	170–172 °C (diethyl ether/petroleum ether).
υ_{max} ($CHCl_3$)	3377 (m), 3028 (w), 2950 (w), 1770 (m), 1619 (s), 1486 (s), 1336 (s), 1050 (m), 994 (w), 761 (m).
δ_H (300 MHz, $CDCl_3$)	7.68 - 7.53 (6 H, m, 6 x Ar**H**)
	7.50–7.41 (2 H, m, 2 x Ar**H**)
	7.40–7.31 (1 H, m, Ar**H**)
	4.12 (3 H, s, OC**H**$_3$)
	4.05 (3 H, s, OC**H**$_3$)
	3.07 (1 H, s, O**H**).
δ_C (75 MHz, $CDCl_3$)	183.8 (**C**=O), 165.9 (**C**), 141.4 (**C**), 140.6 (**C**), 136.0 (**C**), 134.4 (**C**), 128.8 (**C**H x 2), 127.5 (**C**H), 127.4 (**C**H x 2), 127.1 (**C**H x 2), 126.3 (**C**H x 2), 87.6 (**C**), 60.3 (O**C**H$_3$), 58.7 (O**C**H$_3$).
LCMS (ES+)	297 ($[M+H]^+$, 100%).
HRMS (ES+)	Found 319.0939, $C_{18}H_{16}NaO_4$ $[M+Na]^+$ requires 319.0946.

_N_,_N_-Diisopropyl-4-(1-hydroxy-2,3-dimethoxy-4-oxocyclobut-2-en-1-yl)-benzamide (258f)

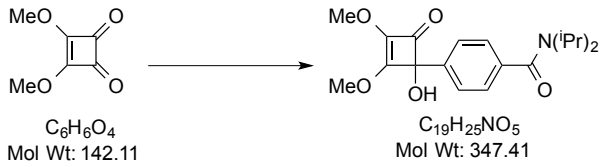

To a solution of *N*,*N*-diisopropyl-4-bromobenzamide (1.20 g, 4.22 mmol) in THF (20 mL) at –78 °C was added ^{n}BuLi (1.76 mL, 2.4 M solution in hexane, 4.22 mmol) dropwise. After 20 min the resulting solution was added *via* cannula to a solution of dimethyl squarate (0.50 g, 3.52 mmol) in THF (20 mL) at –78 °C, giving a yellow solution. After 30 min sat. NH_4Cl (75 mL) was added. The reaction mixture was allowed to warm to RT then extracted with DCM (20 mL x 3). The combined organic layers were washed with brine (20 mL x 2), dried ($MgSO_4$), filtered, concentrated *in vacuo* and purified by flash column chromatography (0%→75% EtOAc:petroleum ether with 2% NEt_3) to afford the title compound as a white solid (0.139 g, 0.40 mmol, 18%).

MP	98–100 °C (diethyl ether/petroleum ether).
υ_{max} ($CHCl_3$)	3308 (m), 2966 (w), 2360 (s), 2342 (s), 1772 (w), 1636 (m), 1338 (s), 1054 (w), 995 (w).
δ_H (400 MHz, $CDCl_3$)	7.55 (2 H, d, *J*=7.5 Hz, 2 x Ar**H**)
	7.33 (2 H, d, *J*=7.5 Hz, 2 x Ar**H**)
	4.07 (3 H, s, OC**H**$_3$)
	4.05 (3 H, s, OC**H**$_3$)
	3.65 (2 H, br. s, N((C**H**$(CH_3)_2)_2$)
	2.70 (1 H, s, O**H**)
	1.32 (12 H, br. s, N((CH(C**H**$_3)_2)_2$).
δ_C (100 MHz, $CDCl_3$)	207.3 (**C**=O), 183.8 (**C**=O), 171.1 (**C**), 166.1 (**C**), 139.2 (**C**), 138.0 (**C**), 126.5 (**C**H x 2), 126.3 (**C**H x 2), 87.2 (**C**), 60.7 (O**C**H_3), 59.1 (O**C**H_3), 31.3 (**C**H x 2), 21.1 (**C**H_3 x 4).
LRMS (ES+)	348 ($[M+H]^+$, 100%).

4-Hydroxy-2,3-dimethoxy-4-(4-methoxyphenyl)cyclobut-2-enone (258g)

$C_6H_6O_4$
Mol Wt: 142.11

$C_{13}H_{14}O_5$
Mol Wt: 250.25

To a solution of *p*-bromoanisole (0.97 mL, 7.74 mmol) in THF (70 mL) at –78 °C was added ^{n}BuLi (3.14 mL, 2.47 M solution in hexane, 7.74 mmol) dropwise. After 30 min the resulting solution was added *via* cannula to a solution of dimethyl squarate (1.00 g, 7.04 mmol) in THF (10 mL) at –78 °C, giving a yellow solution. After 1 h sat. NH_4Cl (50 mL) was added. The reaction mixture was allowed to warm to RT then extracted with DCM (50 mL x 3). The combined organic layers were washed with brine (50 mL x 2), dried ($MgSO_4$), filtered, concentrated *in vacuo* and purified by flash column chromatography (5%→50% EtOAc:petroleum ether with 2% NEt_3) to afford the title compound as an off-white solid (0.534 g, 2.14 mmol, 30%).

Data is consistent with literature.[6]

MP	98–100 °C (diethyl ether/petroleum ether).
υ_{max} ($CHCl_3$)	3392 (m), 2953 (w), 2839 (w), 2359 (s), 2342 (s), 1771 (m), 1619 (s), 1511 (s), 1466 (s), 1386 (s), 1048 (s), 992 (m), 854 (m).
δ_H (300 MHz, $CDCl_3$)	7.45 (2 H, d, *J*=8.8 Hz, 2 x Ar**H**)
	6.90 (2 H, d, *J*=8.8 Hz, 2 x Ar**H**)
	4.07 (3 H, s, OC**H**$_3$)
	4.01 (3 H, s, OC**H**$_3$)
	3.81 (3 H, s, Ar-OC**H**$_3$)
	2.75 (1 H, s, O**H**).
δ_C (75 MHz, $CDCl_3$)	184.4 (**C**=O), 166.3 (**C**), 159.6 (**C**), 135.1 (**C**), 129.3 (**C**), 127.1 (**C**H x 2), 114.0 (**C**H x 2), 87.2 (**C**), 60.2 (O**C**H$_3$), 58.6 (O**C**H$_3$), 55.3 (Ar-O**C**H$_3$).
LRMS (ES+)	273 ([M+Na]$^+$, 100%).

4-(4-Fluorophenyl)-4-hydroxy-2,3-dimethoxycyclobut-2-enone (258h)

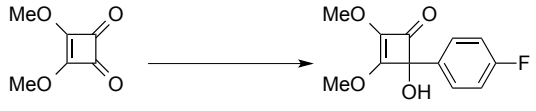

$C_6H_6O_4$
Mol Wt: 142.11

$C_{12}H_{11}FO_4$
Mol Wt: 238.21

To a solution of 1-bromo-4-fluorobenzene (0.69 mL, 6.34 mmol) in THF (30 mL) at –78 °C was added ^{n}BuLi (2.63 mL, 2.46 M solution in hexane, 6.34 mmol) dropwise. After 30 min the resulting solution was added *via* cannula to a solution of dimethyl squarate (0.75 g, 5.28 mmol) in THF (30 mL) at –78 °C, giving a yellow solution. After 30 min sat. NH_4Cl (30 mL) was added. The reaction mixture was allowed to warm to RT then extracted with DCM (20 mL x 3). The combined organic layers were washed with brine (20 mL x 2), dried ($MgSO_4$), filtered, concentrated *in vacuo* and purified by flash column chromatography (0%→40% EtOAc:petroleum ether with 2% NEt_3) to afford the title compound as a white solid (0.31 g, 2.05 mmol, 39%).

MP	98–100 °C (diethyl ether/petroleum ether).
υ_{max} ($CHCl_3$)	3385 (m), 2954 (w), 2360 (s), 2341 (s), 1772 (s), 1601 (s), 1468 (s), 1337 (s), 1047 (s), 994 (m), 858 (m).
δ_H (300 MHz, $CDCl_3$)	7.52 (2 H, dd, *J*=8.8, 5.3 Hz, 2 x Ar**H**)
	7.08 (2 H, app. t, *J*=8.8 Hz, 2 x Ar**H**)
	4.11 (3 H, s, OC**H**$_3$)
	4.04 (3 H, s, OC**H**$_3$)
	2.67 (1 H, s, O**H**).
δ_C (75 MHz, $CDCl_3$)	184.0 (**C**=O), 166.1 (**C**), 161.5 (**C**), 135.3 (**C**), 133.0 (**C**), 127.8 (**C**H x 2), 115.4 (**C**H x 2), 87.2 (**C**), 60.3 (O**C**H$_3$), 58.7 (O**C**H$_3$).
δ_F (282 MHz, $CDCl_3$)	–113.5 (C**F**);
LRMS (ES+)	477 ([2M+H]$^+$, 100%).

4-Hydroxy-2,3-dimethoxy-4-(4-(trifluoromethyl)phenyl)cyclobut-2-enone (258i)

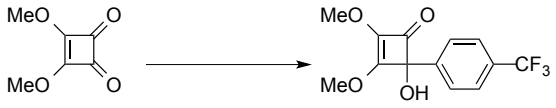

$C_6H_6O_4$
Mol Wt: 142.11

$C_{13}H_{11}F_3O_4$
Mol Wt: 288.22

To a solution of 1-bromo-4-(trifluoromethyl)-benzene (0.54 mL, 3.87 mmol) in THF (20 mL) at –78 °C was added ^{n}BuLi (1.57 mL, 2.47 M solution in hexane, 3.87 mmol) dropwise. After 30 min the resulting solution was added *via* cannula to a solution of dimethyl squarate (0.50 g, 3.52 mmol) in THF (20 mL) at –78 °C, giving an orange solution. After 20 min sat. NH_4Cl (30 mL) was added. The reaction mixture was allowed to warm to RT then extracted with DCM (20 mL x 3). The combined organic layers were washed with brine (20 mL x 2), dried ($MgSO_4$), filtered, concentrated *in vacuo* and purified by flash column chromatography (5%→50% EtOAc:petroleum ether with 2% NEt_3) to afford the title compound as a white solid (0.59 g, 2.05 mmol, 59%).

MP	180–182 °C (diethyl ether/petroleum ether).
υ_{max} ($CHCl_3$)	3365 (m), 2956 (w), 2360 (s), 2341 (s), 1772 (m), 1616 (s), 1470 (s), 1324 (s), 994 (m), 864 (w).
δ_H (300 MHz, $CDCl_3$)	7.64 (4 H, app. s, 4 x Ar**H**)
	4.08 (3 H, s, OC**H**$_3$)
	4.03 (3 H, s, OC**H**$_3$)
	2.62 (1 H, s, O**H**).
δ_C (75 MHz, $CDCl_3$)	183.0 (**C**=O), 165.6 (**C**), 141.0 (**C**), 138.7 (**C**), 136.5 (**C**), 126.8 (**C**H x 2), 125.9 (**C**H x 2), 87.4 (**C**), 60.4 (O**C**H$_3$), 58.8 (O**C**H$_3$).
δ_F (282 MHz, $CDCl_3$)	–62.8 (C**F**$_3$).
LCMS (ES+)	287 ([M–H]$^-$, 64%).
HRMS (ES+)	Found 311.0507, $C_{13}H_{11}F_3NaO_4$ [M+Na]$^+$ requires 311.0507.

4-Hydroxy-2,3-dimethoxy-4-(pyridin-2-yl)cyclobut-2-enone (267)

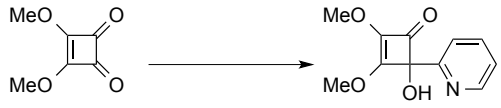

$C_6H_6O_4$
Mol Wt: 142.11

$C_{11}H_{11}NO_4$
Mol Wt: 221.21

To a solution of 2-bromopyridine (0.82 mL, 8.45 mmol) in THF (30 mL) at –78 °C was added ^{n}BuLi (3.52 mL, 2.40 M solution in hexane, 8.45 mmol) dropwise. After 15 min the resulting solution was added *via* cannula to a solution of dimethyl squarate (1.00 g, 7.04 mmol) in THF (10 mL) at –78 °C, giving a red solution. After 30 min sat. NH_4Cl (20 mL) was added. The reaction mixture was allowed to warm to RT then extracted with DCM (50 mL x 3). The combined organic layers were washed with brine (50 mL x 2), dried ($MgSO_4$), filtered, concentrated *in vacuo* and purified by flash column chromatography (5%→50% EtOAc:petroleum ether with 2% NEt_3) to afford the title compound as a pale brown oil (0.97 g, 4.37 mmol, 62%).

υ_{max} ($CHCl_3$)	3463 (w), 2951 (w), 2360 (s), 2339 (s), 1776 (m), 1632 (s), 1468 (m), 1337 (s), 1061 (m), 1003 (w), 852 (w).
δ_H (300 MHz, $CDCl_3$)	8.62 (1 H, d + fine splitting, *J*=4.5 Hz, Ar**H**)
	7.77 (1 H, td, *J*=7.5, 1.5 Hz, Ar**H**)
	7.48 (1 H, d, *J*=7.5 Hz, Ar**H**)
	7.30 (1 H, ddd, *J*=7.5, 4.5, 1.0 Hz, Ar**H**)
	6.07 (1 H, s, O**H**)
	4.09 (3 H, s, OC**H**$_3$)
	3.98 (3 H, s, OC**H**$_3$).
δ_C (75 MHz, $CDCl_3$)	182.6 (**C**=O), 164.4 (**C**), 154.6 (**C**H), 148.3 (**C**), 137.6 (**C**), 137.4 (**C**H), 123.2 (**C**H), 120.0 (**C**H), 80.0 (**C**), 59.9 (O**C**H$_3$), 58.8 (O**C**H$_3$).
LRMS (ES+)	222 ([M+H]$^+$, 100%)
HRMS (ES+)	Found 222.0766, $C_{11}H_{12}NO_4$ [M+H]$^+$ requires 222.0775.

4-Hydroxy-2,3-dimethoxy-4-(thiophen-2-yl)cyclobut-2-en-1-one (270)

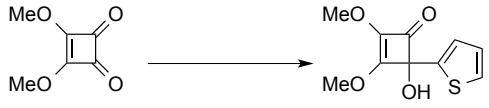

$C_6H_6O_4$
Mol Wt: 142.11

$C_{10}H_{10}O_4S$
Mol Wt: 226.25

To a solution of ^{n}BuLi (2.42 mL, 1.6 M solution in hexane, 3.87 mmol) in THF (15 mL) at –78 °C was added 2-bromothiopene (0.376 mL, 3.87 mmol) dropwise. After 15 min a solution of dimethyl squarate (0.50 g, 3.52 mmol) in THF (10 mL) was added over 5 min, giving an orange solution. After 1 h sat. NH_4Cl (20 mL) was added. The reaction mixture was allowed to warm to RT then extracted with DCM (20 mL x 3). The combined organic layers were washed with brine (20 mL x 2), dried ($MgSO_4$), filtered, concentrated *in vacuo* and purified by flash column chromatography (5%→40% EtOAc:petroleum ether with 2% NEt_3) to afford the title compound as a white solid (0.257 g, 1.14 mmol, 32%).

Data is consistent with literature.[6]

MP	66-68 °C (diethyl ether/petroleum ether).
υ_{max} ($CHCl_3$)	3400 (w), 3008 (w), 2956 (w), 1781 (m), 1644 (s), 1635 (m), 1470 (m), 1348 (s), 1040 (m), 984 (w).
δ_H (300 MHz, $CDCl_3$)	7.33 (1 H, dd, *J*=5.0, 1.3 Hz, Ar**H**)
	7.11 (1 H, dd, *J*=3.5, 1.3 Hz, Ar**H**)
	7.02 (1 H, dd, *J*=5.0, 3.5 Hz, Ar**H**)
	4.11 (3 H, s, OC**H**$_3$)
	4.02 (3 H, s, OC**H**$_3$)
	3.56 (1 H, s, O**H**).
δ_C (75 MHz, $CDCl_3$)	183.1 (**C**=O), 166.0 (**C**), 140.7 (**C**), 135.2 (**C**), 127.2 (**C**H), 126.2 (**C**H), 125.0 (**C**H), 85.7 (**C**), 60.3 (O**C**H$_3$), 58.8 (O**C**H$_3$).
LCMS (ES+)	290 ([M+Na+MeCN]$^+$, 100%).

General Experimental for Flow Reactions

2 mL aliquots of **258a-i** in 1,4-dioxane were taken from bulk solutions (0.25 g in 25 mL) and heated at 150 °C under flow in stainless steel tubing for the stated residence time using a Vapourtec R4/R2+ device. The resulting solutions were concentrated *in vacuo* then analyzed by ^{1}H NMR to determine their composition (**258**, **260** and **261**) by comparison of the respective integrals as indicated below.

2,3-Dimethoxynaphthalene-1,4-dione (261a)

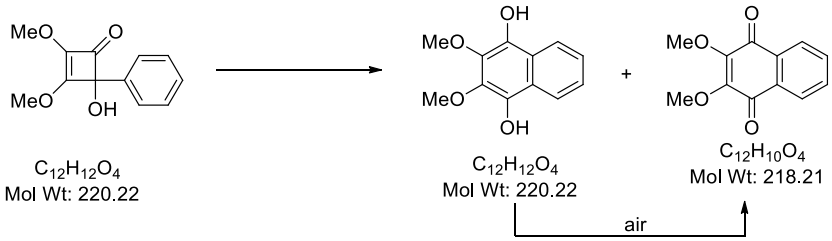

Naphthalene-1,4-dione **261a** could be formed in near quantitative yield using the aforementioned method by applying a residence time of 30 min and stirring the resulting solution in air for 1 h.

Data is consistent with literature.[6]

MP	116–118 °C (diethyl ether/petroleum ether).
υ_{max} ($CHCl_3$)	3385 (m), 2954 (w), 2360 (s), 2341 (s), 1772 (s), 1601 (s), 1468 (s), 1337 (s), 1047 (s), 994 (m), 858 (m).
δ_H (300 MHz, $CDCl_3$)	7.71 (2 H, m, 2 x Ar**H**)
	8.07 (2 H, m, 2 x Ar**H**)
	4.13 (6 H, s, OC**H**$_3$ x 2).
δ_C (75 MHz, $CDCl_3$)	182.0 (**C**=O x 2), 154.5 (**C** x 2), 133.8 (**C** x 2), 130.8 (**C** x 2), 126.3 (**C**H x 2), 61.5 (O**C**H$_3$ x 2).
LRMS (ES+)	241 ([M+Na]$^+$, 46%), 219 ([M+H]$^+$, 16%).

Rate determination

Stacked NMR data at various residence times with an expansion of the integrated region, followed by a tabulated summary of the acquired data and 1st order rate plot.

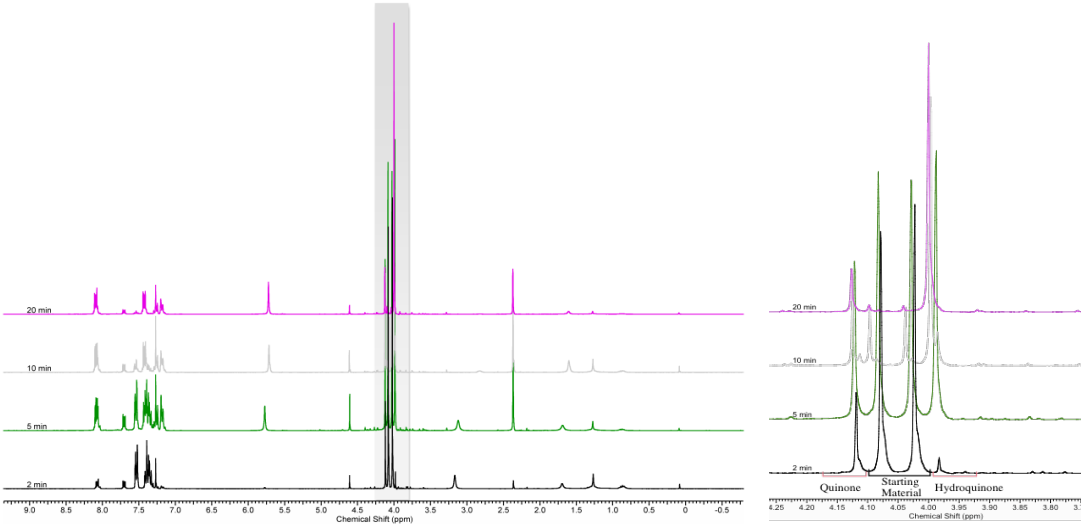

Time (s)	261a (%)	ln [SM]	1st order rate plot
0	100	4.61	
300	63.2	4.15	
450	53.5	3.98	
600	39.6	3.68	
900	25.1	3.22	
1200	17.1	2.84	

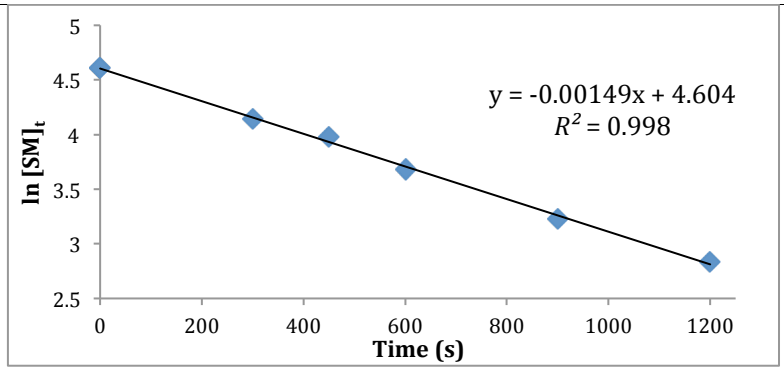

2,3-Dimethoxy-6-methylnaphthalene-1,4-dione (261b)

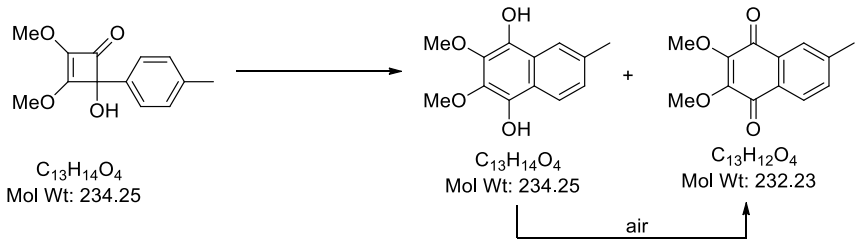

Naphthalene-1,4-dione **261b** could be formed in 94% yield using the general method by applying a residence time of 2 h and stirring the resulting solution in air for 3 h.

Data is consistent with literature.[6]

MP	89–91 °C (aq. MeOH).
υ_{max} ($CHCl_3$)	2950 (w), 1659 (s), 1611 (s), 1600 (s), 1306 (s), 1269 (s), 1040 (m).
δ_H (400 MHz, $CDCl_3$)	7.96 (1 H, d, *J*=7.8 Hz, Ar**H**)
	7.87 (1 H, br. s, Ar**H**)
	7.53–7.47 (1 H, ddq, *J*=7.8, 1.5, 0.8 Hz, Ar**H**)
	4.12 (3 H, s, OC**H**$_3$)
	4.10 (3 H, s, OC**H**$_3$)
	2.48 (3 H, br. s, C**H**$_3$).
δ_C (100 MHz, $CDCl_3$)	182.3 (**C**=O), 181.8 (**C**=O), 147.6 (**C**), 144.9 (**C**), 134.4 (**C**), 130.8 (**C**H), 128.6 (**C**), 126.7 (**C**H), 126.4 (**C**H), 119.7 (**C**), 61.4 (O**C**H$_3$ × 2), 21.8 (**C**H$_3$).
LRMS (ES+)	233 ($[M+H]^+$, 100%).

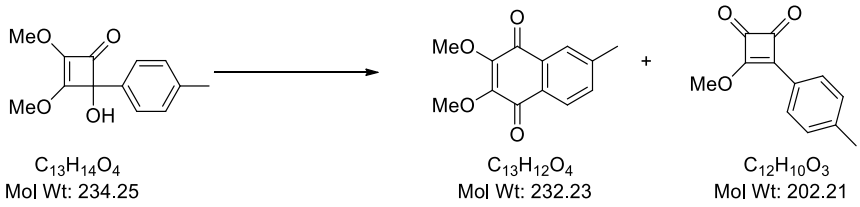

As an alternative to the general method, crude reaction mixtures could be concentrated *in vacuo*, dissolved in DCM then exposed to 23% CAN on silica. The procedure facilitates the quantitative oxidation of the benzohydroquinone (**260b**) to the corresponding benzoquinone (**261b**) with remaining starting material (**258b**) cleanly converted to the corresponding cyclobuten-1,2-dione (**259b**) as a clear oil.

Data is consistent with literature.[120]

υ_{max} ($CHCl_3$)	2361 (s), 2340 (s), 1784 (s), 1750 (w), 1595 (m), 1369 (s), 1032 (w), 833 (w).
δ_H (400 MHz, $CDCl_3$)	7.94 (2 H, d, *J*=8.1 Hz, 2 x Ar**H**)
	7.32 (2 H, d, *J*=8.1 Hz, 2 x Ar**H**)
	4.60 (3 H, s, OC**H**$_3$)
	2.44(3 H, s, C**H**$_3$).
δ_C (100 MHz, $CDCl_3$)	193.8(**C**=O), 184.7 (**C**=O), 174.0 (**C**), 143.9 (**C**), 129.9 (**C**H x 2), 127.9 (**C**H x 2), 125.0 (**C**), 116.3 (**C**), 61.4 (O**C**H$_3$), 22.0 (**C**H$_3$).
LRMS (ES+)	266 ([M+MeCN+Na]$^+$, 100%), 203 ([M+H]$^+$, 2%).

Rate determination

Stacked NMR data at various residence times with an expansion of the integrated region, followed by a tabulated summary of the acquired data and 1st order rate plot. In this case, integration of the methyl ether resonances of **261b** and **259b** provided a reliable means of assessing the progress of the reaction.

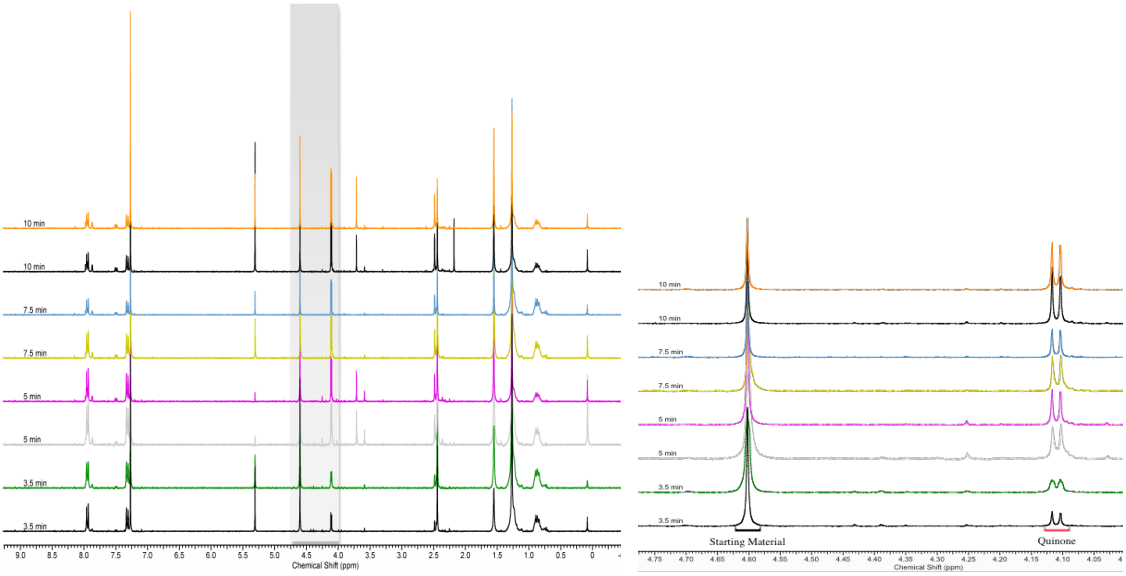

Time (s)	261b (%)	ln [SM]	1st order rate plot
0	100	4.61	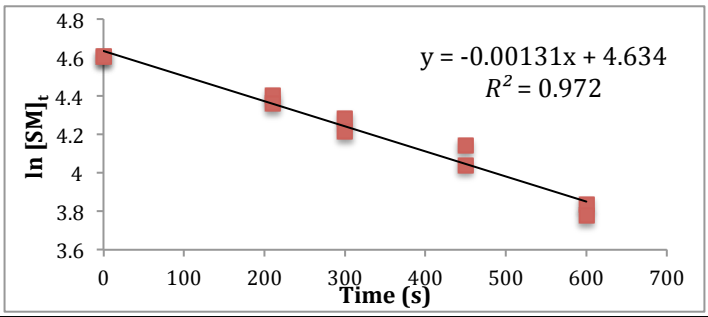
	100	4.61	
210	81.9	4.41	
	78.4	4.36	
300	72.4	4.28	
	67.5	4.21	
450	62.7	4.14	
	56.9	4.04	
600	46.5	3.84	
	43.7	3.78	

2,3-Dimethoxy-6-(trimethylsilyl)naphthalene-1,4-dione (261c)

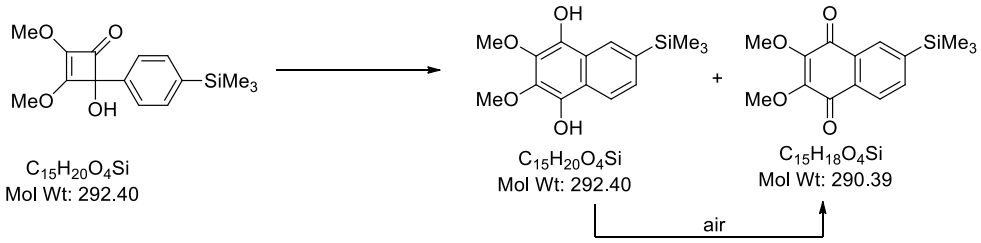

Naphthalene-1,4-dione **261c** could be formed in 94% yield using the general method with a residence time of 2 h, followed by stirring of the resulting solution in air for 3 h.

MP	69-71 °C (diethyl ether/petroleum ether).
υ_{max} ($CHCl_3$)	2953 (w), 1661 (s), 1608 (s), 1600 (s), 1220 (s), 1030 (s), 840 (s).
δ_H (400 MHz, $CDCl_3$)	8.18–8.22 (1 H, d, *J*=1.2 Hz, Ar**H**)
	8.01 (1 H, d, *J*=7.6 Hz, Ar**H**)
	7.85 (1 H, dd, *J*=7.6, 1.2 Hz, Ar**H**)
	4.12 (3 H, s, OC**H**$_3$)
	4.12 (3 H, s, OC**H**$_3$)
	0.34 (9 H, s, Si(C**H**$_3$)$_3$).
δ_C (100 MHz, $CDCl_3$)	182.6 (**C**=O), 182.3 (**C**=O), 179.0 (**C**)148.7 (**C**), 147.6 (**C**), 147.4 (**C**), 138.7 (**C**H), 130.9 (**C**H), 129.5 (**C**), 125.0 (**C**H), 61.4 (O**C**H$_3$ x 2), –1.4 (Si(**C**H$_3$)$_3$).
LCMS (ES+)	598 ([2M+NH_4]$^+$, 100%), 291 ([M+H]$^+$, 70%).
HRMS (ES+)	Found 291.1053, $C_{15}H_{19}O_4Si$ [M+H]$^+$ requires 291.1055.

Rate determination

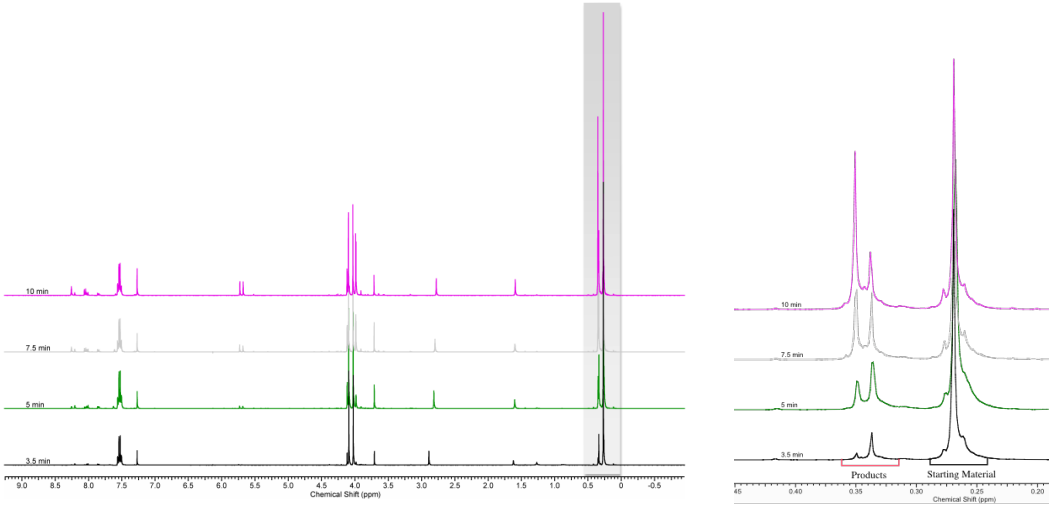

Time (s)	261c (%)	ln [SM]	1st order rate plot
0 210 300 450 600	100 86.6 74.0 60.4 49.4	4.61 4.46 4.30 4.10 3.90	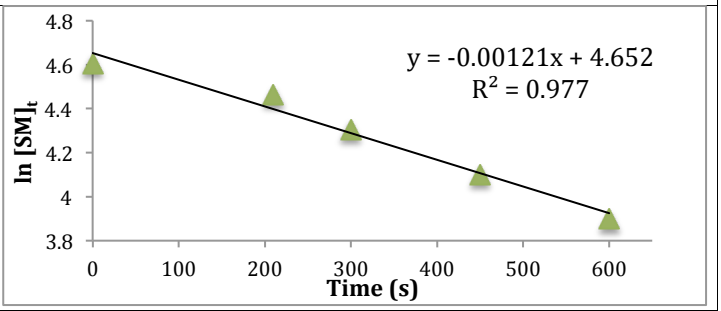

6-(*tert*-Butyl)-2,3-dimethoxynaphthalene-1,4-dione (261d)

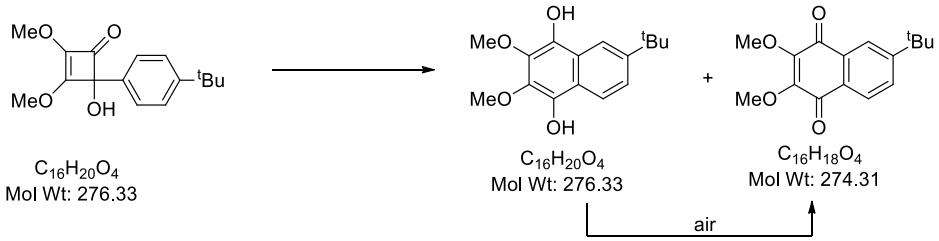

Naphthalene-1,4-dione **261d** could be formed in 94% yield using the general method with a residence time of 2 h, followed by stirring of the resulting solution in air for 3 h.

MP	88–90 °C (diethyl ether/petroleum ether).
υ_{max} ($CHCl_3$)	2960 (w), 1663 (s), 1610 (w), 1597 (s), 1220 (s), 1038 (s), 950 (w).
δ_H (300 MHz, $CDCl_3$)	8.08 (1 H, d, *J*=2.0 Hz, Ar**H**)
	7.99 (1 H, d, *J*=8.2 Hz, Ar**H**)
	7.71 (1 H, dd, *J*=8.2, 2.0 Hz, Ar**H**)
	4.11 (3 H, s, OC**H**$_3$)
	4.10 (3 H, s, OC**H**$_3$)
	1.38 (9 H, s, C(C**H**$_3$)$_3$).
δ_C (75 MHz, $CDCl_3$)	182.4 (**C**=O), 181.8 (**C**=O), 158.0 (**C**), 147.6 (**C**), 147.5 (**C**), 130.7 (**C**H), 130.7 (**C**), 128.5 (**C**), 126.3 (**C**H), 123.2 (**C**H), 61.4 (O**C**H$_3$ x 2), 35.5 (**C**), 30.9 ((**C**H$_3$)$_3$).
LCMS (ES+)	566 ([2M+NH_4]$^+$, 100%), 275 ([M+H]$^+$, 70%).
HRMS (ES+)	Found 275.1283, $C_{16}H_{19}O_4$ [M+H]$^+$ requires 275.1286.

Rate determination

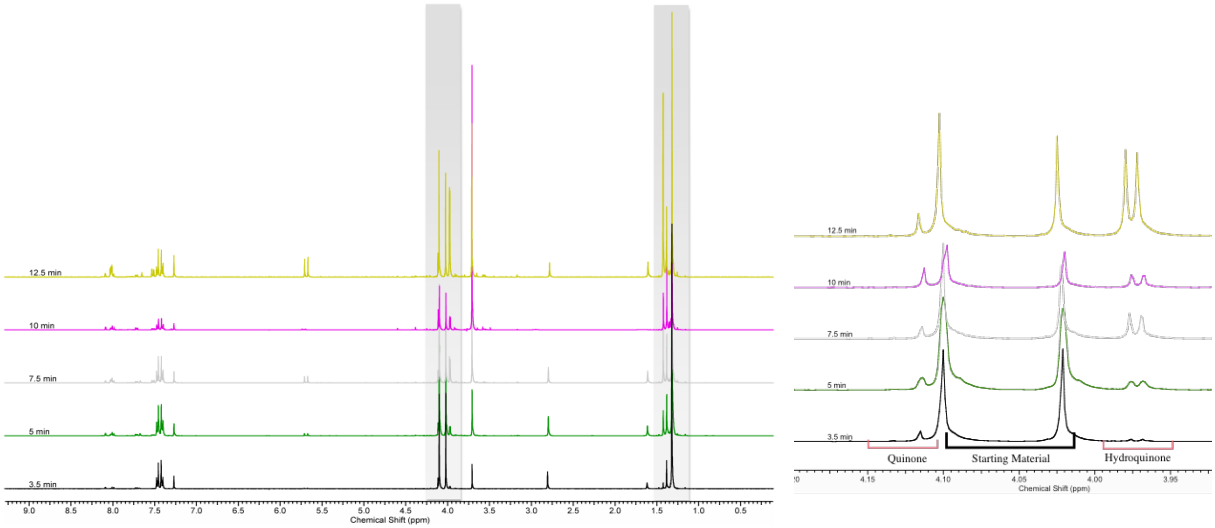

Time (s)	261d (%)	ln [SM]	1st order rate plot
	^{t}Bu signal		
0	100	4.61	
210	86.1	4.46	
300	77.5	4.35	
450	65.7	4.19	
600	53.4	3.98	
750	46.4	3.84	
	Me signal		
0	100	4.61	
210	84.9	4.44	
300	78.7	4.37	
450	67.6	4.21	
600	54.4	4.00	
750	47.9	3.87	

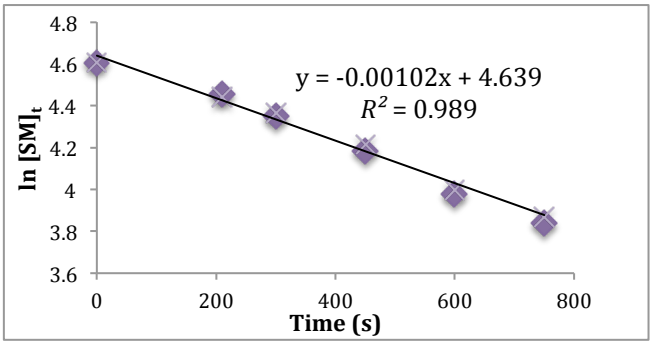

2,3-Dimethoxy-6-phenylnaphthalene-1,4-diol (261e)

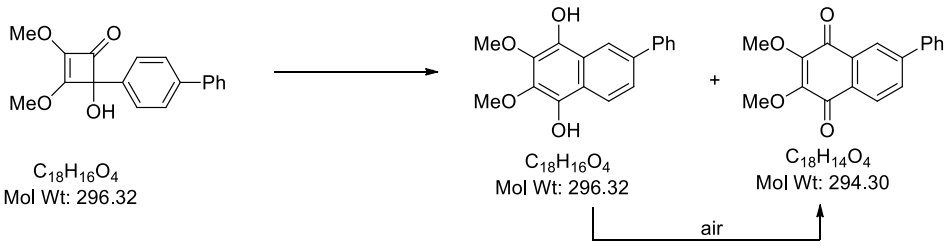

Naphthalene-1,4-dione **261e** could be formed in 95% yield using the general method with a residence time of 3 h, followed by stirring of the resulting solution in air for 4 h.

MP	75–77 °C (diethyl ether/petroleum ether).
υ_{max} ($CHCl_3$)	2928 (m), 1667 (s), 1598 (m), 1216 (s), 1220 (m), 1034 (s), 914 (w).
δ_H (300 MHz, $CDCl_3$)	8.31 (1 H, d, *J*=2.0 Hz, Ar**H**) 8.14 (1 H, d, *J*=7.7 Hz, Ar**H**) 7.92 (1 H, dd, *J*=7.7, 2.0 Hz, Ar**H**) 7.69 (2 H, dd, *J*=7.1, 1.5 Hz, 2 x Ar**H**) 7.54–7.44 (3 H, m, 3 x Ar**H**) 4.15 (3 H, s, OC**H**$_3$) 4.14 (3 H, s, OC**H**$_3$).
δ_C (75 MHz, $CDCl_3$)	180.1 (**C**=O), 180.1 (**C**=O), 166.4 (**C**), 146.7 (**C**), 138.9 (**C**), 133.9 (**C**), 131.9 (**C**H), 129.1 (**C**H x 2), 128.9 (**C**H), 127.3 (**C**H x 2), 127.04 (**C**H), 124.7 (**C**H), 112.8 (**C**), 110.1 (**C**), 61.5 (O**C**H$_3$ x 2).
LRMS (ES+)	358 ([M+MeCN+Na]$^+$, 100%).

Rate determination

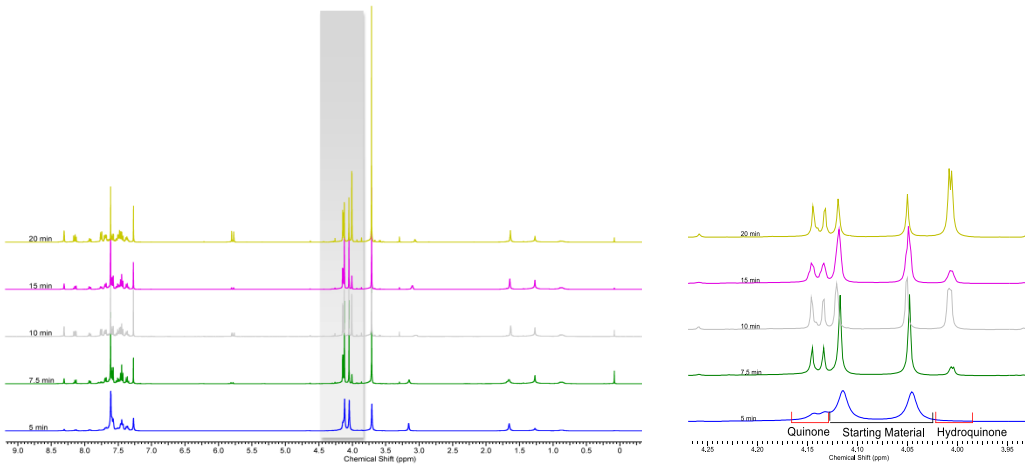

Time (s)	261e (%)	ln [SM]	1st order rate plot
0	100	4.61	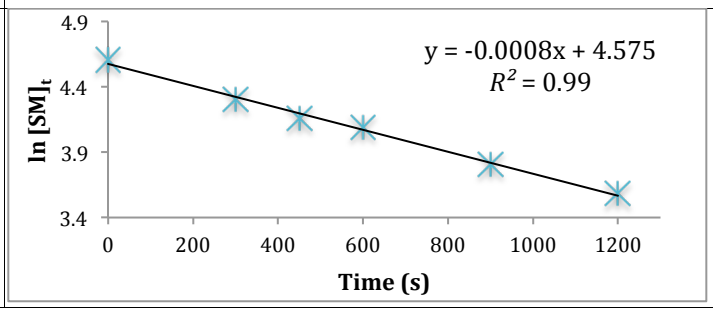
300	73.7	4.30	
450	63.6	4.16	
600	59.8	4.09	
900	44.8	3.80	
1200	35.7	3.58	

_N,N_-Diisopropyl-5,8-dihydroxy-6,7-dimethoxy-2-naphthamide (261f)

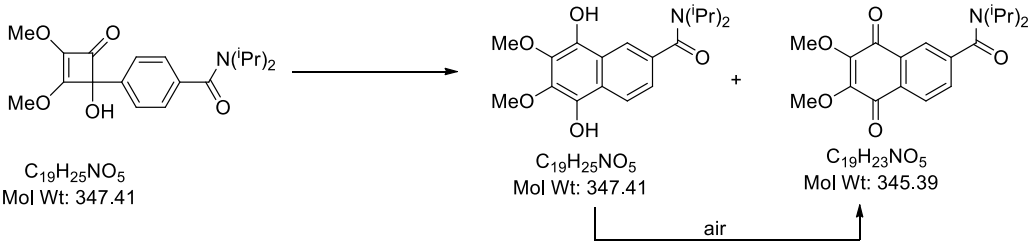

Naphthalene-1,4-dione **261f** could be formed in 84% yield using the general method with a residence time of 90 min, followed by stirring of the resulting solution in air for 2 h.

MP	130–132 °C (diethyl ether/petroleum ether).
υ_{max} ($CHCl_3$)	2946 (w), 1674 (s), 1667 (s), 1612 (s), 1600 (s), 1583 (s), 1300 (s), 1235 (s), 1037 (s), 749 (s).
δ_H (400 MHz, $CDCl_3$)	8.09 (1 H, d, *J*=7.8 Hz, Ar**H**)
	7.98 (1 H, d, *J*=1.5 Hz, Ar**H**)
	7.62 (1 H, dd, *J*=7.8, 1.5 Hz, Ar**H**)
	4.12 (3 H, s, OC$\mathbf{H}_3$)
	4.12 (3 H, s, OC$\mathbf{H}_3$)
	3.67 (1 H, br. s, NC**H**$(CH_3)_2$)
	3.58 (1 H, br. s, NC**H**$(CH_3)_2$)
	1.55 (6 H, br. s, NCH$(C\mathbf{H}_3)_2$)
	1.17 (6 H, br. s, NCH$(C\mathbf{H}_3)_2$).
δ_C (100 MHz, $CDCl_3$)	181.3 (**C**=O), 181.3 (**C**=O), 168.7 (**C**=O), 147.7 (**C**), 144.0, (**C**), 131.0 (**C**), 130.7 (**C**), 130.5 (**C**), 126.8 (**C**H), 123.3 (**C**H), 103.6 (**C**), 61.5 (O**C**H_3 x 2), 51.2 (br., **C**H), 46.3 (br., **C**H), 20.6 ($(\mathbf{C}H_3)_2)_2$.
LRMS (ES+)	387 ($[M+MeCN+H]^+$, 100%), 346 ($[M+H]^+$, 75%).

Rate determination

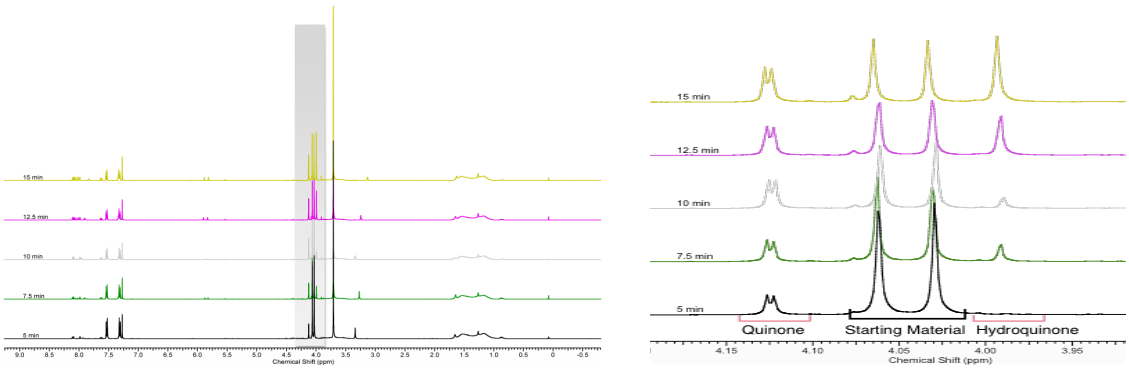

Time (s)	261f (%)	ln [SM]	1st order rate plot
0	100	4.61	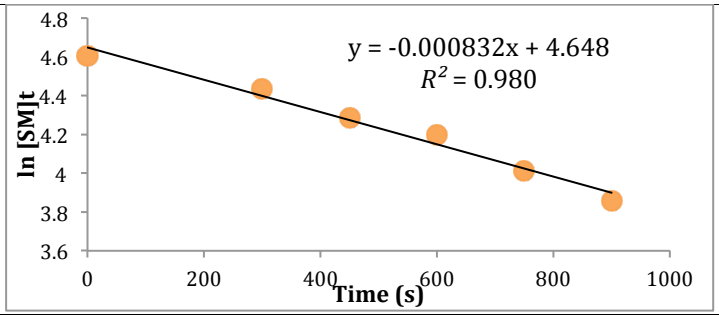
300	84.4	4.44	
450	72.5	4.28	
600	66.5	4.20	
750	55.2	4.01	
900	47.5	3.86	

2,3,6-Trimethoxynaphthalene-1,4-diol (261g)

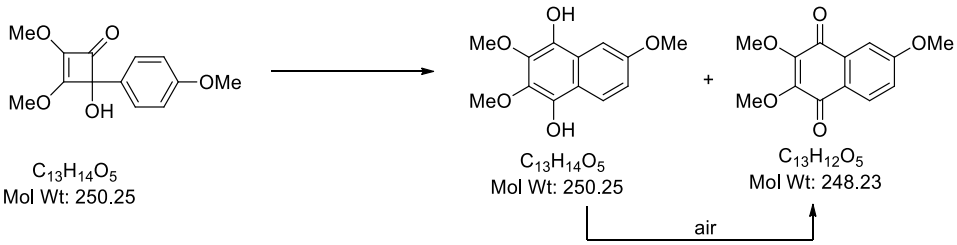

Naphthalene-1,4-dione **261g** could be formed in 94% yield using the general method with a residence time of 4 h, followed by stirring of the resulting solution in air for 5 h.

Data is consistent with literature.[6]

MP	116–118 °C (diethyl ether/petroleum ether).
υ_{max} ($CHCl_3$)	2955 (w), 1669 (s), 1657 (m), 1596 (s), 1311 (s), 1011 (s), 837 (m).
δ_H (400 MHz, $CDCl_3$)	8.01 (1 H, d, *J*=8.6 Hz, Ar**H**)
	7.52 (1 H, d, *J*=2.6 Hz, Ar**H**)
	7.16 (1 H, dd, *J*=8.6, 2.6 Hz, Ar**H**)
	4.13 (3 H, s, OC**H**$_3$)
	4.08 (3 H, s, OC**H**$_3$)
	3.95 (3 H, s, OC**H**$_3$).
δ_C (100 MHz, $CDCl_3$)	182.0 (**C**=O), 181.1 (**C**=O), 164.2 (**C**), 147.8 (**C**), 147.0 (**C**), 132.9 (**C**), 128.7 (**C**H), 124.1 (**C**), 119.9 (**C**H), 110.0 (**C**H), 61.4 (O**C**H$_3$ x 2), 55.9 (O**C**H$_3$).
LRMS (ES+)	514 ([2M+NH_4]$^+$, 40%), 249 ([M+H]$^+$, 100%).

Rate determination

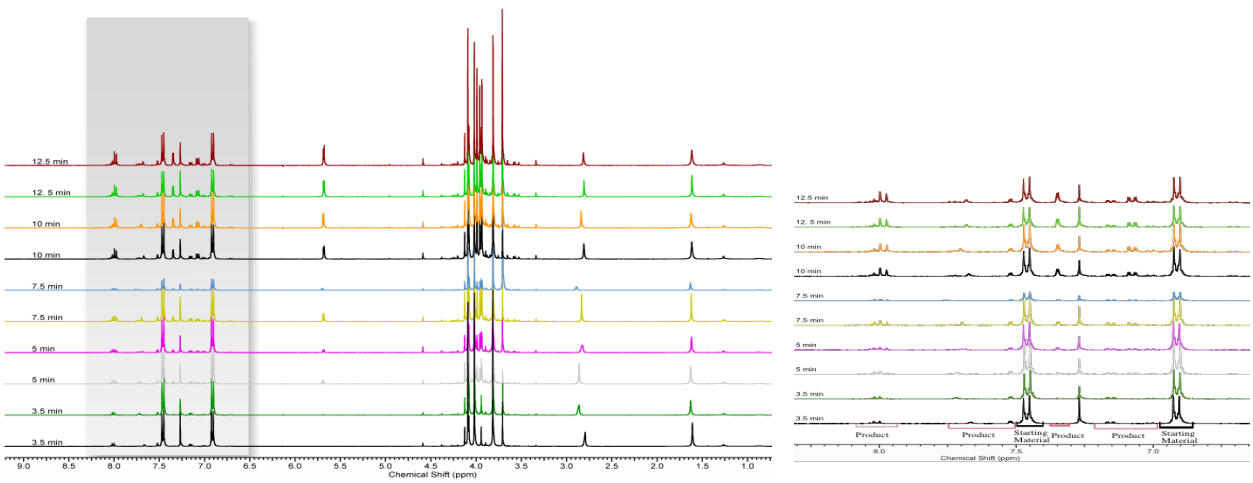

Time (s)	261g (%)	ln [SM]	1st order rate plot
0	100	4.61	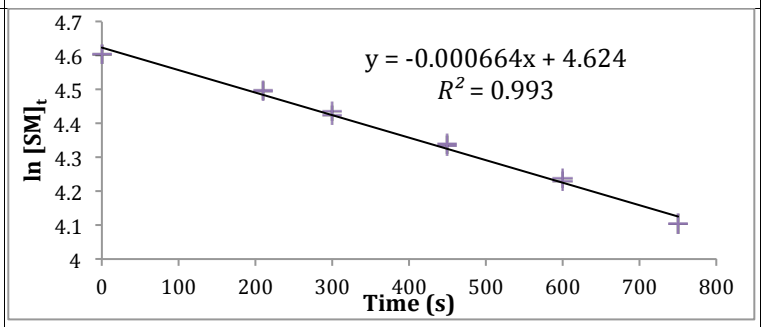
	100	4.61	
210	89.7	4.50	
	89.5	4.50	
300	84.4	4.44	
	83.5	4.43	
450	76.2	4.33	
	76.7	4.34	
600	69.3	4.24	
	68.8	4.23	
750	60.6	4.10	
	60.6	4.10	

6-Fluoro-2,3-dimethoxynaphthalene-1,4-diol (261h)

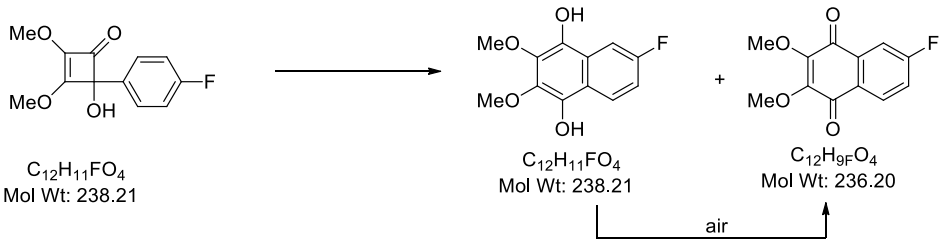

Naphthalene-1,4-dione **261h** could be formed in 92% yield using the general method with a residence time of 4 h, followed by stirring of the resulting solution in air for 5 h.

MP	110–111 °C (diethyl ether/petroleum ether).
υ_{max} ($CHCl_3$)	2922 (w), 1658 (s), 1614 (m), 1585 (s), 1301 (s), 1238 (s), 1038 (s), 842 (m).
δ_H (400 MHz, $CDCl_3$)	8.11 (1 H, dd, *J*=8.6, 5.1 Hz, Ar**H**)
	7.73 (1 H, d, *J*=8.6, 2.5 Hz, Ar**H**)
	7.36 (1 H, td, *J*=8.2, 2.8 Hz, Ar**H**)
	4.13 (3 H, s, OC**H**$_3$)
	4.11 (3 H, s, OC**H**$_3$).
δ_C (100 MHz, $CDCl_3$)	184.0 (**C**=O), 167.9 (**C**=O), 130.5 (**C**), 129.4 (**C**), 129.3 (**C**H), 120.9 (**C**), 120.6 (**C**H), 116.5 (**C**), 113.3 (**C**H), 113.1 (**C**), 61.5 (O**C**H$_3$ x 2).
δ_F (282.4 MHz, $CDCl_3$)	–102.4 (C**F**),
LRMS (ES+)	237 ([M+H]$^+$, 100%).

Rate determination

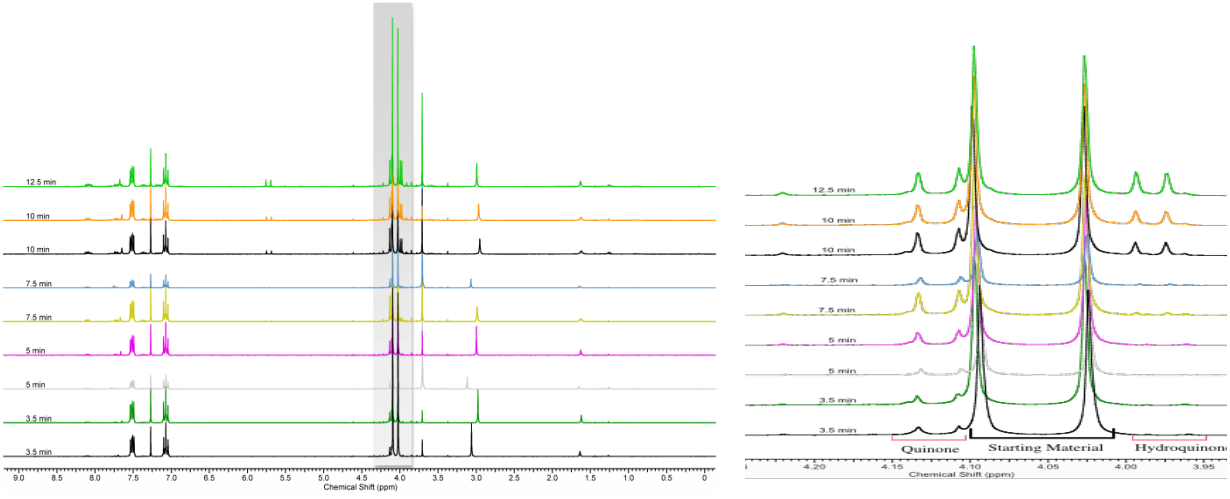

Time (s)	261h (%)	ln [SM]	1st order rate plot
0	100	4.61	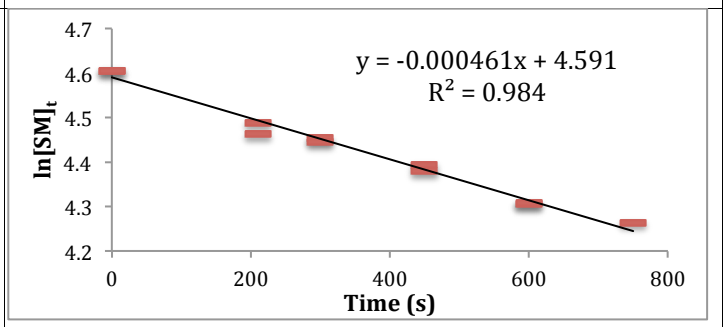
	100	4.61	
210	89.0	4.49	
	86.8	4.46	
300	86.0	4.45	
	85.2	4.45	
450	79.7	4.38	
	81.0	4.39	
600	74.1	4.31	
	74.3	4.31	
750	71.1	4.26	

2,3-Dimethoxy-6-(trifluoromethyl)naphthalene-1,4-diol (261i)

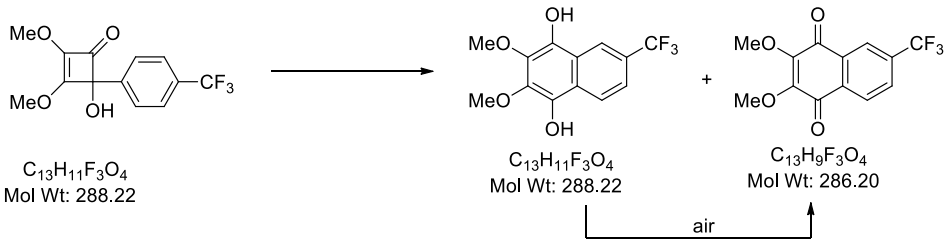

Naphthalene-1,4-dione **261i** could be formed in 93% yield using the general method with a residence time of 4 h, followed by stirring of the resulting solution in air for 5 h.

MP	98–100 °C (diethyl ether/petroleum ether).
υ_{max} ($CHCl_3$)	2958 (w), 2839 (w), 1661 (s), 1610 (s), 1296 (s), 1209 (s), 1084 (s), 1032 (m), 914 (s), 732 (s).
δ_H (300 MHz, $CDCl_3$)	8.33–8.36 (1 H, d, *J*=1.3 Hz, Ar**H**)
	8.21 (1 H, d, *J*=8.0 Hz, Ar**H**)
	7.95 (1 H, dd, *J*=8.2, 1.1 Hz, Ar**H**)
	4.15 (3 H, s, OC**H**$_3$)
	4.15 (3 H, s, OC**H**$_3$).
δ_C (75 MHz, $CDCl_3$)	180.8 (**C**=O), 180.6 (**C**=O), 147.9 (**C**), 147.8 (**C**), 135.5 (**C**CF_3, q, J_{CF} = 33.6 Hz), 133.0 (**C**), 131.2 (**C**), 130.2 (**C**H, q, J_{CF} = 3.9 Hz), 127.0 (**C**H), 123.4 (**C**H, q, J_{CF} = 3.9 Hz), 123.1 (**C**F_3, q, J_{CF} = 273 Hz), 61.6 (O**C**H_3 x 2).
δ_F (282.4 MHz, $CDCl_3$)	–63.60 (C**F**$_3$).
LRMS (ES+)	287 ($[M+H]^+$, 100%).
HRMS (ES+)	Found 287.0531, $C_{13}H_{10}O_4F_3$ $[M+H]^+$ requires 287.0540.

Rate determination

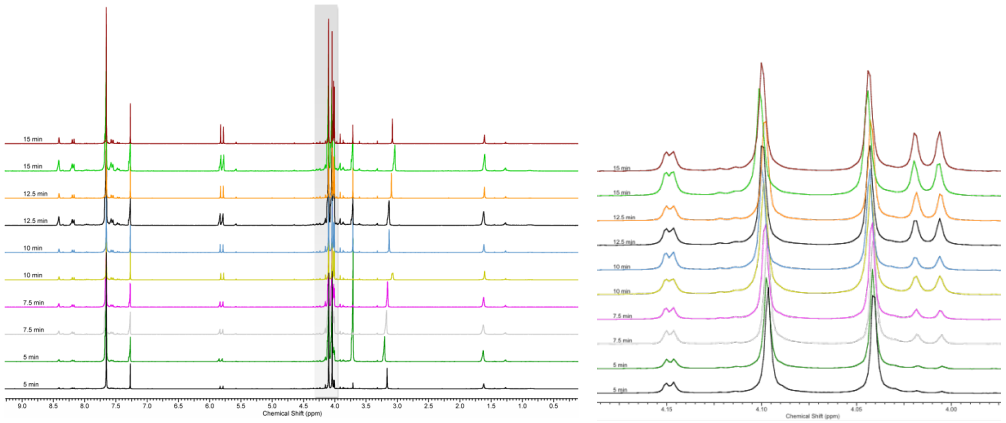

Time (s)	261i (%)	ln [SM]	1st order rate plot
0	100	4.61	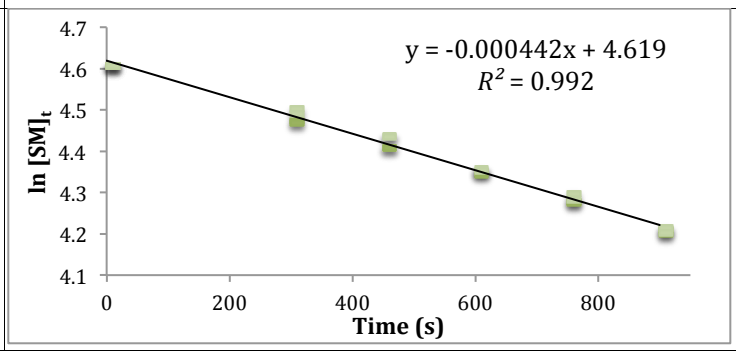
	100	4.61	
300	87.5	4.47	
	87.2	4.47	
450	82.2	4.41	
	82.1	4.41	
600	77.0	4.341	
	77.5	4.35	
750	71.9	4.28	
	72.0	4.28	
900	67.4	4.21	
	66.7	4.20	

1-Hydroxy-2,3-dimethoxy-4H-quinolizin-4-one (268)

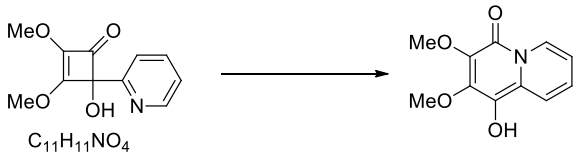

$C_{11}H_{11}NO_4$
Mol Wt: 221.21

$C_{11}H_{11}NO_4$
Mol Wt: 221.21

A solution of **267** (5.0 mg, 0.023 mmol) in 1,4-dioxane (2 mL) was heated at 100 °C in stainless steel tubing for a residence time of 10 min using a Vapourtec R4/R2+ device. The resulting solution was stirred in air for 1 h then concentrated *in vacuo* to afford the title compound as a pale brown solid (4.9 mg, 0.022 mmol, 99%).

MP	110–112 °C (EtOAc/petroleum ether).
υ_{max} ($CHCl_3$)	2955 (w), 2925 (w), 1733 (m), 1634 (w), 1595 (w), 1457 (w), 1288 (m), 1122 (w), 759 (w), 682 (w).
δ_H (400 MHz, DMSO)	8.88 (1 H, s, O**H**)
	8.70 (1 H, d, *J*=7.6 Hz, Ar**H**)
	7.73 (1 H, d, *J*=9.0 Hz, Ar**H**)
	7.16 (1 H, dd, *J*=8.0, 6.6 Hz, Ar**H**)
	6.86 – 6.97 (1 H, m, Ar**H**)
	4.03 (3 H, s, OC**H**$_3$)
	3.87 (3 H, s, OC**H**$_3$).
δ_C (100 MHz, DMSO)	152.07 (**C**=O), 150.16 (**C**), 132.8 (**C**), 128.6 (**C**), 128.4 (**C**), 124.7 (**C**H), 124.6 (**C**H), 120.9 (**C**H), 114.0 (**C**H), 60.9 (O**C**H$_3$), 59.3 (O**C**H$_3$).
LCMS (ES+)	222 ([M+H]$^+$, 100%).
HRMS (ES+)	Found 222.0766, $C_{11}H_{12}NO_4$ [M+H]$^+$ requires 222.0775.

5,6-Dimethoxybenzo[*b*]thiophene-4,7-dione (272)

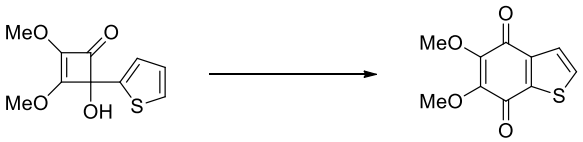

$C_{10}H_{10}O_4S$
Mol Wt: 226.25

$C_{10}H_8O_4S$
Mol Wt: 224.23

A solution of **270** (5.0 mg, 0.022 mmol) in 1,4-dioxane (2 mL) was heated at 150 °C in stainless steel tubing for a residence time of 10 min using a Vapourtec R4/R2+ device. The resulting solution was stirred in air for 1 h then concentrated *in vacuo* to afford the title compound as an orange solid (4.9 mg, 0.022 mmol, 98%).

Data is consistent with literature.[6]

MP	169–172 °C (diethyl ether/petroleum ether).
υ_{max} ($CHCl_3$)	3033 (m), 3008 (m), 2929 (w), 1651 (s), 1340 (s), 1292 (s), 858 (m).
δ_H (400 MHz, $CDCl_3$)	7.33 (1 H, dd, *J*=5.1, 1.3 Hz, Ar**H**)
	7.11 (1 H, dd, *J*=5.3, 1.3 Hz, Ar**H**)
	4.09 (6 H, app. s, 2 x O**C**$\mathbf{H}_3$).
δ_C (100 MHz, $CDCl_3$)	178.0 (**C**=O), 176.6 (**C**=O), 147.2 (**C**), 146.7 (**C**), 141.4 (**C**), 139.5 (**C**), 133.4 (**C**H), 125.9 (**C**H), 61.5 (O**C**H_3), 61.6 (O**C**H_3).
LCMS (ES+)	225 ($[M+H]^+$, 100%).

(3-Bromopyridin-2-yl)methanamine (300)

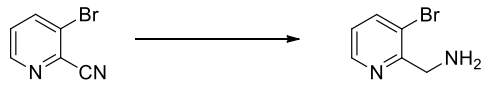

$C_6H_3BrN_2$
Mol Wt: 183.01

$C_6H_7BrN_2$
Mol Wt: 187.04

To a cooled (0 °C) solution of 3-bromo-2-cyanopyridine (0.100 g, 0.546 mmol) in toluene (20 mL) was added alane•Me_2NEt complex (0.5 M solution in toluene, 2.2 mL, 1.093 mmol) dropwise. The resulting mixture was warmed to RT then re-cooled to 0 °C after 16 h. Methanol (10 mL) then sat. potassium sodium tartare (50 mL) were cautiously added and the aqueous phase separated and extracted with $CHCl_3$ (20 mL x 3). The combined organic phases were then washed with brine (20 mL x 2), dried ($MgSO_4$), filtered and concentrated *in vacuo* to afford the title compound as a yellow oil (60.5 mg, mmol, 60%).

Data is consistent with literature.

δ_H (300 MHz, $CDCl_3$)	8.52 (1 H, dd, *J*=5.0, 1.5 Hz, Ar**H**)
	7.85 (1 H, dd, *J*=7.9, 1.5 Hz, Ar**H**)
	7.11 (1 H, dd, *J*=7.9, 5.0 Hz, Ar**H**)
	4.14 (2 H, s, C**H**$_2$)
	2.77 (2H, s, N**H**$_2$).
δ_C (75 MHz, $CDCl_3$)	162.4 (**C**), 150.2 (**C**H), 145.2 (**C**H), 123.1 (**C**), 115.9 (**C**H), 45.2 (**C**H_2).
LCMS (ES+)	189 ([M{^{81}Br}+H]$^+$, 100%), 187 ([M{^{79}Br}+H]$^+$, 100%).

N-((3-Bromopyridin-2-yl)methyl)acetamide (301a)

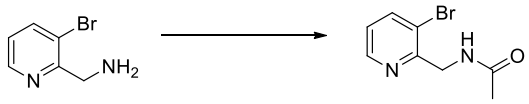

$C_6H_7BrN_2$
Mol Wt: 187.04

$C_8H_9BrN_2O$
Mol Wt: 229.07

To a solution *N*-(3-dimethylaminopropyl)-N'-ethylcarbodiimide hydrochloride (2.84 g, 14.83 mmol) in DCM (30 mL) at RT were added sequentially acetic acid (0.850 mL, 14.83 mmol) and triethylamine (4.13 mL, 29.7 mmol). After 1 h a solution of **300** (1.422 g, 5.93 mmol) in DMF and (15 mL) and DCM (10 mL) was added, followed after a further 1 h by 2M aq Na_2CO_3 (30 mL). The aqueous phase was separated and extracted with DCM (3 x 20 mL). The organic phases were combined, dried ($MgSO_4$), filtered, concentrated *in vacuo* and purified by chromatography (EtOAc) to afford the title compound as a white solid (0.730 g, 3.187 mmol, 52%).

Data is consistent with literature.[109]

MP	62–64 °C (EtOAc).
υ_{max} ($CHCl_3$)	3314 (m), 1642 (s), 1560 (m), 812 (w).
δ_H (400 MHz, $CDCl_3$)	8.50 (1 H, dd, *J*=4.5, 1.3 Hz, Ar**H**)
	7.89 (1 H, dd, *J*=7.9, 1.4 Hz, Ar**H**)
	7.18 (1H, br. s, N**H**)
	7.16 (1 H, dd, *J*=7.9, 4.3 Hz, Ar**H**)
	4.64 (2 H, d, *J*=4.3 Hz, C**H**$_2$)
	2.13 (3 H, s, C**H**$_3$).
δ_C (100 MHz, $CDCl_3$)	170.0 (**C**=O), 153.7 (**C**), 146.9 (**C**H), 140.4 (**C**H), 123.5 (**C**), 120.3 (**C**H), 44.1 (**C**H_2), 23.3 (**C**H_3).
LCMS (ES+)	231 ([M{^{81}Br}+H]$^+$, 100%), 229 ([M{^{79}Br}+H]$^+$, 100%)

(Ethoxyethynyl)trimethylsilane

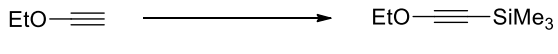

C_4H_6O
Mol Wt: 70.09

$C_7H_{14}OSi$
Mol Wt: 142.27

To a solution of ethoxyacetylene (4 g, 40 wt % in hexanes, 22.83 mmol) in diethyl ether (60 mL) stirring under nitrogen at 0 °C was added a solution of methyllithium (1.6 M in diethyl ether, 15.69 mL, 25.1 mmol) dropwise. The reaction mixture was stirred for 10 min at 0 °C after which freshly distilled chlorotrimethylsilane (3.21 mL, 25.1 mmol) was added dropwise. After the addition was complete, the mixture was allowed to stir at RT for 16 h. The reaction mixture was then filtered through celite at low vacuum and the filter cake washed with anhydrous diethyl ether (10 mL x 2) and concentrated *in vacuo* to half its volume. The remaining solution was purified by fractional distillation to remove the diethyl ether followed by vacuum distillation (28 °C at 13 mbar) to afford the title compound as a clear oil (1.0939 g, 7.69 mmol, 34%).

Data is consistent with literature.[121]

δ_H (400 MHz, $CDCl_3$)	4.13 (2 H, q, *J*=7.1 Hz, $CH_3C\mathbf{H}_2O$)
	7.89 (3 H, t, *J*=7.1 Hz, $C\mathbf{H}_3CH_2O$)
	0.14 (9 H, s, $Si(C\mathbf{H}_3)_3$).
δ_C (100 MHz, $CDCl_3$)	109.5 (**C**), 74.8 (**C**H_2), 36.8 (**C**), 14.2 (**C**H_3), 0.68 ($Si(\mathbf{C}H_3)_3$).

***N*-((3-Bromopyridin-2-yl)methyl)-2-(trimethylsilyl)acetamide (301b)**

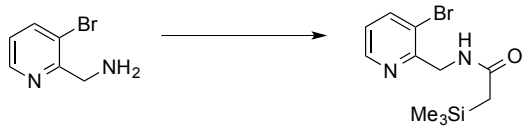

$C_6H_7BrN_2$
Mol Wt: 187.04

$C_{11}H_{17}BrN_2OSi$
Mol Wt: 301.26

A solution of **300** (1.00 g, 5.35 mmol), in toluene (15 mL) and a solution of (ethoxyethynyl)trimethylsilane (0.761 g, 5.35 mmol) were heated at 110 °C under flow in stainless steel tubing for 90 min. The resulting solution was concentrated *in vacuo* and purified by flash column chromatography (0→10% MeOH:*tert*-butyl methyl ether) to afford the title compound as a brown oil (1.428 g, 4.74 mmol, 89%).

υ_{max} ($CHCl_3$)	3301 (m), 2955 (w), 1638 (s), 1423 (m), 854 (w).
δ_H (400 MHz, $CDCl_3$)	8.49 (1 H, dd, *J*=4.5, 1.2 Hz, Ar**H**)

	7.87 (1 H, dd, *J*=8.1, 1.5 Hz, Ar**H**)
	7.13 (1 H, dd, *J*=7.9, 4.8 Hz, Ar**H**)
	6.84 (1H, br. s, N**H**)
	4.62 (2 H, d, *J*=4.4 Hz, C**H**$_2$NH)
	1.95 (2 H, s, C**H**$_2$)
	0.16 (9 H, s, Si(C**H**$_3$)$_3$).
δ_C (100 MHz, $CDCl_3$)	172.1 (**C**=O), 154.2 (**C**), 146.9 (**C**H), 140.2 (**C**H), 123.3 (**C**), 123.4 (**C**H), 44.1 (**C**H$_2$), 29.2 (**C**H$_2$), –1.32 (**C**H$_3$ x 3).
LCMS (ES+)	303 ([M{^{81}Br}+H]$^+$, 100%), 229 ([M{^{79}Br}+H]$^+$, 100%)
HRMS (ES+)	Found 301.0370, $C_{11}H_{18}N_2OSiBr$ [M+H]$^+$ requires 301.0372.

8-Bromo-3-methylimidazo[1,5-a]pyridine (302)

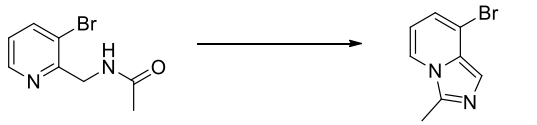

$C_8H_9BrN_2O$
Mol Wt: 229.07

$C_8H_7BrN_2$
Mol Wt: 211.06

To a solution of acetamide **301a** (0.730 g, 3.19 mmol) in toluene (10 mL) at RT was added phosphorus oxychloride (1.07 mL, 11.5 mmol) dropwise. The reaction mixture was heated at reflux for 4 h then cooled to 0 °C and saturated $NaHCO_3$ (30 mL) added. The aqueous phase was separated and extracted with EtOAc (10 mL x 3), then the combined organic phases were washed with water (10 mL x 2), dried ($MgSO_4$), filtered and concentrated *in vacuo* to afford the title compound as a brown oil (0.680 g, 3.222 mmol, 99%, 98% purity).

Data is consistent with literature.[109]

δ_H (400 MHz, $CDCl_3$)	7.68 (1 H, d, *J*=7.3 Hz, Ar**H**)
	7.46 (1 H, s, Ar**H**)
	6.92 (1 H, d, *J*=6.8 Hz, Ar**H**)
	6.47 (1 H, app. t, *J*=7.1 Hz, Ar**H**)
	2.69 (3 H, s, C**H**$_3$).
δ_C (100 MHz, $CDCl_3$)	179.0 (**C**), 136.6 (**C**), 130.0 (**C**), 120.8 (**C**H), 119.8 (**C**H), 119.5 (**C**H), 112.7 (**C**H), 12.6 (**C**H$_3$).
LCMS (ES+)	213 ([M{^{81}Br}+H]$^+$, 100%), 211 ([M{^{79}Br}+H]$^+$, 100%)

Alternative route to 302 from 301b

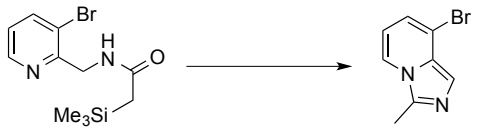

$C_{11}H_{17}BrN_2OSi$
Mol Wt: 301.26

$C_8H_7BrN_2$
Mol Wt: 211.06

To a solution of **301b** (1.43 g, 4.75 mmol) in toluene (20 mL) stirred under nitrogen at RT was added phosphorus oxychloride (1.59 mL, 17.09 mmol) dropwise. The reaction mixture was then refluxed for 4 h. The reaction mixture was cooled to 0 °C and saturated $NaHCO_3$ (50 mL) added. The aqueous phase was separated and extracted with EtOAc (20 mL x 3), then the combined organic phases were washed with water (10 mL x 2), dried ($MgSO_4$), filtered and concentrated *in vacuo* to afford the title compound as a brown oil (0.852 g, 4.037 mmol, 85%).

*Data in accordance with the previously synthesised substrate **302**.*

3-Ethoxy-4-hydroxy-2-methyl-4-(3-methylimidazo[1,5-a]pyridin-8-yl)cyclobut-2-enone (303)

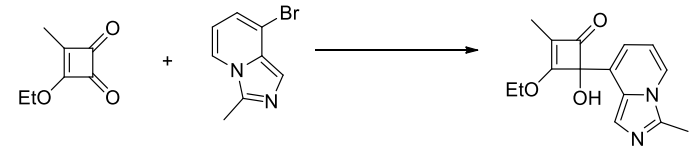

$C_7H_8O_3$
Mol Wt: 140.14

$C_8H_7BrN_2$
Mol Wt: 211.06

$C_{15}H_{16}N_2O_3$
Mol Wt: 272.30

To a solution of 8-bromo-3-methylimidazo[1.5-a]pyridine **302** (242 mg, 1.15 mmol), in THF (5 mL) at –78 °C was added ^{n}BuLi (1.6 M in hexane, 0.788 mL, 1.26 mmol). After 30 min a solution of 3-ethoxy-4-methyl-3-cyclobutene-1,2-dione **292** (0.161 g, 1.147 mmol) in THF (5 mL) was added dropwise, followed after a further 1 h by sat. NH_4Cl (20 mL). On warming to RT the aqueous phase was separated and extracted with DCM (20 mL x 3). The combined organic phases were washed with brine (20 mL x 2), dried ($MgSO_4$), filtered, concentrated *in vacuo* and purified by flash column chromatography (0%→5% MeOH:DCM with 1% NEt_3) to afford the title compound as a pale orange oil (175 mg, 0.642 mmol, 56%).

υ_{max} ($CHCl_3$) 2928 (w), 2861 (w), 2360 (s), 2339 (s), 1715 (m), 1731 (m), 1617 (m), 1332 (m), 1135 (w), 1078 (w), 878 (w), 669 (w).

δ_H (400 MHz, $CDCl_3$)	7.64 (1H, d, *J*=7.0 Hz, Ar**H**)
	7.39 (1H, s, Ar**H**)
	6.97 (1H, d, *J*=6.8 Hz, Ar**H**)
	6.60 (1H, t, *J*=6.9 Hz, Ar**H**)
	4.45 (1H, dq, *J*=9.8, 7.1 Hz, OC**H**$_2$CH$_3$)
	4.26 (1H, dq, *J*=9.9, 7.1 Hz, OC**H**$_2$CH$_3$)
	2.66 (3H, s, OC**H**$_3$)
	2.05 (1H, s, O**H**)
	1.85 (3H, s, OC**H**$_3$)
	1.36 (3H, t, *J*=7.0 Hz, OCH$_2$C**H**$_3$).
δ_C (100 MHz, $CDCl_3$)	189.5 (**C**=O), 182.2 (**C**=O), 135.5 (**C**), 127.8 (**C**), 127.6 (**C**), 125.2 (**C**), 120.7 (**C**H), 118.5 (**C**H), 116.5 (**C**H), 112.0 (**C**H), 91.6 (**C**), 69.2 (**C**H$_2$), 15.0 (**C**H$_3$), 12.6 (**C**H$_3$), 6.9 (**C**H$_3$).
LCMS (ES+)	273 ([M+H]$^+$, 100%)
HRMS (ES+)	Found 273.1232, $C_{15}H_{17}N_2O_3$ [M+H]$^+$ requires 273.1161.

9-Ethoxy-3,8-dimethylimidazo[5,1-a]isoquinoline-7,10-dione, Cribrostatin 6 (273)

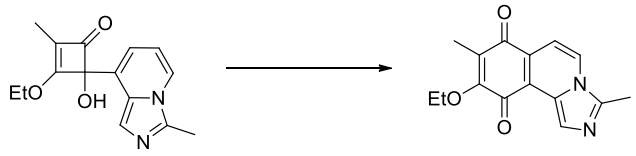

$C_{15}H_{16}N_2O_3$
Mol Wt: 272.30

$C_{15}H_{14}N_2O_3$
Mol Wt: 270.28

Cyclobutenone **303** (59 mg, 0.217 mmol) in 1,4-dioxane (2 mL) was heated at 110 °C in stainless steel tubing for a residence time of 1 h using a Vapourtec R4/R2+ device. The resulting solution was stirred in air for 30 min then concentrated *in vacuo* and purified by chromatography (2% MeOH:DCM) to give cribrostatin 6 **273** as a light blue solid (52 mg, 0.193 mmol, 90%).

Data is consistent with literature.[113]

MP	167–169 °C.
υ_{max} ($CHCl_3$)	2925 (m), 1662 (s), 1626 (s), 1611 (s), 1527 (m), 1172 (m).
δ_H (400 MHz, $CDCl_3$)	8.52 (1H, s, Ar**H**)
	8.10 (1H, d, *J*=7.6 Hz, Ar**H**)
	7.26 (1H, d, *J*=7.6 Hz, Ar**H**)
	4.49 (2H, q, *J*=6.8 Hz, OC**H**$_2$CH$_3$)

	3.09 (3H, br. s, C**H**$_3$)
	2.13 (3H, s, C**H**$_3$)
	1.45 (3H, t, *J*=6.8 Hz, OCH$_2$C**H**$_3$).
δ_C (100 MHz, $CDCl_3$)	184.9 (**C**=O), 180.7 (**C**=O), 156.2 (**C**), 137. 7 (**C**), 130.1 (**C**), 125.9 (**C**), 125.0 (**C**), 124.7 (**C**), 123.9 (**C**H), 123.5 (**C**H), 107.6 (**C**), 69.6 (O**C**H$_2$), 16.0 (**C**H$_3$), 12.6 (**C**H$_3$), 9.2 (**C**H$_3$).
LRMS (ES+)	271 ([M+H]$^+$, 100%).

6.3 Experimental Procedures for Chapter 4

4-Hydroxy-2,3-dimethoxy-4-(phenylethynyl)cyclobut-2-enone (240b)

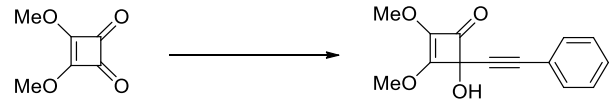

$C_6H_6O_4$
Mol Wt: 142.11

$C_{14}H_{12}O_4$
Mol Wt: 244.24

To a solution of phenylacetylene (0.85 mL, 7.74 mmol) in THF (20 mL) at –78 °C was added ^{n}BuLi (2.30 M in hexanes, 3.44 mL, 7.74 mmol) over 3 min. After 30 min the resulting solution was added *via* cannula to a solution of dimethyl squarate (1.00 g, 7.04 mmol) in THF (20 mL) at –78 °C, giving a bright yellow solution. After 20 min, sat. NH_4Cl (75 mL) was added. The reaction mixture was allowed to warm to RT then extracted with EtOAc (25 mL x 3). The combined organic layers were washed with brine (20 mL x 2), dried ($MgSO_4$), filtered, concentrated *in vacuo* and purified by flash column chromatography (10%→20% EtOAc:DCM with 2% NEt_3) to afford the title compound as a bright yellow solid (1.35 g, 5.53 mmol, 79%).

Data is consistent with literature.[14]

MP	138-140 °C (diethyl ether/petroleum ether).
υ_{max}	3273 (m), 2950 (w), 2222 (s), 2190 (s), 1771 (m), 1624 (s), 1467 (m), 1335 (s), 1086 (w), 1030 (w), 883 (w), 748 (s).
δ_H (400 MHz, $CDCl_3$)	7.47 (2 H, dd, *J*=7.8, 1.5 Hz, 2 x Ar**H**)
	7.36–7.30 (3 H, m, 3 x Ar**H**)
	4.24 (3 H, s, OC**H**$_3$)
	3.99 (3 H, s, OC**H**$_3$)
	3.35 (1 H, br. s, O**H**).
δ_C (100 MHz, $CDCl_3$)	180.4 (**C**=O), 164.5 (**C**), 135.7 (**C**), 131.9 (**C**H x 2), 129.0 (**C**H), 128.3 (**C**H x 2), 121.6 (**C**), 89.1 (**C**), 83.0 (**C**), 79.1 (**C**), 60.2 (O**C**H$_3$), 58.7 (O**C**H$_3$).
LRMS (ES+)	308 ([M+MeCN+Na]$^+$, 100%)

4-(*tert*-Butyl)-4-hydroxy-2,3-dimethoxycyclobut-2-enone (240c)

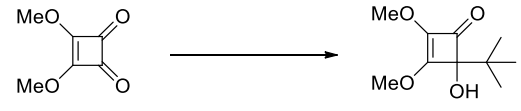

$C_6H_6O_4$
Mol Wt: 142.11

$C_{10}H_{16}O_4$
Mol Wt: 200.23

To a solution of dimethyl squarate (0.50 g, 3.52 mmol) in THF (15 mL) at –78 °C was added ^{t}BuLi (1.78 M in hexanes, 2.5 mL, 4.40 mmol) over 2 min, giving a bright yellow solution. After 60 min, sat. NH_4Cl (20 mL) was added. The reaction mixture was allowed to warm to RT then extracted with diethyl ether (20 mL x 3). The combined organic layers were washed with brine (20 mL x 2), dried ($MgSO_4$), filtered, concentrated *in vacuo* and purified by flash column chromatography (30% EtOAc:petroleum ether with 2% NEt_3) to afford the title compound as a white solid (0.612 g, 3.06 mmol, 86%).

Data is consistent with literature.[69]

MP	76–78 °C (diethyl ether/petroleum ether).
υ_{max} ($CHCl_3$)	3417(m), 2957 (w), 2361 (s), 2343 (s), 1765 (m), 1618 (s), 1463 (m), 1330 (s), 1064 (w), 729 (s).
δ_H (400 MHz, $CDCl_3$)	4.09 (3 H, s, OC**H**$_3$)
	3.91 (3 H, s, OC**H**$_3$)
	2.90 (1 H, br. s, O**H**)
	1.02 (9H, s, C(C**H**$_3$)$_3$).
δ_C (100 MHz, $CDCl_3$)	187.2 (**C**=O), 168.0 (**C**), 133.9 (**C**), 90.9 (**C**), 60.4 (O**C**H$_3$), 58.5 (O**C**H$_3$), 35.3 (**C**(CH$_3$)$_3$), 25.9 (**C**H$_3$ x 3).
LRMS (ES+)	264 ([M+MeCN+Na]$^+$, 100%)

4-Butyl-4-hydroxy-2,3-dimethoxycyclobut-2-enone (240e)

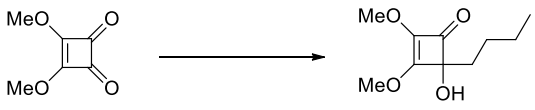

$C_6H_6O_4$
Mol Wt: 142.11

$C_{10}H_{16}O_4$
Mol Wt: 200.23

To a solution of dimethyl squarate (0.75 g, 5.28 mmol) in THF (25 mL) at –78 °C was added ^{n}BuLi (2.35 M in hexanes, 2.47 mL, 5.81 mmol) over 2 min, giving a pale yellow solution. After 60 min, sat. NH_4Cl (20 mL) was added and the reaction mixture was allowed to warm to RT then extracted with DCM (30 mL x 3). The combined organic layers were washed with brine (20 mL x 2), dried ($MgSO_4$), filtered, concentrated *in vacuo*

and purified by flash column chromatography (40%→50% EtOAc:petroleum ether with 2% NEt_3) to afford the title compound as a pale yellow oil (0.912 g, 4.56 mmol, 86%).

υ_{max} ($CHCl_3$)	3389 (w), 2956 (s), 2360 (m), 1766 (m), 1620 (s), 1465 (s), 1334 (s), 1032 (m).
δ_H (400 MHz, $CDCl_3$)	4.12 (3 H, s, OC**H**$_3$)
	3.95 (3 H, s, OC**H**$_3$)
	2.52 (1 H, br. s, O**H**)
	1.89–1.79 (2 H, m, C**H**$_2$)
	1.35–1.31 (4 H, m, 2 x C**H**$_2$)
	0.92–0.89 (3 H, t, *J*=7.0 Hz, C**H**$_3$).
δ_C (100 MHz, $CDCl_3$)	186.8 (**C**=O), 167.8 (**C**), 133.9 (**C**), 86.8 (**C**), 60.1 (O**C**H_3), 58.5 (O**C**H_3), 32.6 (**C**H_2), 27.2 (**C**H_2), 22.8 (**C**H_2), 13.9 (**C**H_3).
LRMS (ES+)	264 ([M+MeCN+Na]$^+$, 100%)
HRMS (ES+)	Found 223.0941, $C_{10}H_{16}NaO_4$ [M+Na]$^+$ requires 223.0946.

4-Hydroxy-2,3-dimethoxy-4-(2-methoxyphenyl)cyclobut-2-enone (240d)

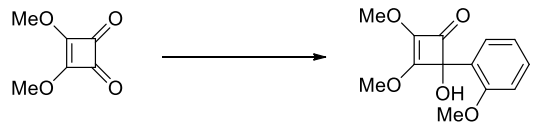

$C_6H_6O_4$
Mol Wt: 142.11

$C_{13}H_{14}O_5$
Mol Wt: 250.25

To a stirred solution of 1-bromo-2-methoxybenzene (0.26 mL, 2.11 mmol) in THF (10 mL) at -78 °C was added ^{n}BuLi (1.57 mL, 2.19 mmol) dropwise and the pale yellow reaction mixture left to stir for 15 min. The resulting solution was added *via* cannula to a solution of dimethyl squarate (0.25 g, 1.76 mmol) in THF (10 mL) at –78 °C. After 20 min, sat. NH_4Cl (50 mL) was added. The reaction mixture was allowed to warm to RT then extracted with DCM (25 mL x 3). The combined organic layers were washed with brine (25 mL x 2), dried ($MgSO_4$), filtered, concentrated *in vacuo* and purified by flash column chromatography (25%→100% *tert*-butyl methyl ether:cyclohexane with 2% NEt_3) to afford the title compound as a white solid (0.384 g, 1.54 mmol, 87%)

Data is consistent with literature.[69]

MP	100-102 °C (chloroform/cyclohexane).
υ_{max} ($CHCl_3$)	3407 (w), 2951 (w), 1775 (m), 1629 (s), 1465 (m), 1334 (s), 1039 (m), 991 (w).

δ_H (400 MHz, $CDCl_3$)	7.35–7.28 (2 H, m, 2 x Ar**H**)
	7.03–6.94 (2 H, m, 2 x Ar**H**)
	4.96 (1 H, s, O**H**)
	4.14 (3 H, s, OC**H**$_3$)
	4.00 (3 H, s, OC**H**$_3$)
	3.95 (3 H, s, OC**H**$_3$).
δ_C (100 MHz, $CDCl_3$)	183.9 (**C**=O), 164.5 (**C**), 157.4 (**C**), 134.7 (**C**), 129.7 (**C**H), 127.4 (**C**H), 125.4 (**C**), 121.4 (**C**H), 112.1 (**C**H) 88.6 (**C**), 60.2 (O**C**H$_3$), 58.5 (O**C**H$_3$), 56.3 (O**C**H$_3$).
LRMS (ES+)	251 ([M+H]$^+$, 100%).

4-Hydroxy-2,3-dimethoxy-4-(pyridin-3-yl)cyclobut-2-enone (240h)

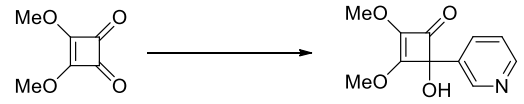

$C_6H_6O_4$
Mol Wt: 142.11

$C_{11}H_{11}NO_4$
Mol Wt: 221.21

To a clear solution of 3-bromopyridine (1.2 mL, 12.67 mmol) in Diethyl ether (45 mL) stirring at –50 °C was added ^{n}BuLi (8.25 mL, 1.6 M in hexane, 13.19 mmol) dropwise and then stirred at -50 °C for 15 min. The reaction mixture was cooled down to –78 °C and cannulated over into a solution of 3, 4-dimethoxycyclobut-3-ene-1,2-dione (1.5 g, 10.56 mmol) in THF (35 mL) at -78 °C. The resultant reaction mixture was stirred at –78 °C for 20 mins, after which it was warmed to and stirred at -60 ºC for 15 min. The reaction mixture was quenched at –78 °C with NH_4Cl (sat) (50 mL) and warmed to RT. The aqueous solution was extracted with DCM (50 mL x 3). The combined organic layers were washed with brine (50 mL x 2), dried ($MgSO_4$), filtered, concentrated *in vacuo* and purified by flash column chromatography (0%→10% MeOH:DCM with 1% NEt_3) to afford the title compound as an yellow solid (1.419 g, 6.42 mmol, 61%).

MP	114-116 °C (DCM/cyclohexane).
υ_{max} ($CHCl_3$)	3037 (w), 2845 (w), 1774 (m), 1628 (s), 1466 (m), 1330 (s), 1059 (m), 992 (w).
δ_H (400 MHz, $CDCl_3$)	8.96 (1 H, dd, *J*=2.0, 0.6 Hz, Ar**H**)
	8.47 (1 H, dd, *J*=4.9, 1.6 Hz, Ar**H**)
	7.90 (1 H, dt, *J*=8.0, 1.9 Hz, Ar**H**)
	7.30 (1 H, ddd, *J*=8.0, 4.9, 0.8 Hz, Ar**H**)
	5.89 (1 H, s, O**H**)

	4.08 (3 H, s, OC**H**$_3$)
	3.98 (3 H, s, OC**H**$_3$).
δ_C (100 MHz, $CDCl_3$)	183.6 (**C**=O), 165.9 (**C**), 148.7 (**C**H), 146.9 (**C**H), 135.4 (**C**), 134.4 (**C**H), 133.8 (**C**), 123.5 (**C**H), 86.0 (**C**), 60.4 (O**C**H$_3$), 58.7 (O**C**H$_3$).
LRMS (ES+)	222 ([M+H]$^+$, 100%).
HRMS (ES+)	Found 222.0759, $C_{11}H_{12}NO_4$ [M+H]$^+$ requires 222.0766.

General Experimental for Photo-Flow Reactions

Solutions of **240** in degassed acetonitrile at a concentration of 0.05 M were pumped using the Vapourtec R4/R2+ device into the photo-reactor. The resulting solutions were concentrated *in vacuo* then purified by flash column chromatography.

3,4-Dimethoxy-5-phenylfuran-2(5*H*)-one (241a)

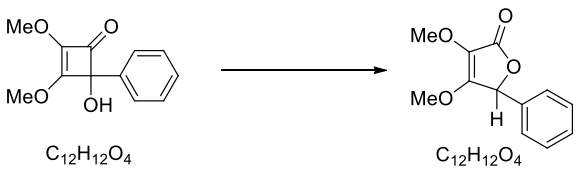

$C_{12}H_{12}O_4$
Mol Wt: 220.22

$C_{12}H_{12}O_4$
Mol Wt: 220.22

A prepared solution of **240a** (0.110 g, 0.5 mmol) in acetonitrile (10 mL) was pumped into the photo-reactor for 90 min. The resulting solution was concentrated *in vacuo* then purified by flash column chromatography (30% EtOAc:petroleum ether) to afford the title compound as a pale yellow oil (0.109 g, 0.495 mmol, 99%).

Data is consistent with literature.

υ_{max} ($CHCl_3$)	2922 (w), 2360 (s), 2340 (m), 1761 (m), 1675 (s), 1459 (s), 1336 (s), 1336 (m), 1049 (s), 764 (w).
δ_H (300 MHz, $CDCl_3$)	7.42–7.34 (3 H, m, 3 x Ar**H**)
	7.54 (2 H, dd, *J*=6.7, 3.3 Hz, 2 x Ar**H**)
	5.52 (1 H, s, C**H**)
	4.07 (3 H, s, OC**H**$_3$)
	3.90 (3 H, s, OC**H**$_3$).
δ_C (75 MHz, $CDCl_3$)	169.2 (**C**=O), 159.1 (**C**), 134.2 (**C**), 129.5 (**C**H x 2), 128.8 (**C**H), 126.8 (**C**H x 2), 122.1 (**C**), 76.7 (**C**H), 60.5 (O**C**H$_3$), 59.4 (O**C**H$_3$).
LRMS (ES+)	284 ([M+Na+MeCN]$^+$, 56%)

3,4-Dimethoxy-5-(4-(trimethylsilyl)phenyl)furan-2(5*H*)-one (241g)

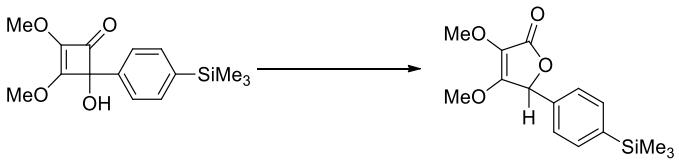

$C_{15}H_{20}O_4Si$
Mol Wt: 292.40

$C_{15}H_{20}O_4Si$
Mol Wt: 292.40

A prepared solution of **240g** (0.146 g, 0.5 mmol) in acetonitrile (10 mL) was pumped into the photo-reactor for 90 min. The resulting solution was concentrated *in vacuo* then purified by flash column chromatography (10%→30% EtOAc:petroleum ether) to afford the title compound as a pale yellow oil (0.135 g, 0.462 mmol, 92%).

υ_{max} ($CHCl_3$)	2954 (w), 2360 (s), 2340 (m), 1765 (m), 1677 (s), 1460 (s), 1335 (s), 1127(m), 1049 (s), 832 (w).
δ_H (300 MHz, $CDCl_3$)	7.54 (2 H, d, *J*=8.1 Hz, 2 x Ar**H**)
	7.29 (2 H, d, *J*=7.9 Hz, 2 x Ar**H**)
	5.51 (1 H, s, C**H**)
	4.07 (3 H, s, OC**H**$_3$)
	3.90 (3 H, s, OC**H**$_3$)
	0.27 (9 H, s, Si(C**H**$_3$)$_3$).
δ_C (75 MHz, $CDCl_3$)	170.5 (**C**=O), 160.3 (**C**), 143.5 (**C**), 135.8 (**C**), 135.8 (**C**H x 2), 127.2 (**C**H x 2), 123.4 (**C**), 78.0 (**C**H), 61.7 (O**C**H$_3$), 60.6 (O**C**H$_3$), 0.01 (Si(**C**H$_3$)$_3$).
LRMS (ES+)	356 ([M+MeCN+Na]$^+$, 100%)
HRMS (ES+)	Found 315.1023, $C_{15}H_{20}NaO_4Si$ [M+Na]$^+$ requires 315.1023.

5-(4-(*tert*-Butyl)phenyl)-3,4-dimethoxyfuran-2(5*H*)-one (241c)

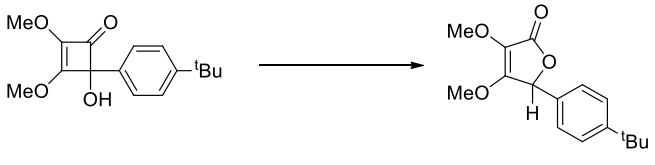

$C_{16}H_{20}O_4$
Mol Wt: 276.33

$C_{16}H_{20}O_4$
Mol Wt: 276.33

A prepared solution of **240c** (0.138 g, 0.5 mmol) in acetonitrile (10 mL) was pumped into the photo-reactor for 90 min. The resulting solution was concentrated *in vacuo* then purified by flash column chromatography (10%→30% EtOAc:petroleum ether) to afford the title compound as a pale yellow oil (0.127 g, 0.46 mmol, 92%).

υ_{max} ($CHCl_3$)	2959 (w), 2361 (s), 2340 (m), 1764 (m), 1679 (s), 1461 (s), 1337 (s), 1130(m), 1051 (s), 844 (w).
δ_H (300 MHz, $CDCl_3$)	7.41 (2 H, d, *J*=8.5 Hz, 2 x Ar**H**)
	7.24 (2 H, d, *J*=8.3 Hz, 2 x Ar**H**)
	5.50 (1 H, s, C**H**)
	4.07 (3 H, s, OC**H**$_3$)
	3.90 (3 H, s, OC**H**$_3$)
	1.32 (9 H, s, C(C**H**$_3$)$_3$).
δ_C (75 MHz, $CDCl_3$)	169.3 (**C**=O), 159.1 (**C**), 152.6 (**C**), 131.1 (**C**), 126.8 (**C**H x 2), 125.8 (**C**H x 2), 122.2 (**C**), 76.7 (**C**H), 60.5 (O**C**H$_3$), 59.3 (O**C**H$_3$), 34.7 (**C**(CH$_3$)$_3$), 31.3 (C(**C**H$_3$)$_3$).
LRMS (ES+)	340 ([M+MeCN+Na]$^+$, 100%)
HRMS (ES+)	Found 299.1254, $C_{16}H_{20}NaO_4$ [M+Na]$^+$ requires 299.1259.

3,4-Dimethoxy-5-(phenylethynyl)furan-2(5*H*)-one (241b)

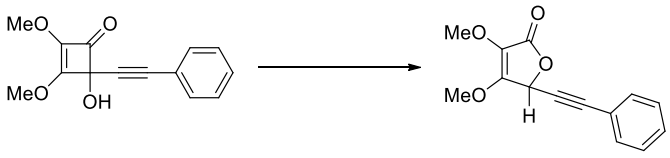

$C_{14}H_{12}O_4$
Mol Wt: 244.24

$C_{14}H_{12}O_4$
Mol Wt: 244.24

A prepared solution of **240b** (0.122 g, 0.5 mmol) in acetonitrile (10 mL) was pumped into the photo-reactor for 90 min. The resulting solution was concentrated *in vacuo* then purified by flash column chromatography (10%→30% EtOAc:petroleum ether) to afford the title compound as a yellow oil (0.115 g, 0.471 mmol, 95%).

Data is consistent with literature.[23]

υ_{max} ($CHCl_3$)	2952 (w), 2233 (s), 1767 (m), 1679 (s), 1461 (s), 1337 (s), 1037 (s), 946 (s), 757 (s), 691 (s).
δ_H (300 MHz, $CDCl_3$)	7.49–7.46 (2 H, m, 2 x Ar**H**)
	7.39–7.30 (3 H, m, 3 x Ar**H**)
	5.47 (1 H, s, C**H**)
	4.20 (3 H, s, OC**H**$_3$)
	3.88 (3 H, s, OC**H**$_3$).
δ_C (75 MHz, $CDCl_3$)	168.1 (**C**=O), 156.0 (**C**), 132.0 (**C**H x 2), 129.4 (**C**H), 128.4 (**C**H x 2), 122.2 (**C**), 121.2 (**C**), 88.24 (**C**), 80.3 (**C**), 65.4(**C**H), 60.3 (O**C**H$_3$), 59.6 (O**C**H$_3$).

LRMS (ES+) 511 ([2M+Na]$^+$, 100%), 308 ([M+MeCN+Na]$^+$, 57%).

5-(*tert*-Butyl)-3,4-dimethoxyfuran-2(5*H*)-one (241c)

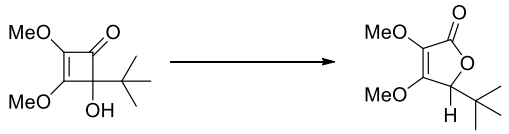

$C_{10}H_{16}O_4$
Mol Wt: 200.23

$C_{10}H_{16}O_4$
Mol Wt: 200.23

A prepared solution of **240c** (0.081 g, 0.36 mmol) in acetonitrile (7.4 mL) was pumped into the photo-reactor for 90 min. The resulting solution was concentrated *in vacuo* then purified by flash column chromatography (10%→30% EtOAc:petroleum ether) to afford the title compound as a pale yellow oil (0.0776 g, 0.354 mmol, 97%).

Data is consistent with literature.[69]

υ_{max} ($CHCl_3$)	2959 (w), 2360 (s), 1762 (s), 1674 (s), 1344 (s), 1065 (s).
δ_H (300 MHz, $CDCl_3$)	4.26 (1 H, s, C**H**)
	4.12 (3 H, s, OC**H**$_3$)
	3.82 (3 H, s, OC**H**$_3$)
	0.99 (9H, s, C(C**H**$_3$)$_3$).
δ_C (75 MHz, $CDCl_3$)	169.4 (**C**=O), 160.0 (**C**), 123.2 (**C**), 82.3 (**C**H), 60.5 (O**C**H$_3$), 59.1 (O**C**H$_3$), 34.9 (**C**(CH$_3$)$_3$), 25.3 (C(**C**H$_3$)$_3$).
LRMS (ES+)	264 ([M+MeCN+Na]$^+$, 55%)

5-Butyl-3,4-dimethoxyfuran-2(5*H*)-one (241e)

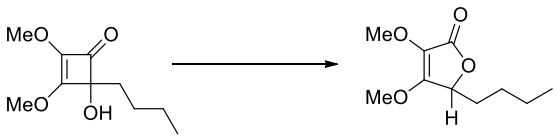

$C_{10}H_{16}O_4$
Mol Wt: 200.23

$C_{10}H_{16}O_4$
Mol Wt: 200.23

A prepared solution of **240e** (0.100 g, 0.5 mmol) in acetonitrile (10 mL) was pumped into the photo-reactor for 90 min. The resulting solution was concentrated *in vacuo* then purified by flash column chromatography (10%→30% EtOAc:petroleum ether) to afford the title compound as a pale yellow oil (0.0951 g, 0.475 mmol, 95%).

υ_{max} ($CHCl_3$) 2956 (w), 2361 (s), 1760 (s), 1677 (s), 1325 (s), 1075 (s).

δ_H (300 MHz, $CDCl_3$)	4.56 (1 H, dd, *J*=7.6, 3.6 Hz, C**H**)
	4.11 (3 H, s, OC**H**$_3$)
	3.81 (3 H, s, OC**H**$_3$)
	1.88–1.82 (1 H, m, C**H**$_2$(CH$_2$)$_2$CH$_3$)
	1.57–1.48 (1 H, m, C**H**$_2$(CH$_2$)$_2$CH$_3$)
	1.42–1.27 (4 H, m, CH$_2$(C**H$_2$**)$_2$CH$_3$)
	0.89 (3H, t, *J*=7.1 Hz, CH$_2$(CH$_2$)$_2$C**H$_3$**).
δ_C (75 MHz, $CDCl_3$)	169.5 (**C**=O), 160.0 (**C**), 122.1 (**C**), 75.4 (**C**H), 60.4 (O**C**H$_3$), 59.2 (O**C**H$_3$), 31.6 (**C**H$_2$), 26.1 (**C**H$_2$), 22.3 (**C**H$_2$), 13.8 (**C**H$_3$).
LRMS (ES+)	264 ([M+MeCN+Na]$^+$, 77%)
HRMS (ES+)	Found 201.1121, $C_{10}H_{17}O_4$ [M+H]$^+$ requires 201.1121.

3,4-Dimethoxy-5-(pyridin-2-yl)furan-2(5*H*)-one (241i) and 1-Hydroxy-2,3-dimethoxy-4*H*-quinolizin-4-one (268)

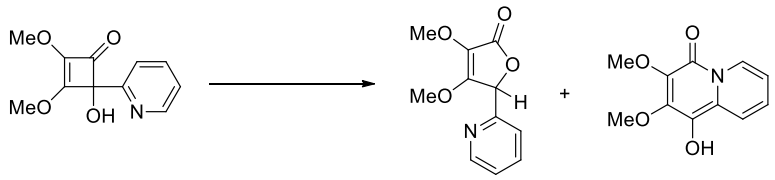

$C_{11}H_{11}NO_4$
Mol Wt: 221.21

$C_{11}H_{11}NO_4$
Mol Wt: 221.21

A prepared solution of **267** (0.221 g, 1.0 mmol) in acetonitrile (20 mL) was pumped into the photo-reactor for 150 min. The resulting solution was concentrated *in vacuo* then purified by flash column chromatography (20%→60% EtOAc:DCM) to afford **241i** as a pink oil (0.095 g, 0.43 mmol, 43%) and **268** as a brown solid (0.089 g, 0.40 mmol, 40%).

Data for **241i**

υ_{max} ($CHCl_3$)	2954 (w), 2358 (s), 1762 (s), 1675 (s), 1335 (s), 1127 (s), 1047 (s), 953 (m), 752 (m).
δ_H (400 MHz, $CDCl_3$)	8.61 (1 H, ddd, *J*=4.9, 1.7, 1.0 Hz, Ar**H**)
	7.74 (1 H, td, *J*=7.7, 1.8 Hz, Ar**H**)
	7.31 (1 H, dd, *J*=6.8, 1.0 Hz, Ar**H**)
	7.28 (1 H, ddd, *J*=7.6, 5.1, 1.0 Hz, Ar**H**)
	5.65 (1 H, s, C**H**)
	4.07 (3 H, s, OC**H**$_3$)
	3.90 (3 H, s, OC**H**$_3$).
δ_C (100 MHz, $CDCl_3$)	169.1 (**C**=O), 158.7 (**C**), 154.1 (**C**), 149.7 (**C**H), 137.3 (**C**H),

	123.4 (**C**H), 122.3 (**C**), 122.2(**C**H), 77.5 (**C**H), 60.3 (O**C**H_3), 59.5 (O**C**H_3).
LRMS (ES+)	285 ([M+MeCN+Na]$^+$, 100%)
HRMS (ES+)	Found 222.0761, $C_{11}H_{12}NO_4$ [M+H]$^+$ requires 222.0766.

Data for **268**

*Data in accordance with the previously synthesised substrate **268**.*

3,4-Dimethoxy-5-(pyridin-3-yl)furan-2(5H)-one (241h)

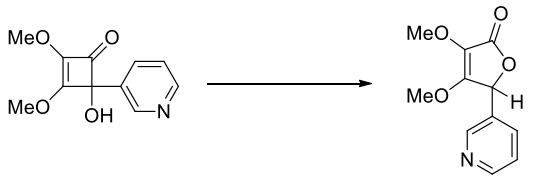

$C_{11}H_{11}NO_4$
Mol Wt: 221.21

$C_{11}H_{11}NO_4$
Mol Wt: 221.21

A prepared solution of **240h** (0.100 g, 1.0 mmol) in acetonitrile (9.04 mL) was pumped into the photo-reactor for 90 min. The resulting solution was concentrated *in vacuo* then purified by flash column chromatography (80%→100% EtOAc:cyclohexane) to afford the title compound as an off-white oil (0.094 g, 0.43 mmol, 94%).

δ_H (600 MHz, $CDCl_3$)	8.65 (1 H, d, *J*=4.0 Hz, Ar**H**)
	8.61 (1 H, br. s, Ar**H**)
	7.68 (1 H, d, *J*=7.7 Hz, Ar**H**)
	7.38 (1 H, dd, *J*=7.9, 4.9 Hz, Ar**H**)
	5.58 (1 H, s, C**H**)
	4.11 (3 H, s, OC**H**$_3$)
	3.91 (3 H, s, OC**H**$_3$).
δ_C (150 MHz, $CDCl_3$)	168.5 (**C**=O), 158.2 (**C**), 150.1(**C**H), 147.9 (**C**H), 134.5 (**C**H), 130.7 (**C**), 123.9 (**C**H), 122.2 (**C**), 74.3 (**C**H), 60.4 (O**C**H_3), 59.6 (O**C**H_3).
LRMS (ES+)	222 ([M+H]$^+$, 100%)

3,4-Dimethoxy-5-(2-methoxyphenyl)furan-2(5H)-one (241d)

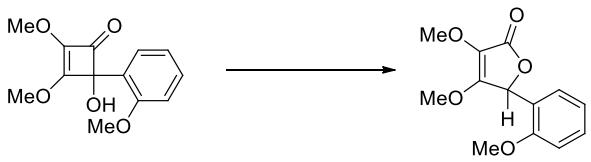

$C_{13}H_{14}O_5$
Mol Wt: 250.25

$C_{13}H_{14}O_5$
Mol Wt: 250.25

A prepared solution of **240d** (0.100 g, 0.400 mmol) in acetonitrile (7.9 mL) was pumped into the photo-reactor for 90 min. The resulting solution was concentrated *in vacuo* then purified by flash column chromatography (10%→30% EtOAc:petroleum ether) to afford the title compound as a pale yellow oil (0.088 g, 0.352 mmol, 88%).

Data is consistent with literature.[69]

υ_{max} ($CHCl_3$)	2951 (w), 2841 (s), 1759 (s), 1676 (s), 1336 (s), 1050 (s), 756 (s).
δ_H (400 MHz, $CDCl_3$)	7.32–7.40 (1 H, m, Ar**H**)
	7.15 (1 H, dd, *J*=7.7, 1.6 Hz, Ar**H**)
	7.02–6.90 (2 H, m, 2 x Ar**H**)
	6.05 (1 H, s, C**H**)
	4.06 (3 H, s, OC$\mathbf{H}_3$)
	3.91 (3 H, s, OC$\mathbf{H}_3$)
	3.86 (3 H, s, OC$\mathbf{H}_3$).
δ_C (100 MHz, $CDCl_3$)	169.5 (**C**=O), 159.4 (**C**), 158.1 (**C**), 130.8 (**C**H), 127.8 (**C**H), 122.7 (**C**), 122.1 (**C**), 120.8 (**C**H), 111.3 (**C**H), 71.7 (**C**H), 60.4 (O**C**H_3), 59.2 (O**C**H_3), 55.8 (O**C**H_3).
LCMS (ES+)	251 ($[M+H]^+$, 60%)

6.4 Experimental Procedures for Chapter 5

1,1-dibromo-3,7-dimethylocta-1,6-diene (315)

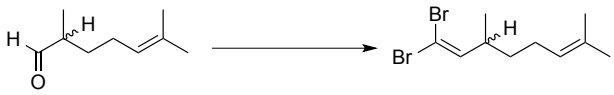

$C_9H_{16}O$
Mol Wt: 140.23

$C_{10}H_{16}Br_2$
Mol Wt: 296.05

A grey suspension of triphenylphosphine (9.35 g, 35.7 mmol), zinc dust (2.56 g, 39.2 mmol) and carbon tetrabromide (11.82 g, 35.7 mmol) in DCM (150 mL) was stirred under nitrogen for 24 h after which was added a solution of 2,6-dimethylhept-5-enal (2.94 mL, 17.83 mmol) in DCM (20 mL). The reaction mixture was stirred at RT for 2 h, after which it was quenched with a saturated solution of potassium carbonate (50 mL). The organic layer was separated and the aqueous layer washed with more DCM (20 mL x 2). The combined organic layers were washed with water (20 mL x 2), followed by brine (30 mL), dried ($MgSO_4$) and concentrated *in vacuo*. The crude product was suspended in diethyl ether and the solid formed filtered, and the filtrate concentrated *in vacuo*. This process was repeated 5 times with diethyl ether followed by cyclohexane to give the title compound (3.39 g, 11.23 mmol, 63% yield) as a yellow oil which was used without further purification.

υ_{max}	2964 (m), 2924 (m), 2852 (w), 1452 (w), 780 (s).
δ_H (400 MHz, $CDCl_3$)	6.19 (1 H, d, *J*=9.5 Hz, Br_2C=C**H**)
	5.09 (1 H, t (with fine splitting), *J*=7.1 Hz, C**H**=C(CH_3)$_2$)
	2.48 (1 H, m, C**H**)
	1.99 (2 H, q, *J*=7.3 Hz, C**H**$_2$)
	1.70 (3 H, d, *J*=1.0 Hz, C**H**$_3$)
	1.62 (3 H, s, C**H**$_3$)
	1.46–1.32 (2 H, m, C**H**$_2$)
	1.01 (3 H, d, *J*=6.9 Hz, C**H**$_3$).
δ_C (100 MHz, $CDCl_3$)	144.3 (**C**H), 132.0 (**C**), 123.9 (**C**H), 87.4 (**C**Br_2), 38.0 (**C**H), 36.2 (**C**H_2), 25.75 (**C**H_2), 25.74 (**C**H_3), 19.2 (**C**H_3), 17.7(**C**H_3).
LRMS (EI)	224 ([M{2^{79}Br}–CH_3CH=C(CH_3)$_2$]$^{+\bullet}$, 226 [M{^{79}Br, ^{81}Br}–CH_3CH=C(CH_3)$_2$]$^{+\bullet}$, 228 [M{2^{81}Br}–CH_3CH=C(CH_3)$_2$]$^{+\bullet}$, 15%), 215 [M{^{79}Br}–Br]$^{+\bullet}$, 217 [M{^{81}Br}–Br]$^{+\bullet}$, 27%), 135 (100%).

4-(3,7-Dimethyloct-6-en-1-yn-1-yl)-4-hydroxy-2,3-dimethoxycyclobut-2-en-1-one (316)

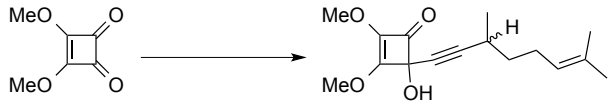

$C_6H_6O_4$
Mol Wt: 142.11

$C_{16}H_{22}O_4$
Mol Wt: 278.35

To a solution of **315** (0.306 g, 1.013 mmol) in THF (20 mL) stirring under N_2 at –78 °C was added ^{n}BuLi (1.11 ml, 1.6 M in hexanes, 1.77 mmol) dropwise. The reaction mixture was stirred at –78 °C for 30 min and then warmed to RT and stirred for a further 30 min. The reaction mixture was then cooled back to –78 °C, and cannulated into a solution of **16** (0.120 g, 0.844 mmol) in THF (10 mL) at -78 °C and the reaction mixture stirred for 30 min. The reaction mixture was quenched at –78 °C with NH_4Cl (15 mL) and extracted with DCM (10 mL x 3). The organic phase was washed with water (10 mL), followed by saturated brine (10 mL), dried ($MgSO_4$), filtered and concentrated *in vacuo* and purified by flash column chromatography (0%→50% EtOAc: petroleum ether) to afford the title compound as a clear oil (0.171 g, 0.614 mmol, 73%).

υ_{max}	3367 (w), 2931 (w), 2859 (w), 1776 (m), 1624 (s), 1469 (m), 1335 (s), 1036 (m), 984 (w).
δ_H (400 MHz, $CDCl_3$)	5.09 (1 H, t (with fine splitting), *J*=7.1 Hz, $CH_2C\mathbf{H}(CH_3)_2$)
	4.19 (3 H, s, $OC\mathbf{H}_3$)
	3.97 (3 H, s, $OC\mathbf{H}_3$)
	2.95 (1 H, s, O**H**)
	2.51 (1 H, sxt, *J*=6.9 Hz, C**H**)
	2.09 (2 H, q, *J*=7.5 Hz, $C\mathbf{H}_2$)
	1.69 (3 H, s, $C\mathbf{H}_3$)
	1.62 (3 H, s, $C\mathbf{H}_3$)
	1.35–1.56 (2 H, m, $C\mathbf{H}_2$)
	1.17 (3 H, q, *J*=7.1 Hz, $C\mathbf{H}_3$).
δ_C (100 MHz, $CDCl_3$)	181.1 (**C**=O), 164.8 (**C**), 135.4 (**C**), 132.2 (**C**), 123.6 (**C**H), 94.9 (**C**), 78.7 (**C**), 74.7 (**C**), 59.9 ($O\mathbf{C}H_3$), 58.6 ($O\mathbf{C}H_3$), 36.6 ($\mathbf{C}H_2$), 25.8 ($\mathbf{C}H_2$), 25.7 (**C**H), 25.6 ($\mathbf{C}H_3$), 20.5 ($\mathbf{C}H_3$), 17.6 ($\mathbf{C}H_3$).
LCMS (ES+)	296 ($[M+NH_4]^+$, 65%).

2,3-Dimethoxy-5-(6-methylhept-5-en-2-yl)cyclohexa-2,5-diene-1,4-dione (318) and 5-Isopropyl-2,3-dimethoxy-8-methyl-5,6,7,8-tetrahydronaphthalene-1,4-dione (320)

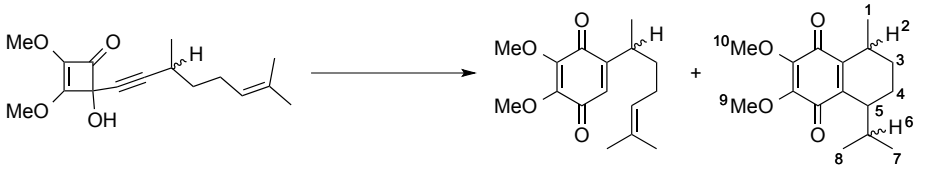

$C_{16}H_{22}O_4$
Mol Wt: 278.35

$C_{16}H_{22}O_4$
Mol Wt: 278.35

A solution of **316** (50 mg, 0.180 mmol) in 1,4-dioxane (2 mL) was heated under flow at 150 °C for 30 min. The output was collected and concentrated *in vacuo*. The crude product was purified by preparative reverse phase HPLC (15%→55% acetonitrile (with 0.1% ammonia):10 mM ammonium bicarbonate solution in water) to give **318** as a orange oil (8 mg, 0.029 mmol, 16%) and **320** as a orange oil (30 mg, 0.126 mmol, 70%).

Data for **318**

υ_{max}	2929 (w), 1652 (m), 1601 (s), 1452 (m), 1139 (m).
δ_H (400 MHz, $CDCl_3$)	6.34 (1 H, d, *J*= 1.0 Hz, C**H**)
	5.05 (1 H, t (with fine splitting), *J*= 7.1 Hz, $CH_2C\mathbf{H}(CH_3)_2$)
	4.02 (3 H, s, $OC\mathbf{H}_3$)
	4.00 (3 H, s, $OC\mathbf{H}_3$)
	2.94 (1 H, sxt, *J*= 6.8 Hz, $C\mathbf{H}_2CH(CH_3)_2$)
	1.96 (2 H, dq, *J*= 15.3, 7.6 Hz, $CC\mathbf{H}_2CH_2$)
	1.67 (3 H, d, *J*=1.1 Hz, $C\mathbf{H}_3$)
	1.56 (3 H, s, $C\mathbf{H}_3$)
	1.61–1.50 (1 H, m, $C\mathbf{H}_2$)
	1.49–1.36 (1 H, m, $C\mathbf{H}_2$)
	1.11 (3 H, d, *J*= 6.8 Hz, $C\mathbf{H}_3$).
δ_C (100 MHz, $CDCl_3$)	184.46(**C**=O), 183.8 (**C**=O), 152.5 (**C**), 145.1 (**C**), 144.3 (**C**), 132.15 (**C**H), 129.2 (**C**H), 123.8 (**C**), 61.2 (OCH_3), 61.1 (OCH_3), 35.8 (CH_2), 31.4 (**C**H), 25.8 (CH_2), 25.7 (CH_3), 19.5 (CH_3), 17.7 (CH_3).
LCMS (ES+)	579 ($[2M+Na]^+$, 65%), 342 ($[M+Na+MeCN]^+$, 73%), 279 ($[M+H]^+$, 58%).
HRMS (ES+)	Found 301.1410, $C_{16}H_{22}NaO_4$ $[M+Na]^+$ requires 301.1410.

Data for **320**

υ_{max}	2929 (w), 1651 (m), 1601 (s), 1452 (m), 1139 (m).
δ_H (600 MHz, $CDCl_3$)	4.01 (6H, s, OC**H**$_3$$^{9'}$ and OC**H**$_3$$^{10'}$)
	3.97 (3H, s, OC**H**$_3$$^{9/10}$)
	3.97 (3H, s, OC**H**$_3$$^{9/10}$)
	3.01–2.94 (2 H, m, C**H**^{2} and C**H**$^{2'}$)
	2.85–2.78 (1 H, m, C**H**^{5})
	2.71 (1 H, br. t, *J*= 5.5 Hz, C**H**$^{5'}$)
	2.22 (1 H, app. octet, *J*= 6.7 Hz, C**H**^{6})
	1.90–1.80 (2 H, m, C**H**$^{6'}$ and C**H**^{3})
	1.77 (1 H, br. dq, *J*=14.1, 1.3 Hz, C**H**^{4})
	1.65–1.56 (5 H, m, C**H**$_2$$^{3'}$, C**H**$_4$, and C**H**$_2$$^{4'}$)
	1.46 (1 H, br. dt, *J*= 13.6, 4.2 Hz, C**H**^{3})
	1.14 (3 H, d, *J*=7.3 Hz, C**H**$_3$^{1})
	1.09 (3 H, d, *J*=7.0 Hz, C**H**$_3$$^{1'}$)
	0.95 (3 H, d, *J*=7.0 Hz, C**H**$_3$^{7})
	0.91 (3 H, d, *J*=6.6 Hz, C**H**$_3$$^{7'/8'}$)
	0.88 (3 H, d, *J*=7.0 Hz, C**H**$_3$$^{7'/8'}$)
	0.77 (3 H, d, *J*=7.0 Hz, C**H**$_3$^{8}).
δ_C (150 MHz, $CDCl_3$)	184.7 (**C**=O'), 184.6 (**C**=O), 183.9 (**C**=O'), 183.8 (**C**=O), 145.4 (**C'**), 145.2 (**C'**), 144.8 (**C**), 144.5 (**C**), 144.4 (**C'**), 144.3 (**C**), 144.2 (**C**), 143.9 (**C'**), 61.2 ($^{9'/10'}$O**C**H$_3$), 61.03 ($^{9/10}$O**C**H$_3$ and $^{9'/10'}$O**C**H$_3$), 61.0 ($^{9/10}$O**C**H$_3$), 38.3 (^{5}**C**H$_2$), 36.5 ($^{5'}$**C**H$_2$), 32.0 ($^{6'}$**C**H$_2$), 29.9 (^{6}**C**H$_2$), 27.4 ($^{3'}$**C**H$_2$), 26.58 (^{2}**C**H), 26.5 ($^{2'}$**C**H), 25.5 (^{3}**C**H$_2$), 22.0 ($^{7'/8'}$**C**H$_3$), 21.11 ($^{1'}$**C**H$_3$), 21.09 (^{7}**C**H$_3$), 20.6 ($^{7/8}$**C**H$_3$), 20.5 (^{1}**C**H$_3$), 19.0 (^{4}**C**H$_2$), 18.9 ($^{4'}$**C**H$_2$), 17.8 (^{8}**C**H$_3$).
LCMS (ES+)	279 ([M+H]$^+$, 100%).
HRMS (ES+)	Found 301.1404, $C_{16}H_{22}NaO_4$ [M+Na]$^+$ requires 301.1410.

Synthesis towards 1,1-dibromo-7-methylocta-1,6-diene (**351**)

6-Methylhept-5-en-1-ol (350)

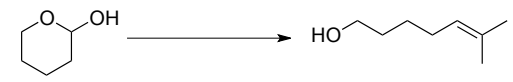

$C_5H_{10}O_2$
Mol Wt: 102.13

$C_8H_{16}O$
Mol Wt: 128.21

To a suspension of potassium hydride (1.24 g, 30.84 mmol) in THF (120 mL) was added isopropyltriphenylphosphine iodide (15.24 g, 35.25 mmol) and the resulting suspension stirred at RT while a solution of tetrahydro-2*H*-pyran-2-ol (3.00 g, 29.38 mmol) in THF (10 mL) was cannulated into the above suspension dropwise. The resulting mixture was refluxed for 3 h, and then cooled to RT. The reaction mixture was diluted with water (200 mL) and extracted with diethyl ether (100 mL x 3). The combined organic layers were washed with brine (200 mL), dried ($MgSO_4$), filtered, the solvent removed under reduced presure and purified by flash column chromatography (10–50% diethyl ether:pentane) to afford the title compound as a clear oil (2.22 g, 17.32 mmol, 59%).

υ_{max} ($CHCl_3$)	2929 (m), 2858 (m), 1444 (w), 1378 (s), 1060 (m), 729 (s).
δ_H (400 MHz, $CDCl_3$)	5.113–5.09 (1 H, m, $CH_2C\mathbf{H}(CH_3)_2$)
	3.63 (2 H, br. t, *J*=6.6 Hz, $C\mathbf{H}_2OH$)
	2.00 (2 H, q, *J*=7.2 Hz, $C\mathbf{H}_2CH(CH_3)_2$)
	1.87 (1 H, br. s, O**H**)
	1.68 (3H, s, $C\mathbf{H}_3$)
	1.60 (3H, s, $C\mathbf{H}_3$)
	1.59–1.53 (2H, m, $C\mathbf{H}_2$)
	1.43–1.35 (2H, m, $C\mathbf{H}_2$).
δ_C (100 MHz, $CDCl_3$)	131.6 (**C**), 124.4 (**C**H), 62.9 (**C**H_2), 32.3 (**C**H_2), 27.7 (**C**H_2), 25.9 (**C**H_2), 25.7 (**C**H_3), 17.6 (**C**H_3).
LRMS (ES+)	146 ($[M+NH_4]^+$, 100%)

1,1-Dibromohepta-1,6-diene (351)

$C_8H_{16}O$
Mol Wt: 128.21

$C_9H_{14}Br_2$
Mol Wt: 282.02

Oxidation of the alcohol to the aldehyde followed by Corey-Ramirez-Fuchs reaction.

To a solution of oxalyl chloride (1.47 mL, 17.16 mmol) in DCM (150 mL) at –78 °C was added DMSO (2.44 mL, 34.32 mmol) dropwise. After stirring for 10 min at –78 °C, a solution of **350** (2.00 g, 15.59 mmol) in DCM (30 mL) was added dropwise, and the resultant cloudy reaction mixture stirred for a further 1 h at –78 °C. Triethylamine (10.9 mL, 78.00 mmol) was added to the cloudy reaction mixture and stirred for 30 mins at –78 °C before warming to RT over 2 h. The reaction mixture was quenched with 1% HCl in NaCl solution (200 mL) and the organic layer separated and further washed further 1% HCl in NaCl solution (100 mL x 2), followed by brine (100 mL). The organic layer was dried ($MgSO_4$), filtered, the solvent removed under reduced pressure to afford the aldehyde as a solution in DCM (20 mL), which was carried forward without purification.

To a solution of triphenylphosphine (16.37 g, 62.39 mmol) in DCM (100 mL) at 0 °C was add carbon tertrabromide (10.34 g, 31.20 mmol) and the orange reaction mixture stirred under Ar for 5 min, after which the above aldehyde in DCM (20 mL) was added. The reaction mixture was quenched after 15 mins, by addition of a saturated solution of K_2CO_3 (200 mL) and the organic layer separated, washed with brine (150 mL), dried ($MgSO_4$), filtered and the solvent removed under reduced pressure to give a brown solid, which was purified by flash column chromatography (neat pentane) to afford the title compound as an pale yellow oil (3.77 g, 13.37 mmol, 86%).

υ_{max} ($CHCl_3$)	2925 (w), 1620 (w), 1444 (w), 1377 (w), 766 (s).
δ_H (300 MHz, $CDCl_3$)	6.40 (1 H, t, *J*=7.2 Hz, Br_2C=C**H**CH_2)
	5.10 (1 H, tdt, *J*=7.2, 2.8, 1.4 Hz, CH_2C**H**=C$(CH_3)_2$)
	2.10 (2 H, q, *J*=7.4 Hz, C**H**$_2$)
	2.02 (2 H, q, *J*=7.3 Hz, C**H**$_2$)
	1.70 (3 H, s, C**H**$_3$)
	1.62 (3 H, s, C**H**$_3$)
	1.47 (2 H, quin, *J*=7.5 Hz, C**H**$_2$).
δ_C (75 MHz, $CDCl_3$)	138.8 (**C**H), 132.3 (**C**), 123.7 (**C**H), 88.6 (**C**Br_2), 32.6 (**C**H_2), 27.9 (**C**H_2), 27.4 (**C**H_2), 25.7 (**C**H_3), 17.7(**C**H_3).

LRMS (EI) 241 ([M{2^{81}Br}– $HC(CH_3)_2]^{+\bullet}$, 6%), 239 ([M{^{79}Br, ^{81}Br}–$HC(CH_3)_2]^{+\bullet}$, 12%), 237 ([M{2^{79}Br}–$HC(CH_3)_2]^{+\bullet}$, 7%), 214 ([M{2^{81}Br}–$CH_3HC(CH_3)_2]^{+\bullet}$, 12%), 212 ([M{^{79}Br, ^{81}Br}–$CH_3HC(CH_3)_2]^{+\bullet}$, 26%), 210 ([M{$2^{79}$Br}–$CH_3HC(CH_3)_2]^{+\bullet}$, 13%), 203 ([M{^{81}Br}–Br]$^+$, 34%), 201 ([M{^{79}Br}–Br]$^+$, 44%), 121 ([M–$HBr_2]^+$, 54%).

4-Hydroxy-2,3-dimethoxy-4-(7-methyloct-6-en-1-yn-1-yl)cyclobut-2-enone (323)

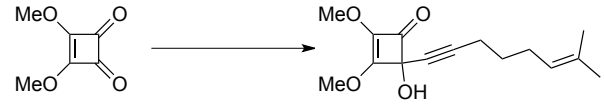

$C_6H_6O_4$
Mol Wt: 142.11

$C_{15}H_{20}O_4$
Mol Wt: 264.32

To a solution of **351** (0.595 g, 1.759 mmol) in THF (25 mL) stirring at –78 °C was added ^{n}BuLi (1.84 mL, 2.4 M in hexane, 4.398 mmol) dropwise and the reaction mixture stirred at –78 °C for 30 min and then warmed to RT over 30 min. The reaction mixture was cooled back down to –78 °C and cannulated over into a solution of **16** (0.250 g, 1.759 mmol) in THF (10 mL) at –78 °C. The resultant reaction mixture was stirred at –78 °C for 30 min, and then quenched with NH_4Cl (sat.) (50 mL) at –78 °C. The reaction mixture was warmed up to RT, and the aqueous solution extracted with DCM (50 mL x 2). The combined organic layers were dried ($MgSO_4$), filtered, concentrated *in vacuo* and purified by flash column chromatography (0%→40% EtOAc:petroleum ether) to afford the title compound as an off-white waxy solid (0.449 g, 1.591 mmol, 90%).

MP Decomposition at 40 °C.

υ_{max} ($CHCl_3$) 3367 (w), 2929 (w), 2859 (w), 1777 (m), 1622 (s), 1468 (m), 1339 (s), 1034 (m), 983 (w).

δ_H (400 MHz, $CDCl_3$) 5.08 (1 H, t (with fine splitting) *J*=6.7 Hz, $CH_2C\mathbf{H}(CH_3)_2$)

4.19 (3 H, s, $OC\mathbf{H}_3$)

3.96 (3 H, s, $OC\mathbf{H}_3$)

3.05 (1 H, s, O**H**)

2.25 (2 H, t, *J*=7.2 Hz, $C\mathbf{H}_2$)

2.06 (2 H, q, *J*=7.2 Hz, $C\mathbf{H}_2$)

1.69 (3 H, s, $C\mathbf{H}_3$)

1.60 (3 H, s, $C\mathbf{H}_3$)

1.59–1.50 (2 H, m, $C\mathbf{H}_2$).

δ_C (100 MHz, $CDCl_3$) 181.1 (**C**=O), 164.9 (**C**), 135.4 (**C**), 132.6 (**C**), 123.3 (**C**H), 90.7 (**C**), 78.7 (**C**), 74.5 (**C**), 60.0 (OCH_3), 58.6 (OCH_3), 28.4 (CH_2), 27.1 (CH_2), 25.7 (CH_3), 18.4 (CH_2), 17.6 (CH_3).

LRMS (ES+) 551 ([2M+Na]$^+$, 100%), 328 ([M+Na+MeCN]$^+$, 25%).

HRMS (ES+) Found 265.1438, $C_{15}H_{21}O_4$ [M+H]$^+$ requires 265.1434.

2,3-Dimethoxy-5-(5-methylhex-4-en-1-yl)cyclohexa-2,5-diene-1,4-dione (325)

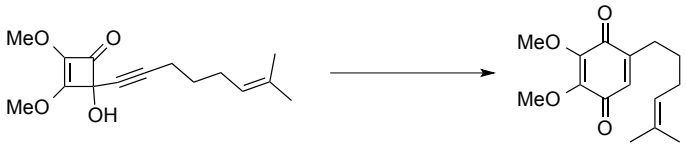

$C_{15}H_{20}O_4$
Mol Wt: 264.32

$C_{15}H_{20}O_4$
Mol Wt: 264.32

A solution of **323** (0.050 g, 0.189 mmol) in 1,4-dioxane + 1% H_2O (5 mL) was heated at 150 °C under flow in stainless steel tubing for 30 min. The resulting solution was concentrated *in vacuo* then purified by high performance liquid chromatography (8% EtOAc:cyclohexane) to afford the title compound as an orange oil (48 mg, 0.177 mmol, 95%).

υ_{max} ($CHCl_3$) 2931 (w), 2895 (w), 1675 (s), 1601 (s), 1453 (m), 1136 (m), 1077 (m).

δ_H (300 MHz, $CDCl_3$) 6.38 (1 H, t, *J*= 1.5 Hz, C**H**)

5.15–5.03 (1 H, m, $CH_2C\mathbf{H}(CH_3)_2$)

4.02 (3 H, s, $OC\mathbf{H}_3$)

4.00 (3 H, s, $OC\mathbf{H}_3$)

2.46–2.35 (2 H, m, $C\mathbf{H}_2CH(CH_3)_2$)

2.04 (2 H, q, *J*= 7.1 Hz, $CC\mathbf{H}_2CH_2$)

1.69 (3 H, d, *J*=1.1 Hz, $C\mathbf{H}_3$)

1.60 (3 H, s, $C\mathbf{H}_3$)

1.58–1.48 (2 H, m, $C\mathbf{H}_2$).

δ_C (75 MHz, $CDCl_3$) 184.4 (**C**=O), 184.1 (**C**=O), 147.9 (**C**), 144.6 (**C**), 132.5 (**C**), 130.4 (**C**H), 123.5 (**C**H), 110.0 (**C**), 61.2 ($O\mathbf{C}H_3$), 61.1 ($O\mathbf{C}H_3$), 28.3 ($\mathbf{C}H_2$), 27.9 ($\mathbf{C}H_2$), 27.5 ($\mathbf{C}H_2$), 25.7 ($\mathbf{C}H_3$), 17.8 ($\mathbf{C}H_3$).

LRMS (ES+) 551 ([2M+Na]$^+$, 57%), 328 ([M+Na+MeCN]$^+$, 34%), 265 ([M+H]$^+$, 12%).

HRMS (ES+) Found 287.1267, $C_{15}H_{20}NaO_4$ [M+Na]$^+$ requires 287.1254.

2,3-Dimethoxy-4-(methoxymethoxy)-4-(7-methyloct-6-en-1-yn-1-yl)cyclobut-2-enone (328)

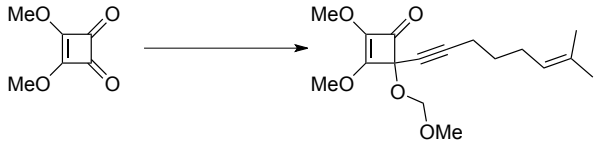

$C_6H_6O_4$
Mol Wt: 142.11

$C_{17}H_{24}O_5$
Mol Wt: 308.37

To a solution of 1,1-dibromo-7-methylocta-1,6-diene (0.595 g, 1.759 mmol) in THF (25 mL) stirring at –78 °C was added ^{n}BuLi (1.84 mL, 2.4 M in hexane, 4.398 mmol) dropwise and the reaction mixture stirred at –78 °C for 30 min and then warmed to RT over 30 min. The reaction mixture was cooled back down to –78 °C and cannulated over into a solution of 3, 4-dimethoxycyclobut-3-ene-1,2-dione (0.250 g, 1.759 mmol) in THF (10 mL) at –78 °C. The resultant reaction mixture was stirred at –78 °C for 30 min, and MOMCl (0.17 mL, 2.199 mmol) added at –78 °C and allowed to warm to RT overnight. The reaction mixture was quenched with H_2O (50 mL) and aqueous solution extracted with DCM (50 mL x 2). The combined organic layers were dried ($MgSO_4$), filtered, concentrated *in vacuo* and purified by flash column chromatography (0%→40% EtOAc:petroleum ether) to afford the title compound as an pale yellow oil (0.391 g, 1.267 mmol, 72%).

υ_{max} ($CHCl_3$)	2931 (w), 1782 (m), 1640 (s), 1468 (m), 1339 (s), 1021 (m), 980 (w).
δ_H (400 MHz, $CDCl_3$)	5.07 (1 H, t (with fine splitting), *J*=7.2 Hz, $CH_2C\mathbf{H}(CH_3)_2$)
	4.90 (1H, d, *J*=7.8 Hz, $C\mathbf{H}_2OCH_3$)
	4.87 (1H, d, *J*=7.8 Hz, $C\mathbf{H}_2OCH_3$)
	4.17 (3 H, s, $OC\mathbf{H}_3$)
	3.98 (3 H, s, $OC\mathbf{H}_3$)
	3.39 (3 H, s, $OC\mathbf{H}_3$)
	2.28 (2 H, t, *J*=7.3 Hz, $C\mathbf{H}_2$)
	2.06 (2 H, q, *J*=6.8 Hz, $C\mathbf{H}_2$)
	1.68 (3 H, s, $C\mathbf{H}_3$)
	1.60 (3 H, s, $C\mathbf{H}_3$)
	1.59–1.51 (2 H, m, $C\mathbf{H}_2$).
δ_C (100 MHz, $CDCl_3$)	179.6 (**C**=O), 164.3 (**C**), 136.1 (**C**), 132.5 (**C**), 123.3 (**C**H), 93.0 ($\mathbf{C}H_2$), 92.4 (**C**), 83.1 (**C**), 72.0 (**C**), 60.1($O\mathbf{C}H_3$), 58.6 ($O\mathbf{C}H_3$), 55.9 ($O\mathbf{C}H_3$), 28.4 ($\mathbf{C}H_2$), 27.1 ($\mathbf{C}H_2$), 25.7 ($\mathbf{C}H_3$), 18.5 ($\mathbf{C}H_2$), 17.6 ($\mathbf{C}H_3$).
LRMS (ES+)	639 ($[2M+Na]^+$, 45%), 372 ($[M+Na+MeCN]^+$, 56%), 331

([M+Na]$^+$, 100%).

HRMS (ES+) Found 331.1513, $C_{17}H_{24}NaO_5$ [M+Na]$^+$ requires 331.1516.

7,8-Dimethoxy-6-(methoxymethoxy)-2-(2-methylprop-1-en-1-yl)chroman (331)

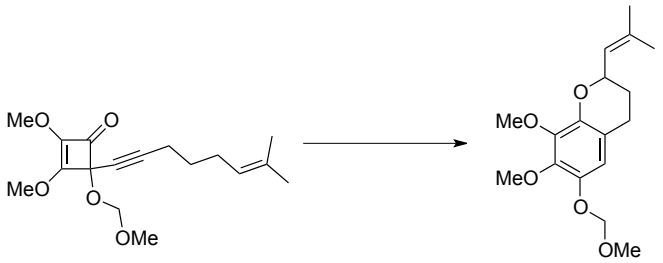

$C_{17}H_{24}O_5$
Mol Wt: 308.37

$C_{17}H_{24}O_5$
Mol Wt: 308.37

A solution of **328** (0.200 g, 0.649 mmol) in 1,4-dioxane (5 mL) was heated at 150 °C under flow in stainless steel tubing for 30 min. The resulting solution was concentrated *in vacuo* then purified by high performance liquid chromatography (8% EtOAc:cyclohexane) to afford the title compound as a pale yellow oil (0.133 mg, 0.474 mmol, 73%).

υ_{max} ($CHCl_3$) 2932 (w), 1485 (m), 1461 (s), 1404 (m), 1062 (m), 990 (w).

δ_H (400 MHz, $CDCl_3$) 6.60 (1 H, s, Ar**H**)

5.38 (1H, ddt, *J*=8.2, 2.7, 1.5 Hz, C**H**$(CH_3)_2$)

5.13 (2 H, s, C**H**$_2$OCH_3)

4.76–4.66 (1H, m, OC**H**CH_2)

3.88 (3 H, s, OC**H**$_3$)

3.87 (3 H, s, OC**H**$_3$)

3.53 (3 H, s, OC**H**$_3$)

2.88–2.76 (1 H, m, C**H**$_2$)

2.76–2.66 (1 H, m, C**H**$_2$)

1.99–1.91 (1 H, m, C**H**$_2$)

1.87–1.78 (1 H, m, C**H**$_2$)

1.77 (3 H, d, *J*=1.2 Hz, C**H**$_3$)

1.74 (3 H, d, *J*=1.2 Hz, C**H**$_3$).

δ_C (100 MHz, $CDCl_3$) 144.0 (**C**), 143.6 (**C**), 142.5 (**C**), 142.3 (**C**), 136.4 (**C**H), 124.6 (**C**H), 117.2 (**C**), 112.2 (**C**H), 96.2 (**C**H$_2$), 72.8 (**C**H), 61.3 (O**C**H$_3$), 61.0 (O**C**H$_3$), 59.1 (O**C**H$_3$), 27.9 (**C**H$_2$), 25.8 (**C**H$_3$), 24.5 (**C**H$_2$), 18.4 (**C**H$_3$).

LRMS (ES+) 639 ([2M+Na]$^+$, 29%), 372 ([M+Na+MeCN]$^+$, 100%).

HRMS (ES+) Found 331.1517, $C_{17}H_{24}NaO_5$ $[M+H]^+$ requires 331.1516.

3,4-Di-*tert*-butoxycyclobut-3-ene-1,2-dione (*tert*-butyl squarate)

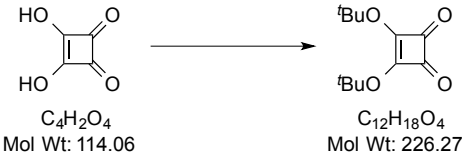

A solution of squaric acid (2.0 g, 17.54 mmol) in ^{t}BuOH (70 mL) stirring under Ar was refluxed for 1 h while trimethyl orthoformate (19.38 mL, 175 mmol) was added dropwise. The resulting distillate was collected simultaneously by short-path distillation. The crude reaction mixture was cooled to RT and concentrated *in vacuo* where the crude product was purified by column chromatography (0%→25% EtOAc:petroleum ether) to afford the title compound as a white solid (2.78 g, 12.28 mmol, 70%).

Data is consistent with literature.[119]

MP	106–108 °C (EtOAc/hexane).
υ_{max} ($CHCl_3$)	2980 (w), 1804 (m), 1726 (s), 1573 (s), 1374 (s).
δ_H (400 MHz, $CDCl_3$)	1.62 (18 H, s, 2 x OC($C\mathbf{H}_3$)$_3$).
δ_C (100 MHz, $CDCl_3$)	188.6 (**C**=O x 2), 186.3 (**C** x 2), 87.0 (O**C**(CH_3)$_3$ x 2), 28.7 (OC(**C**H_3)$_3$ x 2).
LCMS (ES+)	244 ($[M+NH_4]^+$, 100%).

3-(*tert*-Butoxy)-4-methylcyclobut-3-ene-1,2-dione (185)

$C_{12}H_{18}O_4$
Mol Wt: 226.27

$C_9H_{12}O_3$
Mol Wt: 168.19

To a solution of *tert*-butyl squarate (2.0 g, 8.84 mmol) in THF (100 mL) stirring under N_2 at –78 °C was added MeLi (6.08 mL, 1.6 M in ether, 9.72 mmol). The reaction mixture was stirred at –78 °C for 15 min, after which TFAA (1.5 mL, 10.6 mmol) was added, and the stirring was continued for a further 15 min. The reaction mixture was quenched with NH_4Cl (20 mL) and the resulting solution warmed to RT and stirred for 1 h at RT. The aqueous solution was extracted with diethyl ether (20 mL x 2). The combined organic layers were washed with brine (50 mL), dried ($MgSO_4$), filtered, concentrated *in vacuo* and purified by flash column chromatography (0%→25% methyl *tert*-butyl ether:cyclohexane) to afford the title compound as an off-white solid (1.05 g, 6.24 mmol, 71%).

Data is consistent with literature.[15]

MP	67–69 °C (EtOAc/petroleum ether).
υ_{max} ($CHCl_3$)	2981 (w), 1793 (s), 1739 (s), 1574 (s), 1395 (s).
δ_H (300 MHz, $CDCl_3$)	2.19 (3 H, s, C**H**$_3$) 1.62 (9 H, s, C(C**H**$_3$)$_3$).
δ_C (75 MHz, $CDCl_3$)	199.9 (**C**=O), 195.9 (**C**=O), 192.7 (**C**), 182.7 (**C**), 87.5 (**C**(CH$_3$)$_3$), 28.7 (C(**C**H$_3$)$_3$), 9.3 (**C**H$_3$).
LCMS (ES+)	186 ([M+NH_4]$^+$, 70%).

2-(*tert*-Butoxy)-3-methyl-4-oxo-1-(phenylethynyl)cyclobut-2-en-1-yl acetate (341b)

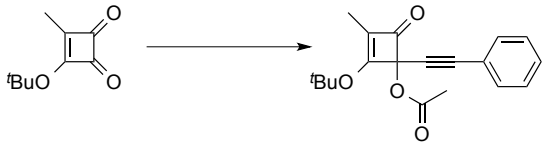

$C_9H_{12}O_3$
Mol Wt: 168.19

$C_{19}H_{20}O_4$
Mol Wt: 312.36

To a solution of phenylacetylene (0.3 mL, 2.705 mmol) in THF (30 mL) stirring at –78 °C was added ^{n}BuLi (1.27 mL, 2.3 M in hexane, 2.914 mmol) dropwise. The reaction mixture was stirred at –78 °C for 15 min and cannulated into a solution of 3-(*tert*-butoxy)-4-methylcyclobut-3-ene-1,2-dione (0.350 g, 2.081 mmol) in THF (10 mL) at –78 °C. The resultant reaction mixture was stirred at –78 °C for 30 min. Acetic anhydride (0.26 mL, 2.705 mmol) was then added and the reaction mixture stirred for a further 1 h at –78 °C. The reaction mixture was quenched with $NaHCO_3$ (sat.) (100 mL) and extracted with DCM (50 mL x 3). The combined organic layers were dried ($MgSO_4$), filtered, concentrated *in vacuo* and purified by flash column chromatography (0%→40% EtOAc:petroleum ether) to afford the title compound as a yellow solid (0.460 g, 1.473 mmol, 71%).

MP	112-114 °C (DCM/hexane).
υ_{max} ($CHCl_3$)	2983 (w), 2233 (w), 1753 (m), 1602 (s), 1466 (m), 1345 (s), 1146 (m), 914 (w).
δ_H (400 MHz, $CDCl_3$)	7.46 (2 H, dd, *J*=7.7, 1.8 Hz, 2 x Ar**H**)
	7.34–7.28 (3 H, m, 3 x Ar**H**)
	2.12 (3 H, s, C**H**$_3$)
	1.83 (3 H, s, C**H**$_3$)
	1.59 (9 H, s, C(C**H**$_3$)$_3$).
δ_C (100 MHz, $CDCl_3$)	183.0 (**C**=O), 174.7 (**C**=O), 168.5 (**C**), 132.0 (**C**H x 2), 128.9 (**C**H), 128.2 (**C**H x 2), 125.8 (**C**), 121.9 (**C**), 90.0 (**C**), 88.4 (**C**), 85.2 (**C**), 81.3 (**C**), 28.8 (C(**C**H$_3$)$_3$), 21.3 (**C**H$_3$), 9.1 (**C**H$_3$).
LRMS (ES+)	647 ([2M+Na]$^+$, 100%), 376 ([M+Na+MeCN]$^+$, 30%).
HRMS (ES+)	Found 335.1261, $C_{19}H_{20}NaO_4$ [M+Na]$^+$ requires 335.1254.

4-(*tert*-Butoxy)-6-hydroxy-3-methyl-[1,1'-biphenyl]-2,5-dione (349)

$C_{19}H_{20}O_4$
Mol Wt: 312.36

$C_{17}H_{18}O_4$
Mol Wt: 286.33

A solution of **341b** (0.100 g, 0.324 mmol) in 1,4-dioxane (+ 1% H_2O) (5 mL) was heated at 150 °C under flow in stainless steel tubing for 30 min and the resulting solution concentrated *in vacuo*. The crude material was dissolved in THF (5 mL) and to it added 2M NaOH (3 mL) and stirred for 30 min at RT. The reaction mixture was acidified to pH 9 using 2M HCl and partitioned between EtOAc (20 mL x 2) and H_2O (20 mL). The combined organic layers were washed with brine (20 mL), dried ($MgSO_4$), filtered and concentrated *in vacuo*. The crude orange oil was stirred as a DCM solution in air for 2 h, concentrated *in vacuo*, and purified by flash column chromatography (30%→50% EtOAc:petroleum ether) to afford the title compound as an orange solid (88 mg, 0.308 mmol, 95%).

MP	180–182 °C (diethyl ether/hexane).
υ_{max} ($CHCl_3$)	3366 (w), 2972 (w), 1658 (s), 1632 (s), 1362 (s), 1294 (s), 738(m).
δ_H (400 MHz, $CDCl_3$)	7.47–7.34 (5 H, m, 5 x Ar**H**)
	7.19 (1 H, s, Ar**H**)
	2.09 (3 H, s, C**H**$_3$)
	1.46 (9 H, s, C(C**H**$_3$)$_3$).
δ_C (100 MHz, $CDCl_3$)	187.1 (**C**=O), 181.4 (**C**=O), 151.1 (**C**), 149.3 (**C**), 137.5 (**C**), 130.5 (**C**H x 2), 129.8 (**C**), 128.4 (**C**H), 127.9 (**C**H x 2), 118.8 (**C**), 84.6 (**C**), 29.5 (C(**C**H$_3$)$_3$), 11.5 (**C**H$_3$).
LRMS (ES–)	285 ([M–H]$^-$, 100%).
HRMS (ES+)	Found 309.1101, $C_{17}H_{18}NaO_4$ $[M+Na]^+$ requires 309.1.97.

3-(*tert*-Butoxy)-4-hydroxy-2-methyl-4-(phenylethynyl)cyclobut-2-en-1-one (341a)

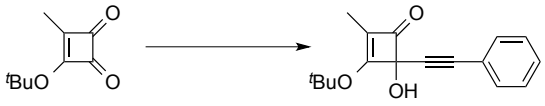

$C_9H_{12}O_3$
Mol Wt: 168.19

$C_{17}H_{18}O_3$
Mol Wt: 270.33

To a solution of phenylacetylene (0.2 mL, 1.858 mmol) in THF (20 mL) stirring at –78 °C was added ^{n}BuLi (0.77 mL, 2.4 M in hexane, 1.858 mmol) dropwise. The reaction mixture was stirred at –78 °C for 15 min and cannulated into a solution of 3-(*tert*-butoxy)-4-methylcyclobut-3-ene-1,2-dione (0.250 g, 1.486 mmol) in THF (10 mL) at –78 °C. The resultant reaction mixture was stirred at –78 °C for 30 min, and quenched with NH_4Cl (sat.) (50 mL) and extracted with DCM (50 mL x 2). The combined organic layers were dried ($MgSO_4$), filtered, concentrated *in vacuo* and purified by flash column chromatography (0%→60% EtOAc:petroleum ether) to afford the title compound as a yellow solid (0.375 g, 1.387 mmol, 93%).

MP	85–87 °C (DCM/hexane at 4 °C).
υ_{max} ($CHCl_3$)	3316 (w), 2981 (w), 1753 (m), 1590 (s), 1388 (m), 1339 (s), 1145 (m), 910 (w).
δ_H (400 MHz, $CDCl_3$)	7.43 (2 H, d, *J*=7.7, 1.6 Hz, 2 x Ar**H**)
	7.36–7.28 (3 H, m, 3 x Ar**H**)
	3.71 (1 H, s, O**H**)
	1.73 (3 H, s, C$\mathbf{H}_3$)
	1.64 (9 H, s, C(C$\mathbf{H}_3$)$_3$).
δ_C (100 MHz, $CDCl_3$)	188.2 (**C**=O), 179.4 (**C**), 131.8 (**C**H x 2), 128.8 (**C**H), 128.2 (**C**H x 2), 126.9 (**C**), 122.0 (**C**), 89.5 (**C**), 85.6 (**C**), 84.8 (**C**), 84.2 (**C**), 29.0 (C(**C**H_3)$_3$), 7.5 (**C**H_3).
LRMS (ES+)	563 ([2M+Na]$^+$, 100%), 334 ([M+Na+MeCN]$^+$, 13%).
HRMS (ES+)	Found 293.1155, $C_{17}H_{18}NaO_3$ [M+Na]$^+$ requires 293.1148.

4-(*tert*-Butoxy)-6-hydroxy-3-methyl-[1,1'-biphenyl]-2,5-dione (343) and **(*E*)-2-Benzylidene-4-(*tert*-butoxy)-5-methylcyclopent-4-ene-1,3-dione (345).**

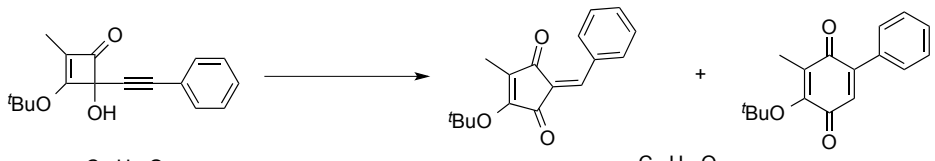

A solution of **341a** (0.100 g, 0.369 mmol) in 1,4-dioxane (5 mL) was heated at 150 °C under flow in stainless steel tubing for 30 min. The resulting solution was concentrated *in vacuo* and purified by flash column chromatography (30%→50% DCM:hexane) to afford **343** as a white solid (36 mg, 0.133 mmol, 36%) and **345** as an yellow oil (51 mg, 0.189 mmol, 51%).

Data for **343**

MP	125–127 °C (diethyl ether/hexane).
υ_{max} ($CHCl_3$)	3073 (w), 2975 (w), 1666 (m), 1625 (s), 1598 (m), 1380 (s), 1119 (m), 780 (w).
δ_H (400 MHz, $CDCl_3$)	8.32–8.24 (2 H, m, 2 x Ar**H**)
	7.48–7.42 (3 H, m, 3 x Ar**H**)
	7.41 (1 H, s, C**H**)
	2.02 (3 H, s, C$\mathbf{H}_3$)
	1.56 (9 H, s, C(C$\mathbf{H}_3$)$_3$).
δ_C (100 MHz, $CDCl_3$)	190.2 (**C**=O), 189.4 (**C**=O), 165.9 (**C**), 144.6 (**C**), 139.1 (**C**H), 133.2 (**C**H x 2), 132.9 (**C**), 131.7 (**C**H), 128.5 (**C**H x 2), 126.8 (**C**), 85.2 (**C**), 29.5 (C(**C**H_3)$_3$), 7.8 (**C**H_3).
LRMS (ES+)	563 ([2M+Na]$^+$, 34%), 334 ([M+Na+MeCN]$^+$, 100%).
HRMS (ES+)	Found 293.1150, $C_{17}H_{18}NaO_3$ [M+Na]$^+$ requires 293.1148.

Data for **345**

υ_{max} ($CHCl_3$)	2976 (w), 2359 (w), 1652 (s), 1596 (m), 1369 (s), 1144 (m), 841 (w).
δ_H (400 MHz, $CDCl_3$)	7.51–7.41 (5 H, m, 5 x Ar**H**)
	6.75 (1 H, s, C**H**)
	2.08 (3 H, s, C$\mathbf{H}_3$)
	1.45 (9 H, s, C(C$\mathbf{H}_3$)$_3$).
δ_C (100 MHz, $CDCl_3$)	187.8 (**C**=O), 185.0 (**C**=O), 154.5 (**C**), 145.8 (**C**), 134.9 (**C**), 133.1 (**C**), 131.5 (**C**H), 129.8 (**C**H), 129.3 (**C**H x 2), 128.3

	(**C**H x 2), 84.7 (**C**), 29.5 (C(**C**H_3)$_3$), 11.0 (**C**H_3).
LRMS (ES+)	563 ([2M+Na]$^+$, 65%), 334 ([M+Na+MeCN]$^+$, 56%).
HRMS (ES+)	Found 293.1148, $C_{17}H_{18}NaO_3$ [M+Na]$^+$ requires 293.1148.

Chapter 7.References

(1) Perri, S. T.; Foland, L. D.; Decker, O. H. W.; Moore, H. W. *J. Org. Chem.* **1986**, *51*, 3067.
(2) Moore, H. W.; Yerxa, B. R. *Chemtracts–Organic Chemistry* **1992**, *5*, 273.
(3) Moore, H. W.; Yerxa, B. R. *Adv. Strain Org. Chem.* **1995**, *4*, 81.
(4) Birchler, A. G.; Liu, F. Q.; Liebeskind, L. S. *J. Org. Chem.* **1994**, *59*, 7737.
(5) Zhang, D. W.; Llorente, I.; Liebeskind, L. S. *J. Org. Chem.* **1997**, *62*, 4330.
(6) Moore, H. W.; Perri, S. T. *J. Org. Chem.* **1988**, *53*, 996.
(7) Harrowven, D. C.; Pascoe, D. D.; Demurtas, D.; Bourne, H. O. *Angew. Chem. Int. Ed.* **2005**, *44*, 1221.
(8) Harrowven, D. C.; Pascoe, D. D.; Guy, I. L. *Angew. Chem. Int. Ed.* **2007**, *46*, 425.
(9) Liebeskind, L. S.; Iyer, S.; Jewell, C. F. *J. Org. Chem.* **1986**, *51*, 3065.
(10) Kirmse, W.; Rondan, N. G.; Houk, K. N. *J. Am. Chem. Soc.* **1984**, *106*, 7989.
(11) Liebeskind, L. S. *Tetrahedron* **1989**, *45*, 3053.
(12) Xu, S. L.; Moore, H. W. *J. Org. Chem.* **1989**, *54*, 4024.
(13) Xu, S. L.; Moore, H. W. *J. Org. Chem.* **1992**, *57*, 326.
(14) Reed, M. W.; Pollart, D. J.; Perri, S. T.; Foland, L. D.; Moore, H. W. *J. Org. Chem.* **1988**, *53*, 2477.
(15) Liebeskind, L. S.; Fengl, R. W.; Wirtz, K. R.; Shawe, T. T. *J. Org. Chem.* **1988**, *53*, 2482.
(16) Turnbull, P.; Moore, H. W. *J. Org. Chem.* **1995**, *60*, 644.
(17) Dess, D. B.; Martin, J. C. *J. Org. Chem.* **1983**, *48*, 4155.
(18) Comins, D. L. *Tetrahedron Lett.* **1983**, *24*, 2807.
(19) Lee, K. H.; Moore, H. W. *J. Org. Chem.* **1995**, *60*, 735.
(20) Lohse, P.; Loner, H.; Acklin, P.; Sternfeld, F.; Pfaltz, A. *Tetrahedron Lett.* **1991**, *32*, 615.
(21) Karlsson, J. O.; Nguyen, N. V.; Foland, L. D.; Moore, H. W. *J. Am. Chem. Soc.* **1985**, *107*, 3392.
(22) Perri, S. T.; Dyke, H. J.; Moore, H. W. *J. Org. Chem.* **1989**, *54*, 2032.
(23) Foland, L. D.; Karlsson, J. O.; Perri, S. T.; Schwabe, R.; Xu, S. L.; Patil, S.; Moore, *J. Am. Chem. Soc.* **1989**, *111*, 975.
(24) Xiong, Y. F.; Moore, H. W. *J. Org. Chem.* **1996**, *61*, 9168.
(25) Hergueta, A. R.; Moore, H. W. *J. Org. Chem.* **1999**, *64*, 5979.
(26) Xu, S. L.; Taing, M.; Moore, H. W. *J. Org. Chem.* **1991**, *56*, 6104.
(27) Xia, H. J.; Moore, H. W. *J. Org. Chem.* **1992**, *57*, 3765.
(28) Wipf, P.; Hopkins, C. R. *J. Org. Chem.* **1999**, *64*, 6881.
(29) Thomson, R. H. *Naturally Occurring Quinones III--Recent Advances;* Chapman Hall: London, New York, 1987.
(30) Park, A.; Schmitz, F. J. *Tetrahedron Lett.* **1993**, *34*, 3983.
(31) Davidson, B. S. *Tetrahedron Lett.* **1992**, *33*, 3721.
(32) McKee, T. C.; Ireland, C. M. *J. Nat. Prod.* **1987**, *50*, 754.
(33) McKillop, A.; Brown, S. P. *Syn. Commun.* **1987**, *17*, 657.
(34) Kobayashi, M.; Rao, S. R.; Chavakula, R.; Sarma, N. S. *J. Chem. Res. (S)*, *1994*, 282.
(35) Krane, B. D.; Fagbule, M. O.; Shamma, M. *J. Nat. Prod.* **1984**, *47*, 1.
(36) Sotomayor, N.; Dominguez, E.; Lete, E. *Tetrahedron Lett.* **1994**, *35*, 2973.
(37) Seraphin, D.; Lynch, M.; Duval, O. *Tetrahedron Lett.* **1995**, *36*, 5731.
(38) Katritzky, A. R.; Black, M.; Fan, W. Q. *J. Org. Chem.* **1991**, *56*, 5045.
(39) Xiong, Y. F.; Xia, H. J.; Moore, H. W. *J. Org. Chem.* **1995**, *60*, 6460.
(40) Perri, S. T.; Moore, H. W. *Tetrahedron Lett.* **1987**, *28*, 4507.
(41) Jones, G. H.; Venuti, M. C.; Young, J. M.; Murthy, D. V. K.; Loe, B. E.; Simpson, R. A.; Berks, A. H.; Spires, D. A.; Maloney, P. J.; Kruseman, M.; Rouhafza, S.; Kappas, K. C.; Beard, C. C.; Unger, S. H.; Cheung, P. S. *J. Med. Chem.* **1986**, *29*, 1504.
(42) Reed, M. W.; Moore, H. W. *J. Org. Chem.* **1988**, *53*, 4166.

(43) Reed, M. W.; Moore, H. W. *J. Org. Chem.* **1987**, *52*, 3491.
(44) Gammill, R. B.; Day, C. E.; Schurr, P. E. *J. Med. Chem.* **1983**, *26*, 1672.
(45) Trost, B. M.; Thiel, O. R.; Tsui, H. C. *J. Am. Chem. Soc.* **2003**, *125*, 13155.
(46) Winters, M. P.; Stranberg, M.; Moore, H. W. *J. Org. Chem.* **1994**, *59*, 7572.
(47) Kwan, H. L.; Moore, H. W. *Tetrahedron Lett.* **1993**, *34*, 235.
(48) Fieser, L. F.; Hartwell, J. L.; Seligman, A. M. *J. Am. Chem. Soc.* **1936**, *58*, 1223.
(49) Hooker, S. C. *J. Am. Chem. Soc.* **1936**, *58*, 1174.
(50) Hooker, S. C.; Steyermark, A. *J. Am. Chem. Soc.* **1936**, *58*, 1179.
(51) Hooker, S. C. *J. Am. Chem. Soc.* **1936**, *58*, 1168.
(52) Fieser, L. F.; Fieser, M. *J. Am. Chem. Soc.* **1948**, *70*, 3215.
(53) Fieser, L. F.; Bader, A. R. *J. Am. Chem. Soc.* **1951**, *73*, 681.
(54) Packard, E.; Pascoe, D. D.; Maddaluno, J.; Gonçalves, T. P.; Harrowven, D. C. *Angew. Chem. Int. Ed.* **2013**, *52*, 13076.
(55) Bettólo, G. B. M.; Casinovi, C. G.; Galeffi, C. *Tetrahedron Lett.* **1965**, *6*, 4857.
(56) Garcia, E.; Mendoza, V.; Guzman, J. A. *Nat. Prod. Lett.* **1997**, *11*, 67.
(57) Shapiro, R. H.; Lipton, M. F.; Kolonko, K. J.; Buswell, R. L.; Capuano, L. A. *Tetrahedron Lett.* **1975**, 1811.
(58) Enhsen, A.; Karabelas, K.; Heerding, J. M.; Moore, H. W. *J. Org. Chem.* **1990**, *55*, 1177.
(59) Decker, O. H. W.; Moore, H. W. *J. Org. Chem.* **1987**, *52*, 1174.
(60) Foland, L. D.; Decker, O. H. W.; Moore, H. W. *J. Am. Chem. Soc.* **1989**, *111*, 989.
(61) Parnes, J. S.; Carter, D. S.; Kurz, L. J.; Flippin, L. A. *J. Org. Chem* **1994**, *59*, 3497.
(62) Ghosal, S.; Saini, K. S.; Frahm, A. W. *Phytochemistry* **1983**, *22*, 2305.
(63) Grundon, M. F. *Nat. Prod. Rep.* **1989**, *6*, 79.
(64) Cheng, R. K. Y.; Yan, S. J.; Chen, C. C. *J. Med. Chem.* **1978**, *21*, 199.
(65) Torregrosa, J.; Baboulene, M.; Speziale, V.; Lattes, A. *J. Organomet. Chem.* **1983**, *244*, 311.
(66) Breyer, S.; Effenberger-Neidnicht, K.; Schobert, R. *J. Org. Chem.* **2010**, *75*, 6214.
(67) Pena-Cabrera, E.; Liebeskind, L. S. *J. Org. Chem.* **2002**, *67*, 1689.
(68) Nichols, A. L.; Zhang, P.; Martin, S. F. *Tetrahedron* **2012**, *68*, 7591.
(69) Perri, S. T.; Foland, L. D.; Moore, H. W. *Tetrahedron Lett.* **1988**, *29*, 3529.
(70) Yamamoto, Y.; Ohno, M.; Eguchi, S. *Tetrahedron* **1994**, *50*, 7783.
(71) Rondan, N. G.; Houk, K. N. *J. Am. Chem. Soc.* **1985**, *107*, 2099.
(72) Houk, K. N.; Spellmeyer, D. C.; Jefford, C. W.; Rimbault, C. G.; Wang, Y.; Miller, R. D. *J. Org. Chem.* **1988**, *53*, 2125.
(73) Exner, O. *Correlation Analysis of Chemical Data*; Plenum: New York, 1988.
(74) Hammett, L. P. *Physical Organic Chemistry*, 2nd ed.; McGraw-Hill: New York, 1970.
(75) Baxendale, I. R.; Hayward, J. J.; Ley, S. V. *Comb. Chem. High Throughput Screening* **2007**, *10*, 802.
(76) Ley, S. V.; Baxendale, I. R. *Chimia* **2008**, *62*, 162.
(77) Carter, C. F.; Lange, H.; Ley, S. V.; Baxendale, I. R.; Wittkamp, B.; Goode, J. G.; , N. L. *Org. Process Res. Dev.* **2010**, *14*, 393.
(78) Lévesque, F.; Seeberger, P. H. *Angew. Chem. Int. Ed.* **2012**, *51*, 1706.
(79) Tucker, J. W.; Zhang, Y.; Jamison, T. F.; Stephenson, C. R. J. *Angew. Chem. Int. Ed.* **2012**, *51*, 4144.
(80) Gutierrez, A. C.; Jamison, T. F. *Org. Lett.* **2011**, *13*, 6414.
(81) Bourne, R. A.; Han, X.; Poliakoff, M.; George, M. W. *Angew. Chem. Int. Ed.* **2009**, 48, 5322.
(82) Knowles, J. P.; Elliott, L. D.; Booker-Milburn, K. I. *Beilstein J. Org. Chem.* **2012**, *8*, 2025.
(83) Jaffé, H. H. *Chem. Rev.* **1953**, *53*, 191.
(84) Smith, M. O.; March, J. *March's Advanced Organic Chemistry: Reactions, Mechanisms, and Structure*, 6th ed.; Wiley: Chichester, 2007.

(85) Isaacs, N. S. *Physical Organic Chemistry*; Longman Scientific & Technical: Harlow, 1987.
(86) Jas, G.; Kirschning, A. *Chem. Eur. J.* **2003**, *9*, 5708.
(87) Bogdan, A. R.; Sach, N. W. *Adv. Synth. Catal.* **2009**, *351*, 849.
(88) Vapourtec R4/R2+ devices can be purchased from Vapourtec Ltd., Place Farm, Suffolk, IP31 1NQ; http://www.vapourtec.co.uk/
(89) Valera, F. E.; Quaranta, M.; Moran, A.; Blacker, J.; Armstrong, A.; Cabral, J. T.; Blackmond, D. G. *Angew. Chem. Int. Ed.* **2010**, *49*, 2478.
(90) Hammett, L. P. *J. Am. Chem. Soc.* **1937**, *59*, 96.
(91) Hine, J. *J. Am. Chem. Soc.* **1960**, *82*, 4877.
(92) Dubois, J. E.; Ruasse, M. F.; Argile, A. *J. Am. Chem. Soc.* **1984**, *106*, 4840.
(93) Ruasse, M. F.; Argile, A.; Dubois, J. E. *J. Am. Chem. Soc.* **1984**, *106*, 4846.
(94) Lee, I.; Shim, C. S.; Chung, S. Y.; Kim, H. Y.; Lee, H. W. *J. Chem. Soc., Perkin Trans. 2* **1988**, 1919.
(95) Hansch, C.; Leo, A.; Taft, R. W. *Chem. Rev.* **1991**, *91*, 165.
(96) Ananchenko, G.; Beaudoin, E.; Bertin, D.; Gigmes, D.; Lagarde, P.; Marque, S. R. Valor, E.; Tordo, P. *J. Phys. Org. Chem.* **2006**, *19*, 269.
(97) Fujita, T.; Takayama, C.; Nakajima, M. *J. Org. Chem.* **1973**, *38*, 1623.
(98) Taft, R. W. *J. Am. Chem. Soc.* **1952**, *74*, 2729.
(99) Taft, R. W. *J. Am. Chem. Soc.* **1952**, *74*, 3120.
(100) Taft, R. W. *J. Am. Chem. Soc.* **1953**, *75*, 4538.
(101) Gaussian 09, Revision A.1, Frisch, M. J.; Trucks, G. W.; Schlegel, H. B.; Scuseria, G. E.; Robb, M. A.; Cheeseman, J. R.; Scalmani, G.; Barone, V.; Mennucci, B.; Petersson, G. A.; Nakatsuji, H.; Caricato, M.; Li, X.; Hratchian, H. P.; Izmaylov, A. F.; Bloino, J.; Zheng, G.; Sonnenberg, J. L.; Hada, M.; Ehara, M.; Toyota, K.; Fukuda, R.; Hasegawa, J.; Ishida, M.; Nakajima, T.; Honda, Y.; Kitao, O.; Nakai, H.; Vreven, T.; Montgomery, Jr., J. A.; Peralta, J. E.; Ogliaro, F.; Bearpark, M.; Heyd, J. J.; Brothers, E.; Kudin, K. N.; Staroverov, V. N.; Kobayashi, R.; Normand, J.; Raghavachari, K.; Rendell, A.; Burant, J. C.; Iyengar, S. S.; Tomasi, J.; Cossi, M.; Rega, N.; Millam, N. J.; Klene, M.; Knox, J. E.; Cross, J. B.; Bakken, V.; Adamo, C.; Jaramillo, J.; Gomperts, R.; Stratmann, R. E.; Yazyev, O.; Austin, A. J.; Cammi, R.; Pomelli, C.; Ochterski, J. W.; Martin, R. L.; Morokuma, K.; Zakrzewski, V. G.; Voth, G. A.; Salvador, P.; Dannenberg, J. J.; Dapprich, S.; Daniels, A. D.; Farkas, Ö.; Foresman, J. B.; Ortiz, J. V.; Cioslowski, J.; Fox, D. J. Gaussian, Inc., Wallingford CT, 2009.
(102) Musch, P. W.; Remenyi, C.; Helten, H.; Engels, B. *J. Am. Chem. Soc.* **2002**, *124*, 1823.
(103) Schreiner, P. R.; Bui, B. H. *Eur. J. Org. Chem.* **2006**, 1162.
(104) Liebeskind, L. S.; Birchler, A. G.; Liu, F. Q. *J. Org. Chem.* **1995**, *59*, 7737.
(105) As the value of σ_I for CON^iPr_2 is not known, we used as an estimate the known for $CONH_2$.
(106) Nakahara, S.; Kubo, A. *Heterocycles* **2004**, *63*, 2355.
(107) Nakahara, S.; Kubo, A.; Mikami, Y.; Ito, J. *Heterocycles* **2006**, *68*, 515.
(108) Yerxa, B. R.; Moore, H. W. *Abstr. Pap. Am. Chem. Soc.* **1992**, *203*, 395.
(109) Jiajie, Z. China, CN101239978(A), 2008.
(110) Ramsbeck, S.; Heiser, U.; Buchholz, M.; Niestroj, A. J. US pat. US2008/234313 08.
(111) AbdelMagid, A. F.; Carson, K. G.; Harris, B. D.; Maryanoff, C. A.; Shah, R. D. *J. Org.* **1996**, *61*, 3849.
(112) Yoon, N. M.; Brown, H. C. *J. Am. Chem. Soc.* **1968**, *90*, 2927.
(113) Pettit, G. R.; Collins, J. C.; Knight, J. C.; Herald, D. L.; Nieman, R. A.; Williams, M. D.; Pettit, R. K. *J. Nat. Prod.* **2003**, *66*, 544.
(114) Pettit, R. K.; Fakoury, B. R.; Knight, J. C.; Weber, C. A.; Pettit, G. R.; Cage, G. D.; Pon, S. *J. Med. Microbiol.* **2004**, *53*, 61.
(115) Knueppel, D.; Martin, S. F. *Angew. Chem. Int. Ed.* **2009**, *48*, 2569.
(116) Markey, M. D.; Kelly, T. R. *J. Org. Chem.* **2008**, *73*, 7441.

(117) Hook, B. D. A.; Dohle, W.; Hirst, P. R.; Pickworth, M.; Berry, M. B.; Booker-Milburn, K. I. *J. Org. Chem.* **2005**, *70*, 7558.
(118) All light bulbs used were purchased either directly from Philips or the appropriate supplier. Datasheets on all the bulbs include UV visible spectra can be found in the appendix on the website http://www.ecat.lighting.philips.com/
(119) Liu, H.; Tomooka, C. S.; Moore, H. W. *Synth. Commun.* **1997**, *27*, 2177.
(120) Schmidt, A. H.; Kircher, G.; Maus, S.; Bach, H. *J. Org. Chem.* **1996**, *61*, 2085.
(121) Black, T. H.; Farrell, J. R.; Probst, D. A.; Zotz, M. C. *Synth. Commun.* **2002**, *32*, 2083.

Chapter 8.Appendix

8.1 X-Ray Crystallography Data

Details of X-ray Crystal Structure Determination for **268**

Table 1. Crystal data and structure refinement details.

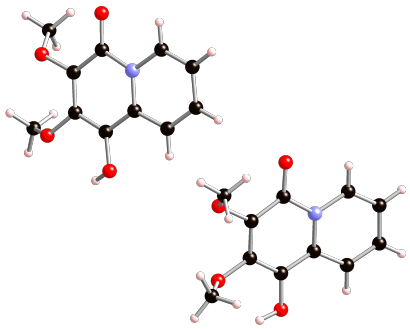

Identification code	**2010sot0772**
Empirical formula	$C_{11}H_{11}NO_4$
Formula weight	221.21
Temperature	120(2) K
Wavelength	0.71073 Å
Crystal system	Orthorhombic
Space group	*Pccn*
Unit cell dimensions	a = 30.0640(7) Å
	b = 8.9261(2) Å
	c = 14.6848(4) Å
Volume	3940.73(17) Å^3
Z	16
Density (calculated)	1.491 Mg / m^3
Absorption coefficient	0.115 mm^{-1}
F(000)	1856
Crystal	Block; Dark Orange
Crystal size	0.10 × 0.10 × 0.08 mm^3
θ range for data collection	2.99 – 25.03°
Index ranges	$-35 \le h \le 35$, $-10 \le k \le 10$, $-17 \le l \le 16$
Reflections collected	18484
Independent reflections	3480 [R_{int} = 0.0604]
Completeness to θ = 25.03°	99.7 %
Absorption correction	Semi–empirical from equivalents
Max. and min. transmission	0.9909 and 0.9886
Refinement method	Full-matrix least-squares on F^2
Data / restraints / parameters	3480 / 0 / 293
Goodness-of-fit on F^2	1.082
Final R indices [$F^2 > 2\sigma(F^2)$]	$R1$ = 0.0619, $wR2$ = 0.1159
R indices (all data)	$R1$ = 0.0831, $wR2$ = 0.1269
Largest diff. peak and hole	0.240 and –0.245 e Å^{-3}

Diffractometer: *Nonius KappaCCD* area detector (ϕ scans and ω scans to fill *asymmetric unit*). **Cell determination:** DirAx (Duisenberg, A.J.M.(1992). J. Appl. Cryst. 25, 92-96.) **Data collection:** Collect (Collect: Data collection software, R. Hooft, Nonius B.V., 1998). **Data reduction and cell refinement**: *Denzo* (Z. Otwinowski & W. Minor, *Methods in Enzymology* (1997) Vol. **276**: *Macromolecular Crystallography*, part A, pp. 307–326; C. W. Carter, Jr. & R. M. Sweet, Eds., Academic Press). **Absorption correction**: Sheldrick, G. M. SADABS - Bruker Nonius area detector scaling and absorption correction - V2.10 S**tructure solution**: *SHELXS97* (G. M. Sheldrick, Acta Cryst. (1990) A**46** 467–473). S**tructure refinement**: *SHELXL97* (G. M. Sheldrick (1997), University of Göttingen, Germany). **Graphics:** Cameron - A Molecular Graphics Package. (D. M. Watkin, L. Pearce and C. K. Prout, Chemical Crystallography Laboratory, University of Oxford, 1993).
Special details: All hydrogen atoms were placed in idealised positions and refined using a riding model.

Table 2. Atomic coordinates [× 10^4], equivalent isotropic displacement parameters [Å^2 × 10^3] and site occupancy factors. U_{eq} is defined as one third of the trace of the orthogonalized U^{ij} tensor.

Atom	*x*	*y*	*z*	U_{eq}	*S.o.f.*
O101	245(1)	3342(2)	6727(1)	30(1)	1
O102	–552(1)	1986(2)	6323(1)	23(1)	1
O103	–809(1)	1595(2)	4531(1)	24(1)	1
O104	–227(1)	2581(3)	3169(1)	29(1)	1
N101	279(1)	3373(3)	4258(2)	20(1)	1
C101	399(1)	3607(3)	5171(2)	20(1)	1
C102	115(1)	3131(3)	5853(2)	22(1)	1
C103	–281(1)	2409(3)	5622(2)	18(1)	1
C104	–399(1)	2197(3)	4725(2)	20(1)	1
C105	–129(1)	2704(3)	4002(2)	21(1)	1
C106	567(1)	3836(3)	3570(2)	26(1)	1
C107	961(1)	4474(3)	3757(2)	28(1)	1
C108	1095(1)	4702(3)	4673(2)	28(1)	1
C109	815(1)	4296(3)	5353(2)	25(1)	1
C110	–573(1)	400(4)	6481(3)	38(1)	1
C111	–793(1)	200(4)	4039(2)	35(1)	1
O201	2124(1)	–1113(2)	136(1)	28(1)	1
O202	2924(1)	335(2)	279(1)	33(1)	1
O203	3271(1)	1017(2)	2017(1)	24(1)	1
O204	2761(1)	229(2)	3524(1)	30(1)	1
N201	2226(1)	–844(3)	2587(2)	23(1)	1
C201	2062(1)	–1171(3)	1720(2)	19(1)	1
C202	2300(1)	–747(3)	955(2)	21(1)	1
C203	2701(1)	26(3)	1063(2)	23(1)	1
C204	2860(1)	361(3)	1931(2)	20(1)	1
C205	2630(1)	–68(3)	2726(2)	22(1)	1
C206	1983(1)	–1285(3)	3353(2)	24(1)	1
C207	1586(1)	–1953(3)	3277(2)	26(1)	1
C208	1403(1)	–2247(3)	2407(2)	26(1)	1
C209	1640(1)	–1888(3)	1656(2)	24(1)	1
C210	3094(1)	1802(4)	127(2)	40(1)	1
C211	3268(1)	2499(3)	2403(2)	29(1)	1

Table 3. Bond lengths [Å] and angles [°].

Bond lengths [Å]		Bond angles [°]			
O101–C102	1.354(3)	C103–O102–C110	114.9(2)	C103–O102–C110	114.9(2)
O102–C103	1.365(3)	C104–O103–C111	114.4(2)	C104–O103–C111	114.4(2)
O102–C110	1.436(4)	C106–N101–C101	119.1(2)	C106–N101–C101	119.1(2)
O103–C104	1.375(3)	C106–N101–C105	118.1(2)	C106–N101–C105	118.1(2)
O103–C111	1.440(4)	C101–N101–C105	122.7(2)	C101–N101–C105	122.7(2)
O104–C105	1.264(3)	C102–C101–N101	119.1(2)	C102–C101–N101	119.1(2)
N101–C106	1.395(4)	C102–C101–C109	122.7(3)	C102–C101–C109	122.7(3)
N101–C101	1.404(4)	N101–C101–C109	118.2(3)	N101–C101–C109	118.2(3)
N101–C105	1.413(4)	O101–C102–C101	117.8(3)	O101–C102–C101	117.8(3)
C101–C102	1.383(4)	O101–C102–C103	122.7(3)	O101–C102–C103	122.7(3)
C101–C109	1.419(4)	C101–C102–C103	119.5(3)	C101–C102–C103	119.5(3)
C102–C103	1.398(4)	O102–C103–C104	122.1(2)	O102–C103–C104	122.1(2)
C103–C104	1.376(4)	O102–C103–C102	117.0(2)	O102–C103–C102	117.0(2)
C104–C105	1.410(4)	C104–C103–C102	120.9(3)	C104–C103–C102	120.9(3)
C106–C107	1.342(4)	O103–C104–C103	118.8(2)	O103–C104–C103	118.8(2)
C107–C108	1.419(4)	O103–C104–C105	119.0(2)	O103–C104–C105	119.0(2)
C108–C109	1.356(4)	C103–C104–C105	121.9(3)	C103–C104–C105	121.9(3)
O201–C202	1.356(3)	O104–C105–C104	124.5(3)	O104–C105–C104	124.5(3)
O202–C203	1.361(3)	O104–C105–N101	119.8(3)	O104–C105–N101	119.8(3)
O202–C210	1.424(4)	C104–C105–N101	115.7(3)	C104–C105–N101	115.7(3)
O203–C204	1.375(3)	C107–C106–N101	121.7(3)	C107–C106–N101	121.7(3)
O203–C211	1.439(4)	C106–C107–C108	120.4(3)	C106–C107–C108	120.4(3)
O204–C205	1.265(3)	C109–C108–C107	118.9(3)	C109–C108–C107	118.9(3)
N201–C201	1.395(4)	C108–C109–C101	121.6(3)	C108–C109–C101	121.6(3)
N201–C206	1.399(4)	C203–O202–C210	119.8(2)	C203–O202–C210	119.8(2)
N201–C205	1.415(4)	C204–O203–C211	114.9(2)	C204–O203–C211	114.9(2)
C201–C202	1.385(4)	C201–N201–C206	119.4(2)	C201–N201–C206	119.4(2)
C201–C209	1.423(4)	C201–N201–C205	122.6(2)	C201–N201–C205	122.6(2)
C202–C203	1.397(4)	C206–N201–C205	118.0(2)	C206–N201–C205	118.0(2)
C203–C204	1.393(4)	C202–C201–N201	120.0(3)	C202–C201–N201	120.0(3)
C204–C205	1.410(4)	C202–C201–C209	121.9(3)	C202–C201–C209	121.9(3)
C206–C207	1.340(4)	N201–C201–C209	118.0(2)	N201–C201–C209	118.0(2)
C207–C208	1.415(4)	O201–C202–C201	116.9(3)	O201–C202–C201	116.9(3)
C208–C209	1.352(4)	O201–C202–C203	123.9(3)	O201–C202–C203	123.9(3)
		C201–C202–C203	119.2(3)	C201–C202–C203	119.2(3)
		O202–C203–C204	124.1(3)	O202–C203–C204	124.1(3)
		O202–C203–C202	115.4(3)	O202–C203–C202	115.4(3)
		C204–C203–C202	120.3(3)	C204–C203–C202	120.3(3)
		O203–C204–C203	119.0(3)	O203–C204–C203	119.0(3)
		O203–C204–C205	118.7(3)	O203–C204–C205	118.7(3)
		C203–C204–C205	122.1(3)	C203–C204–C205	122.1(3)
		O204–C205–C204	124.0(3)	O204–C205–C204	124.0(3)
		O204–C205–N201	120.3(3)	O204–C205–N201	120.3(3)
		C204–C205–N201	115.7(3)	C204–C205–N201	115.7(3)
		C207–C206–N201	121.5(3)	C207–C206–N201	121.5(3)
		C206–C207–C208	120.3(3)	C206–C207–C208	120.3(3)
		C209–C208–C207	119.2(3)	C209–C208–C207	119.2(3)
		C208–C209–C201	121.5(3)	C208–C209–C201	121.5(3)

Table 4. Anisotropic displacement parameters [Å^2× 10^3]. The anisotropic displacement factor exponent takes the form: $-2\pi^2[h^2a^{*2}U^{11} + \cdots + 2\ h\ k\ a^*\ b^*\ U^{12}]$.

Atom	U^{11}	U^{22}	U^{33}	U^{23}	U^{13}	U^{12}
O101	30(1)	43(1)	18(1)	1(1)	−2(1)	−8(1)
O102	24(1)	26(1)	20(1)	2(1)	3(1)	0(1)
O103	20(1)	29(1)	25(1)	−3(1)	−4(1)	−1(1)
O104	32(1)	41(1)	15(1)	−2(1)	−1(1)	0(1)
N101	19(1)	23(1)	18(1)	−2(1)	3(1)	1(1)
C101	19(1)	20(2)	21(2)	−1(1)	−1(1)	4(1)
C102	22(2)	23(2)	19(2)	−1(1)	−4(1)	4(1)
C103	16(1)	20(2)	18(2)	1(1)	4(1)	4(1)
C104	20(1)	17(1)	23(2)	0(1)	−2(1)	2(1)
C105	23(2)	22(2)	18(2)	1(1)	2(1)	3(1)
C106	32(2)	28(2)	19(2)	2(1)	7(1)	5(1)
C107	25(2)	29(2)	30(2)	1(1)	11(1)	−4(1)
C108	17(1)	23(2)	43(2)	−1(1)	0(1)	2(1)
C109	24(2)	24(2)	27(2)	0(1)	−1(1)	1(1)
C110	44(2)	30(2)	42(2)	13(2)	14(2)	3(2)
C111	34(2)	33(2)	38(2)	−6(2)	−9(2)	−2(2)
O201	29(1)	37(1)	18(1)	3(1)	−1(1)	−5(1)
O202	43(1)	38(1)	17(1)	−3(1)	9(1)	−12(1)
O203	23(1)	22(1)	26(1)	−3(1)	0(1)	−1(1)
O204	42(1)	32(1)	16(1)	−1(1)	−2(1)	−2(1)
N201	25(1)	22(1)	21(1)	2(1)	4(1)	1(1)
C201	26(2)	16(1)	14(2)	0(1)	0(1)	6(1)
C202	25(2)	23(2)	16(2)	−1(1)	−5(1)	4(1)
C203	25(2)	24(2)	19(2)	2(1)	4(1)	4(1)
C204	19(1)	17(1)	23(2)	1(1)	−1(1)	3(1)
C205	27(2)	23(2)	16(2)	1(1)	0(1)	3(1)
C206	28(2)	29(2)	16(2)	0(1)	1(1)	−1(1)
C207	28(2)	30(2)	21(2)	5(1)	4(1)	0(1)
C208	24(2)	24(2)	31(2)	0(1)	1(1)	−1(1)
C209	25(2)	24(2)	23(2)	−2(1)	−4(1)	5(1)
C210	50(2)	39(2)	32(2)	6(2)	11(2)	−10(2)
C211	35(2)	22(2)	29(2)	−4(1)	−2(2)	−1(1)

Table 5. Hydrogen coordinates [× 10^4] and isotropic displacement parameters [Å^2 × 10^3].

Atom	*x*	*y*	*z*	U_{eq}	*S.o.f.*
H101	47	3018	7080	46	1
H106	483	3696	2952	31	1
H107	1151	4775	3274	34	1
H108	1376	5132	4807	33	1
H109	899	4478	5967	30	1
H11A	−274	−30	6423	58	1
H11B	−771	−64	6033	58	1
H11C	−686	212	7096	58	1
H11D	−663	−578	4427	52	1
H11E	−611	322	3490	52	1
H11F	−1096	−95	3865	52	1
H201	2239	−580	−272	42	1
H206	2103	−1108	3942	29	1
H207	1426	−2229	3809	32	1
H208	1117	−2692	2351	32	1
H209	1523	−2119	1072	29	1
H21A	2927	2524	495	61	1
H21B	3064	2057	−519	61	1
H21C	3409	1833	300	61	1
H21D	3128	3195	1974	43	1
H21E	3573	2820	2525	43	1
H21F	3099	2489	2974	43	1

Table 6. Hydrogen bonds [Å and °].

D–H···*A*	*d*(*D*–H)	*d*(H···*A*)	*d*(*D*···*A*)	∠(*DHA*)
O101–H101···O104^{i}	0.84	1.88	2.679(3)	159.1
O101–H101···O102	0.84	2.31	2.750(3)	113.1
O201–H201···O204^{ii}	0.84	1.91	2.674(3)	150.9

Symmetry transformations used to generate equivalent atoms:
(i) x,–y+1/2,z+1/2 (ii) –x+1/2,y,z–1/2

Details of X-ray Crystal Structure Determination for **349**

Table 1. Crystal data and structure refinement details.

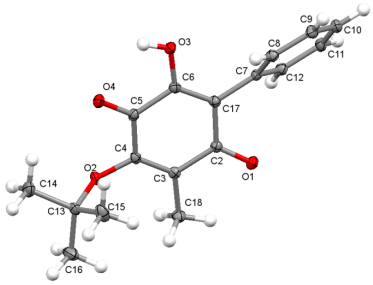

Identification code	**2013mr006_R**	
Empirical formula	$C_{17}H_{18}O_4$	
Formula weight	286.31	
Temperature	100(2) K	
Wavelength	0.71073 Å	
Crystal system	Triclinic	
Space group	*P*–1	
Unit cell dimensions	a = **6.208(2) Å**	α = **107.422(8)°**
	b = **10.002(4) Å**	β = **96.887(6)°**
	c = **12.196(5) Å**	γ = **91.925(6)°**
Volume	715.4(5) Å^3	
Z	2	
Density (calculated)	1.329 Mg / m^3	
Absorption coefficient	0.094 mm^{-1}	
F(000)	304	
Crystal	?; ?	
Crystal size	? x ? x ? mm^3	
θ range for data collection	3.528 – 27.482°	
Index ranges	$-8 \le h \le 8$, $-12 \le k \le 12$, $-15 \le l \le 15$	
Reflections collected	15039	
Independent reflections	3257 [R_{int} = 0.0186]	
Completeness to θ = 25.242°	99.7 %	
Refinement method	Full-matrix least-squares on F^2	
Data / restraints / parameters	3257 / 0 / 194	
Goodness-of-fit on F^2	1.064	
Final *R* indices [$F^2 > 2\sigma(F^2)$]	*R1* = 0.0437, *wR2* = 0.1248	
R indices (all data)	*R1* = 0.0462, *wR2* = 0.1271	
Extinction coefficient	n/a	
Largest diff. peak and hole	0.584 and –0.585 e Å^{-3}	

Diffractometer: *Rigaku AFC12 Kappa 3-circle with Saturn724+* area detector (ω scans to fill *asymmetric unit* sphere). **Cell determination:** *CrystalClear-SM Expert 2.0 r7* (Rigaku, 2011). **Data collection:** *CrystalClear-SM Expert 2.0 r7* (Rigaku, 2011). **Data reduction and cell refinement**: *CrystalClear-SM Expert 2.0 r7* (Rigaku, 2011). **Absorption correction**: *CrystalClear-SM Expert 2.0 r7* (Rigaku, 2011). **Structure solution**: *SHELXS-2013* (Sheldrick, G.M. (2013)) **Structure refinement**: *SHELXL-2013* (G Sheldrick, G.M. (2013)). **Graphics:** *OLEX2* (Dolomanov, O. V., Bourhis, L. J., Gildea, R. J., Howard, J. A. K. & Puschmann, H. (2009). J. Appl. Cryst. 42, 339-341.)

Table 2. Atomic coordinates [× 10^4], equivalent isotropic displacement parameters [$Å^2$ × 10^3] and site occupancy factors. U_{eq} is defined as one third of the trace of the orthogonalized U^{ij} tensor.

Atom	*x*	*y*	*z*	U_{eq}	*S.o.f.*
O2	8673(2)	514(1)	3411(1)	16(1)	1
O1	9029(2)	4968(1)	6218(1)	16(1)	1
O3	14726(2)	2030(1)	6468(1)	18(1)	1
O4	12771(2)	284(1)	4448(1)	18(1)	1
C2	9824(2)	3838(1)	5869(1)	12(1)	1
C6	12826(2)	2361(1)	5996(1)	14(1)	1
C7	12757(2)	4585(1)	7628(1)	13(1)	1
C3	8704(2)	2762(1)	4798(1)	13(1)	1
C17	11879(2)	3550(1)	6494(1)	13(1)	1
C4	9673(2)	1582(1)	4330(1)	13(1)	1
C8	14925(2)	5142(1)	7868(1)	15(1)	1
C5	11821(2)	1327(1)	4878(1)	14(1)	1
C12	11384(2)	5036(1)	8475(1)	15(1)	1
C9	15681(2)	6136(1)	8933(1)	18(1)	1
C13	9138(2)	340(1)	2211(1)	16(1)	1
C10	14308(2)	6569(1)	9768(1)	19(1)	1
C11	12158(2)	6014(1)	9540(1)	18(1)	1
C18	6548(2)	3085(2)	4283(1)	17(1)	1
C14	9914(3)	−1129(2)	1780(1)	25(1)	1
C15	10821(3)	1459(2)	2172(1)	24(1)	1
C16	6964(3)	446(2)	1527(1)	27(1)	1

Table 3. Bond lengths [Å] and angles [°].

O2–C4	1.3620(15)
O2–C13	1.4863(16)
O1–C2	1.2256(16)
O3–C6	1.3455(16)
O3–H3	0.8400
O4–C5	1.2243(16)
C2–C17	1.4886(18)
C2–C3	1.4956(17)
C6–C17	1.3528(18)
C6–C5	1.4920(17)
C7–C12	1.3985(18)
C7–C8	1.4016(18)
C7–C17	1.4844(17)
C3–C4	1.3442(18)
C3–C18	1.4962(18)
C4–C5	1.4840(18)
C8–C9	1.3949(19)
C8–H8	0.9500
C12–C11	1.3899(19)
C12–H12	0.9500
C9–C10	1.386(2)
C9–H9	0.9500
C13–C15	1.5206(19)
C13–C14	1.521(2)
C13–C16	1.523(2)
C10–C11	1.391(2)
C10–H10	0.9500
C11–H11	0.9500
C18–H18A	0.9800
C18–H18B	0.9800
C18–H18C	0.9800
C14–H14A	0.9800

C14–H14B	0.9800
C14–H14C	0.9800
C15–H15A	0.9800
C15–H15B	0.9800
C15–H15C	0.9800
C16–H16A	0.9800
C16–H16B	0.9800
C16–H16C	0.9800
C4–O2–C13	121.47(10)
C6–O3–H3	109.5
O1–C2–C17	120.46(11)
O1–C2–C3	118.82(11)
C17–C2–C3	120.72(11)
O3–C6–C17	122.61(11)
O3–C6–C5	115.56(11)
C17–C6–C5	121.83(11)
C12–C7–C8	118.88(12)
C12–C7–C17	119.37(11)
C8–C7–C17	121.74(11)
C4–C3–C2	119.60(11)
C4–C3–C18	123.14(12)
C2–C3–C18	117.24(11)
C6–C17–C7	124.14(11)
C6–C17–C2	117.95(11)
C7–C17–C2	117.91(11)
C3–C4–O2	122.52(12)
C3–C4–C5	120.60(11)
O2–C4–C5	116.60(11)
C9–C8–C7	120.15(12)
C9–C8–H8	119.9
C7–C8–H8	119.9
O4–C5–C4	121.88(12)
O4–C5–C6	119.28(11)
C4–C5–C6	118.84(11)
C11–C12–C7	120.59(12)
C11–C12–H12	119.7
C7–C12–H12	119.7
C10–C9–C8	120.45(12)
C10–C9–H9	119.8
C8–C9–H9	119.8
O2–C13–C15	111.97(10)
O2–C13–C14	105.68(10)
C15–C13–C14	111.82(12)
O2–C13–C16	105.32(11)
C15–C13–C16	110.95(12)
C14–C13–C16	110.80(12)
C9–C10–C11	119.74(12)
C9–C10–H10	120.1
C11–C10–H10	120.1
C12–C11–C10	120.18(12)
C12–C11–H11	119.9
C10–C11–H11	119.9
C3–C18–H18A	109.5
C3–C18–H18B	109.5
H18A–C18–H18B	109.5
C3–C18–H18C	109.5
H18A–C18–H18C	109.5
H18B–C18–H18C	109.5
C13–C14–H14A	109.5
C13–C14–H14B	109.5

H14A–C14–H14B	109.5
C13–C14–H14C	109.5
H14A–C14–H14C	109.5
H14B–C14–H14C	109.5
C13–C15–H15A	109.5
C13–C15–H15B	109.5
H15A–C15–H15B	109.5
C13–C15–H15C	109.5
H15A–C15–H15C	109.5
H15B–C15–H15C	109.5
C13–C16–H16A	109.5
C13–C16–H16B	109.5
H16A–C16–H16B	109.5
C13–C16–H16C	109.5
H16A–C16–H16C	109.5
H16B–C16–H16C	109.5

Symmetry transformations used to generate equivalent atoms:

Table 4. Anisotropic displacement parameters [Å^2× 10^3]. The anisotropic displacement factor exponent takes the form: $-2\pi^2[h^2a^{*2}U^{11} + \cdots + 2\,h\,k\,a^*\,b^*\,U^{12}]$.

Atom	U^{11}	U^{22}	U^{33}	U^{23}	U^{13}	U^{12}
O2	19(1)	14(1)	12(1)	0(1)	2(1)	−3(1)
O1	17(1)	14(1)	17(1)	3(1)	4(1)	4(1)
O3	18(1)	15(1)	17(1)	1(1)	−1(1)	8(1)
O4	23(1)	14(1)	17(1)	3(1)	3(1)	6(1)
C2	13(1)	13(1)	12(1)	4(1)	4(1)	1(1)
C6	15(1)	14(1)	13(1)	5(1)	2(1)	2(1)
C7	15(1)	11(1)	12(1)	4(1)	2(1)	3(1)
C3	13(1)	14(1)	13(1)	5(1)	2(1)	−1(1)
C17	14(1)	13(1)	12(1)	4(1)	2(1)	1(1)
C4	15(1)	12(1)	12(1)	3(1)	2(1)	−2(1)
C8	15(1)	16(1)	16(1)	5(1)	2(1)	2(1)
C5	17(1)	12(1)	13(1)	4(1)	4(1)	2(1)
C12	15(1)	14(1)	15(1)	5(1)	3(1)	2(1)
C9	17(1)	15(1)	21(1)	6(1)	−2(1)	−1(1)
C13	21(1)	14(1)	11(1)	1(1)	1(1)	1(1)
C10	26(1)	13(1)	15(1)	2(1)	−3(1)	1(1)
C11	23(1)	15(1)	15(1)	4(1)	5(1)	5(1)
C18	14(1)	19(1)	18(1)	4(1)	0(1)	1(1)
C14	36(1)	18(1)	18(1)	2(1)	5(1)	8(1)
C15	33(1)	23(1)	16(1)	4(1)	6(1)	−7(1)
C16	27(1)	30(1)	18(1)	3(1)	−4(1)	6(1)

Table 5. Hydrogen coordinates [× 10^4] and isotropic displacement parameters [Å^2 × 10^3].

Atom	*x*	*y*	*z*	U_{eq}	*S.o.f.*
H3	15026	1236	6064	27	1
H8	15882	4842	7303	18	1
H12	9908	4672	8321	18	1
H9	17147	6518	9087	22	1
H10	14832	7242	10494	23	1
H11	11216	6304	10113	21	1
H18A	6153	3994	4762	26	1
H18B	5439	2350	4253	26	1
H18C	6641	3122	3496	26	1
H14A	11268	−1189	2261	37	1
H14B	10172	−1325	972	37	1
H14C	8801	−1818	1831	37	1
H15A	10324	2393	2520	36	1
H15B	11015	1345	1364	36	1
H15C	12210	1362	2606	36	1
H16A	5852	−186	1659	40	1
H16B	7100	177	698	40	1
H16C	6540	1414	1783	40	1

Table 6. Torsion angles [°].

O1–C2–C3–C4	172.65(12)
C17–C2–C3–C4	−6.80(18)
O1–C2–C3–C18	−5.83(17)
C17–C2–C3–C18	174.72(11)
O3–C6–C17–C7	−2.7(2)
C5–C6–C17–C7	177.39(11)
O3–C6–C17–C2	177.43(11)
C5–C6–C17–C2	−2.49(18)
C12–C7–C17–C6	−129.79(14)
C8–C7–C17–C6	51.18(18)
C12–C7–C17–C2	50.09(16)
C8–C7–C17–C2	−128.93(13)
O1–C2–C17–C6	−172.06(12)
C3–C2–C17–C6	7.38(17)
O1–C2–C17–C7	8.05(17)
C3–C2–C17–C7	−172.51(11)
C2–C3–C4–O2	174.78(10)
C18–C3–C4–O2	−6.83(19)
C2–C3–C4–C5	1.19(18)
C18–C3–C4–C5	179.58(11)
C13–O2–C4–C3	99.93(15)
C13–O2–C4–C5	−86.24(14)
C12–C7–C8–C9	−0.42(18)
C17–C7–C8–C9	178.61(11)
C3–C4–C5–O4	−177.57(12)
O2–C4–C5–O4	8.48(18)
C3–C4–C5–C6	3.60(18)
O2–C4–C5–C6	−170.36(10)
O3–C6–C5–O4	−1.71(17)
C17–C6–C5–O4	178.22(12)
O3–C6–C5–C4	177.15(11)
C17–C6–C5–C4	−2.92(18)
C8–C7–C12–C11	−0.40(19)
C17–C7–C12–C11	−179.45(11)
C7–C8–C9–C10	0.78(19)
C4–O2–C13–C15	0.70(16)

C4–O2–C13–C14	122.67(13)
C4–O2–C13–C16	–119.98(13)
C8–C9–C10–C11	–0.3(2)
C7–C12–C11–C10	0.85(19)
C9–C10–C11–C12	–0.5(2)

Symmetry transformations used to generate equivalent atoms:

8.2 Wavelengths of UV Lamps Used in Photochemical Experiments.

Philips UVB Broad (280 – 370 nm); PL-S 9W/12/2P

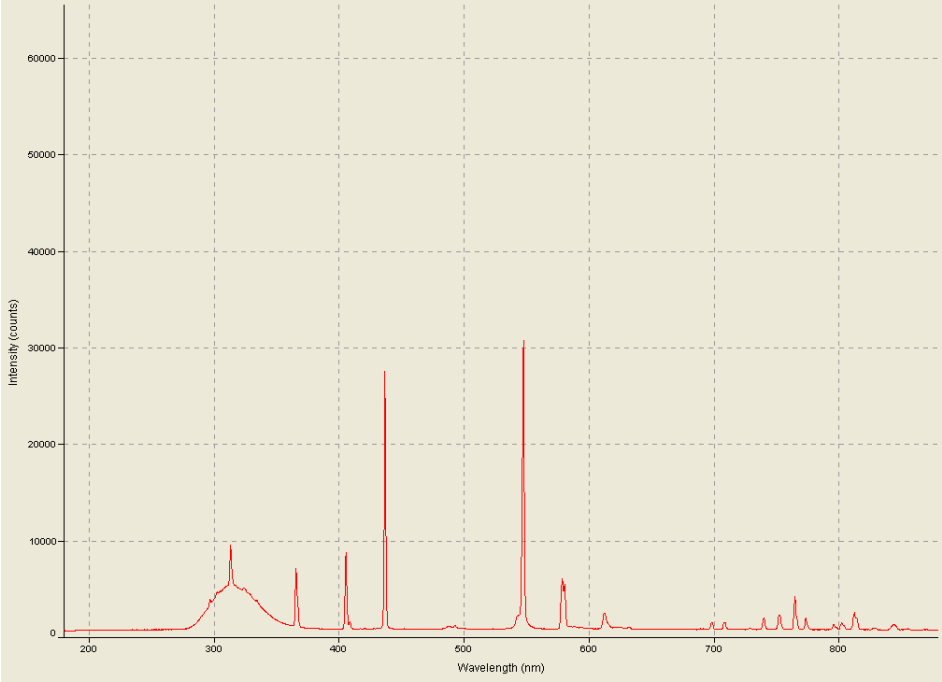

Philips UVB Narrow (310 – 320 nm); PL-S 9W/01/2P

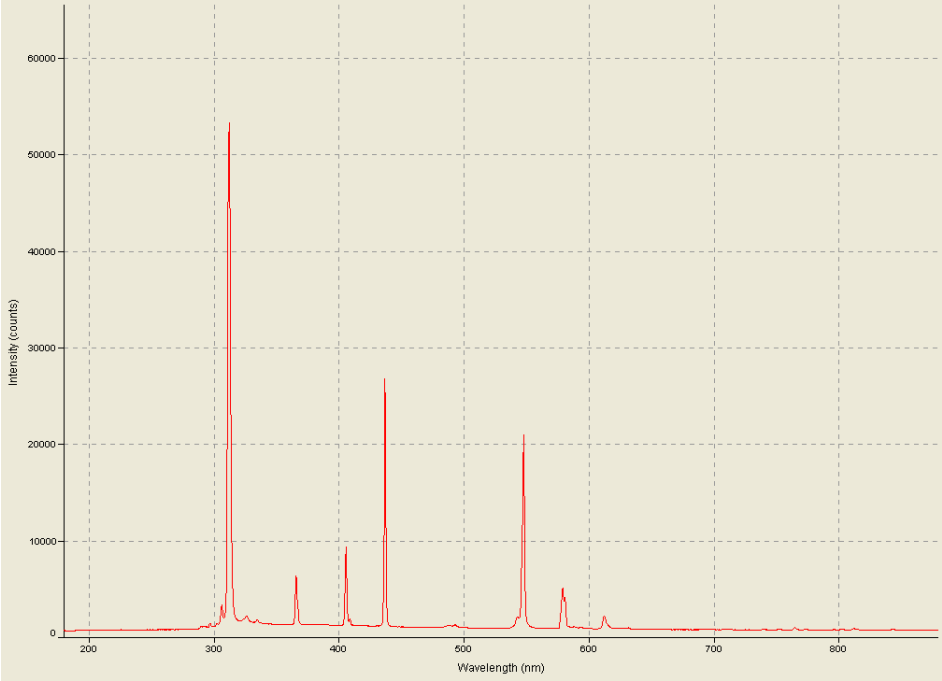

OSRAM UVC (254 nm); HNS S 92, GCF9Ds/G23/Se/OF

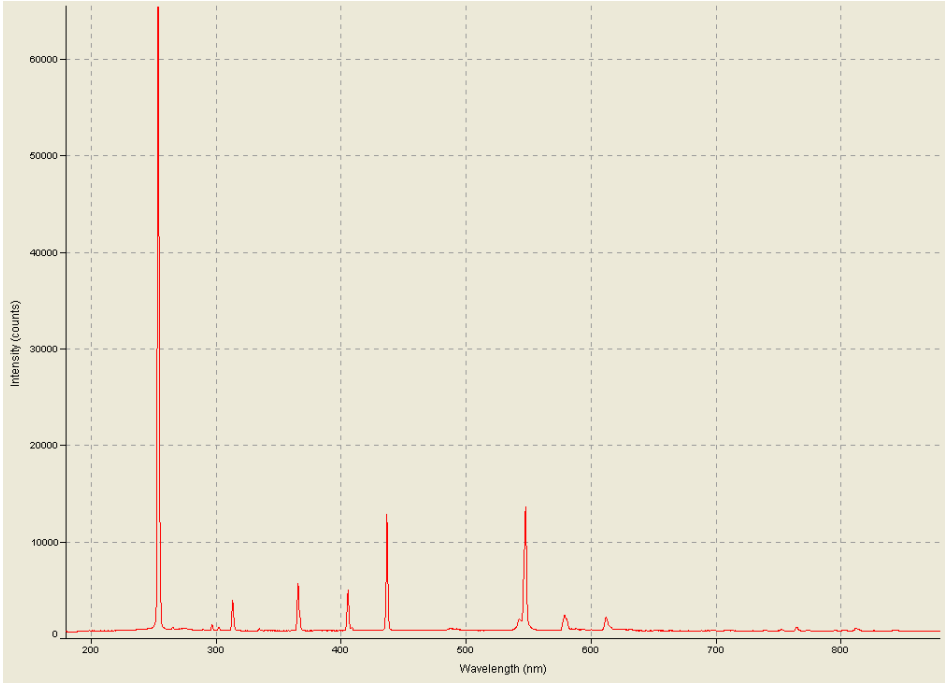

Philips UVA (360 – 395 nm); PL-S/9W/10/2P

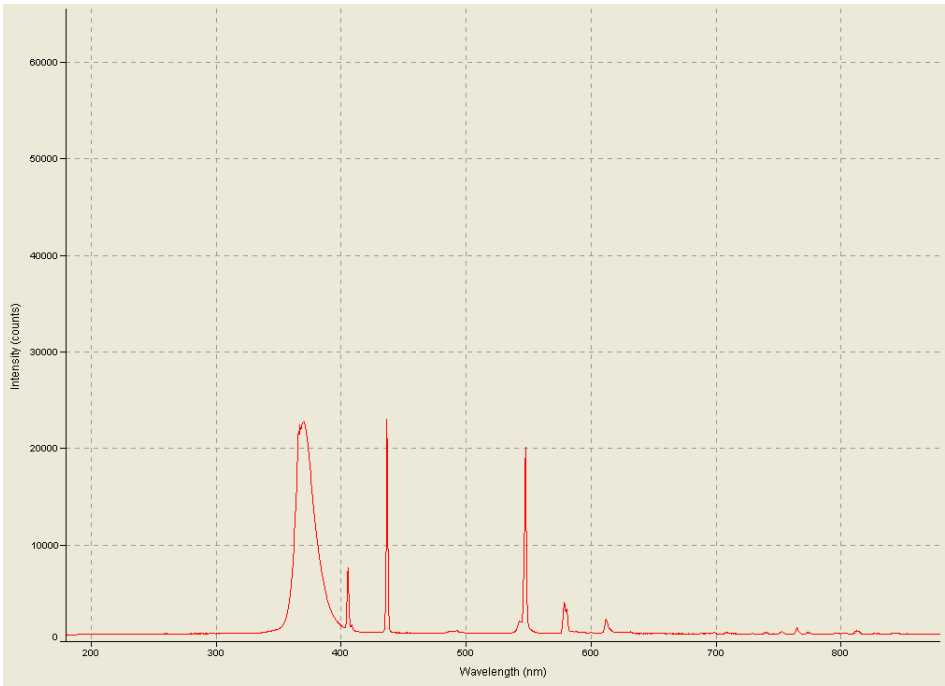

8.3 Publications

CHEMISTRY
A EUROPEAN JOURNAL

DOI: 10.1002/chem.201102263

New Insights into Cyclobutenone Rearrangements: A Total Synthesis of the Natural ROS-Generating Anti-Cancer Agent Cribrostatin 6**

Mubina Mohamed,[a] Théo P. Gonçalves,[a] Richard J. Whitby,[a] Helen F. Sneddon,[b] and David C. Harrowven*[a]

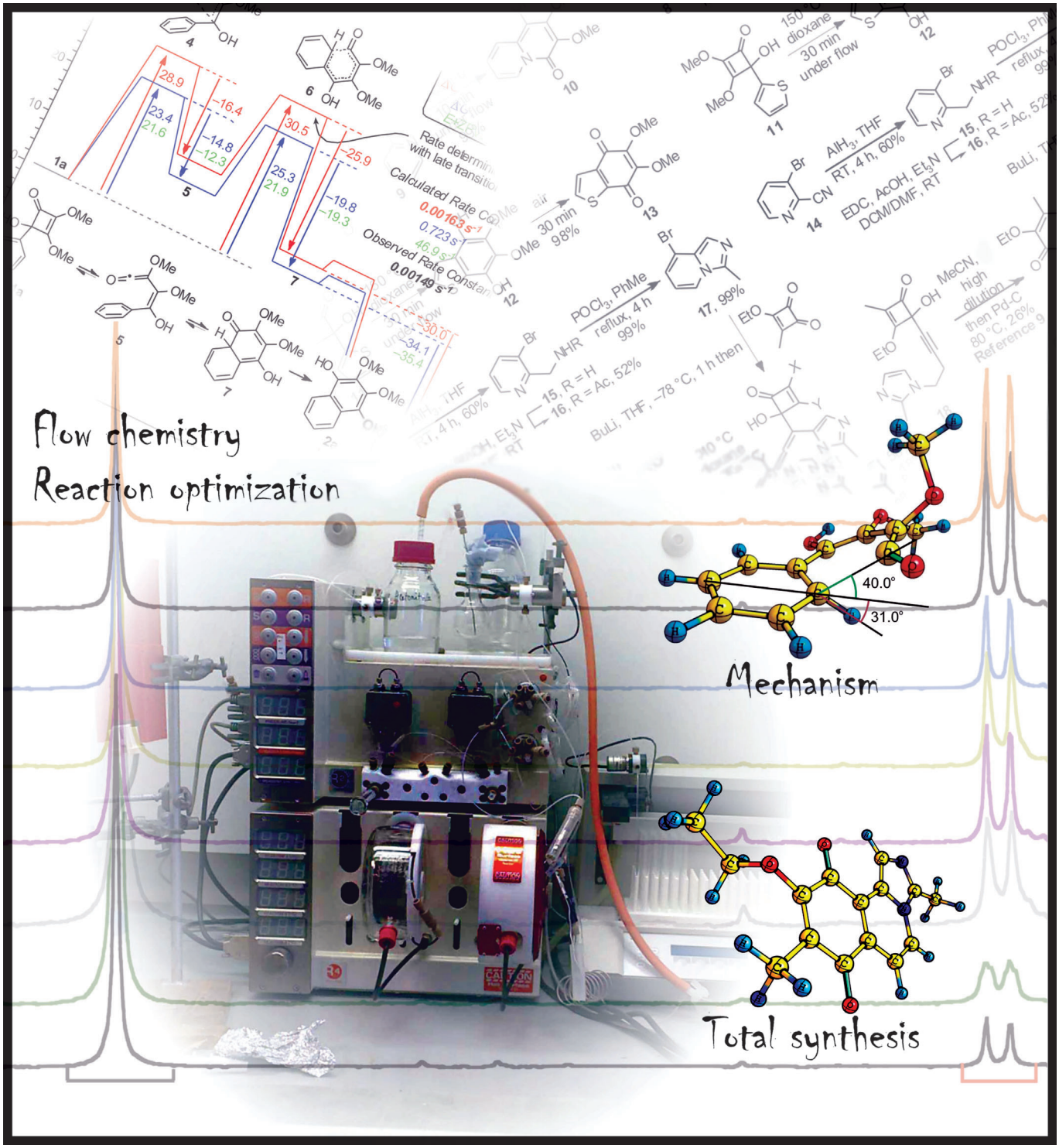

Abstract: Aryl- and heteroarylcyclobutenone rearrangements proceed in excellent yield under continuous-flow conditions. The former shows a Hammett correlation with σ_I providing strong evidence that electrocyclisation is the rate-determining step and has a late transition state. The reaction has been modelled by using DFT and CCSD(T) methods, with the latter giving excellent correlation with the experimental rate constant. A short and efficient total synthesis of cribrostatin 6, an anti-neoplastic and anti-microbial agent, provides a topical demonstration of the value of this method.

Keywords: density functional calculations · flow chemistry · Hammett correlation · reaction mechanisms · thermochemistry

Introduction

Thermal rearrangements of aryl- and heteroarylcyclobutenones have become established as useful methods for the de novo synthesis of many polyaromatic and heteroaromatic ring systems, especially those with dense substitution patterns.[1–3] Though widely used, little is known about the factors that influence the course of these reactions, or indeed the optimal conditions for effecting them. Herein we present a detailed study of the rearrangement and show how it is possible to achieve near-quantitative conversions under continuous flow. In turn, this has allowed us to establish a Hammett relationship for the reaction which,[4] in conjunction with an in silico study, provides new insights into the mechanistic course. Extensions to heteroarylcyclobutenone rearrangements include a short and efficient total synthesis of the marine natural product cribrostatin 6,[5–9] which displays useful anti-microbial and anti-cancer activity through a reactive-oxygen species (ROS)-generating mechanism.[5,7]

Results and Discussion

Reaction optimization under continuous flow and establishment of a Hammett relationship: Our investigation began with a survey of the arylcyclobutenone rearrangement, **1**→**2**+**3** (Scheme 1).[1] In batch, reactions of this type are usually conducted in xylenes at reflux (ca. 135 °C) and typically give yields of 70–85 % after 2–10 h.[1–3] By contrast, under continuous flow on a Vapourtec R4/R2+ instrument with stainless-steel tubing of 1 mm diameter,[10] it was possible to employ dioxane as the solvent at 150 °C to induce rearrangement of cyclobutenone **1a** to benzohydroquinone **2a** in 99 % isolated yield in less than 1 h.

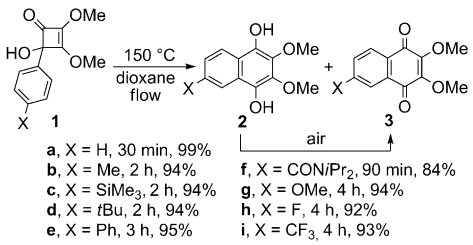

Scheme 1. Arylcyclobutenone rearrangements under continuouse flow (with isolated yields quoted for the formation of **3** from **1**).

By reasoning that the marked improvement in efficiency was due to a tight control of temperature across the narrow tubing, we were pleased to observe similar results for the rearrangement of a range of related substrates **1b–i** (Scheme 1). In each case, reactions took longer to proceed to completion than the parent compound **1a**, with electron-withdrawing substituents (F, CF_3, amide) and some electron donors (OMe) slowing the reaction down significantly. To delineate the nature of substituent effects, the progress of each reaction was determined at various residence times by using ^{1}H NMR analysis to assess the extent of conversion.[11] Though complicated by incomplete aerial oxidation of the product hydroquinones **2** to the respective benzoquinones **3**, the method proved reliable in establishing that each rearrangement exhibited first-order kinetics (Figure 1).

With these data a Hammett relationship for the reaction was sought. No correlation was evident with either the σ_m or σ_p parameter sets, as would be expected if the electrocyclic opening of the cyclobutenone were involved in the rate-determining step (Figure 2, **1a**→**5**). A reasonable correlation was given with the σ_I (inductive) parameter set (R^2=0.8584, Figure 3, grey line),[4b] with the parent compound **1a** (X= H) and those with large substituents (*t*Bu, Me_3Si, CF_3) showing greatest deviation from the line of best fit. This suggested a significant steric component to the reaction.[4,12] Indeed, by introducing a small steric correction factor (σ_I−6 % E_s) the correlation was improved to R^2=0.989 (Figure 3, bold line).[4,12]

Computational studies on the reaction mechanism: The Hammett relationship observed suggests that the electrocyc-

[a] M. Mohamed, T. P. Gonçalves, Prof. R. J. Whitby, Prof. D. C. Harrowven
Chemistry, University of Southampton
Highfield, Southampton, Hampshire, SO17 1BJ (UK)
Fax: (+44) 23-8059-6805
E-mail: dch2@soton.ac.uk

[b] Dr. H. F. Sneddon
c/o GlaxoSmithKline Medicines Research Centre
Gunnels Wood Road, Stevenage, SG1 2NY (UK)

[**] ROS = reactive-oxygen species

Supporting information for this article is available on the WWW under http://dx.doi.org/10.1002/chem.201102263.

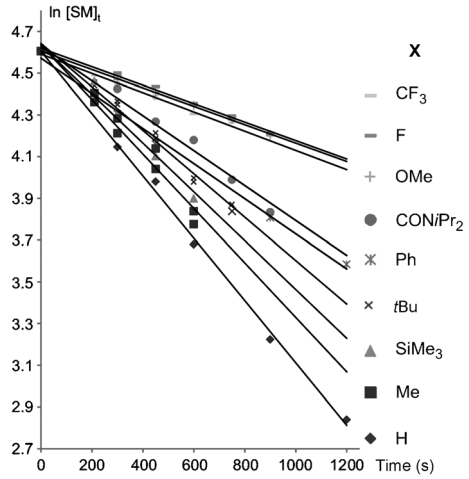

Figure 1. Determination of rate constants for **1**→**2**+**3**. X=CF_3: $k=4.4\times10^{-4}\,s^{-1}$, $R^2=0.96$; X=F: $k=4.6\times10^{-4}\,s^{-1}$, $R^2=0.98$; X=OMe: $k=6.6\times10^{-4}\,s^{-1}$, $R^2=0.99$; X=CON*i*Pr_2: $k=8.0\times10^{-4}\,s^{-1}$, $R^2=0.98$; X=Ph: $k=8.2\times10^{-4}\,s^{-1}$, $R^2=1.00$; X=*t*Bu: $k=10.2\times10^{-4}\,s^{-1}$, $R^2=0.99$; X=$SiMe_3$: $k=12.1\times10^{-4}\,s^{-1}$, $R^2=0.98$; X=Me: $k=13.1\times10^{-4}\,s^{-1}$, $R^2=0.97$; X=H: $k=14.9\times10^{-4}\,s^{-1}$, $R^2=1.00$. $[SM]_t$=concentration of starting material at a given time.

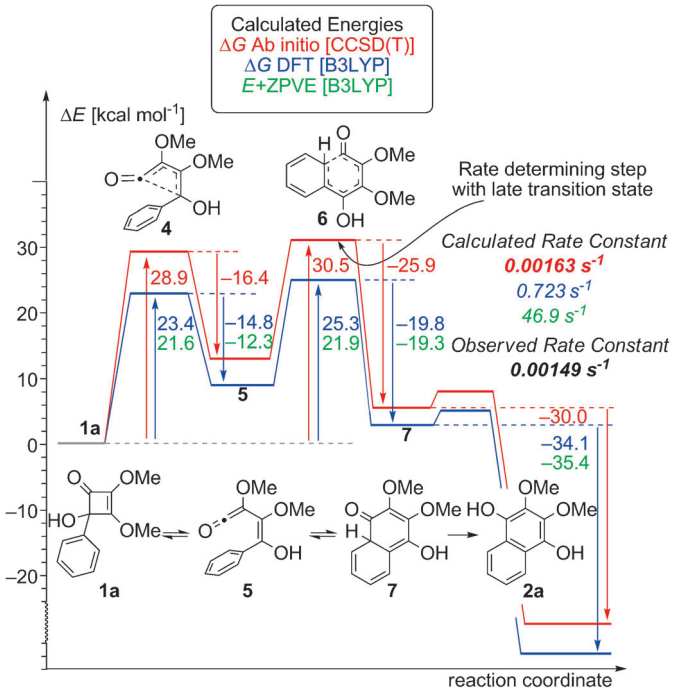

Figure 2. Summary of the energies calculated for the rearrangement **1a**→**2a** in the gas phase at 150°C computed by Δ(*E*+ZPE) UB3LYP/6-311G(d,p) (in green), Δ*G*(UB3LYP/6-311G(d,p)) (in blue) and Δ*G*(RCCSD(T)/6-31G(d)//UB3LYP/6-311G(d,p)) (in red) as well as associated rate constants.[15–18]

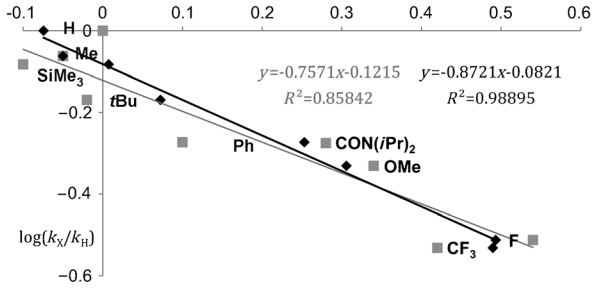

Figure 3. Hammett plot for the arylcyclobutenone rearrangement **1**→**2**+**3** with the σ_I parameter set (■) and with a steric correction (σ_I–6% E_s, ◆).[13]

lisation of ketene **5** to bicyclic ketone **7** is rate determining and has a late transition state (i.e., **6** is more akin to intermediate **7** than precursor ketene **5**, Figure 2). The rate of reaction is thus dictated by the ease with which the sigma bond, which is developing between the arene and the carbonyl in **6**, is established; this explains the observed influence of inductive rather than resonance effects. To test this hypothesis, the course of the reaction was modelled by DFT calculations at the UB3LYP/6-311G(d,p) level with the Gaussian 09 program.[14,15] The estimated *E*+ZPVE values (Figure 2, in green) were interesting in that they showed little difference between the activation barrier for electrocyclic ring opening (21.6 kcal mol^{-1}) and ring closing (21.9 kcal mol^{-1}). However, when these were corrected to reflect free energy, the calculated values for Δ*G* at 150°C (23.4 and 25.3 kcal mol^{-1}, respectively) supported our postulate that electrocyclisation of vinylketene **5**→**7** is rate determining. Importantly, they also showed the electrocyclic opening of **1a**→**5** to be reversible with the equilibrium favouring the cyclobutenone rather than the ketene.

A limitation of the DFT method was exposed when we sought to relate the predicted Δ*G* values to the reaction rates observed experimentally for the rearrangement **1a**→**2a**. The calculated values implied a reaction rate substantially faster than the observed one, underestimating the energy requirements by nearly 5 kcal mol^{-1}. Consequently, we refined our analysis further by employing high ab initio single-point energy calculations [RCCSD(T)/6-31G(d)] with the GAMESS(US) package.[17,18] The results attained predicted a rate constant for the rearrangement of **1a**→**2a** of 0.0016 s^{-1} after correction for the free energy at 150°C; this is in excellent agreement with the observed value (0.00149 s^{-1}). In addition, these calculations reaffirmed that the electrocyclic closure **5**→**7** is rate limiting (30.5 kcal mol^{-1} compared with 28.9 kcal mol^{-1} for **1a**→**5**).

The calculated geometry for transition-state **6** (Figure 4) is also instructive as it shows an angle of incidence of 40.0° between the developing σ bond and the plane of the arene. The angle is reduced to 22.1° as the reaction progresses to intermediate **7**. Thus, interaction between this nascent σ bond and the residual π system is limited as it develops to become part of the σ framework—an observation that is consistent with a late transition state under the influence of inductive rather than resonance effects.

Further exemplifications of the method and a total synthesis of cribrostatin 6: Our attention next turned to the rear-

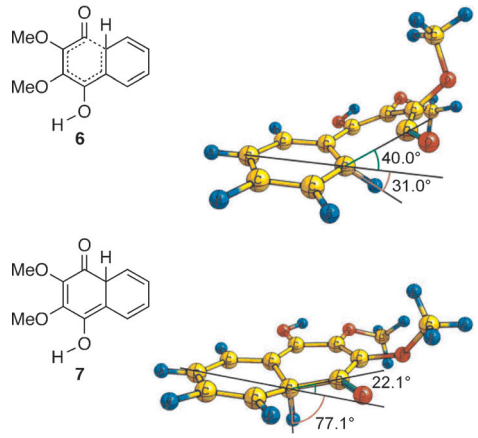

Figure 4. Calculated structures for the transition state **6** and intermediate **7**.[16]

rangement of heteroarylcyclobutenones. With a myriad of options available, we limited our study to representative electron-rich (thiophene) and electron-poor (pyridine) systems, and an exemplification through total synthesis. The thermolysis of (2-pyridyl)cyclobutenones provides rapid access to quinolizidones,[2a] for example, **9**→**10**, which are used widely in medicinal chemistry as isosteres for naphthalenes. In spite of this, the reaction has found little favour, perhaps due to modest yields (29–60%) and a need to protect the alcohol moiety formed on addition of a 2-lithiopyridine to a cyclobutendione. Under continuous-flow conditions, the thermal rearrangement of pyridylcyclobutenone **9** in dioxane at 100°C gave quinolizidone **10** in quantitative yield after a residence time of just 10 min without the need for alcohol protection (Scheme 2). Although the related synthesis of quino[*b*]thiophene **13** from thiophene **11** required a higher temperature (150°C) and an aerial oxidation, it too proceeded efficiently, to give a 98% yield over the two steps (Scheme 2).[19]

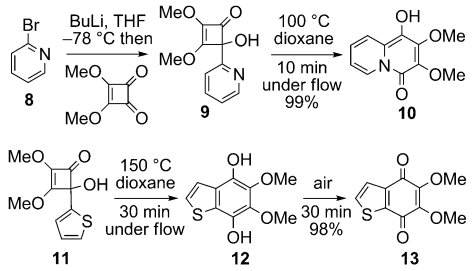

Scheme 2. Representative heteroarylcyclobutenone rearrangements under continuous-flow conditions.[17,18]

To demonstrate the value of the method, we chose to tackle the synthesis of the marine natural product cribrostatin 6 (**19**), a popular target since it was identified by Pettit et al. in 2003, that exhibits useful anti-neoplastic and antimicrobial activity.[5,6] In 2010, cribrostatin 6 was reported to induce death in cancer cells by inducing oxidative stress and the build-up of ROS.[20] As an approach to cancer chemotherapy, ROS-inducing therapies are still in their infancy. Esclomol, for example, was recently advanced to phase III clinical trials in combination with taxol, though these were halted because of increased mortality.[20] To date, four total syntheses of **19** have been reported.[6–9,20] The shortest, by Knueppel and Martin, was reported in 2009 and featured an alkynylcyclobutenone rearrangement as a key step, namely, **18**→**19**.[9] Although this step gave a low yield (26%), it allowed the total synthesis to be completed in just five linear steps.

Our plan was to achieve a synthesis of cribrostatin 6 in a similar step count, but with greater efficiency. To that end, nitrile **14** was reduced to the corresponding amine **15** with alane (AlH_3) (Scheme 3).[21] Acylation to **16** was followed by cyclisation with $POCl_3$ to give imidazopyridine **17** in a near-quantitative yield. Halogen–lithium exchange then facilitated the union of **17** and 2-ethoxy-3-methylcyclobutendione, to give a separable 3:1 mixture of adduct **20** and a regioisomer **20a** derived from addition to the vinylogous ester carbonyl. Finally, thermolysis of **20** in dioxane for 1 h at 110°C under continuous flow, followed by exposure to air for a further 45 min, gave **19** in 90% yield after purification by column chromatography.

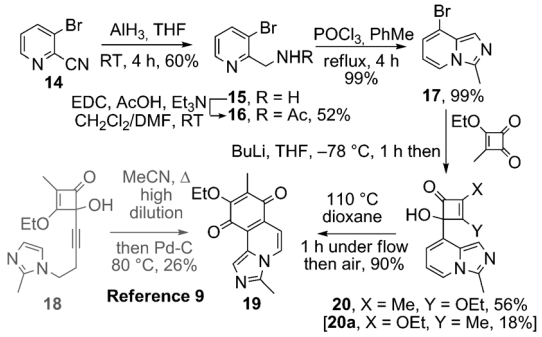

Scheme 3. A short total synthesis of cribrostatin 6 (**19**). EDC = 1-ethyl-3-(3-dimethylaminopropyl)carbodiimide.

Conclusion

In conclusion, we have shown that aryl- and heteroarylcyclobutenone rearrangements can be conveniently performed under continuous flow in dioxane at 150°C and proceed with excellent yields. The approach has allowed us to determine a Hammett relationship for the reaction. This, in conjunction with DFT and ab initio modelling,[11] provides strong evidence that the electrocyclisation of ketene **5** to bicyclic ketone **7** is rate determining in arylcyclobutenone rearrangements and has a late transition state. From a computational perspective, the excellent performance of RCCSD(T)/6-31G(d)//UB3LYP/6-311G(d,p) in predicting reaction kinetics is notable. The short and efficient total syn-

thesis of cribrostatin 6 (**19**), a useful anti-neoplastic and anti-microbial agent, provides a topical demonstration of the value of the method for the rapid construction of condensed quinones.

Experimental Section

General procedure for continuous-flow reactions: Aliquots of **1a–i** (2 mL) in dioxane were taken from bulk solutions (0.25 g in 25 mL) and heated at 150 °C under continuous flow in stainless-steel tubing (internal diameter 1 mm, capacity 10 mL) for the stated residence time by using a Vapourtec R4/R2+ device. The resulting solutions were concentrated in vacuo then analyzed by ^{1}H NMR to determine the composition (**1**, **2** and **3**) by comparison of the respective integrals as indicated in the Supporting Information.

*2,3-Dimethoxynaphthalene-1,4-dione (**3a**)*:[1a,f] Compound **3a** could be formed in a near-quantitative yield by using the general procedure with a residence time of 30 min and stirring the resulting solution in air for 1 h. M.p.: 116–118 °C (Et_2O/petroleum ether; previously reported: 115–117 °C (Et_2O));[1a,f] ^{1}H NMR (300 MHz, $CDCl_3$): δ = 7.71 (m, 2H), 8.07 (m, 2H), 4.13 ppm (s, 6H); ^{13}C NMR (75 MHz, $CDCl_3$): δ = 182.0 (2×C), 147.5 (2×C), 133.8 (2×CH), 130.8 (2×C), 126.3 (2×CH), 61.5 ppm (2×CH_3); IR ($CHCl_3$): $\tilde{\nu}$ = 3385, 2954, 1772, 1601, 1468, 1337, 1047, 994, 858 cm^{-1}; MS (ES$^+$): *m/z* (%): 241 $[M+Na]^+$ (46), 219 $[M+H]^+$ (16). See Figure 5 and Table 1.

*2,3-Dimethoxy-6-methylnaphthalene-1,4-dione (**3b**)*:[1a] Compound **3b** could be formed in 94% yield by using the general procedure with a residence time of 2 h and stirring the resulting solution in air for 3 h. M.p.: 89–91 °C (MeOH; previously reported: 90–92 °C (aq MeOH));[1a] ^{1}H NMR (400 MHz, $CDCl_3$): δ = 7.96 (d, J = 7.8 Hz, 1H), 7.87 (br s, 1H), 7.53–7.47 (ddq, J = 7.8, 1.5, 0.8 Hz, 1H), 4.12 (s, 3H), 4.10 (s, 3H), 2.48 ppm (br s, 3H); ^{13}C NMR (100 MHz, $CDCl_3$): δ = 182.3 (C), 181.8 (C), 147.6 (C), 144.9 (C), 134.4 (C), 130.8 (CH), 128.6 (C), 126.7 (CH), 126.4 (CH), 119.7 (C), 61.4 (2×CH_3), 21.8 ppm (CH_3); IR ($CHCl_3$): $\tilde{\nu}$ = 2950, 1659, 1611, 1600, 1306, 1269, 1040 cm^{-1}; MS (ES$^+$): *m/z* (%): 482 $[2M+NH_4]^+$ (60), 233 $[M+H]^+$ (100). See Scheme 4, Figure 6 and Table 2.

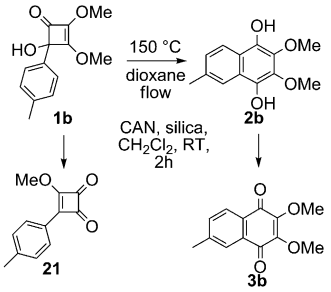

Scheme 4. Synthesis of **3b**. CAN = ceric ammonium nitrate.

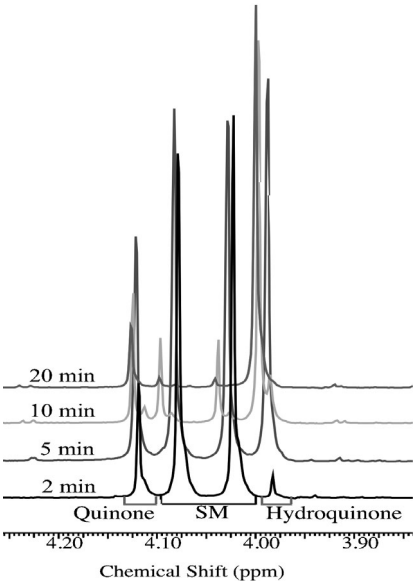

Figure 5. NMR spectra used to extract data presented in Table 1.

Table 1. Concentration of **1a** after thermolysis in dioxane at 150 °C for the stated residence time, as determined by NMR integration.

Time [s]	**1a** [%]	ln[SM]
0	100	4.61
300	63.2	4.15
450	53.5	3.98
600	39.6	3.68
900	25.1	3.22
1200	17.1	2.84

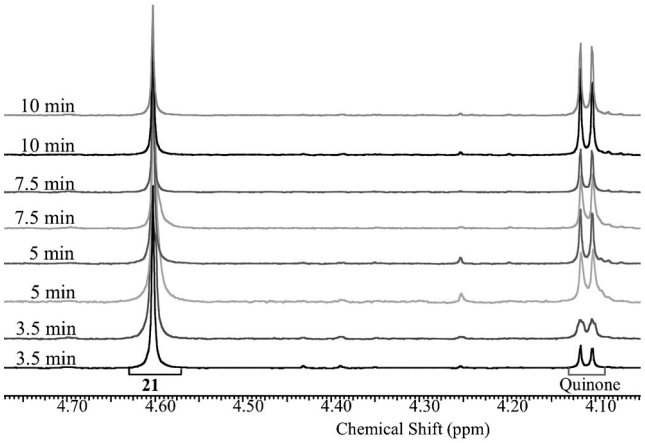

Figure 6. NMR spectra used to extract data presented in Table 2.

Table 2. Concentration of **1b** after thermolysis in dioxane at 150 °C for the stated residence time, as determined by NMR integration; the reactions were run in duplicate.

Time [s]	**1b** [%]	ln[SM]
0	100	4.61
	100	4.61
210	81.9	4.41
	78.4	4.36
300	72.4	4.28
	67.5	4.21
450	62.7	4.14
	56.9	4.04
600	46.5	3.84
	43.7	3.78

As an alternative to the general method, the crude reaction mixture could be concentrated in vacuo, dissolved in CH_2Cl_2 then exposed to 23% CAN on silica. The procedure facilitates the quantitative oxidation of the benzohydroquinone **2b** to benzoquinone **3b** with remaining starting-material **1b** converted to 3-methoxy-4-(4-methylphenyl)cyclobuten-1,2-dione (**21**). ^{1}H NMR (400 MHz, $CDCl_3$): $\delta=7.94$ (d, $J=8.1$ Hz, 2H), 7.32 (d, $J=8.1$, Hz, 2H), 4.60 (3H, s), 2.44 ppm (s, 3H); ^{13}C NMR (100 MHz, $CDCl_3$): $\delta=193.8$ (C), 184.7 (C), 174.9 (C), 143.9 (C), 129.9 (2×CH), 127.9 (2×CH), 125.0 (C), 116.3 (C), 61.6 (CH_3), 22.0 ppm (CH_3); IR ($CHCl_3$): $\tilde{\nu}=1784$, 1595, 1369 cm^{-1}; MS (ES$^+$): *m/z* (%): 266 $[M+MeCN+Na]^+$ (100), 203 $[M+H]^+$ (2).[22]

*4-Hydroxy-2,3-dimethoxy-4-(pyridin-2-yl)cyclobut-2-enone (**9**)*: *n*BuLi (3.52 mL, 2.40 M solution in hexane, 8.45 mmol) was added to a solution of 2-bromopyridine (0.82 mL, 8.45 mmol) in THF (30 mL) at −78 °C over 5 min. After 15 min the resulting solution was added, through a cannula, to a solution of dimethyl squarate (1.00 g, 7.04 mmol) in THF (10 mL) at −78 °C, giving a red solution. After 30 min, saturated NH_4Cl (20 mL) was added. The reaction mixture was allowed to warm to RT then extracted with CH_2Cl_2 (50 mL×3). The combined organic layers were washed with brine (50 mL×2), dried ($MgSO_4$), filtered, concentrated in vacuo and purified by flash column chromatography (5%→50% EtOAc/petroleum ether with 2% NEt_3) to afford the title-compound **9** as a pale brown oil (0.97 g, 4.37 mmol, 62%). ^{1}H NMR (400 MHz, $CDCl_3$): $\delta=8.62$ (d+fine splitting, $J=4.5$ Hz, 1H), 7.77 (td, $J=7.5$, 1.5 Hz, 1H), 7.48 (d, $J=7.5$ Hz, 1H), 7.30 (ddd, $J=7.5$, 4.5, 1.0 Hz, 1H), 6.07 (s, 1H), 4.09 (s, 3H), 3.98 ppm (s, 3H); ^{13}C NMR (75 MHz, $CDCl_3$): $\delta=182.6$ (C), 164.4 (C), 154.6 (CH), 148.3 (C), 137.6 (C), 137.4 (CH), 123.2 (CH), 120.0 (CH), 80.0 (C), 59.9 (CH_3), 58.8 ppm (CH_3); IR ($CHCl_3$): $\tilde{\nu}=3463$, 2951, 1776, 1632, 1468, 1337, 1061 cm^{-1}; MS (ES$^+$): *m/z* (%): 222 $[M+H]^+$ (100); HRMS (ES$^+$): *m/z*: calcd for $C_{11}H_{12}NO_4$: 222.0775 $[M+H]^+$; found: 222.0766.

*1-Hydroxy-2,3-dimethoxy-4H-quinolizin-4-one (**10**)*: A solution of **9** (5.0 mg, 0.023 mmol) in dioxane (2 mL) was heated at 100 °C in stainless-steel tubing for a residence time of 10 min with a Vapourtec R4/R2+ device. The resulting solution was stirred in air for 1 h and then concentrated in vacuo to give **10** as a pale brown solid (4.9 mg, 0.022 mmol, 99%). M.p.: 110–112 °C (EtOAc/petroleum ether); ^{1}H NMR (400 MHz, [D$_6$]DMSO): $\delta=8.88$ (s, 1H), 8.70 (d, $J=7.6$ Hz, 1H), 7.73 (d, $J=9.0$ Hz, 1H), 7.16 (dd, $J=8.0$, 6.6 Hz, 1H), 6.86–6.97 (m, 1H), 4.03 (s, 3H), 3.87 ppm (s, 3H); ^{13}C NMR (100 MHz, [D$_6$]DMSO): $\delta=152.1$ (C), 150.2 (C), 131.7 (C), 127.2 (C), 126.7 (C), 125.4 (CH), 125.2 (CH), 120.0 (CH), 114.0 (CH), 60.9 (CH_3), 59.3 ppm (CH_3); IR ($CHCl_3$): $\tilde{\nu}=2955$, 2925, 1733, 1634, 1595, 1457, 1288, 1122 cm^{-1}; MS (ES$^+$): *m/z* (%): 222 $[MH]^+$ (100); HRMS (ES$^+$): *m/z*: calcd for $C_{11}H_{12}NO_4$: 222.0775 $[M+H]^+$; found: 222.0766.

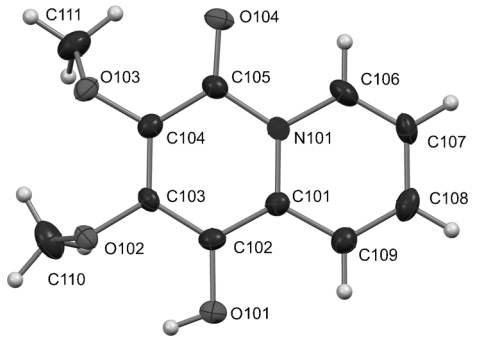

*4-Hydroxy-2,3-dimethoxy-4-(thiophen-2-yl)cyclobut-2-en-1-one (**11**)*:[1a] 2-Bromothiopene (0.376 mL, 3.87 mmol) was added to a solution of *n*BuLi (2.42 mL, 1.6 M solution in hexane, 3.87 mmol) in THF (15 mL) over 5 min at −78 °C. After 15 min, a solution of dimethyl squarate (0.50 g, 3.52 mmol) in THF (10 mL) was added over 5 min, giving an orange solution. After 1 h, saturated NH_4Cl (20 mL) was added. The reaction mixture was allowed to warm to RT then extracted with CH_2Cl_2 (20 mL×3). The combined organic layers were washed with brine (20 mL×2), dried ($MgSO_4$), filtered, concentrated in vacuo and purified by flash column chromatography (5%→40% EtOAc/petroleum ether with 2% NEt_3) to afford the title-compound **11** as a white solid (0.257 g, 1.14 mmol, 32%). M.p.: 66–68 °C (Et_2O/petroleum ether; previously reported: 68–69 °C (Et_2O));[1a] ^{1}H NMR (400 MHz, $CDCl_3$): $\delta=7.33$ (dd, $J=5.0$, 1.3 Hz, 1H), 7.11 (dd, $J=3.5$, 1.3 Hz, 1H), 7.02 (dd, $J=5.0$, 3.5 Hz, 1H), 4.11 (s, 3H), 4.02 (s, 3H), 3.56 ppm (s, 1H); ^{13}C NMR (100 MHz, $CDCl_3$): $\delta=$ 183.1 (C), 166.0 (C), 140.7 (C), 135.2 (C), 127.2 (CH), 126.2 (CH), 125.0 (CH), 85.7 (C), 60.3 (CH_3), 58.8 ppm (CH_3); IR ($CHCl_3$): $\tilde{\nu}=3400$, 3008, 2956, 1781, 1644, 1635, 1470, 1348, 1040 cm^{-1}; MS (ES$^+$): *m/z* (%): 227 $[M+H]^+$ (100).

*5,6-Dimethoxybenzo[b]thiophene-4,7-dione (**13**)*:[1a] A solution of **11** (5.0 mg, 0.022 mmol) in dioxane (2 mL) was heated at 150 °C in stainless-steel tubing for a residence time of 30 min by using a Vapourtec R4/R2+ device. The resulting solution was stirred in air for 1 h then concentrated in vacuo to give the title-compound **13** as an orange solid (4.9 mg, 0.022 mmol, 98%). M.p.: 169–172 °C (Et_2O/petroleum ether; previously reported: 171.5–173 °C (CH_2Cl_2/petroleum ether));[1a] ^{1}H NMR (400 MHz, $CDCl_3$): $\delta=7.63$ (d, $J=5.0$ Hz, 1H), 7.50 (d, $J=5.0$ Hz, 1H), 4.09 ppm (apparent s, 6H); ^{13}C NMR (100 MHz, $CDCl_3$): $\delta=178.0$ (C), 176.6 (C), 147.2 (C), 146.7 (C), 141.4 (C), 139.5 (C), 133.4 (CH), 125.9 (CH), 61.5 (CH_3), 61.6 ppm (CH_3); IR ($CHCl_3$): $\tilde{\nu}=3033$, 3008, 2929, 1651, 1340, 1292, 858 cm^{-1}; MS (ES$^+$): *m/z* (%): 225 $[M+H]^+$ (100).

*(3-Bromopyridin-2-yl)methanamine (**15**)*:[21] To a cooled (0 °C) solution of 3-bromo-2-cyanopyridine (0.100 g, 0.546 mmol) in toluene (20 mL) was added alane·Me_2NEt complex (0.5 M solution in toluene, 2.2 mL, 1.093 mmol) over 4 min. The resulting mixture was warmed to RT and then, after 16 h, was re-cooled to 0 °C. Methanol (10 mL) and saturated sodium potassium tartare (50 mL) were cautiously added, then the aqueous phase was separated and extracted with $CHCl_3$ (20 mL×3). The combined organic phases were then washed with brine (20 mL×2), dried ($MgSO_4$), filtered and concentrated in vacuo to afford the title-compound **15** as an yellow oil (60.5 mg, mmol, 60%). ^{1}H NMR (300 MHz, $CDCl_3$): $\delta=8.52$ (dd, $J=5.0$, 1.5 Hz, 1H), 7.85 (dd, $J=7.9$, 1.5 Hz, 1H), 7.11 (dd, $J=7.9$, 5.0 Hz, 1H), 4.14 (s, 2H), 2.77 ppm (s, 2H); ^{13}C NMR (75 MHz, $CDCl_3$): $\delta=162.4$ (C), 150.2 (CH), 145.2 (CH), 123.1 (C), 115.9 (CH), 45.2 ppm (CH_2); MS (ES$^+$): *m/z* (%): 189 $[M(^{81}Br)+H]^+$ (100), 187 $[M(^{79}Br)+H]^+$ (100).

*N-((3-Bromopyridin-2-yl)methyl)acetamide (**16**)*:[21] Acetic acid (0.850 mL, 14.83 mmol) and triethylamine (4.13 mL, 29.7 mmol) were added sequentially to a solution of *N*-(3-dimethylaminopropyl)-*N*′-ethylcarbodiimide hydrochloride (2.84 g, 14.83 mmol) in dichloromethane (30 mL) at RT. After 1 h, a solution of **15** (1.422 g, 5.93 mmol) in DMF (15 mL) and CH_2Cl_2 (10 mL) was added, followed by 2 M sodium carbonate (30 mL) after an additional 1 h. The aqueous phase was separated and extracted with dichloromethane (3×20 mL) and then the organic phases were dried ($MgSO_4$), concentrated in vacuo and purified by column chromatography (EtOAc) to give the title-compound **16** as a white solid (0.730 g, 3.187 mmol, 52%). M.p.: 62–64 °C (EtOAc); ^{1}H NMR (400 MHz, $CDCl_3$): $\delta=8.50$ (d, $J=4.4$, 1.3 Hz, 1H), 7.89 (d, $J=$ 7.9, 1.3 Hz, 1H), 7.18 (brs, 1H), 7.16 (dd, $J=7.9$, 4.4 Hz, 1H), 4.62 (d, $J=4.3$, 2H), 2.13 ppm (s, 3H); ^{13}C NMR (100 MHz, $CDCl_3$): $\delta=170.0$ (C), 153.7 (C), 146.9 (CH), 140.4 (CH), 123.5 (C), 120.3 (CH), 44.1 (CH_2), 23.3 ppm (CH_3); IR ($CHCl_3$): $\tilde{\nu}=3314$, 1642, 1560, 812 cm^{-1}; MS (ES$^+$): *m/z* (%): 231 $[M(^{81}Br)+H]^+$ (100), 229 $[M(^{79}Br)+H]^+$ (100).

*8-Bromo-3-methylimidazo[1,5-a]pyridine (**17**)*: Phosphorus oxychloride (1.07 mL, 11.5 mmol) was added to a solution of acetamide **16** (0.730 g, 3.19 mmol) in toluene (10 mL) at RT over 5 min. The reaction mixture was heated at reflux for 4 h then cooled to 0 °C and saturated sodium bicarbonate (30 mL) was added. The aqueous phase was separated and extracted with ethyl acetate (10 mL×3), then the combined organic phases were washed with water (10 mL×2), dried ($MgSO_4$) and concentrated to give the title-compound **17** as a brown oil (0.680 g, 3.222 mmol, 99%, ca. 98% purity). ^{1}H NMR (400 MHz, $CDCl_3$): $\delta=7.68$ (d, $J=7.3$ Hz, 1H), 7.46 (s, 1H), 6.92 (d, $J=6.8$ Hz, 1H), 6.47 (apparent t, $J=7.1$ Hz, 1H), 2.69 ppm (s, 3H); ^{13}C NMR (100 MHz, $CDCl_3$): $\delta=179.0$ (C), 136.6 (C),

130.0 (C), 120.8 (CH), 119.8 (CH), 119.5 (CH), 112.7 (CH), 12.6 ppm (CH_3); IR ($CHCl_3$): $\tilde{\nu}$ = 3314, 1642, 1560, 812 cm^{-1}; MS (ES^+): *m/z* (%): 213 $[M(^{81}Br)+H]^+$ (100), 211 $[M(^{79}Br)+H]^+$ (100).

*3-Ethoxy-4-hydroxy-2-methyl-4-(3-methylimidazo[1,5-a]pyridin-8-yl)cyclobut-2-enone (**20**)*: *n*BuLi (1.6 M in hexane, 0.79 mL, 1.26 mmol) was added to a solution of imidazo[1,5-*a*]pyridine **17** (242 mg, 1.15 mmol) in THF (5 mL) at −78 °C. After 30 min a solution of 3-ethoxy-4-methyl-3-cyclobutene-1,2-dione (0.161 g, 1.147 mmol)[1,9] in THF (5 mL) was added over 4 min, followed by saturated NH_4Cl (20 mL) after an additional 1 h. After warming to RT the aqueous phase was separated and extracted with dichloromethane (20 mL × 3). The combined organic phases were washed with brine (20 mL × 2), dried ($MgSO_4$), concentrated in vacuo and purified by flash column chromatography (0 % → 5 % methanol/dichloromethane with 1 % NEt_3) gave firstly **20a** (59 mg, 0.204 mmol, 18 %) then the title-compound **20** as a pale orange oil (175 mg, 0.642 mmol, 56 %). ^1H NMR (400 MHz, $CDCl_3$): δ = 7.64 (d, *J* = 7.0 Hz, 1H), 7.39 (s, 1H), 6.97 (d, *J* = 6.8 Hz, 1H), 6.60 (t, *J* = 6.9 Hz, 1H), 4.45 (dq, *J* = 9.8, 7.1 Hz, 1H), 4.26 (dq, *J* = 9.9, 7.1 Hz, 1H), 2.66 (s, 3H), 1.85 (s, 3H), 1.36 ppm (t, *J* = 7.1 Hz, 3H); ^{13}C NMR (100 MHz, $CDCl_3$): δ = 189.5 (C), 182.2 (C), 135.5 (C), 127.8 (C), 127.6 (C), 125.2 (C), 120.7 (CH), 118.5 (CH), 116.5 (CH), 112.0 (CH), 91.6 (C), 69.2 (CH_2), 15.0 (CH_3), 12.6 (CH_3), 6.9 ppm (CH_3); IR ($CHCl_3$): $\tilde{\nu}$ = 2928, 2861, 1715, 1731, 1617, 1332, 1135, 1078 cm^{-1}; MS (ES^+): *m/z* (%): 273 $[M+H]^+$ (100); HRMS (ES^+): *m/z*: calcd for $C_{15}H_{17}N_2O_3$: 273.1161 $[M+H]^+$; found: 273.1232.

*9-Ethoxy-3,8-dimethylimidazo[5,1-a]isoquinoline-7,10-dione (**19**, Cribrostatin 6)*: Cyclobutenone **20** (59 mg, 0.217 mmol) in dioxane (2 mL) was heated at 110 °C in stainless-steel tubing for a residence time of 1 h by using a Vapourtec R4/R2+ device. The resulting solution was stirred in air for 30 min then concentrated in vacuo and purified by chromatography (2 % MeOH in CH_2Cl_2) to give **19** as a light-blue solid (52 mg, 0.193 mmol, 90 %). M.p.: 167–169 °C (acetone at −4 °C; previously reported: 165–167 °C (acetone)[8,9], 169–171 °C (acetone)[5], 171–172 °C (acetone)[6,7]); ^1H NMR (400 MHz, $CDCl_3$): δ = 8.52 (s, 1H); 8.10 (d, *J* = 7.6 Hz, 1H), 7.62 (d, *J* = 7.6 Hz, 1H), 4.49 (q, *J* = 6.8 Hz, 2H), 3.09 (br s, 3H), 2.13 (s, 3H), 1.45 ppm (t, *J* = 7 Hz, 3H); ^{13}C NMR (100 MHz, $CDCl_3$): δ = 184.9 (C), 180.7 (C), 156.2 (C), 137. 7 (C), 130.1 (C), 125.9 (C), 125.0 (C), 124.7 (C), 123.9 (CH), 123.5 (CH), 107.6 (C), 69.6 (CH_2), 16.0 (CH_3), 12.6 (CH_3), 9.2 ppm (CH_3); IR ($CHCl_3$): $\tilde{\nu}$ = 2925, 1662, 1626, 1611, 1527, 1172 cm^{-1}; MS (ES^+): *m/z* (%): 271 $[M+H]^+$ (100).

CCDC-808547 contains the supplementary crystallographic data for this paper. These data can be obtained free of charge from The Cambridge Crystallographic Data Centre via www.ccdc.cam.ac.uk/data_request/cif.

Acknowledgements

We gratefully acknowledge GSK, ERDF (IS:CE-Chem & InterReg IVa program 4061) and the EPSRC for funding, and for the support of the Iridis 3 cluster. Rob Wheeler and Dr. Andy Craven are thanked for valuable advice and Dr. M. E. Light for the X-ray analysis.

[1] a) H. W. Moore, S. T. Perri, *J. Org. Chem.* **1988**, *53*, 996–1003; b) S. T. Perri, H. J. Dyke, H. W. Moore, *J. Org. Chem.* **1989**, *54*, 2032–2034; c) A. Enhsen, K. Karabelas, J. M. Heerding, H. W. Moore, *J. Org. Chem.* **1990**, *55*, 1177–1185; d) J. M. Heerding, H. W. Moore, *J. Org. Chem.* **1991**, *56*, 4048–4050; e) M. P. Winters, M. Stranberg, H. W. Moore, *J. Org. Chem.* **1994**, *59*, 7572–7574; f) H. W. Moore, O. H. W. Decker, *Chem. Rev.* **1986**, *86*, 821–830; g) M. W. Reed, D. J. Pollart, S. T. Perri, L. D. Foland, H. W. Moore, *J. Org. Chem.* **1988**, *53*, 2477–2482.

[2] a) A. G. Birchler, F. Liu, L. S. Liebeskind, *J. Org. Chem.* **1994**, *59*, 7737–7745; b) D. Zhang, I. Llorente, L. S. Liebeskind, *J. Org. Chem.* **1997**, *62*, 4330–4338; c) S. Zhang, L. S. Liebeskind, *J. Org. Chem.* **1999**, *64*, 4042–4049.

[3] For an excellent review see a) R. L. Danheiser, G. B. Dudley, W. F. Austin in *Science in Synthesis, Vol. 23*, (Ed.: R. Danheiser), Thieme Chemistry, Stuttgart, **2006**, pp. 493–568; see also b) D. C. Harrowven, D. D. Pascoe, D. Demurtas, H. O. Bourne, *Angew. Chem.* **2005**, *117*, 1247–1248; *Angew. Chem. Int. Ed.* **2005**, *44*, 1221–1222; c) D. C. Harrowven, D. D. Pascoe, I. L. Guy, *Angew. Chem.* **2007**, *119*, 429–432; *Angew. Chem. Int. Ed.* **2007**, *46*, 425–428.

[4] a) L. P. Hammett, *Physical Organic Chemistry*, 2nd ed., McGraw-Hill, New York, **1970**; b) O. Exner, *Correlation Analysis of Chemical Data*, Plenum Press, New York, **1988**.

[5] G. R. Pettit, J. C. Collins, J. C. Knight, D. L. Herald, R. A. Nieman, M. D. Williams, R. K. Pettit, *J. Nat. Prod.* **2003**, *66*, 544–547; R. K. Pettit, B. R. Fakoury, J. C. Knight, C. A. Weber, G. R. Pettit, G. D. Cage, S. Pon, *J. Med. Microbiol.* **2004**, *53*, 61–65.

[6] S. Nakahara, A. Kubo, *Heterocycles* **2004**, *63*, 2355–2362.

[7] S. Nakahara, A. Kubo, Y. Mikami, J. Ito, *Heterocycles* **2006**, *68*, 515–520.

[8] M. D. Markey, T. R. Kelly, *J. Org. Chem.* **2008**, *73*, 7441–7443.

[9] D. Knueppel, S. F. Martin, *Angew. Chem.* **2009**, *121*, 2607–2609; *Angew. Chem. Int. Ed.* **2009**, *48*, 2569–2571.

[10] The flow system employed is shown in Figure 2 of S. V. Ley, I. R. Baxendale, *Chimia* **2008**, *62*, 162–168. Further details may be found on the manufacturer's web site http://www.vapourtec.co.uk/products/rseriessystem accessed 21/7/2011.

[11] a) A. Odedra, P. H. Seebergera, *Angew. Chem.* **2009**, *121*, 2737–2740; *Angew. Chem. Int. Ed.* **2009**, *48*, 2699–2702; b) F. E. Valera, M. Quaranta, A. Moran, J. Blacker, A. Armstrong, J. Cabral, D. G. Blackmond, *Angew. Chem.* **2010**, *122*, 2530–2537; *Angew. Chem. Int. Ed.* **2010**, *49*, 2478–2485.

[12] a) V. P. Andreev, *Chem. Heterocycl. Compd.* **2010**, *46*, 184–195; b) E. Kutter, C. Hansch, *J. Med. Chem.* **1969**, *12*, 647–651; c) T. Fujita, C. Takayama, M. Nakajima, *J. Org. Chem.* **1973**, *38*, 1623–1630; d) G. Ananchenko, E. Beaudoin, D. Bertin, D. Gigmes, P. Lagarde, S. R. A. Marque, E. Revalor. P. Tordo, *J. Phys. Org. Chem.* **2006**, *19*, 269–275.

[13] As the value of σ_I for CON*i*Pr_2 is not known, we used as an estimate, namely, the known value for $CONH_2$.

[14] Gaussian 09, Revision A.02, M. J. Frisch, G. W. Trucks, H. B. Schlegel, G. E. Scuseria, M. A. Robb, J. R. Cheeseman, G. Scalmani, V. Barone, B. Mennucci, G. A. Petersson, H. Nakatsuji, M. Caricato, X. Li, H. P. Hratchian, A. F. Izmaylov, J. Bloino, G. Zheng, J. L. Sonnenberg, M. Hada, M. Ehara, K. Toyota, R. Fukuda, J. Hasegawa, M. Ishida, T. Nakajima, Y. Honda, O. Kitao, H. Nakai, T. Vreven, J. A. Montgomery, Jr., J. E. Peralta, F. Ogliaro, M. Bearpark, J. J. Heyd, E. Brothers, K. N. Kudin, V. N. Staroverov, R. Kobayashi, J. Normand, K. Raghavachari, A. Rendell, J. C. Burant, S. S. Iyengar, J. Tomasi, M. Cossi, N. Rega, N. J. Millam, M. Klene, J. E. Knox, J. B. Cross, V. Bakken, C. Adamo, J. Jaramillo, R. Gomperts, R. E. Stratmann, O. Yazyev, A. J. Austin, R. Cammi, C. Pomelli, J. W. Ochterski, R. L. Martin, K. Morokuma, V. G. Zakrzewski, G. A. Voth, P. Salvador, J. J. Dannenberg, S. Dapprich, A. D. Daniels, Ö. Farkas, J. B. Foresman, J. V. Ortiz, J. Cioslowski, D. J. Fox, Gaussian, Inc., Wallingford CT, 2009.

[15] a) P. W. Musch, C. Remenyi, H. Helten, B. Engels, *J. Am. Chem. Soc.* **2002**, *124*, 1823–1828; b) P. R. Schreiner, B. H. Bui, *Eur. J. Org. Chem.* **2006**, 1162–1165; c) P. W. Musch, B. Engels, *J. Am. Chem. Soc.* **2001**, *123*, 5557–5562.

[16] All calculations were performed at the B3LYP/6–311G(d,p) level with Gaussian 09,[14] with GAMESS(US)[17] used for all RCCSD(T)/6–31G(d) calculations.[18] For each optimized structure an analytical Hessian was calculated to obtain vibrational frequencies, zero-point energies and thermodynamic corrections at 423 K, additionally confirming each as a minimum or transition-state structure. Post-processing visualization was carried out with the ChemCraft (G. A. Zhurko, *ChemCraft version 1.6*; http://www.chemcraftprog.com) and Gabedit programs (A. R. Allouche, *J. Comput. Chem* **2011**, *32*, 174–182).

[17] Programme used: GAMESS(US), ver. 1-Oct-2010 (R1): M. W. Schmidt, K. K. Baldridge, J. A. Boatz, S. T. Elbert, M. S. Gordon,

J. H. Jensen, S. Koseki, N. Matsunaga, K. A. Nguyen, S. Su, T. L. Windus, M. Dupuis, J. A. Montgomery, *J. Comput. Chem.* **1993**, *14*, 1347–1363.

[18] P. Piecuch, S. A. Kucharski, K. Kowalski, M. Musial, *Comp. Phys. Commun.* **2002**, *149*, 71–96.

[19] S. T. Perri, L. D. Foland, O. H. Decker, H. W. Moore, *J. Org. Chem.* **1986**, *51*, 3067–3068.

[20] M. T. Hoyt, R. Palchaudhuri, P. J. Hergenrother, *Invest. New Drugs* **2010**, DOI: 10.1007 s10637–010–9390-x, accessed 1/12/2010.

[21] This reduction is reported to proceed in >80% yield with the borane·THF complex (a) Z. Jiajie *Chinese Pat.* CN101239978(A); b) S. Ramsbeck, U. Heiser, M. Buchholz, A. J. Niestroj, US Pat. US2008/234313 A1, **2008**). In our hands, isolation of amine **15** from that reaction proved difficult, prompting a switch to alane.

[22] A. H. Schmidt, G. Kircher, S. Maus, H. Bach, *J. Org. Chem.* **1996**, *61*, 2085–2094.

Received: July 22, 2011
Published online: November 14, 2011

VIP Photochemistry

DOI: 10.1002/anie.201200281

An Efficient Flow-Photochemical Synthesis of 5*H*-Furanones Leads to an Understanding of Torquoselectivity in Cyclobutenone Rearrangements**

David C. Harrowven, Mubina Mohamed, Théo P. Gonçalves, Richard J. Whitby, David Bolien, and Helen F. Sneddon*

Dedicated to Professor Philip Parsons on the occasion of his 60th birthday

Thermal rearrangements of cyclobutenones give access to numerous ring systems and have proven especially valuable for the de novo synthesis of quinones, benzoquinones, and related heteroaromatics with dense substitution.[1–3] A classic example is the rearrangement of arylcyclobutenone **1a**→ **3a**,[1a] where the emergence of a protocol to realize this transformation in near quantitative yield means it achieves many of the ideals for a green-chemical reaction.[2,4] In principle, such criteria could also be met by the related photochemical rearrangement of **1a** to 5*H*-furanone **4a**, yet this reaction has lain almost dormant since its introduction by Moore et al. in 1988 because of the low yields attained in each of the published examples (27–51%, Scheme 2).[5]

Herein we show how the photochemical rearrangement of 4-hydroxycyclobutenones can be realized in near quantitative yield under continuous flow using a simple, low-cost device with an interchangeable low-energy light source.[6,7] In addition, our results challenge the long-established view that the electrocyclic opening of cyclobutenones is a torquoselective process, with the thermochemical and photochemical rearrangements displaying complimentary torquoselectivity,[1e] as implicated by the aforementioned examples (Scheme 1).

Before our investigation could begin, we needed to construct a photochemical reactor for use under flow. Taking inspiration from the pioneering work of Booker-Milburn and co-workers,[6] we assembled the apparatus depicted in Figure 1.[8] A key difference between this and the published setup was our use of inexpensive, low-energy 9 W lamps in place of the more conventional 400–600 W medium-pressure mercury discharge lamps. While recognizing that this might limit the throughput of material, we hoped

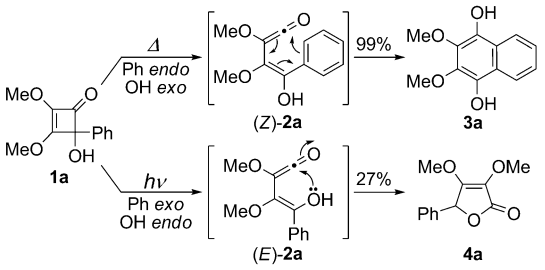

Scheme 1. Thermal and photochemical rearrangements of 4-hydroxycyclobutenone **1**.

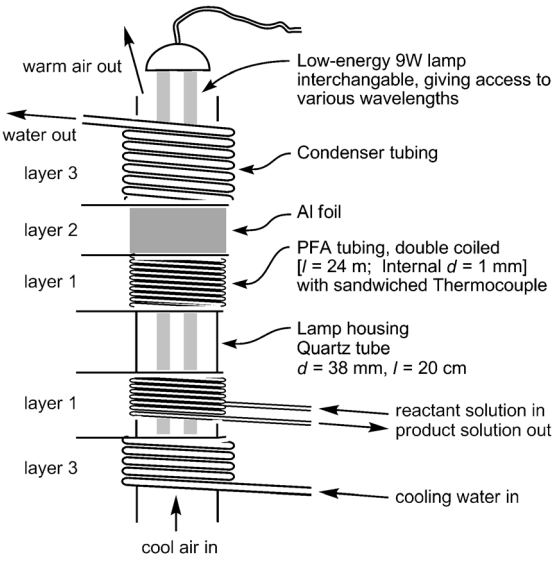

Figure 1. Flow photochemical reactor (cut-away between grey lines). PFA = perfluoroalkoxy.

that it would allow optimization for the wavelength to become "as simple as changing a light bulb", since lamps spanning a wide spectrum of wavelengths have become available at low cost in recent years.[8]

Our study began with an investigation of the rearrangement of phenylcyclobutenone **1a** to 5*H*-furanone **4a** as the reported yield of 27% was among the lowest disclosed in the original study.[5] When conducted under flow using tetrahydrofuran (THF) as solvent, a 9 W broad-spectrum UVB lamp

[*] Prof. D. C. Harrowven, M. Mohamed, T. P. Gonçalves, Prof. R. J. Whitby, D. Bolien
Chemistry, University of Southampton
Highfield, Southampton, SO17 1BJ (UK)
E-mail: dch2@soton.ac.uk
Dr. H. F. Sneddon
GlaxoSmithKline, Stevenage, Hertfordshire, SG1 2NY (UK)

[**] Financial support from GlaxoSmithKline, the ERDF (IS:CE-Chem & InterReg IVa) and the EPSRC (including support for the Iridis cluster) are gratefully acknowledged. Rob Wheeler and Andy Craven are thanked for valuable advice.

Supporting information for this article is available on the WWW under http://dx.doi.org/10.1002/anie.201200281.

(280–370 nm)[8] and a residence time of 120 min, we were pleased to attain 5*H*-furanone **4a** in 54% isolated yield, double that given using a conventional photochemical setup. NMR analysis of crude product mixtures given at various residence times showed many side products, with the ratio of product to by-products worsening as the residence times were increased. In seeking to eliminate side reactions involving the product, a comparison was made between its UV–visible spectrum and that of the starting material. Each showed strong absorbance below 275 nm, with cyclobutenone **1a** exhibiting additional absorbance bands at 295 and 315 nm. A switch to a 9 W UVB narrow-spectrum lamp giving greatest intensity in the region 310–320 nm was therefore implicated and, in the event, this did lead to a modest improvement in yield to 65%.

The step-change in performance we sought was realized with a switch of solvent from THF to acetonitrile. Indeed, through this simple expedient the rearrangement of cyclobutenone **1a** to furanone **4a** was achieved in 97% isolated yield at 0.05 M concentration with a residence time of 1 h. Interestingly, under irradiation from a UVA lamp (350–395 nm) the rearrangement was clean but proceeded at a much slower rate (< 10% conversion after 1 h). The broad-spectrum UVB lamp (280–370 nm) proved as effective as the narrow band lamp, while irradiation for 1 h using a UVC lamp (254 nm) gave complete conversion but the product **4a** was heavily contaminated with by-products which accounted for around 5% of the total mass balance.[8]

To explore the generality of the method, a range of 4-hydroxycyclobutenones **1b–h** were prepared by the addition of alkyl-, aryl-, alkyny-, and heteroaryl-lithium reagents to dimethyl squarate.[1–3] Pleasingly, under the aforementioned conditions, each underwent smooth rearrangement to the corresponding furanones **4b–h** in excellent yield (Scheme 2).

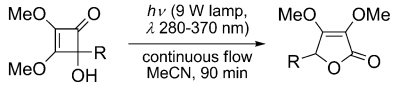

1	yield,	lit. yield	4
a, R = Ph	99%	[27%]	**a**, R = Ph
b, R = *n*Bu	95%		**b**, R = *n*Bu
c, R = *t*Bu	96%	[39%]	**c**, R = *t*Bu
d, R = Ph-CC	95%	[28%]	**d**, R = Ph-CC
e, R = *o*-MeOC$_6$H$_4$	97%	[51%]	**e**, R = *o*-MeOC$_6$H$_4$
f, R = *p*-Me$_3$SiC$_6$H$_4$	93%		**f**, R = *p*-Me$_3$SiC$_6$H$_4$
g, R = *p*-*t*BuC$_6$H$_4$	92%		**g**, R = *p*-*t*BuC$_6$H$_4$
h, R = 3-Pyridyl	94%		**h**, R = 3-Pyridyl

Scheme 2. Photochemically induced cyclobutenone rearrangements of **1a–h** [in a flask] and under continuous flow.

Our survey revealed a striking anomaly in respect of the (2-pyridyl)-cyclobutenone **1i**. In this case the photochemical rearrangement took longer to run to completion and gave a 1:1 mixture of furanone **4i** and quinolizinone **5** (Scheme 3). This anomalous result casts doubt on the view that rearrangements of 4-hydroxycyclobutenones **1** each proceed by torquoselective opening to a vinylketene, with thermolysis giving (*Z*)-**2** and photolysis giving its geometric isomer (*E*)-**2**

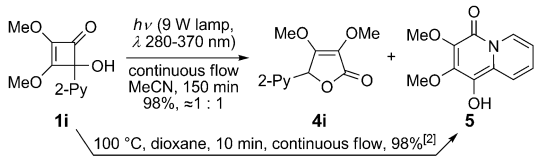

Scheme 3. Photochemical rearrangement of (2-pyridyl)-cyclobutenone **1i** under continuous flow.

(Scheme 1).[1e] Rather, it suggests that the photoinduced electrocyclic opening of **1** gives rise to a mixture of (*E*)- and (*Z*)-vinylketenes **2**, with (*E*)-**2** giving cyclization to furan **6** en route to furanone **4** while (*Z*)-**2** reverts back to cyclobutenone **1** unless it too can be captured by an internal nucleophile (Scheme 4).

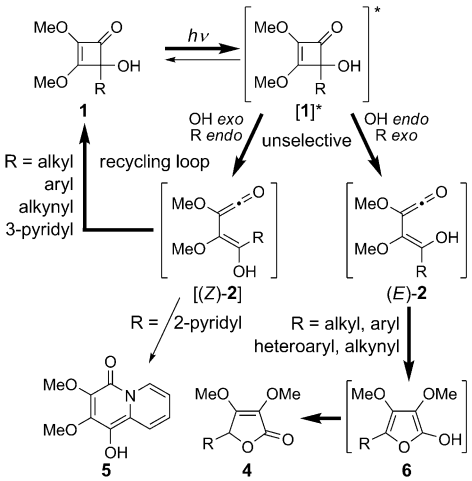

Scheme 4. Revised mechanism for the photochemical rearrangement of 4-hydroxycyclobutenones.

To explore this hypothesis we decided to model the available cyclization pathways for the intermediate (*E*)- and (*Z*)-vinylketenes, **2a** and **2i**, bearing phenyl- and (2-pyridyl)-residues, respectively. The method chosen used DFT calculations at the B3LYP/6-311G(d,p) level to establish the course of the reaction (Gaussian 09),[9–11] with energies refined for required points using the coupled cluster method CCSD(T)/6-31G(d) (GAMESS(US), Schemes 5 and 6).[2,12] Notably, the calculated barrier for 6π-electrocyclic closure of vinylketene (*Z*)-**2a** to **7** at 25 °C (16.7 kcal mol^{-1}) exceeded that for 4π-electrocyclic closure to the starting material **1a** (15.8 kcal mol^{-1}), consistent with the recycling of this intermediate. The situation was reversed for its geometric isomer (*E*)-**2a**, where the calculated barrier for returning cyclobutenone **1a** (20.4 kcal mol^{-1}) exceeded that for cyclization to furan **6a** (12.4 kcal mol^{-1} [13]) leading to the observed product **4a**. For the thermal rearrangement of cyclobutenone **1a** torquoselective opening was evidenced by the calculated activation energies for formation of vinylketenes (*E*)-**2a** (35.0 kcal mol^{-1}) and (*Z*)-**2a** (28.9 kcal mol^{-1}), respectively, at 150 °C.

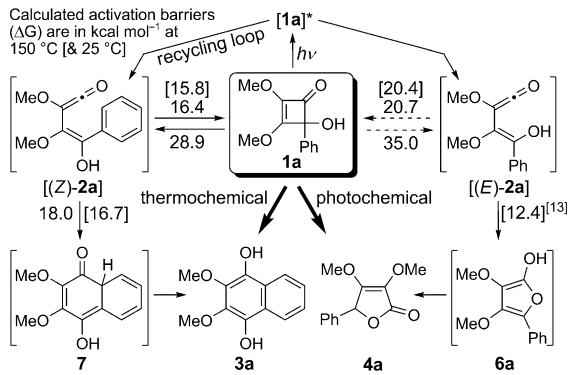

Scheme 5. Calculated energy barriers in photo- and thermochemical rearrangements of cyclobutenone **1b**.

For 2-pyridylcyclobutenone **1i** (Scheme 6), calculations showed that cyclization of vinylketene (*Z*)-**2i** to quinolizinone **5** was spontaneous on adoption of an appropriate reactive conformer, thereby diverting it away from the usual

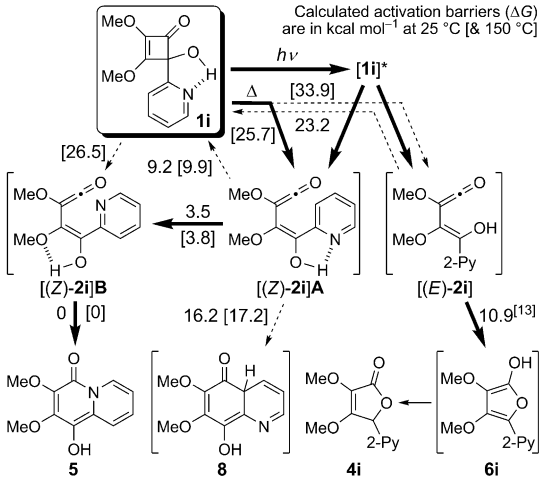

Scheme 6. Calculated activation energies in the photo- and thermochemical rearrangement of cyclobutenone **1i**.

recycling loop. In parallel, the geometric isomer (*E*)-**2i** favors cyclization to furan **6i** (10.9 kcal mol^{-1})[13] over 4π-electrocyclic closure to cyclobutenone **1i** (23.2 kcal mol^{-1}) and gives the expected furanone **4i**. Torquoselectivity in the thermal opening of cyclobutenone **1i** to vinylketene (*Z*)-**2i** was again evidenced, with calculations additionally indicating that a hydrogen bond between the pyridine and hydroxyl residues leads to a significant rate enhancement. This is manifest experimentally by the realization of a near quantitative yield for the thermolysis of **1i** to **5** at 100 °C for 10 min under continuous flow (Scheme 3), when related aryl- and heteroaryl-cyclobutenone rearrangements typically require prolonged heating at 150 °C to achieve a similar outcome.[2] Further observations relating to torquoselectivity in the thermochemical rearrangements of cyclobutenones are given in the Supporting Information.

In conclusion, we have shown that many 4-hydroxycyclobutenones can be transformed into 5*H*-furanones in near quantitative yield using an inexpensive flow-photochemical setup. The results attained challenge a long-held view that the thermal and photochemical rearrangements of cyclobutenones display complementary torquoselectivity in their electrocyclic opening to a vinylketene.[1e] Indeed, they provide a detailed mechanistic understanding of both the thermal and photochemical rearrangements of 4-hydroxycyclobutenones giving valuable insights into their scope and limitations.

Received: January 11, 2012
Revised: March 6, 2012
Published online: March 22, 2012

Keywords: cyclobutenones · density functional calculations · photochemistry · rearrangements · small ring systems

[1] a) S. T. Perri, H. W. Moore, *J. Org. Chem.* **1988**, *53*, 996–1003; b) S. T. Perri, H. J. Dyke, H. W. Moore, *J. Org. Chem.* **1989**, *54*, 2032–2034; c) A. Enhsen, K. Karabelas, J. M. Heerding, H. W. Moore, *J. Org. Chem.* **1990**, *55*, 1177–1185; d) J. M. Heerding, H. W. Moore, *J. Org. Chem.* **1991**, *56*, 4048–4050; e) M. P. Winters, M. Stranberg, H. W. Moore, *J. Org. Chem.* **1994**, *59*, 7572–7574; f) H. W. Moore, O. H. W. Decker, *Chem. Rev.* **1986**, *86*, 821–830; g) A. G. Birchler, F. Liu, L. S. Liebeskind, *J. Org. Chem.* **1994**, *59*, 7737–7745; h) D. Zhang, I. Llorente, L. S. Liebeskind, *J. Org. Chem.* **1997**, *62*, 4330–4338; i) S. Zhang, L. S. Liebeskind, *J. Org. Chem.* **1999**, *64*, 4042–4049.

[2] M. Mohamed, T. P. Gonçalves, R. J. Whitby, H. F. Sneddon, D. C. Harrowven, *Chem. Eur. J.* **2011**, *17*, 13698–13705.

[3] a) D. C. Harrowven, D. D. Pascoe, D. Demurtas, H. O. Bourne, *Angew. Chem.* **2005**, *117*, 1247–1248; *Angew. Chem. Int. Ed.* **2005**, *44*, 1221–1222; b) D. C. Harrowven, D. D. Pascoe, I. L. Guy, *Angew. Chem.* **2007**, *119*, 429–432; *Angew. Chem. Int. Ed.* **2007**, *46*, 425–428.

[4] P. T. Anastas, J. C. Warner, *Green Chemistry: Theory and Practice*, OUP, New York, **1998**, p. 30.

[5] a) S. T. Perri, L. D. Foland, H. W. Moore, *Tetrahedron Lett.* **1988**, *29*, 3529–3532; See also b) Y. Yamamoto, M. Ohno, S. Eguchi, *Tetrahedron* **1994**, *50*, 7783–7798.

[6] a) B. D. Hook, W. Dohle, P. R. Hirst, M. Pickworth, M. B. Berry, K. I. Booker-Milburn, *J. Org. Chem.* **2005**, *70*, 7558–7564; See also b) F. Lévesque, P. H. Seeberger, *Angew. Chem.* **2012**, *124*, 1738–1741; *Angew. Chem. Int. Ed.* **2012**, *51*, 1706–1709; c) M. Nettekoven, B. Püllmann, R. E. Martin, D. Wechsler, *Tetrahedron Lett.* **2012**, *53*, 1363–1366; d) A. C. Gutierrez, T. F. Jamison, *Org. Lett.* **2011**, *13*, 6414–6417; e) F. Lévesque, P. H. Seeberger, *Org. Lett.* **2011**, *13*, 5008–5011; f) T. Fukuyama, Y. Kajihara, Y. Hino, I. Ryu, *J. Flow Chem.* **2011**, *1*, 40–45; g) A. Vasudevan, C. Villamil, J. Trumbull, J. Olson, D. Sutherland, J. Pan, S. Djuric, *Tetrahedron Lett.* **2010**, *51*, 4007–4009; h) M. D. Lainchbury, M. I. Medley, P. M. Taylor, P. Hirst, W. Dohle, K. I. Booker-Milburn, *J. Org. Chem.* **2008**, *73*, 6497–6505.

[7] For excellent recent reviews on photochemical reactions see a) N. Hoffmann, *Chem. Rev.* **2008**, *108*, 1052–1103; b) T. Bach, J. P. Hehn, *Angew. Chem.* **2011**, *123*, 1032–1077; *Angew. Chem. Int. Ed.* **2011**, *50*, 1000–1045, and references therein.

[8] Further details of the photochemical apparatus and lamps used are provided in the Supporting Information.

[9] a) W. Kirmse, N. G. Rondan, K. N. Houk, *J. Am. Chem. Soc.* **1984**, *106*, 7989–7991; b) K. N. Houk, Y. Li, J. D. Evanseck, *Angew. Chem.* **1992**, *104*, 711–739; *Angew. Chem. Int. Ed. Engl.* **1992**, *31*, 682–708; c) R. Ponec, G. Yuzhakov, J. Pecka, *J. Math.*

Chem. **1996**, *20*, 301 – 310; d) P. S. Lee, X. Zhang, K. N. Houk, *J. Am. Chem. Soc.* **2003**, *125*, 5072 – 5079; e) M. Yasui, Y. Naruse, S. Inagaki, *J. Org. Chem.* **2004**, *69*, 7246 – 7249; f) J. M. Um, H. Xu, K. N. Houk, W. Tang, *J. Am. Chem. Soc.* **2009**, *131*, 6664 – 6665.

[10] Gaussian 09, Revision A.02, M. J. Frisch, G. W. Trucks, H. B. Schlegel, G. E. Scuseria, M. A. Robb, J. R. Cheeseman, G. Scalmani, V. Barone, B. Mennucci, G. A. Petersson, H. Nakatsuji, M. Caricato, X. Li, H. P. Hratchian, A. F. Izmaylov, J. Bloino, G. Zheng, J. L. Sonnenberg, M. Hada, M. Ehara, K. Toyota, R. Fukuda, J. Hasegawa, M. Ishida, T. Nakajima, Y. Honda, O. Kitao, H. Nakai, T. Vreven, J. A. Montgomery, Jr., J. E. Peralta, F. Ogliaro, M. Bearpark, J. J. Heyd, E. Brothers, K. N. Kudin, V. N. Staroverov, R. Kobayashi, J. Normand, K. Raghavachari, A. Rendell, J. C. Burant, S. S. Iyengar, J. Tomasi, M. Cossi, N. Rega, N. J. Millam, M. Klene, J. E. Knox, J. B. Cross, V. Bakken, C. Adamo, J. Jaramillo, R. Gomperts, R. E. Stratmann, O. Yazyev, A. J. Austin, R. Cammi, C. Pomelli, J. W. Ochterski, R. L. Martin, K. Morokuma, V. G. Zakrzewski, G. A. Voth, P. Salvador, J. J. Dannenberg, S. Dapprich, A. D. Daniels, Ö. Farkas, J. B. Foresman, J. V. Ortiz, J. Cioslowski, D. J. Fox, Gaussian, Inc., Wallingford CT, **2009**.

[11] All calculations were performed at the B3LYP/6-311G(d,p) level using Gaussian 09,[10] with GAMESS(US) used for all RCCSD(T)/6-31G(d) calculations.[12] For each optimized structure an analytical Hessian was calculated to obtain vibrational frequencies, zero-point energies and thermodynamic corrections at 298 and 423 K, additionally confirming each as a minimum or transition-state structure. Post-processing visualization was carried out using the ChemCraft (G. A. Zhurko, *ChemCraft version 1.6*; http://www.chemcraftprog.com) and Gabedit programs (A. R. Allouche, *J. Comput. Chem.* **2011**, *32*, 174 – 182).

[12] a) GAMESS(US), ver. 1-Oct-2010 (R1): M. W. Schmidt, K. K. Baldridge, J. A. Boatz, S. T. Elbert, M. S. Gordon, J. H. Jensen, S. Koseki, N. Matsunaga, K. A. Nguyen, S. Su, T. L. Windus, M. Dupuis, J. A. Montgomery, *J. Comput. Chem.* **1993**, *14*, 1347 – 1363; b) P. Piecuch, S. A. Kucharski, K. Kowalski, M. Musial, *Comput. Phys. Commun.* **2002**, *149*, 71 – 96.

[13] For reactions involving proton transfer the calculated ΔG presented assumes this to be solvent accelerated: O. Takahashi, K. Kobayashi, A. Oda, *Chem. Biodiversity* **2010**, *7*, 1349 – 1356. See the Supporting Information for details as to how these were estimated.

